

CR 171956

(NASA-CR-171956) LUNAR POWER SYSTEMS Final
Report (System Development Corp.) 324 p
CSCL 10B

N87-17398

Unclas

G3/44 43693

FINAL REPORT: LUNAR POWER SYSTEMS

CONTRACT NAS9 - 17359

12 DECEMBER 1986



**System Development
Corporation**

A Burroughs Company

System Development Corporation
5151 Camino Ruiz
Camarillo CA 93011-6004
Telephone 805 987 6811

TABLE OF CONTENTS

1.0 INTRODUCTION

2.0 SCENARIO AND TRANSPORTATION

3.0 PHOTOVOLTAICS

4.0 HEAT ENGINES

5.0 ENERGY STORAGE

6.0 LUNAR MATERIALS

7.0 LUNAR MATERIALS PROCESSING

1.0 INTRODUCTION

This report presents the findings of a study on the feasibility of several methods of providing electrical power for a permanently manned lunar base. This is the result of a body of thought and activity, stimulated principally by the Solar System Exploration Division of the NASA Lyndon B. Johnson Space Center and identified with the term "Lunar Return Initiative" (LRI). To those involved in the LRI there is an inevitable expectation of a permanent return to the Moon around the year 2000. Funding for this venture has been minimal but is expected to experience a steady growth in the coming years.

In support of the LRI, there is a desire to begin the development of subsystems which will be essential to the survival of the lunar base, so that when an Earth/lunar transportation system becomes available, all will be in readiness for the establishment of the first lunar base. This study has been concerned with the feasibility and the relative merits of several methods of supplying electrical power and suggests some possible approaches. Future work should encompass the preliminary design of the most promising of these. Based upon the results of preliminary design activity, one or two systems could be selected for development and testing.

Two fundamentally different methods for lunar electrical power generation can be considered. One is the use of a small nuclear reactor and the other is the conversion of solar energy to electricity. The lunar environment is characterized, among other things, by the approximate 28 Earth day lunar cycle in which any location on the Moon's surface is sunlit continuously for half of that cycle and is without sunlight for the other half. This circumstance forces the designer of a solar/electric conversion system to provide some means of storing energy for the period of time in which the base is without sunlight. From that point of view, the nuclear approach is the better choice; however this study did not consider any nuclear solutions. The SP-100 program is already active with a goal of having a 300 kW, flight

qualified nuclear power plant by 1992. Although designed for satellite use, it will be adaptable to use at the lunar base. Nevertheless, even if the nuclear option is available to the LRI there is a strong possibility that environmental, sociological and scientific pressure will preclude the establishment of nuclear reactors on the Moon. Therefore, all solar/electric solutions deserve careful consideration.

A baseline goal for the study was to initially provide 300 kW of power with growth capability to first one megawatt and eventually 10 megawatts. There was to be an emphasis on identifying an approach which could use lunar derived materials for the growth of generating capacity. The demand on a power system is never constant, but will vary, in this case with the activity at the base and the size of initial power modules will be constrained by the capacity of the Earth/Moon transportation system. Some understanding of these factors was seen as a necessary ingredient in the study. Section 2 of the report presents a detailed, day by day scenario for the establishment, build-up and operational activity of the lunar base. It also presents a conceptual approach to a supporting transportation system which identifies the number, type and deployment of transportation vehicles required to support the base. Material for this section was developed by Drs. Buzz Aldrin and Harrison Schmitt, with Dr. Schmitt concentrating on the scenario and Dr. Aldrin on the transportation system.

A significant corollary to the scenario which is presented is that an optimum size for a basic power module is 60 kW and all subsequent sections of the report employ that figure as a baseline. A modular build-up to any eventually required capacity is possible. It is also noted that although on Earth we are accustomed to a lower level of activity and of electrical power demand during the time in which we are without sunlight, this

will probably not be true at the lunar base. A night of 336 hours without regular activity is shown to be unrealistic, therefore the demand for electrical power should show little difference throughout the lunar cycle.

The most common method of solar/electric conversion here on Earth is through the use of the photovoltaic or solar cell. Section 3 develops an approach to the use of solar cells in the lunar environment. It is shown that the best baseline system, using currently available technology is one which uses the single crystal silicon solar cell which is the basis for almost all terrestrial and satellite solar/electric systems. Weight and metric size of the baseline system is developed. Some system "cost delivered to the Moon" tradeoffs are shown, which assume technological advances in the manufacture of solar cells. The photovoltaics section of the study and the report were under the direction of Dr. Frederick Allen of UCLA.

There are a number of heat engines which are applicable to solar/electric conversion and these are reported in Section 4. The Stirling, Rankine and Brayton engines are mature heat engine types which are adaptable to the lunar environment. All of them have been operated with closed-cycle working fluids, a necessity on the Moon where replenishment of working fluids for an open cycle system would create a prohibitively expensive Earth/Moon transportation cost.

A particularly interesting engine is the Alkali Metal Thermo Electric Converter (AMTEC). This is a relatively new device with an immature technology, however, it could be available by the year 2000. Section 4 also examines solar concentrators, a necessity for any of the heat engine systems, and the ever present waste heat rejection problem. The latter is amenable to conceptually straight-forward solutions, but which are somewhat more difficult to realize in an engineering sense. The section on heat engines was contributed by Mr. Samuel Melo.

The most difficult part of a lunar based solar/electric conversion system is that subsystem which stores energy for the 336 hours of the lunar cycle when the base is not sunlit. Section 5 examines the several approaches to energy storage which have been used by the electric power utilities and identifies those which could be used at a lunar base. Comparisons are made of the most promising of these in terms of mass for Earth/Moon transportation. Section 5 was the responsibility of Mr. Lee Benbrooks.

As noted in the opening paragraph of this section, the statement of work for the study required the consideration of the feasibility of using lunar derived materials for power system growth. In the first few years of the existence of the base, the materials which appear to be the best candidates for being lunar derived are working fluids, fuels and thermal storage media. The occurrence of these elements and compounds on the Moon is reported in Section 6. Items of particular interest are oxygen as a fuel and as an export commodity, hydrogen as a fuel and as a working fluid, helium³ as an export commodity, sodium and potassium as working fluids and iron, sodium chloride and potassium chloride as thermal storage media.

The occurrence of the desired elements and compounds is one thing and having them in purified form is quite another. The processing of lunar materials on the lunar surface is considered in Section 7. Both Section 6 and Section 7 were under the direction of Dr. Harrison Schmitt.

Drs. David Criswell and Robert Waldron contributed consulting support to the section on photovoltaics and to the section on lunar material processing.

2.0 SCENARIO AND TRANSPORTATION

2.1 LUNAR BASE NETWORK ACTIVATION SCENARIO

The purpose of hypothetical timelines, such as a "Lunar Base Network Activation Scenario," is to begin that long process of bringing realism into the modeling of future mission requirements for the creation and maintenance of a network of bases on the Moon. It is a first step toward the development of a "Design Reference Mission" that can form the basis for developing engineering designs, consumables budgeting, launch support requirements, flight operations requirements, economic analyses, and management structures for such a network. The following detailed scenario or timeline portrays the major day by day activities related to the first two years in one scheme for the establishment and maintenance of a lunar base network. The general assumptions underlying this particular scheme are given in the following subsections.

This scenario for the activation of a lunar base network includes consideration of likely "mission rules," that is, non-negotiable requirements related to crew safety that will be imposed for obvious reasons. Attention is drawn to activities in the timeline which are related to such mission rules with a brief explanation of the rule the first time it is encountered. For example, the status of return modules is checked prior to proceeding with a landing or a departure that might isolate a crew on the moon if one of the return modules were inoperative (see Days 1 and 8).

2.1.1 PRINCIPLE FUNCTIONS AND JUSTIFICATIONS

The principle functions and justifications for the base network, aside from those related to nation building and international policy issues are a) the production of oxygen for use in support

of other space activities and b) the continued scientific exploration and utilization of the Moon. Lunar derived oxygen has the basic advantage over terrestrially derived oxygen of lower export costs from a gravity environment only 1/6th that of the Earth. Potential scientific activities for the network include support of lunar resource development for oxygen and possibly for other materials, further extrapolation of the Moon's special planetological relationships to the Earth and Mars, and use of the Moon's unique advantages as a platform for astronomical observations.

2.1.2 FREQUENCY OF MAJOR SPACECRAFT LANDINGS

The frequency of major spacecraft landings on the moon in support of the activation of the first lunar base (Base I) will be one per lunar cycle. Although higher or lower landing frequencies, and thus frequencies of major launches from Earth, can be accommodated, a frequency of one per lunar cycle appears to give a good balance between the following considerations:

a) a reasonable burden on launch operations on Earth, b) an optimization of sun angle for crew landings, c) a consideration of the operational and safety implications of missing one scheduled landing, and d) a gradual escalation of long duration exposure of humans to the lunar gravity environment. Landing on the moon at a rate of one per lunar cycle also can support the activation of a second base (Base II) provided that launch capabilities can support a step increase (possibly about 50%) in payload mass landed on the moon. The lunar landing frequency required to support the activation of a third base has not been examined, but it is likely that either a higher landing frequency or another major increase in payload mass landed will be required.

2.1.3 ENGINEERING DESIGNS FOR MAJOR SUPPORT SYSTEMS

Engineering designs for the major support systems for a lunar base network will be finalized prior to initiation of the activation of the first

base. These support systems include landers, habitat modules, rovers, power plants, mining plants, oxygen production plants, agricultural plants, storage modules, and oxygen transport modules. On the other hand, it is likely that the operational testing of prototypes at the first base will disclose needed modifications. Thus, the original designs must be compatible with rapidly accomodating such modifications.

2.1.4 SITE FOR FIRST BASE

The site for the first base, (Base I), will be selected as that which is best for the operational testing of all basic support systems as well as being suitable for oxygen production. As it appears that the mineral ilmenite (Fe_2TiO_4) will be the most favorable raw material for oxygen production see (7.2), it would be highly desirable to take advantage of our existing knowledge about ilmenite abundances and variability at an Apollo landing site. Either the Apollo 11 or Apollo 17 sites appear to be the best candidates for Base I.

2.1.5 SITE FOR SECOND BASE

The site for the second base, (Base II) will be that which is best for sustained oxygen production. Although this would appear to be the Apollo 17 area among those about which we have direct knowledge, it may be that our confidence from remote sensing of other ilmenite-rich areas will permit selection of a Base II site that lies in the western region of the Moon. This would be very desirable from a scientific point of view as would be a third base location on the lunar farside such as in the large crater Tsilkovsky.

2.1.6 LUNAR TOUR OF DUTY

The lunar tour of duty for crews will be roughly three lunar cycles for the first year, six lunar cycles for the second year, and 12 lunar cycles for the third and subsequent years. Although longer tours of duty probably can be accomodated, with a

concurrent reduction in launch support requirements, it seems prudent to build up gradually from our base of Skylab and Space Station experience with human adaptation and readaptation in altered gravity environments.

2.1.7 CREW WORK CYCLE

The crew work cycle during base activation and operation normally will be 10 hour days and six day weeks. The Apollo experience indicates that this work load is easily sustainable in 1/6 gravity and, indeed, it may be difficult to resist longer hours and seven day weeks if hardware permits.

2.2 EXPLANATION OF SPECIFIC ACTIVITIES

In the discussions of specific scenario activities which follow, references are made to the daily events listed in section 2.3.

2.2.1 LANDINGS

The first landing at a base site (day -28) is an automated or remotely guided placement of a habitation module (HABMOD) keyed to an existing Apollo lunar module descent stage and to the plan for the final architecture of the base. Twenty-eight days later (day 0) the first crew lands manually, but this landing also is keyed to the descent stage and plan. Sufficient reserves of propellants must be on hand for both landings to maximize the probability of success. Subsequently, both automated and crew landings can be made precisely to landing beacons on sites prepared by preceeding crews (days 50-55). This will reduce the propellant reserves required for landing and consequently increase landed payload capability.

2.2.2 CREW CONSUMABLES

The basic philosophy behind crew consumables supply is to have sufficient margins to maintain normal consumption if the next scheduled resupply mission did not take place. (The chances are that mission rules would require that the crew begin to conserve consumables if a scheduled resupply were indeed missed). Crew consumables are listed in the right hand column of the timeline in units of supply per crew (three persons) per lunar cycle. No allowance has been made for consumables (food and oxygen) that would eventually be produced at the base, however, such consumables would ultimately begin to significantly reduce landed consumables requirements (by day 197 in the case of food and day 309 in the case of oxygen).

2.2.3 POWER

Power production and storage for the base is obtained in two stages. First, relatively small power plants and power storage systems are included as modules with the landings of the habitation modules (days -28 and -29). The first crew lands with a backup power module and power storage system (day 0). These systems must provide power for both day and night operations and habitation. If solar cell and battery systems are utilized, it may be that sun tracking solar arrays will be desirable so that excess power can be generated during the lunar day for battery charging. Consumables for power generation, if required, are listed in the timeline in units of supply needed per lunar cycle. As in the case of crew consumables, it is planned to have margins for power consumables sufficient to maintain normal base operation through at least one missed resupply opportunity.

The second stage power production and storage systems, the central power plant landed on (day 85), must be sized to provide the power necessary for continuous operation of the fully operational base (day 310).

Should fuel cells become a major component of base power systems and should their maintenance require replenishment of significant electrolytes containing Na, K, Cl, or F, the cost of resupply of these elements versus the cost of lunar production should be examined. This subject is treated in part in Section 7.

2.2.4 CREW SELECTION

Crew selection and training leading up to full activation of a base (day 309) will be governed largely by the specialized activities each crew member will be required to perform. An appropriate payload specialist will be on each of the crews through I-PQR whereas subsequent crews responsible for base operation may be more generally trained. Once the upgraded landers are available for Base II activities, additional scientific specialists should be accommodated as permanent personnel at the bases. Habitation module designs should take this possibility into consideration.

Health maintenance considerations will make it highly desirable to have a trained physician at each base at least by the time six persons are in continuous presence (day 309). Such physicians also will be required to fulfill a full range of other base responsibilities as will the scientific payload specialists required throughout the base activation period.

2.2.5 RISK MANAGEMENT

The activation of lunar bases will require some new attitudes as well as new approaches toward risk management. For example, once crews are continuously active on the moon, there cannot be a long-term stand-down in the use of a primary transportation system (as currently is the situation with the Space Shuttle) on which base activities and, indeed, crew survival may depend. Confidence in the transportation systems must be such that it can

be used even in the face of an accident or unforeseen design deficiency. Further, a severely injured or ill person on the Moon must be treated there. Otherwise, the activation or operation of a base will be seriously compromised. Contingency plans should be aimed more toward quickly adding personnel to a base having a personnel problem rather than quickly returning a person or crew back to Earth.

Equipment design must include "fail safe" philosophies as well as the capability to repair and upgrade rather than discard. Major external risks from the environment, such as solar flares, must be managed by initial habitation design and by easily implemented procedures should the crew be caught in an exposed situation during a flare. In this case, appropriate shielding materials should be incorporated in the floor area of lunar rovers so that it can form the roof of an explosively excavated trench.

2.2.6 HABITATION

The delivery (days -28 and -29), checkout (days 2 and 30), inspection and maintenance (day 75), and upgrading (day 186) of habitation modules are sequenced so that sufficient capability is available at all times and the lifetimes of modules are maximized. As the modules will need to be covered by two to three meters of lunar soil for protection from solar flares and cosmic rays, it is anticipated that trenches will be explosively excavated in the regolith next to the lander that delivers each module. In turn, this requires that the lander be designed to protect the modules from the effects of explosive excavation and to provide for off-loading and placement of the module in its trench. The lunar rover must then have the capability to move nearby regolith over the module and cover it to the required depth.

The Apollo experience indicates that a "dust lock" (in contrast to an airlock) will be a highly desirable if not a mandatory

component of the habitation module. Although the absence of a lunar atmosphere prevents the billowing and air transportation of lunar dust, the crews will carry dust on their pressure suits through the entrances to the modules. The highly penetrating and abrasive character of this dust makes it an undesirable addition to the module's interior environment.

Although the scenario provides for the upgrading of the habitation modules (days 186 and 242) to accommodate continuous rather than discontinuous use (2 cycles on, one cycle off) (see day 80), upgrading may not be necessary, depending on the initial design. However, it is likely that the coupling together of new module components as a base develops will be desired as well as the addition of unanticipated new capabilities. Thus, the module design should include provisions for accomodating upgrades.

2.2.7 SCIENCE STATION

Each lunar base will certainly be a major scientific observatory for lunar, solar system, and astronomical phenomena. The base plan should therefore include an appropriately selected site for a scientific station. The timeline provides for the deployment and activation (day 10) and the regular inspection, maintenance, and upgrading (day 79) of the base's scientific systems.

The location of sites which constitute the lunar base network will greatly affect the value of each site's scientific station. If the Apollo 17 site were selected for Base I, then a western ilmenite-rich site for Base II and a farside southern hemisphere site for Base III would make good sense. Base III might well be a purely scientific site, particularly one which could take advantage of the unique astronomical "viewing" potential of the lunar farside.

2.2.8 BASE PLANNING

The layout and architecture of the core of each lunar base must be planned in detail prior to any landing or activation activity. The automated landing of the first habitation module and all subsequent landings should conform to these plans. The first crew must insure that the plan is not only feasible (days 11-20) but can conform to the realities of the selected site.

Some of the considerations for the planning process are as follows:

- Proper location of all landers relative to the site of the oxygen production plant so that they can be used later either to store oxygen, hydrogen, water, or He³ or to be refueled and reused.
- Proper location of the landers bringing oxygen transport modules (OTM) so that the OTM launch area is appropriately spaced relative to the oxygen production plant.
- Proper location of the entire base relative to its ilmenite resource in order to maximize the efficiency of extraction, beneficiation, and transport of ilmenite to the oxygen production plant.
- Proper location of the scientific station and agricultural plant enclosure so that they are unaffected by base activities that create dust, gas, seismic noise, and high velocity particles which could damage these facilities or adversely affect their performance.

2.2.9 SCIENTIFIC ACTIVITIES

Subsequent to the initial scientific survey of the base area (days 36-48) and prior to the activities leading up to full activation of oxygen production (day 253), scientific activities dovetail well with the overlap of crews on three lunar cycle

tours of duty (days 64-72, 120-129, 173-185, and 229-241). The activities contemplated are those that extend our scientific knowledge of the Moon, deploy geophysical and astronomical sensors, and define potential resources accessible to the base.

Once there is preoccupation with the activities of oxygen production (day 253 on), extensive scientific investigation will require the landing of extra payload specialists or entire crews for this purpose. Such augmentation of the scientific activities at a base requires not only additional habitation capacity but also more frequent landings than assumed for this scenario. One other alternative that could increase time available for scientific activities is successful automation of other base operations once systems are activated. Time will tell whether this proves to be practical.

2.2.10 AGRICULTURE

The investigation of food production on the moon (day 59) and the later activation of an agricultural plant (day 127) are related both to the need to minimize imports of food and to the need to dispose of biological waste through recycling. The agricultural experiments and plant will probably involve a large inflatable and pressurized greenhouse and may require a self-contained fuel cell power system to provide water and lunar night lighting for photo-synthesis. Ultimately, food produced on the Moon may become a significant commodity for export to space stations.

2.2.11 ILMENITE RESOURCE EVALUATION

As oxygen production from ilmenite is one of the main functions of a lunar base network, the early and detailed delineation of ilmenite ore grades is essential to the long term operation of each production center. The evaluation of the distribution of ilmenite-rich and ilmenite-poor zones within the regolith (days 60-66) will be an on-going process. Such evaluations will be essential to the development and implementation of a mining plan.

Although ilmenite probably is evenly distributed in individual ilmenite-rich basaltic lavas from which most local regolith is derived, it is also clear that ilmenite-poor zones will be present as a consequent of the deposition of layers of pyroclastic materials, avalanche debris, and impact debris from non-local sources. Surface mapping, the interpretation of local geologic features, and the grid-controlled analysis of bore hole samples will be required to adequately delineate the ilmenite-rich ore zones to be mined and the ilmenite-poor waste zones to be discarded or avoided.

It will probably be desirable to equip the lunar rovers with boring and sampling systems in order to minimize the time required for resource evaluation. It also may be possible as well as desirable to automate the analysis of ilmenite ore grades and integrate that analysis with the drilling of bore holes.

The actual mining of the ilmenite ore will be conceptually similar to large scale dredging operations such as are used to mine rutile in placer deposits. The ilmenite mining plant will need to be mobile with self-contained primary and secondary ilmenite concentration systems. This will minimize the quantity of bulk material transported to the oxygen production plant and provide the capability for real-time control of the ore grade being mined.

2.2.12 READAPTATION PROTOCOL

Although 1/6th gravity has significantly less adaptive effects on human physiology than does total weightlessness, it is probable that some activities related to a crew's readaptation to Earth's gravity will be desirable. The protocol for these activities (day 66) is initiated about two weeks before a crew's return to Earth. The protocol will probably include activities that gradually increase skeletal and cardiovascular stress over this

period. It is hoped that space station research will have defined prophylactic measures against adaptive deterioration by the time we begin to activate a lunar base network.

2.2.13 PLANT ACTIVATION AND TEST

The activation and test of the power plant (day 85), the ilmenite mining plant (day 141), and the oxygen production plant (day 198) are critical not only to future integration of base operations but also to verifying designs. If design flaws are discovered during these activities, it is essential that overall designs make it possible to correct such flaws rapidly and in situ.

2.2.14 STORAGE MODULES

With lengthened tours of duty (day 281) and less frequent landings at Base I (day 364), it will be necessary to bring into service, storage modules (day 253) which can not only provide for the landing and storage of consumables, but can deliver empty oxygen transport modules to the base. These storage modules will probably require use of the step increase in landed payload capability that also will be needed as Base II is activated.

2.2.15 OXYGEN TRANSPORT MODULE

The regular supply of oxygen from the Moon (day 340) implies the existence and regular delivery of empty oxygen transport modules (OTM) to each production base (day 253). The scenario provides for these activities through the cycling of four and eventually five OTM's to and from each base. This cycling of OTM's is best shown in the Summary Timeline (cycles 9 and 16). It appears that, with the assumptions made to develop this scenario, each base might launch a loaded OTM every two lunar cycles. With launches staggered, this means that a lunar oxygen (and perhaps fresh food) delivery to a space station can be made every 28 days

with two operating production bases. However, because landings at each established base in a three base network will occur at an average frequency of less than one every two lunar cycles, it will occasionally be necessary to return empty OTM's in pairs (cycle 25).

2.2.16 INTEGRATED OPERATIONS

With the landing of the I-PQR crew (day 281), the stage is set for a build-up to integrated operations. Initially, the PQR crew integrates ilmenite mining and oxygen (and possibly hydrogen and He³) production with storage in landers and/or oxygen transport modules (day 285).

In order to undertake the full integration of these systems as well as other necessary base functions, it is necessary for the MNO and PQR crews to split into two person shifts (day 294). It appears that this practice will be necessary indefinitely unless a high level of automation and systems reliability is possible.

2.2.17 MAINTENANCE

Throughout the scenario, attention is given to inspection and maintenance of base facilities and plants. Once the base is in full and continuous operation (day 310), it is likely that one of the two person shifts will be an inspection and maintenance shift (day 316). This shift will have to work its way through all base systems on a regular cycle. A capability for repair, replacement, and spares delivery must be clearly defined and implemented if base functions are to be maintained continuously.

2.2.18 BASE II ACTIVATION

It is anticipated that the activation of a second base for oxygen production (day 364) would follow the same general scheme as that

for the first except for the following modifications:

- Landings would be less frequent,
- Crew tours of duty would be longer and responsibilities more varied, and
- Landed payloads would be larger.

2.2.19 MANAGEMENT

A great deal of the management of operating a lunar base network must be contained within the network itself. However, logistics coordination with space stations and Earth will be essential, first, to insure a successful activation of the network and, second, to properly phase exports, imports, and crew replacement. Thus, it would appear that, at least for the first few years, the overall network must be managed from Earth, but the individual bases must be capable of significant operational autonomy.

2.3 DETAILED LUNAR BASE NETWORK ACTIVATION SCENARIO

SUMMARY OF ASSUMPTIONS

- Base Network Functions: Oxygen production and planetary and space science.
- Lunar Landing Frequency: One landing per lunar cycle
- Engineering Designs: Firm prior to start of Base I activity
- Base I Site: Best site for operational testing of engineering designs (such as Apollo 11)
- Base II Site: Best site for oxygen production (such as Apollo 17 area)
- Crew Tour of Duty: First year: 3 lunar cycles
Second year: 6 lunar cycles
Third and subsequent years: 12 lunar cycles
- Crew Work Cycle: 10 hour days/6 day weeks
- Landed Payload Capability: Block change for Base II activation

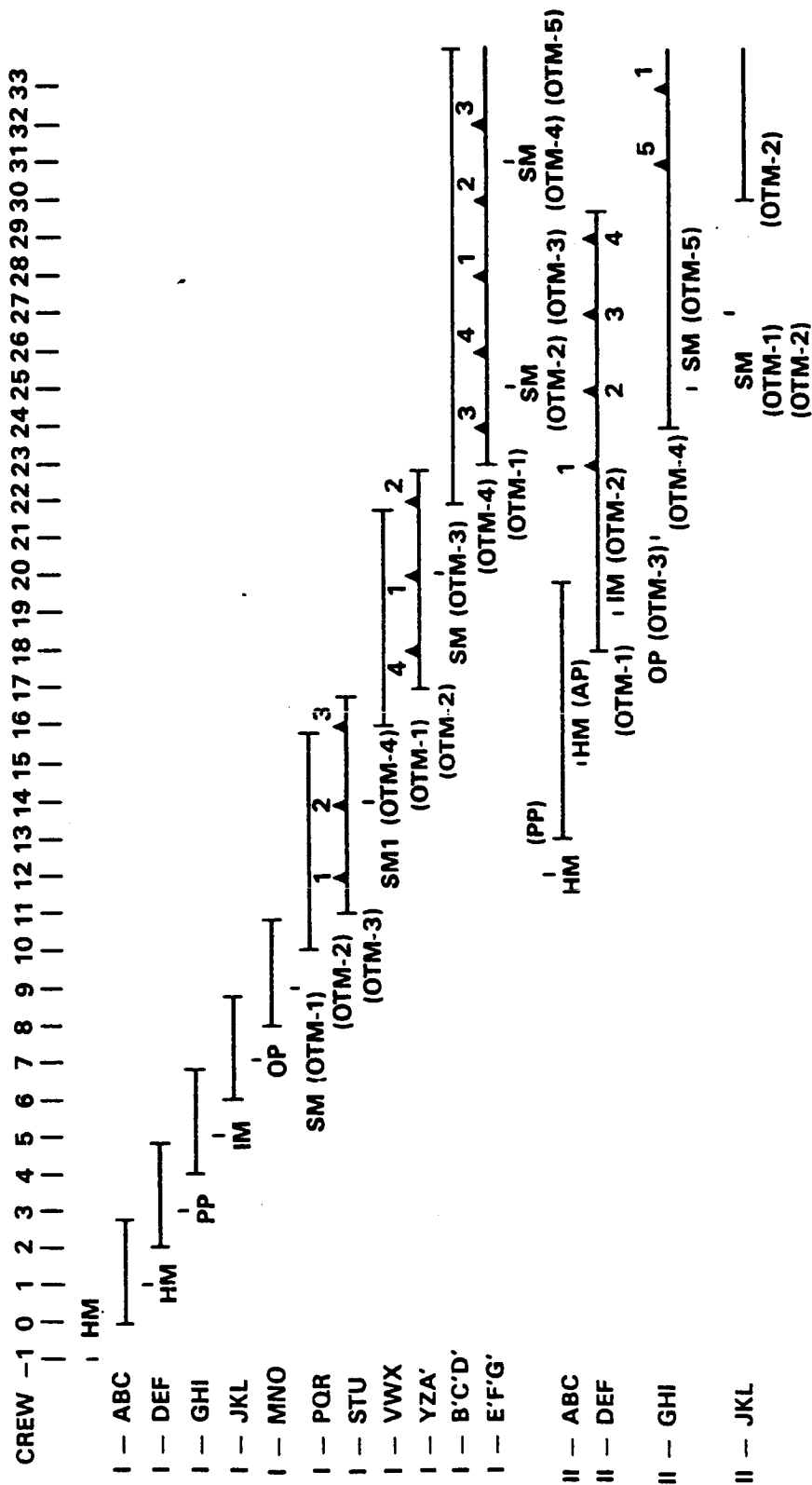


Figure 2.3.1. Scenario Summary Timeline

EARTH DAYS FROM 1ST

CREW LANDINGSMILESTONECONSUMABLE
INVENTORIESCREW* POWER**

-28	HABITATION MODULE I-1 AUTO LANDING	1	1
	<ul style="list-style-type: none"> - Remote landing site selection keyed to Apollo Descent Stage - Includes I-ABC Crew Return Module (short duration - 4 months return module) and habitation power plant module I-1 - Includes crew consumables for 28 days and power consumables for 1 lunar cycle. 		
1	CREW I-ABC LANDING	2	2
	<ul style="list-style-type: none"> - Landing with access to HAB MOD I-1 - Crew consumables for 28 days and power consumables for 1 lunar cycle - Mission Rule: Consumables inventory must be sufficient to back-up next scheduled delivery - Includes LRV, survey equipment, landing beacons back-up habitation power plant module, scientific station, and regolith excavation systems (2) - Includes I-DEF crew return module - Crew Qualifications <ul style="list-style-type: none"> - Knowledge of Base-I plan and habitation systems - Strong geoscientific and agricultural background 		
1	ABC RETURN MODULE CHECKOUT BY I-ABC CREW		
	<ul style="list-style-type: none"> - Mission Rule: Determine status of crew return module before commitment to stay at base. 		

* In requirements per lunar cycle

** In Base requirements per lunar cycle

EARTH DAYS FROM 1ST

CREW LANDINGSMILESTONECONSUMABLE
INVENTORIESCREW* POWER**

2	HABITATION MODULE I-1 ACTIVATION INITIATED BY I-ABC CREW	
3	HABITATION MODULE I-1 ACTIVATION COMPLETED BY I-ABC CREW	
4	HABITATION POWER PLANT MODULE I-1 ACTIVATION INITIATED BY I-ABC	
5	HABITATION POWER PLANT MODULE I-1 ACTIVATION COMPLETED BY I-ABC CREW	
6	HAB POWER MODULE TEST PROTOCOL CONDUCTED BY I-ABC CREW	
7	DAY OFF	
8	I-DEF RETURN MODULE CHECKOUT BY I-ABC CREW -Mission Rule: Determine status of backup crew return module as soon as feasible after landing	
10	SCIENTIFIC STATION I-1 ACTIVATED BY I-ABC CREW	
11	BASE I PLANNING AND SURVEY COMPLETED BY I-ABC CREW	
14	DAY OFF	
20	BASE I PLANNING AND SURVEY COMPLETED BY I-ABC CREW	
21	DAY OFF	

EARTH DAYS FROM 1ST

CREW LANDINGSMILESTONE

CONSUMABLE

INVENTORIESCREW* POWER**

22	HAB MOD I-2 LANDING SITE PREPARATION INITIATED BY I-ABC CREW		
26	HAB MOD I-2 LANDING SITE PREPARATION COMPLETED BY I-ABC CREW		
27	HAB MOD I-2 LANDING BEACON ACTIVATED BY I-ABC CREW		
28	DAY OFF		
29	HABITATION MODULE I-2 LANDING -Includes I-GHI crew return module -Includes crew consumables for 28 days and power consumables for 1 lunar cycle	2	2
30	HABITATION MODULE I-2 ACTIVATION INITIATED BY I-ABC CREW		
33	HABITATION MODULE I-2 ACTIVATION COMPLETED BY I-ABC CREW		
34	HAB MOD I-2 PLACED IN STAND-BY MODE BY I-ABC CREW		
35	DAY OFF		
36	SCIENTIFIC SURVEY OF BASE-I AREA INITIATED BY I-ABC CREW		
42	DAY OFF		
48	SCIENTIFIC SURVEY OF BASE I AREA COMPLETED BY I-ABC CREW		

EARTH DAYS FROM 1ST

CREW LANDINGSMILESTONE

CONSUMABLE

INVENTORIESCREW* POWER**

- 49 DAY OFF
- 50 CREW I-DEF LANDING SITE PREPARATION
INITIATED BY I-ABC CREW
-Landing site placements planned
so that landing module tanks can
be used for cryogenic storage
(O₂, H₂, He³) and/or reuse
- 53 CREW I-DEF LANDING SITE PREPARATION
COMPLETED BY I-ABC CREW
- 54 I-ABC MODULE CHECKOUT BY I-ABC CREW
-Mission Rule: Before new crew
lands, determine status of first
crew's return module
- 55 CREW I-DEF LANDING BEACON ACTIVATED BY I-ABC
CREW
- 55 I-DEF RETURN MODULE CHECKOUT BY I-ABC CREW
-Mission Rule: Before new crew lands
determine status of that crew's return
module
- 56 DAY OFF

EARTH DAYS FROM 1ST
CREW LANDINGS

MILESTONE

CONSUMABLE
INVENTORIES
CREW* POWER*

64	SPECIALIZED SCIENTIFIC ACTIVITIES INITIATED BY I-ABC CREW	
66	READAPTATION PROTOCOL INITIATED BY I-ABC CREW	
66	ILMENITE EVALUATION COMPLETED AND MINE SITE SELECTED BY I-DEF CREW	
70	DAY OFF	
71	PROTO-CENTRAL POWER PLANT LANDING SITE PREPARATION INITIATED BY I-DEF CREW	
72	SPECIALIZED SCIENTIFIC ACTIVITIES BY I-ABC CREW COMPLETED	
73	AGRICULTURAL TEST PROGRAM PLACED IN MONITOR STATUS BY I-ABC CREW	
75	HAB MOD I-1 INSPECTION AND MAINTENANCE INITIATED BY I-ABC CREW	
76	HAB MOD I-1 INSPECTION AND MAINTENANCE COMPLETED BY I-ABC CREW	
76	PROTO-CENTRAL POWER PLANT LANDING SITE PREPARATION COMPLETED BY I-DEF CREW	
77	DAY OFF	

EARTH DAYS FROM 1ST

CREW LANDINGSMILESTONECONSUMABLE
INVENTORIESCREW*POWER**

78 I-ABC RETURN MODULE ACTIVATION
INITIATED BY I-ABC CREW

78 I-DEF RETURN MODULE CHECK-OUT BY DEF CREW
-Mission Rule: Before one crew
departs, status of 2nd crew return
module determined

79 SCIENTIFIC STATION INSPECTION, MAINTENANCE,
AND UPGRADING INITIATED BY I-DEF CREW

80 HAB MOD I-1 PLACED IN STANDBY BY I-ABC CREW

80 DEPARTURE FOR EARTH BY I-ABC CREW

83 PROTO-CENTRAL POWER PLANT LANDING
BEACON ACTIVATED BY I-DEF CREW

83 SCIENTIFIC STATION INSPECTION,
MAINTENANCE, AND UPGRADING COMPLETED
BY I-DEF CREW

84 DAY OFF

85 PROTO-CENTRAL POWER PLANT LANDING
-Includes crew consumables for 56 days
-Includes power consumables for activation
and test of proto-central power plant

3

2

EARTH DAYS FROM 1ST

CREW LANDINGSMILESTONECONSUMABLE
INVENTORIESCREW* POWER**

85	PROTO-CENTRAL POWER PLANT ACTIVATION INITIATED BY I-DEF CREW		
90	PROTO-CENTRAL POWER PLANT ACTIVATION COMPLETED BY I-DEF CREW		
91	DAY OFF		
92	PROTO-CENTRAL POWER PLANT TEST PROTOCOL INITIATED BY I-DEF CREW		
98	DAY OFF		
104	PROTO-CENTRAL POWER PLANT TEST PROTOCOL COMPLETED BY I-DEF CREW		
105	DAY OFF		
106	CREW I-GHI LANDING SITE PREPARATION INITIATED BY I-DEF CREW		
109	I-GHI CREW LANDING SITE PREPARATION COMPLETED BY I-DEF CREW		
110	I-DEF RETURN MODULE CHECKOUT BY I-DEF CREW -Mission Rule		
111	I-GHI CREW LANDING BEACON ACTIVATED BY I-DEF CREW		
111	I-GHI RETURN MODULE CHECKOUT BY I-DEF CREW -Mission Rule		
112	DAY OFF		

EARTH DAYS FROM 1ST

CONSUMABLE
INVENTORIESCREW* POWER**CREW LANDINGSMILESTONE

120	SPECIALIZED SCIENTIFIC ACTIVITIES INITIATED BY I-DEF CREW
122	READAPTATION PROTOCOL INITATED BY I-DEF CREW
125	PROTO-ILMENITE MINING PLANT SITE PREPARATION COMPLETED BY I-GHI CREW
126	DAY OFF
127	PROTO-AGRICULTURAL PLANT ACTIVATION INITIATED BY I-GHI CREW -Includes waste recycling system
129	SPECIALIZED SCIENTIFIC ACTIVITIES BY I-DEF CREW COMPLETED
130	AGRICULTURAL TEST PROGRAM PLACED IN MONITOR STATUS BY I-DEF CREW
130	HAB MOD I-2 INSPECTION AND MAINTENANCE INITIATED BY I-DEF CREW
132	HAB MOD I-2 INSPECTION AND MAINTENANCE COMPLETED BY I-DEF CREW
132	PROTO-AGRICULTURAL PLANT ACTIVATION COMPLETED BY I-GHI CREW
133	DAY OFF
134	I-GHI RETURN MODULE CHECKOUT BY I-GHI CREW

EARTH DAYS FROM 1ST

CREW LANDINGSMILESTONECONSUMABLE
INVENTORIESCREW* POWER**

- | | | | |
|-----|--------------------|---|---|
| 113 | CREW I-GHI LANDING | 4 | 2 |
|-----|--------------------|---|---|
- Includes crew consumables for 56 days and power plant consumables for 2 lunar cycles
 - Includes Proto-Agricultural Plant
 - Includes control power plant consumables for 2 lunar cycles
 - Includes I-MNO crew return module
 - Includes back-up LRV
 - Crew Qualifications
 - Specialists in ilmenite mining plant systems
 - Payload specialist in resource development
-
- | | | | |
|-----|---|--|--|
| 114 | I-JKL CREW RETURN MODULE CHECKOUT BY I-DEF CREW | | |
|-----|---|--|--|
- Mission Rule
-
- | | | | |
|-----|---|--|--|
| 114 | PROTO-CENTRAL POWER PLANT ACTIVATED BY I-DEF CREW | | |
|-----|---|--|--|
-
- | | | | |
|-----|---------------------------------------|--|--|
| 114 | HAB MOD I-1 REACTIVATED BY I-GHI CREW | | |
|-----|---------------------------------------|--|--|
-
- | | | | |
|-----|---|--|--|
| 115 | AGRICULTURAL TEST PROGRAM REACTIVATED BY I-DEF CREW | | |
|-----|---|--|--|
-
- | | | | |
|-----|--|--|--|
| 115 | PROTO-ILMENITE MINING PLANT SITE PREPARATION INITIATED BY I-GHI CREW | | |
|-----|--|--|--|
-
- | | | | |
|-----|---------|--|--|
| 119 | DAY OFF | | |
|-----|---------|--|--|

EARTH DAYS FROM 1ST			CONSUMABLE	
<u>CREW LANDINGS</u>	<u>MILESTONE</u>		<u>INVENTORIES</u>	
			<u>CREW*</u>	<u>POWER**</u>
134	I-DEF RETURN MODULE ACTIVATION INITIATED BY I-DEF CREW			
135	SCIENTIFIC STATION INSPECTION, MAINTENANCE AND UPGRADING INITIATED BY I-GHI CREW			
136	HAB MOD I-2 PLACED IN STANDBY BY I-DEF CREW			
136	DEPARTURE FOR EARTH BY I-DEF CREW			
139	SCIENTIFIC STATION INSPECTION, MAINTENANCE AND UPGRADING COMPLETED BY I-GHI CREW			
139	PROTO-ILMENITE MINING PLANT LANDING BEACON ACTIVATION BY I-GHI CREW			
140	DAY OFF			
141	PROTO-ILMENITE MINING PLANT LANDING -Includes crew consumables for 56 days and power plant consumables for 1 lunar cycle -Includes lunar hydrogen and He ³ extraction capability	4	2	
141	PROTO-ILMENITE MINING PLANT ACTIVATION INITIATED BY I-GHI CREW			
146	PROTO-ILMENITE MINING PLANT ACTIVATION COMPLETED BY I-GHI CREW			
147	DAY OFF			

EARTH DAYS FROM 1ST

CREW LANDINGS

MILESTONE

CONSUMABLE
INVENTORIES

CREW* POWER**

148	PROTO-ILMENITE PLANT INITIAL TEST PROTOCOL INITIATED BY I-GHI CREW		
154	DAY OFF		
160	PROTO-ILMENITE PLANT INITIAL TEST PROTOCOL COMPLETED BY I-GHI CREW		
161	DAY OFF		
162	I-JKL CREW LANDING SITE PREPARATION INITIATED BY I-GHI CREW		
165	I-JKL CREW LANDING SITE PREPARATION COMPLETED BY I-GHI CREW		
166	I-GHI RETURN MODULE CHECKOUT BY I-GHI CREW		
167	I-JKL CREW LANDING BEACON ACTIVATED BY I-GHI CREW		
167	I-JKL CREW RETURN MODULE CHECKOUT BY I-GHI CREW		
168	DAY OFF		

EARTH DAYS FROM 1ST

	<u>CREW LANDINGS</u>	<u>MILESTONE</u>	<u>CONSUMABLE INVENTORIES</u>	
			<u>CREW*</u>	<u>POWER**</u>
169	<u>I-JKL CREW LANDING</u>		4	2
	-Includes crew consumables for 28 days and power plant consumables for one lunar cycle -Includes I-PQR crew return module (1st long duration - 10 months - return module -Includes long duration upgrades for HAB MOD I-1 -Crew Qualifications - Specialists in oxygen plant systems			
170	I-MNO CREW RETURN MODULE CHECK-OUT BY I-GHI CREW			
170	HAB MOD I-2 REACTIVATED BY I-JKL CREW			
171	PROTO-POWER PLANT INSPECTION AND MAINTENANCE INITIATED BY I-GHI CREW			
171	PROTO-OXYGEN PLANT SITE PREPARATION INITIATED BY I-JKL CREW			
172	PROTO-POWER PLANT INSPECTION AND MAINTENANCE COMPLETED BY I-GHI CREW			
173	SPECIALIZED SCIENTIFIC ACTIVITIES INITIATED BY I-GHI CREW			
175	DAY OFF			

EARTH DAYS FROM 1ST

CREW LANDINGSMILESTONE

CONSUMABLE

INVENTORIESCREW* POWER**

- 178 READAPTATION PROTOCOL INITIATED
BY I-GHI CREW
- 181 PROTO-OXYGEN PLANT SITE PREPARATION
COMPLETED BY I-JKL CREW
- 182 DAY OFF
- 183 PROTO-AGRICULTURAL PLANT INSPECTION
AND MAINTENANCE INITIATED BY I-JKL CREW
- 185 SPECIALIZED SCIENTIFIC ACTIVITIES
COMPLETED BY I-GHI CREW
- 186 HAB MOD I-1 INSPECTION MAINTENANCE
AND UPGRADING INITIATED BY I-GHI CREW
-Upgrading required because, with
arrival of I-MNO crew, use of HAB MOD I-1
will be continuous
- 186 PROTO-AGRICULTURAL PLANT INSPECTION AND
MAINTENANCE COMPLETED BY I-JKL CREW
- 187 SCIENTIFIC STATION INSPECTION, MAINTENANCE
AND UPGRADING INITIATED BY I-JKL CREW
- 188 HAB MOD I-1 INSPECTION, MAINTENANCE, AND
UPGRADING COMPLETED BY I-GHI CREW
- 189 DAY OFF

EARTH DAYS FROM 1ST	MILESTONE	CONSUMABLE INVENTORIES	
<u>CREW LANDINGS</u>		<u>CREW*</u>	<u>POWER**</u>
190	I-GHI RETURN MODULE ACTIVATION INITIATED BY I-GHI CREW		
190	I-JKL RETURN MODULE CHECK-OUT BY I-JKL CREW		
192	HAB MOD I-1 PLACED IN STANDBY BY I-GHI CREW		
192	DEPARTURE FOR EARTH BY I-GHI CREW		
195	PROTO-CRYOGENIC PLANT LANDING BEACON ACTIVATION BY I-JKL CREW		
195	SCIENTIFIC STATION INSPECTION, MAINTENANCE, AND UPGRADING COMPLETED BY I-JKL CREW		
196	DAY OFF		
197	PROTO-OXYGEN PLANT LANDING -Includes oxygen production and liquification -Includes crew consumables for 56 days and power plant consumables for 2 lunar cycles -Includes lunar hydrogen and He ³ production capability	4	3
198	PROTO-OXYGEN PLANT ACTIVATION INITIATED BY I-JKL CREW		
202	PROTO-OXYGEN PLANT ACTIVATION COMPLETED BY I-JKL CREW		
203	DAY OFF		

EARTH DAYS FROM 1ST
CREW LANDINGS

MILESTONE

CONSUMABLE
INVENTORIES
CREW* POWER**

204	PROTO-OXYGEN PLANT INITIAL TEST PROTOCOL INITIATED BY I-JKL CREW
210	DAY OFF
216	PROTO-OXYGEN PLANT INITIAL TEST PROTOCOL COMPLETED BY I-JKL CREW
217	DAY OFF
218	I-MNO CREW LANDING SITE PREPARATION INITIATED BY I-JKL CREW
221	I-MNO CREW LANDING SITE PREPARATION COMPLETED BY I-JKL CREW
222	I-JKL CREW RETURN MODULE CHECKOUT BY I-JKL CREW
223	I-MNO CREW LANDING BEACON ACTIVATED BY I-JKL CREW
223	I-MNO CREW RETURN MODULE CHECKOUT BY I-JKL CREW
224	DAY OFF

EARTH DAYS FROM 1ST

CREW LANDINGSMILESTONECONSUMABLE
INVENTORIESCREW* POWER**

225	<p>I-MNO CREW LANDING</p> <p>-Includes crew consumables for 28 days and power plant consumables for 1 lunar cycle</p> <p>-Includes I-STU crew return module I-2</p> <p>-Crew Qualifications</p> <ul style="list-style-type: none"> - Specialists in storage module systems - Specialists in oxygen transfer systems - Note: I-MNO and I-PQR crews are responsible for fully activating BASE-1 	<p>4 3</p>
226	<p>I-PQR CREW RETURN MODULE CHECK-OUT BY I-JKL CREW</p>	
226	<p>HAB MOD I-1 REACTIVATED BY I-MNO CREW</p>	
227	<p>PROTO-CENTRAL POWER PLANT INSPECTION AND MAINTENANCE INITIATED BY I-JKL CREW</p>	
227	<p>STORAGE MODULE I-1 SITE PREPARATION INITIATED BY I-MNO CREW</p>	
228	<p>PROTO-CENTRAL POWER PLANT INSPECTION AND MAINTENANCE COMPLETED BY I-JKL CREW</p>	
229	<p>SPECIALIZED SCIENTIFIC ACTIVITIES INITIATED BY I-JKL CREW</p>	
231	<p>DAY OFF</p>	

EARTH DAYS FROM 1ST

CREW LANDINGSMILESTONE

CONSUMABLE

INVENTORIESCREW* POWER**

- 234 READAPTATION PROTOCOL INITIATED BY
 I-JKL CREW
- 237 STORAGE MODULE SITE PREPARATION COMPLETED
 BY I-MNO CREW
- 238 DAY OFF
- 239 PROTO-AGRICULTURAL PLANT INSPECTION AND
 MAINTENANCE INITIATED BY I-MNO CREW
- 241 SPECIALIZED SCIENTIFIC ACTIVITIES COMPLETED
 BY I-JKL CREW
- 242 HAB MOD I-2 INSPECTION, MAINTENANCE, AND
 UPGRADING INITIATED BY I-JKL CREW
 -Upgrading required because, with
 arrival of I-PQR crew, use of HAB MOD I-2
 will be continuous
- 242 PROTO-AGRICULTURAL PLANT INSPECTION AND
 MAINTENANCE COMPLETED BY I-JKL CREW
- 243 SCIENTIFIC STATION INSPECTION, MAINTENANCE,
 AND UPGRADING INITIATED BY I-MNO CREW
- 244 HAB MOD I-2 INSPECTION, MAINTENANCE, AND
 UPGRADING COMPLETED BY I-JKL CREW
- 245 DAY OFF

EARTH DAYS FROM 1ST

CREW LANDINGSMILESTONECONSUMABLE
INVENTORIESCREW* POWER**

246	I-JKL RETURN MODULE ACTIVATION INITIATED BY I-JKL CREW		
246	I-MNO RETURN MODULE CHECKOUT BY I-MNO CREW		
248	HAB MOD I-2 PLACED IN STANDBY BY I-JKL CREW		
248	DEPARTURE FOR EARTH BY I-JKL CREW		
251	SCIENTIFIC STATION INSPECTION, MAINTENANCE, AND UPGRADING BY I-MNO CREW		
251	STORAGE MODULE LANDING BEACON ACTIVATION BY I-MNO CREW		
252	DAY OFF		
253	STORAGE MODULE I-2 LANDING -Includes crew consumables for 12 months of base operations and power plant consumables for 12 lunar cycles -Includes Oxygen Transport Module I-1	26	14
254	STORAGE MODULE ACTIVATION INITIATED BY I-MNO CREW		
255	STORAGE MODULE ACTIVATION INITIATED BY I-MNO CREW		
256	OXYGEN TRANSPORT MODULE SERVING AND LAUNCH AREA PREPARATION INITIATED BY I-MNO CREW		
259	DAY OFF		

EARTH DAYS FROM 1ST

CREW LANDINGSMILESTONECONSUMABLE
INVENTORIESCREW* POWER**

- 265 OXYGEN TRANSPORT MODULE SERVICING AND
LAUNCH AREA PREPARATION COMPLETED BY
I-MNO CREW
- 266 DAY OFF
- 267 OXYGEN TRANSPORT MODULE I-1 ACTIVATION
AND CHECKOUT INITIATED BY I-MNO CREW
-Includes transport of transport module
to service and launch area
- 272 OXYGEN TRANSPORT MODULE I-1 ACTIVATION
COMPLETED BY I-MNO CREW
- 273 DAY OFF
- 274 I-PQR CREW LANDING SITE PREPARATION
INITIATED BY I-MNO CREW
- 277 I-PQR CREW LANDING SITE PREPARATION
COMPLETED BY I-MNO CREW
- 278 I-MNO CREW RETURN MODULE CHECKOUT BY I-MNO CREW
- 279 I-PQR CREW LANDING BEACON ACTIVATED
BY I-MNO CREW
- I-PQR CREW RETURN MODULE CHECKOUT
BY I-MNO CREW

EARTH DAYS FROM 1ST		CONSUMABLE	
<u>CREW LANDINGS</u>	<u>MILESTONE</u>	<u>INVENTORIES</u>	
		<u>CREW*</u>	<u>POWER**</u>
280	DAY OFF		
281	I-PQR CREW LANDING	25	13
	-Includes I-VWX return module		
	-Includes oxygen transport module I-2		
	-Begins 6 month crew rotation cycle		
	-Crew Qualifications		
	- Operational knowledge of ilmenite mining, oxygen plant and oxygen transport systems		
282	I-STU CREW RETURN MODULE CHECKOUT BY I-MNO CREW		
282	HAB MOD I-2 REACTIVATED BY I-PQR CREW		
283	PROTO-CENTRAL POWER PLANT INSPECTION AND MAINTENANCE INITIATED BY I-MNO CREW		
283	ILMENITE MINING AND OXYGEN PRODUCTION INTEGRATED OPERATIONS INITIATED BY I-PQR CREW		
284	PROTO-CENTRAL POWER PLANT INSPECTION AND MAINTENANCE COMPLETED BY I-MNO CREW		
285	OXYGEN PLANT AND STORAGE SYSTEM INTEGRATED OPERATIONS INITIATED BY I-MNO CREW		
287	DAY OFF		
290	READAPTATION PROTOCOL INITIATED BY I-MNO CREW		

EARTH DAYS FROM 1ST

CREW LANDINGSMILESTONECONSUMABLE
INVENTORIESCREW* POWER**

- 293 OXYGEN PLANT AND STORAGE SYSTEM INTEGRATION
COMPLETED BY I-MNO CREW
-Includes flow of oxygen into landing
module storage or into oxygen transport
module or both
- 293 ILMENITE MINING AND OXYGEN PRODUCTION INTEGRATION
COMPLETED BY I-PQR CREW
- 294 DAY OFF
-I-MNO and I-PQR crews divide into 2 person
shifts: MO, PR, and NQ
- 295 OXYGEN PRODUCTION DURING ONE SHIFT, 6 DAYS
PER WEEK INITIATED BY PR SHIFT
- 295 OXYGEN TRANSPORT MODULE I-2 ACTIVATION AND
CHECKOUT INITIATED BY MO SHIFT
-Includes transport of I-2 to service and
launch area
- 295 PROTO-AGRICULTURAL PLANT INSPECTION,
MAINTENANCE, AND UPGRADING INITIATED BY NQ SHIFT
- 297 OXYGEN TRANSPORT MODULE I-2 STORAGE SYSTEM
ACTIVATION COMPLETED BY MO SHIFT
- 298 HAB MOD I-1 INSPECTION AND MAINTENANCE INITIATED
BY MO SHIFT
- 298 PROTO-AGRICULTURAL PLANT INSPECTION AND MAINTENANCE
COMPLETED BY NQ SHIFT

EARTH DAYS FROM 1ST
CREW LANDINGS

MILESTONE

CONSUMABLE
INVENTORIES
CREW* POWER**

299	SCIENTIFIC STATION INSPECTION, MAINTENANCE, AND UPGRADING INITIATED BY NQ SHIFT		
300	HAB MOD I-1 INSPECTION AND MAINTENANCE COMPLETED BY MO SHIFT		
300	OXYGEN PRODUCTION SYSTEMS PLACED IN STANDBY BY PR SHIFT		
301	DAY OFF		
302	I-MNO RETURN MODULE ACTIVATION INITIATED BY MO SHIFT		
302	I-PQR RETURN MODULE CHECKOUT BY PR SHIFT		
303	SCIENTIFIC STATION INSPECTION, MAINTENANCE, AND UPGRADING COMPLETED BY NQ SHIFT		
304	DEPARTURE FOR EARTH BY I-MNO CREW		
305	I-STU LANDING SITE PREPARATION INITIATED BY I-PQR CREW		
306	I-STU LANDING SITE PREPARATION COMPLETED BY I-PQR CREW		
307	I-STU CREW RETURN MODULE CHECKOUT BY I-PQR CREW		
307	I-STU LANDING BEACON ACTIVATED BY PQR CREW		

EARTH DAYS FROM 1ST

CREW LANDINGSMILESTONECONSUMABLE
INVENTORIESCREW* POWER**

308 DAY OFF

309 I-STU CREW LANDING

24 12

- Begins continuous presence of 6 persons at Base I
- Includes I-VWX return module
- Includes oxygen transport module I-3
- Crew Qualifications
- Same as for I-PQR plus payload specialist in scientific discipline

310 I-VWX CREW RETURN MODULE CHECKOUT
BY I-PQR CREW

310 HAB MOD I-1 OCCUPIED BY I-STU CREW

310 OXYGEN PRODUCTION DURING TWO SHIFTS,
6 DAYS PER WEEK INITIATED BY PR AND SU SHIFT

310 OXYGEN TRANSPORT MODULE I-3 ACTIVATION
AND CHECKOUT INITIATED BY QT SHIFT

314 OXYGEN TRANSPORT MODULE I-3 ACTIVATION
AND CHECKOUT COMPLETED BY QT SHIFT

315 DAY OFF

EARTH DAYS FROM 1ST

CREW LANDINGSMILESTONECONSUMABLE
INVENTORIESCREW* POWER**

316 INSPECTION AND MAINTENANCE SHIFT
INITIATED BY SHIFT IN FOLLOWING BIMONTHLY CYCLE

- Power plant
- Agricultural plant
- Scientific station
- HAB MOD I-1
- HAB MOD I-2
- Ilmenite mining plant
- Oxygen plant
- Cryogenic transfer systems
- Crew return modules

322 DAY OFF

329 DAY OFF

336 DAY OFF

337 HABITATION MODULE II-1
AUTO-LANDING (BASE II)

- Remote landing site selection
- II-ABC return module
- Crew consumables for 56 days

337 OXYGEN TRANSPORT MODULE I-1 LAUNCH
PREPARATIONS INITIATED BY QT SHIFT

339 OXYGEN TRANSPORT MODULE I-1 LAUNCH
PREPARATIONS COMPLETED BY QT SHIFT

2

EARTH DAYS FROM 1ST

CREW LANDINGSMILESTONECONSUMABLE
INVENTORIESCREW* POWER**

340	OXYGEN TRANSPORT MODULE I-1 LAUNCH TO SPACE STATION		
364	CREW II-ABC MANUAL LANDING (BASE II) -Landing with access to HAB MOD II-1 crew and power -Consumables for 56 days -Central power plant module II-1 -II-DEF crew return module	8	6
392	STORAGE MODULE I-2 LANDING -Includes crew consumables for 6 months -Includes power plant consumables for 6 months	30	15
394	OXYGEN TRANSPORT MODULE I-2 LAUNCH TO SPACE STATION		
420	HABITATION MODULE II-2 (BASE II) -Crew and power consumables for 6 months -Agricultural and waste deposit plant	12	10
448	I-VWX CREW LANDING -Includes oxygen transport module I-1 -Includes I-YZA' crew return module	26	13
450	OXYGEN TRANSPORT MODULE I-3 LAUNCH TO SPACE STATION		

EARTH DAYS FROM 1ST		CONSUMABLE INVENTORIES	
<u>CREW LANDINGS</u>	<u>MILESTONE</u>	<u>CREW*</u>	<u>POWER**</u>
472	I-STU CREW DEPARTURE FOR EARTH		
476	I-YZA' CREW LANDING	24	12
	-Includes oxygen transport module I-2		
	-Includes I-B'C'D crew return module		
504	II-DEF CREW LANDING (BASE II)	15	13
	-Oxygen transport module II-1		
	-Crew and Power consumables for 6 months		
	-Initiates crew cycle time of one year		
506	OXYGEN TRANSPORT MODULE I-4 LAUNCH TO SPACE STATION		
532	ILMENITE PLANT LANDING (BASE II)		
	-Oxygen transport module II-2		
556	II-ABC CREW DEPARTURE FOR EARTH (BASE II)		
560	STORAGE MODULE I-3 LANDING	25	13
	- Includes crew consumables for 6 months		
	- Includes power consumables for 6 months		
	- Includes oxygen transport module I-3		
562	OXYGEN TRANSPORT MODULE I-1 LAUNCH TO SPACE STATION		
588	OXYGEN PLANT LANDING (BASE II)		
612	I-VWX CREW DEPARTURE FOR EARTH		

EARTH DAYS FROM 1ST

CREW LANDINGSMILESTONECONSUMABLE
INVENTORIESCREW* POWER*

616	I-B'C'D' CREW LANDING	21	11
	- Includes oxygen transport module I-4		
	- Includes I-E'F'G' crew return module		
618	OXYGEN TRANSPORT MODULE I-2 LAUNCH TO SPACE STATION		
634	I-E'F'G' CREW LANDING	19	10
	- Includes oxygen transport module I-1		
	- Includes I-H'I'J' crew return module		
640	I-YZA' CREW DEPARTURE FOR EARTH		
646	OXYGEN TRANSPORT MODULE II-1 LAUNCH TO SPACE STATION (BASE II)		
672	II-GHI CREW LANDING (BASE II)	13	13
	-Crew and power consumables for 6 months		
	-Oxygen transport module II-4		
674	OXYGEN TRANSPORT MODULE I-3 LAUNCH TO SPACE STATION		
	- Continues every 56 days		
700	STORAGE MODULE II-1 LANDING	19	22
	-Crew and Power consumables for 12 months		
	-Oxygen transport module II-5		

EARTH DAYS FROM 1ST	<u>CREW LANDINGS</u>	<u>MILESTONE</u>	<u>CONSUMABLE INVENTORIES</u>	
			<u>CREW*</u>	<u>POWER**</u>
702	OXYGEN TRANSPORT MODULE II-2 LAUNCH (BASE II)			
718	STORAGE MODULE I-4 LANDING - Includes oxygen transport module I-2 - Includes crew consumables for - Includes power plant consumables for			
			13	7
756	STORAGE MODULE LANDING (BASE II) - Oxygen transport II-1 and II-2			
758	OXYGEN TRANSPORT MODULE II-3 LAUNCH TO SPACE STATION (BASE II) - Continues every 56 days			

2.4 TRANSPORTATION

The scenario for the development of a permanently manned lunar base described in sections 2.1 through 2.3 is dependent upon a transportation system which will support the manned and unmanned landings detailed in the scenario. There are many different approaches to the design of such a transportation system and the many possible variations should be analyzed with the objective of minimizing transportation cost. This will not, incidentally, minimize Earth/Moon transit time.

The development of the transportation system should consider the long-term interplanetary transportation requirements of the space program, and should optimize the selection of staging locations for Mars missions as well as lunar enterprises. This is a complex engineering task which is impacted by the details of the missions must support, and which are not presently well defined. One example of this interrelationship is provided by the first lunar oxygen production plant. This study notes the reduction of ilmenite as the most favorable process for early implementation. A detailed design of this production process would identify the size and mass of equipment for the beneficiation of regolith, the reduction of ilmenite and the storage of oxygen. Only when that has been done can one define the transportation support which is required. There are many more instances of subsystems requiring a detailed level of preliminary design, just for the lunar base, before the full transportation needs can be optimized. The definition of the LEO space station should be reviewed for capability to support the lunar base and the Mars missions.

This section presents a concept for a transportation system which can support both lunar and Mars missions and is approximately related to the scenario in the preceding sections. Vehicles are not sized, because masses of freight are not known. The concept is based upon the use of a Lunar Cyclo-Port, a staging station in

a stable orbit that periodically takes it in close approach to both the Earth and the Moon. Table 2.4.1 illustrates the advantage of this concept in terms of the incremental velocity required for transport from LEO and trans-Mars injection. Preliminary trajectory studies conducted at JPL in 1984 resulted in the definition of three possible configurations (Figure 2.4.0).

- (A) - A retrograde lunar flyby with a backside pass, similar to the Apollo free return. It has one or two coast ellipses between lunar passes and encounters the Moon at 26 day intervals.
- (B) - A posigrade lunar flyby with a frontside pass. It has no coast ellipse between lunar passes and encounters the Moon at 29 day intervals.
- (C) - Alternating posigrade and retrograde lunar passes on a path essentially fixed in inertial space. It has a coast ellipse between lunar passes with an ellipse period equal to one half a lunar period. Lunar encounters are once each 27.3 days.

("Retrograde" and "posigrade" are JPL terms and here both refer to clockwise or East to West orbits of the Moon as in Apollo).

The detail of transportation support to the lunar base is shown in Figures 2.4.1a through 2.4.1e. The following is a list of symbol definition for the figures:

- EOTV - Earth orbit transfer vehicle
- HM - Habitat module
- AVE - Ascent vehicle, emergency, storable propellants
- AVC - Ascent vehicle, contingency, storable propellants
- TK - Tanks, oxygen and hydrogen
- DV - Descent vehicle, cryogenic propellants
- LG - Landing gear, possible mobile structure

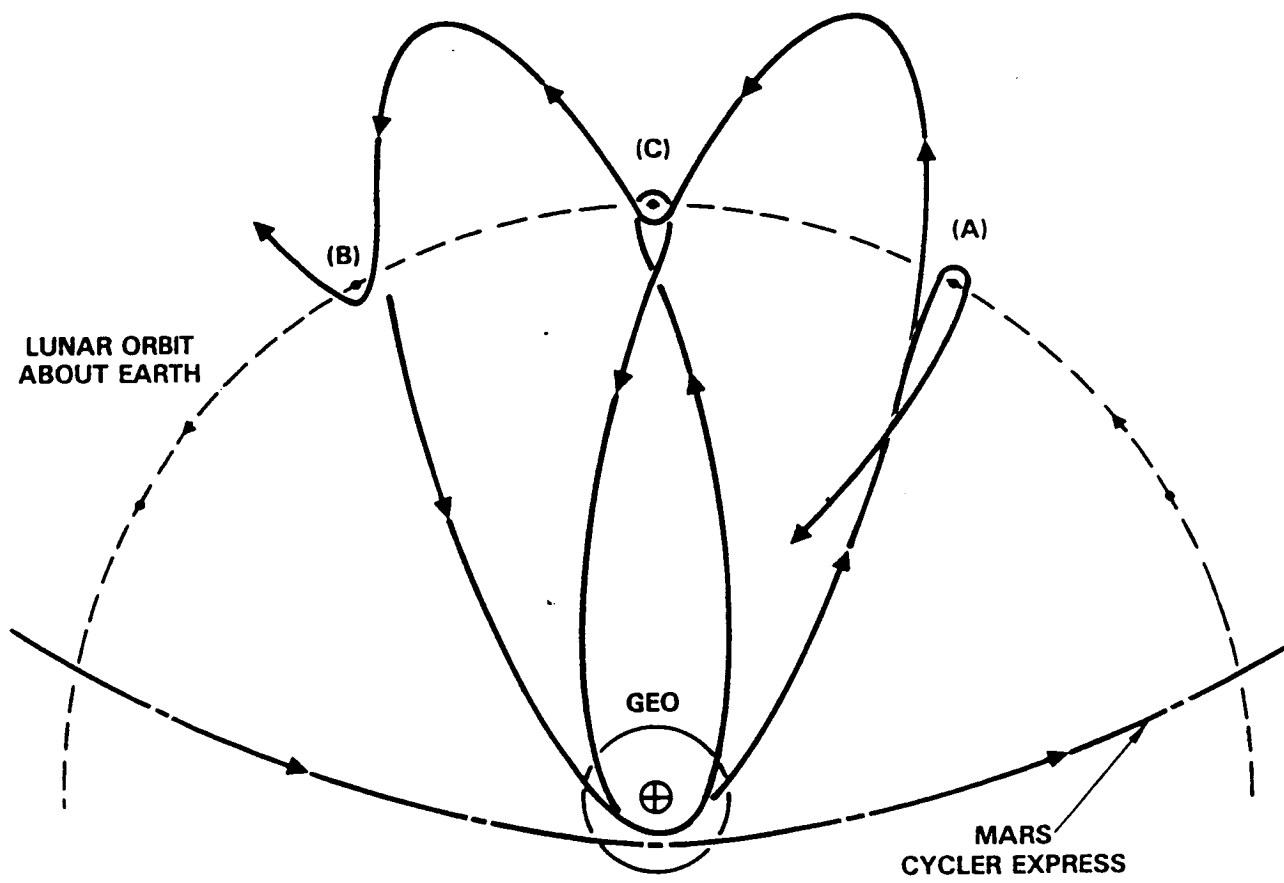


Figure 2.4.0. Lunar Cyclo-Port Staging Options

ABC, DEF, etc. - Three man crews
DAV - Descent, ascent vehicle, unmanned
LAV - Landing ascent vehicle, manned
SR - Solid rocket
HS - Heat shield
PP - Lunar power plant
LCP - Lunar Cyclo-port
OTM - Orbital tank modules
CRV - Crew Return Vehicle - Integral heat shield for normal, aerobraking to LEO and emergency earth landing

Figures 2.4.1a through 2.4.1e are really a single figure, with each succeeding figure being a continuation of the preceding one. A time line of 20 lunar periods is shown. The figures show the vehicles which are required to support the proposed scenario. In Figure 2.4.1a EOTV-1 is first stage burn and EOTV-2 is second stage burn to deliver the stack consisting of HM-1, AVE1 and DV1 first to lunar orbit and then to the lunar surface. The EOTVs return to LEO for refurbishment and reuse.

EOTV-3 and EOTV-4 at lunar period 0 deliver crew ABC, AVC1, TK1 and DV2 to the lunar surface, possibly leaving in lunar orbit a solid rocket and a heat shield as contingency items. Both AVE 1 and AVC 1 are planned for emergency use rather than as routine ferry of crews back to earth. The solid rocket and heat shield are for earth return and aero-braking in the event of an emergency return.

EOTV-5 and EOTV-6 at lunar period 1 carry an unmanned stack containing HM2, DAV1, a crane and a rover. DAV is not man rated.

At lunar period 2, EOTV-1 and EOTV-2 bring crew DEF, LAV1, TK2, TK3, LG-1 and a SRHS to lunar orbit. This shows that six EOTVs are required to support the scenario. The LAV is man rated and will be used to carry crew ABC back to earth at lunar period 3. This is dependent upon EOTV-3 and EOTV-4 having put cryogenic propellants and a heat shield in lunar orbit, for use by LAV1 on its return.

Table 2.4.1. Delta V Requirements for Staging Options in Earth-Moon Space

STAGING LOCATION	TRANS-MARS ⁽¹⁾ INJECTION (m/sec)	TRANSPORT ⁽²⁾ FROM LEO (m/sec)	TRANSPORT FROM ⁽³⁾ LUNAR SURFACE (m/sec)
LEO	4470	—	2670
GEO	3540	3820	3520
EARTH-MOON L ₁	2050	3670	2510
EARTH-MOON CYCLER	1408	3058	2550
LUNAR ORBIT	2230	3880	1730
LUNAR SURFACE	3960	5610	—

(1) ESCAPE ENERGY $C_3 = 30 \text{ km/sec}^2$ TYPICAL OF UP ESCALATOR
TRANSPORT MODE ASSUMES IDEAL GEOMETRY AND FINAL INJECTION
BURN AT 6878 km PERIGEE

(2) LH₂ FROM EARTH

(3) LOX FROM MOON

2) EARTH SURFACE

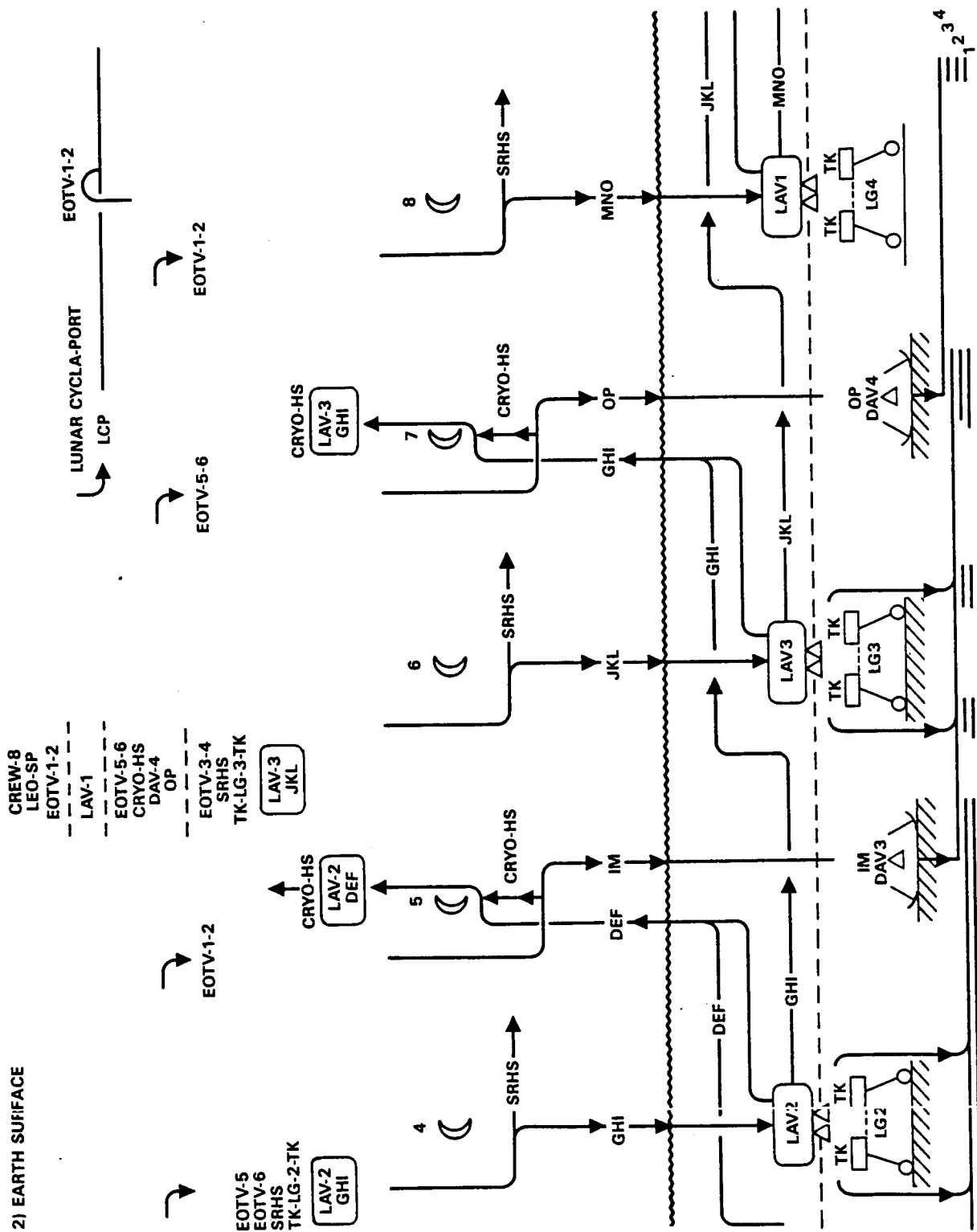


Figure 2.4.1b.

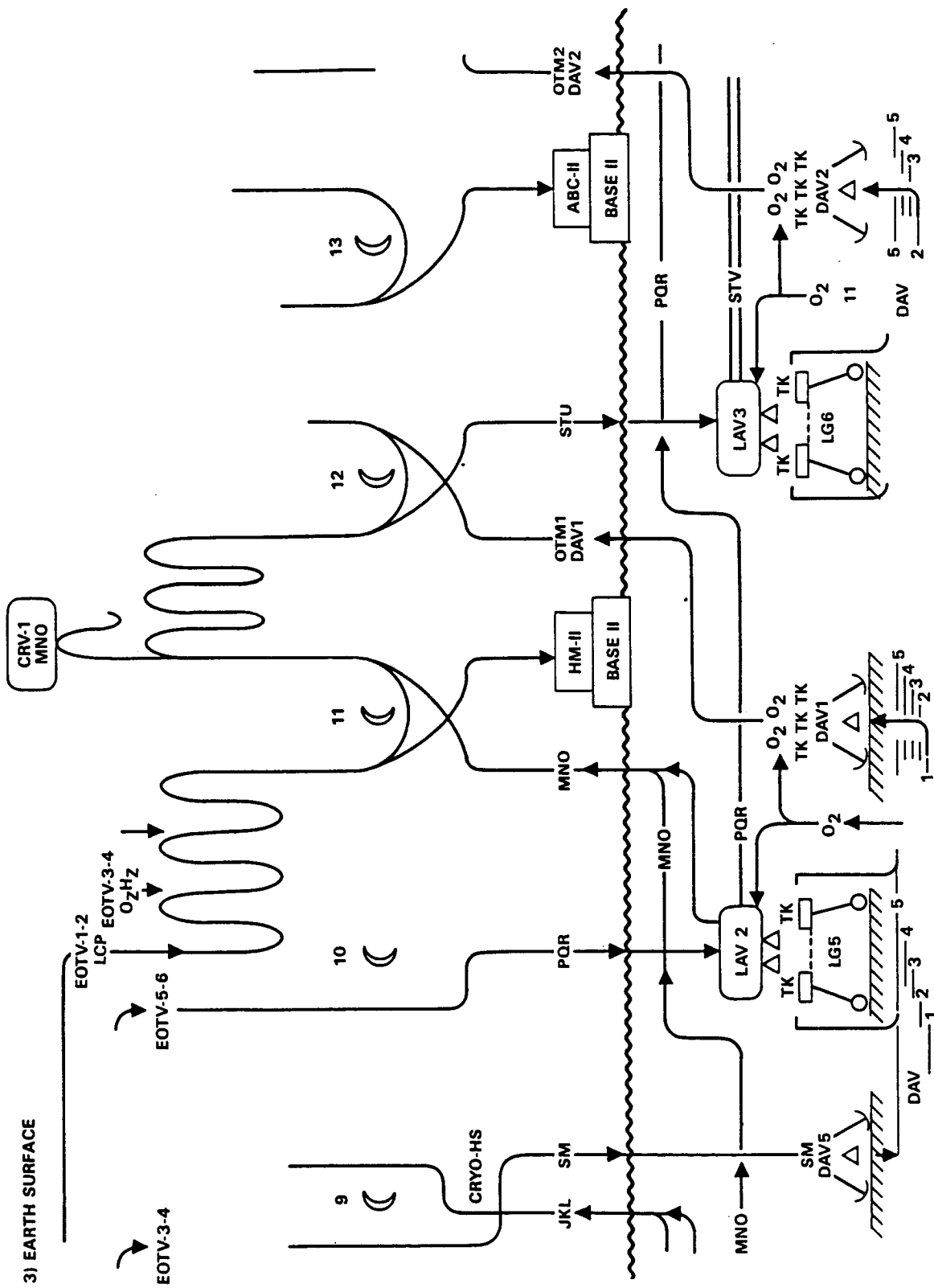


Figure 2.4.1c.

4) BASE I

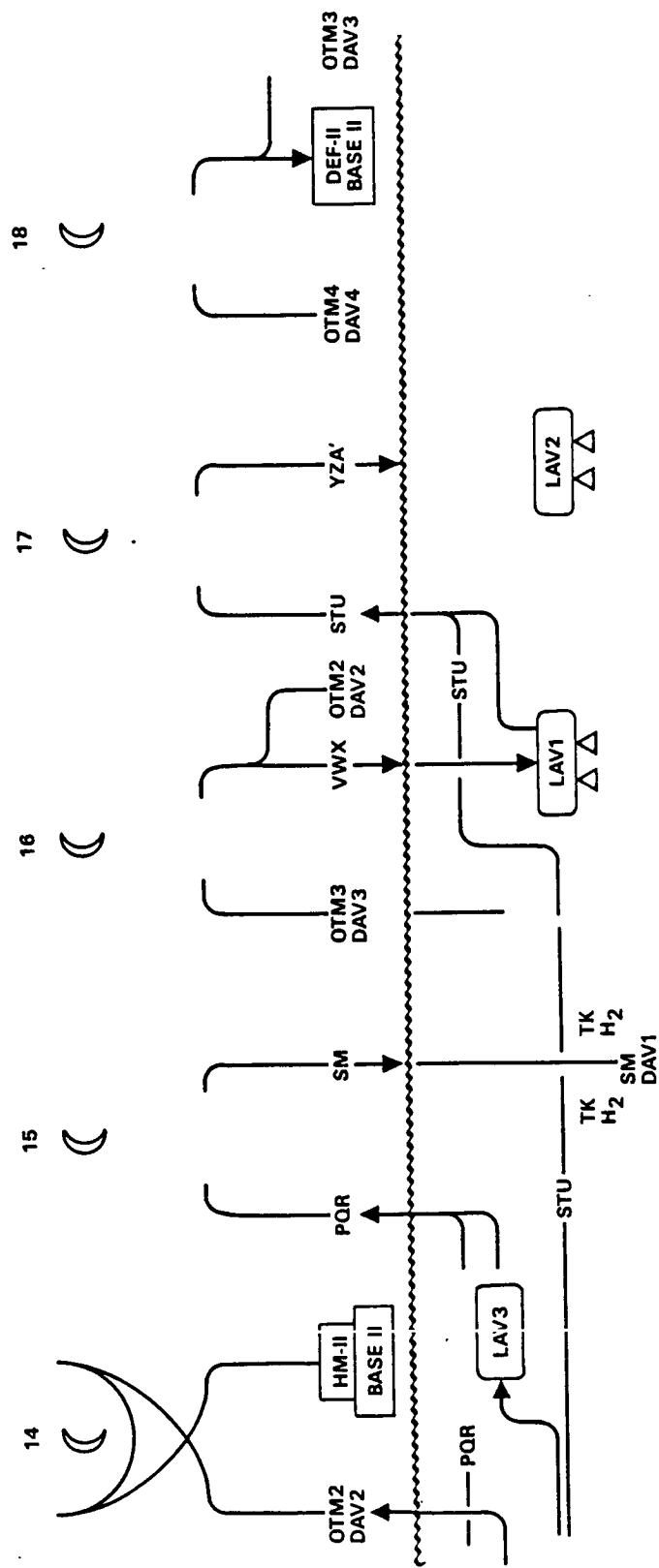


Figure 2.4.1d.

5) BASE II

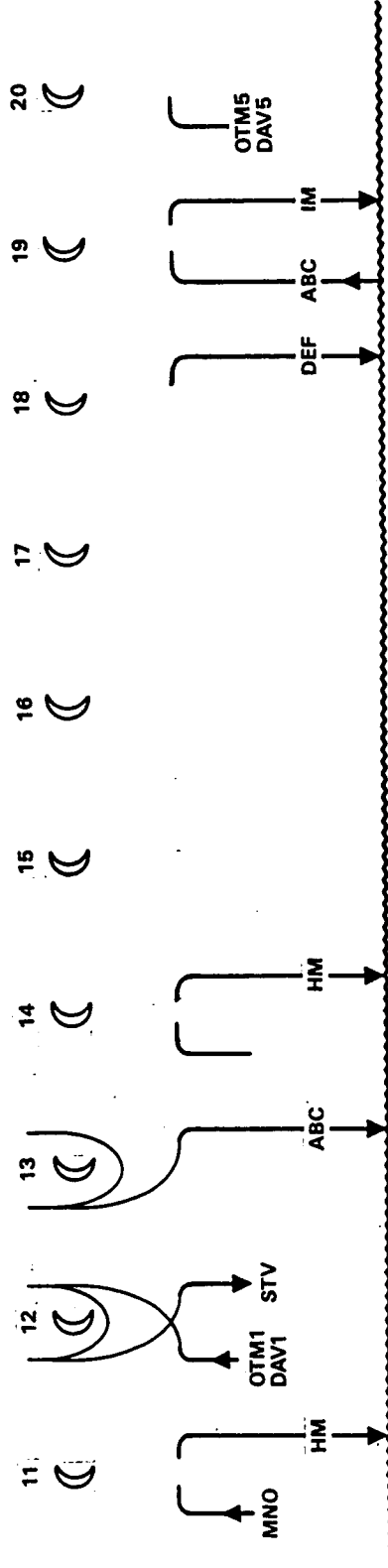


Figure 2.4.1e.

In Figure 2.4.1b the Cyclo-port is being assembled in LEO beginning at lunar period 7 and delivering its first load to the lunar base at lunar period 11.

Shipment of lunar produced oxygen begins at lunar period 12 with DAV 1 delivering the tanks to rendezvous with the Cyclo-port.

2.4.1 GUIDELINES AND CONSIDERATIONS

- Availability of propellants and heat shield for aerobraking to LEO
 - Emergency heatshield and storable propellants available on lunar surface
 - Contingency heatshield and storable propellants available in lunar orbit
 - Normal heatshield and cryo propellants arrive in lunar orbit before lift off from lunar surface.
 - With introduction of Lunar Cyclo-Port a Crew Return Vehicle (CRV) is available for normal return to LEO or contingency pick-up in lunar orbit. Emergency reserve via lunar landing
- Establish confidence in DV and DAV to have early option to land equipment without abort to orbit capability.
- Establish confidence in LAV to have early option to land men without abort to orbit capability - Not possible until Lunar O₂ is available
- Minimize requirement for Lunar Orbit Space Port until Lunar Cyclo-Port available for staging and propellant storage tanks. Consider option of early propellant tank jettisoning in lunar orbit.
- Hydrogen delivery tanks (cycles 10, 12, and 15) should be compatible for use as oxygen tanks modules for return to Lunar Cyclo-Port

- Lunar Cyclo-Port mode depends on
 - Lunar Base sites (LCP in Earth-Moon plane)
 - Landing and Lift-off constraints
 - Inertial orientation of LCP line of opsides to support interplanetary operations (Mars Cyclo Express)
- It is expected that further analysis will establish attractiveness of Lunar Cyclo-Port for staging support of Interplanetary, Lunar and GEO operations. (One would hardly create a LCP to service payloads to GEO, but having an LCP in support of other payload destinations, it appears more than likely that some beneficial use could be made in delivery and retrieval of payloads including manned visits to GEO.
- This study depicted a transition to LCP operations just prior to the availability of Lunar oxygen which fully takes advantage of its staging capability payoffs. It has been evident though, that operations would be considerably simpler, safer potentially cheaper if the Lunar Cyclo-Port were available at the beginning of lunar operations. (CRV available for aerobraking relieves aerobraking structural stress requirements for LAV crew return).

2.4.2 BACKGROUND, LUNAR CYCLO-PORT

The Lunar Cyclo-Port introduced in this study is an outgrowth of concepts pursued by Dr. Buzz Aldrin for the last three years since December 1983. Preliminary trajectory studies were done by JPL in January and July 1984 (1). Further research revealed considerable post-Apollo analysis by Krafft Ehricke (2) which soundly supported the Aldrin concept but did not advantageously make use of lunar gravitational encounters. Paul Keaton (3) in his excellent paper "A Moon Base/Mars Base Transportation Depot" develops the staging base advantages of highly elliptical orbits but then surprisingly quickly dismissed them because of radiation belt passages in favor of various lunar and solar libration points staging options.

REFERENCES

- (1) Periodic Earth-Moon Trajectories Revisited; JPL interoffice memorandum IOM 3121 84.4 - 1005 dated 20 July 1984.
- (2) Cost Reductions in Transportation to Geosynchronous and Lunar Orbits; Krafft A. Ehricke, presented at the 23rd International Congress, October 8-15, 1972; Vienna, Austria.
- (3) A Moon Base/Mars Base Transportation Depot; Paul W. Keaton; Los Alamos Report LA-10552-MS.

3.0 PHOTO-VOLTAIC POWER SYSTEM FOR THE FIRST LUNAR BASE

3.1 INTRODUCTION

The design of a 300 kW solar photo-voltaic power field for a first manned lunar base circa 2000 is considered. The lunar environment, mounting of the solar panels, solar cell technology and later augmentation of the power source using lunar-based processing are discussed. For equatorial locations, energy storage during the 336 hour lunar night is a major technical problem. Storage aside, it is found that all the hardware needed to install an initial solar field adequate to supply 300 kW complete with power conditioning and distribution systems, should have less than 11,364 kg of mass.

Single crystal silicon cells with an efficiency of 15% mounted on fixed or lunar tracking panels represent a technology already proven on Earth and in space. The 300 kW system could be assembled from five separate 60 kW systems.

3.1 BACKGROUND

This section examines the use of a solar photo-voltaic (P-V) power station emplaced on the lunar surface to supply a first manned lunar base in the 2000-2010 time frame. We assume that the base will need 300 kW of electric power during it's early habitable phase and that all the components for this initial power station will be launched from Earth. We assume that the base will have to be located near the lunar equator since at present we cannot plan bases at the polar regions to take advantage of the continuous illumination.

As support equipment and crew are ferried to the Moon on successive launches, it will be desirable to provide a growing electric power capability. Therefore we propose a series of 5 separate 60 kW systems, each to be added to the others as it arrives, till the 300 kW system is complete.

In proposing the most desirable initial photo-voltaic station we shall give special consideration to those systems that could most readily be augmented later by manufacture at the base using lunar materials.

3.2 PROMISING OPTIONS FOR THE INITIAL PHOTO-VOLTAIC POWER STATION

We know from Earth-based solar photo-voltaic systems in operation, as well as from experience with space-qualified solar P-V systems, that a 300 kW system to operate on the lunar surface is perfectly feasible. Further, we know that both cost and launch weight and volume from earth are reasonable and only a small part of those for a total lunar base. So the question is which type of photo-voltaic station would be best for the initial base.

3.2.1 SOLAR CELLS

While there are many types of solar cells, all work on the same principles. Solar photons are absorbed in a thin layer of the semiconductor used. Those photons with sufficient energy (greater than the band gap) produce electron-hole pairs. These diffuse as minority carriers to a space-charge region near a p-n or a metal semiconductor junction where the internal field separates them, producing a photo-voltage that can drive current through an external load.

The important material parameters for good cells for lunar application are 1) the energy band gap, 2) the absorption depth of the useful light, 3) the diffusion length of the minority carriers, 4) temperature sensitivity, 5) the ease of manufacture in producing good semiconductor structure and metal contacts, and 6) the long-term stability of the resulting electrical characteristics in the lunar environment. For later lunar processing, availability of the semiconductor in the lunar regolith and its processing become the dominant factors.

3.2.1.1 MATERIALS

Silicon single crystal cells of high purity have dominated the solar cell field since its inception and constitute the overwhelming majority of all cells in use. This technology is by far the most mature, most understood and most reliable of all types used. It has been long tested in space missions, where vacuum and radiation environment are similar to those on the Moon, so that we know that such cells will operate successfully there with little degradation for many years. The fact that this technology is so well proven makes it difficult to replace with others even though they may offer advantages.

Single silicon solar cell technology is still advancing rapidly. In the past two years, two new cells have been demonstrated each with efficiency higher than ever achieved before and approaching closely the theoretical maximum for Si in the solar spectrum. The latter has achieved efficiencies on the Earth of 22% without and 26% with solar concentrators. This cell has also shown that thicknesses as small as 50 to 100 microns of silicon can achieve these very high efficiencies.

Silicon in the form of SiO_2 is also present in large quantities in the lunar soil so that if extraction and purification processes become feasible, silicon cells to augment the power station could eventually be fabricated on the moon.

Single crystal GaAs is the next best proven solar cell material for space. It has several marked advantages over silicon: 1) the thickness required to absorb all useful solar photons is ~ 1 micron compared to ~ 100 microns for silicon, permitting much thinner films, 2) its band gap is better matched to the solar spectrum permitting slightly higher efficiencies, 3) it is only about half as temperature sensitive as silicon, and 4) it is less sensitive to radiation.

The technology for growth, dopant control and contacts in GaAs is still much less mature than for silicon. Nevertheless, cells of GaAs are now being used in space.

The third contender is polycrystalline or amorphous silicon. In contrast to the single crystal, it has absorption depths of only a micron or two due to reflections at boundaries. It is also much less sensitive to minute amounts of impurity, and is therefore easier to manufacture. Amorphous cells can be evaporated or sputtered onto various substrates including ceramics or flexible sheets of aluminum (with a suitable insulating layer applied first) or plastic. Two big disadvantages are 1) much lower efficiencies than single crystal silicon (5-12% vs 15-18%), and 2) very low reliability due to degradation in time. Whether this degradation is due to atmospheric contact on Earth which would be entirely absent in high vacuum on the Moon is not known, but could be determined by testing in vacuum on Earth.

There are many other solar cell materials being explored. Some such as metal-sulfide combinations can be made simply by electrolytic plating, but have low efficiency and reliability. Others involve two or three different band gaps in tandem to achieve very high efficiency but which are extremely difficult to make. It is unlikely that any of these will be of sufficiently proven technology in time to be used for this first lunar base.

Considering all of the above, we recommend single crystal silicon cells in our promising initial P-V system.

3.2.1.2 MOUNTING AND CONNECTING CELLS

Thin, (typically .25 to .5 mm) wafers of silicon or GaAs single crystal cells, typically a few centimeters across in round or rectangular form, are normally mounted securely on flat panels. The positive and negative leads to each cell are in the form of either

evaporated or sputtered metal layers with shapes defined by masks, or are fine wires bonded to evaporated metal pads on each cell.

Amorphous cells can be mounted on thin flexible sheets of metal or heavy plastic, with evaporated metal film leads for inter-connects.

Since many cell currents must add in parallel, leads have to be brought out to the perimeter of each panel and connected to increasingly large conductors, terminating in large solid conductors of aluminum as they reach central power processing units.

3.2.1.3 TEMPERATURE OF CELLS

The efficiency of both silicon and GaAs solar cells drops linearly with temperature and at 100°C is reduced below its 20°C value by 30% for GaAs and 45% for silicon. Amorphous and polycrystalline cells show similar degradation with temperature. It is highly desirable, therefore, to mount the cells so that they stay as cold as possible. Liquid cooling systems, often used on Earth, especially with solar concentrators, appear very difficult to achieve on the Moon, at least for a relatively simple, reliable initial installation. This is due to the extreme temperature cycles from 380°K (111°C) to 102°K (-117°C), leakage into the ultra-high vacuum environment, and the prohibitive weight of cooling fluid to be launched from Earth.

Good radiative design should be able to keep all temperatures below 50°C during lunar noon, using high emissivity under surfaces and adjusting the reflectivity of top surfaces so that they are absorbative in the most effective wavelength for carrier production but relatively reflective at other parts of the solar spectrum. A simple calculation assuming an emissivity of 1.0 looking down and of 0.5 looking up gives a cell temperature at lunar noon of between 20°C and 100°C depending upon whether the temperature of the lunar surface under the cell is 380°K - its noon temperature with no panel above it, or 100°K, its night low. Since the average lunar surface

temperatures will be somewhere between these two extremes, and can be forced toward the lower extreme by proper shadowing by the panel, 50° C cell temperatures at noon appear feasible.

3.2.2 TRACKING VS NON-TRACKING PANELS (Figure 3.1)

The flat panels holding individual cells can be either tracked to remain perpendicular to the sun's rays at all times, mounted horizontally in fixed positions, or inclined to the surface at chosen angles in rows of triangular cross-section to optimize the diurnal output cycle. In a large solar field with many panels, some mutual shadowing occurs in the triangular or tracking modes.

Considering the relative merits of these three modes the first, Figure 3.1 (a), or the tracking mode, requires the least panel area. Since it has flat output over the lunar day except for some shadowing near dawn and dusk, it requires no energy storage during the day. Since the Sun describes the same arc over an equatorial site on the Moon within $\pm 2^\circ$ over the whole year, tracking need be about only one axis, unlike the case of the Earth where the $\pm 22\frac{1}{2}^\circ$ north-south shift of the solar position requires 2-axis tracking. Clock drive (no feedback control) should be adequate but would still require gears, bearings and electric motor drives for every panel which, in the lunar environment, are prone to failure. The system can be designed so that if tracking fails, it can be returned to the fixed horizontal mode and still be centered to operate at 63.7% of its maximum power output averaged over the day. Adjacent lines of panels should be separated by about five times one panel width to restrict shadowing to about 10 at dawn and dusk.

Additional disadvantages of the tracking mode are the added weight that bearings, heavier frames, and motors would entail, and the added weight of flexible cable electrical conductors to each panel. Liquid cooling through rotating joints would be very difficult with tracking panels.

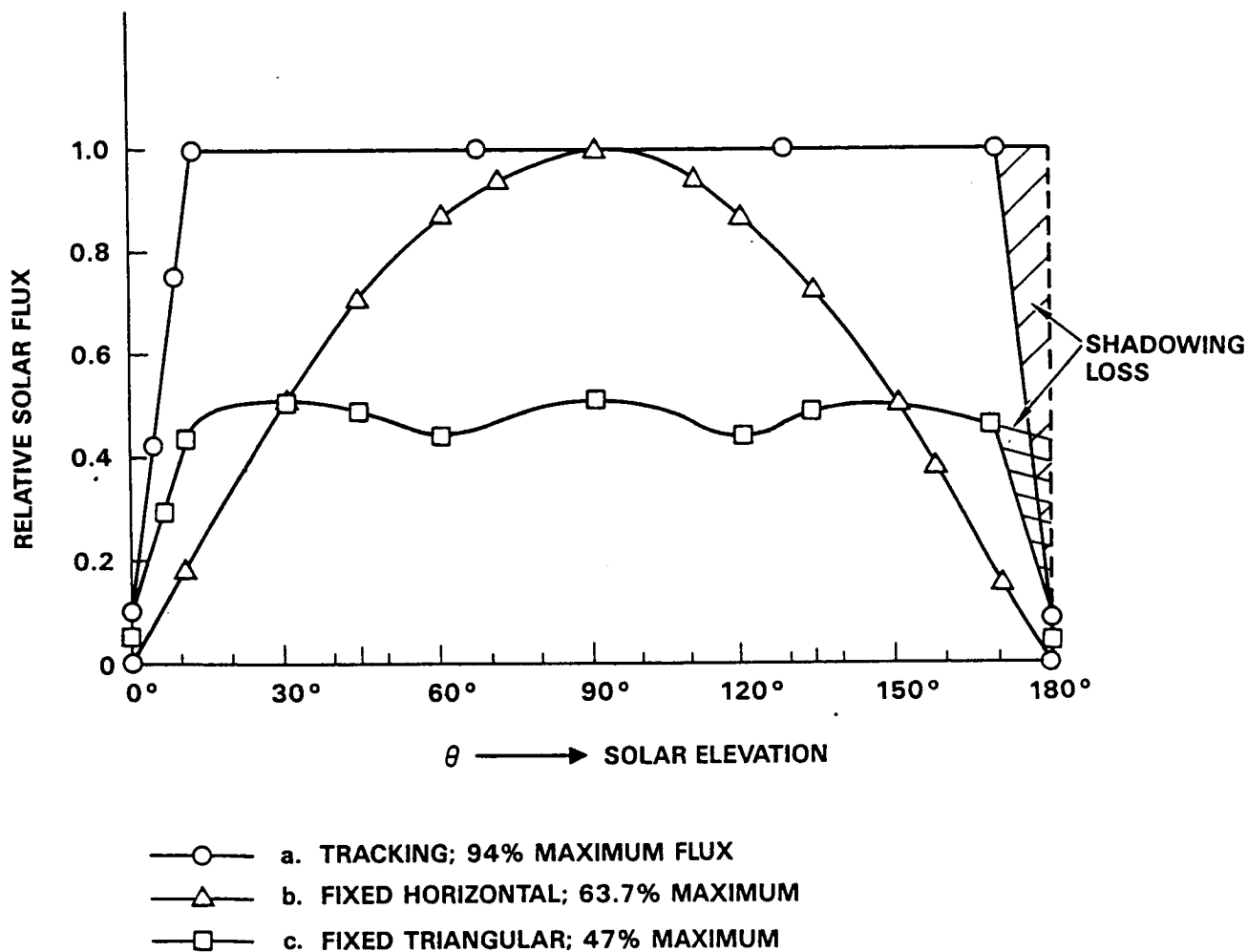


Figure 3.1. Comparison of Solar Flux for Three Panel Arrangements Having Equal Panel Area

- a. Tracking Panels in 10 Rows East to West
 - b. Fixed Horizontal Panels in 10 Rows
 - c. Fixed Triangular Panels in 5 Rows.
- Rows Separated by 5 Times Width in a. and c.

Figure 3.1 (b) shows that fixed horizontal panels operate on a pure cosine law and deliver 63.7% of the maximum solar flux available. They thus require 36.3% more panels than the tracking mode. (Actually, the anti-reflection coatings will cause the output to drop off more rapidly at glancing angles). The very non-uniform power output vs time curve for this cosine law requires a very high energy storage of 36.3% of the daily power requirement just to flatten out the daily cycle. Dust accumulations on the cell surfaces will be the worst of the three modes considered.

This mode does have the advantage of the densest packing possible since no shadowing is involved, and thus results in the smallest overall size of solar field. This mode is also the simplest to erect and is highly reliable.

Figure 3.1 (c) shows the lunar daily cycle of power output from solar panels arranged on the sides of equilateral triangles. A spacing of 5 times the side of each equilateral triangle between adjacent rows of panels in the E-W direction, limits mutual shadowing to about 10 of solar angle at dawn and dusk.

This triangular arrangement is especially interesting because it gives a virtually flat output vs time cycle during the lunar day, and thus minimizes energy storage needed while using fixed panels. It still provides 46% as much power over the full day for a given area of solar panels as the maximum possible. The area of solar panels required will be

$1/.46 = 2.17$ times that for the tracking - no shadowing mode, while the size of solar field required will be comparable to that for the tracking mode.

3.2.3 SOLAR CONCENTRATORS

Some systems on earth use large Fresnel lenses to focus the Sun's light onto small cell areas at their centers. The principal

advantage is cost - since the cell area is more expensive than the lens area. Cooling the cells is then required - usually by flowing liquids - since cell efficiency deteriorates rapidly with temperature, (on the order of 0.4% per degree centigrade for silicon near 20°C). If well-cooled, efficiency of the cell can be improved slightly (a few percent) by concentration.

It appears that the added complexity of lenses and cooling would not be advisable in the initial installation where reliability and low maintenance will be more important than slightly added cost.

If, however, a thermal storage system could use the low temperature heat collected from the cells, concentration would be more attractive.

3.2.4 INSTALLATION AND REPAIR

While by-pass diodes can keep the system working in case some cells fail in an open mode, and the system can cope with some shorted cells, replacement of some panels will probably be required over a lifetime of several years. The system must be designed so that, during initial installation, astronauts can remove the components from the lander, transport them some distance to the solar field and then assemble them, all with relatively simple and fool-proof operations. Electrical interconnections of all panels, made at the site, must also be simple and absolutely secure electrically. High quality couplings that can be plugged or clamped together should be possible and will also permit later removal and replacement with new panels or sub-panels. While it would be desirable to replace individual cells as they failed, making disconnectible plugs on each cell would probably be impossible while maintaining high electrical reliability of the overall system, since the total number of such connections is on the order of one million for this field, (assuming 75 mm cells are used). Such connections are best made in a permanent fashion when the cells are assembled on the sub-panels where they are first made.

For access to all panels there must be path-ways between each row of panels so that astronauts can either walk or ride a small vehicle to all parts of the field.

3.2.5 LUNAR ENVIRONMENT

The radiation and micrometeorite environment on the lunar surface are well enough known so that cell life and degradation can be predicted during design. Solar cells on satellites have already survived many years in similar environments.

A potentially greater problem is coating of cell surfaces by lunar dust. Solar cell fields on Earth require occasional washing of dust from the upper surfaces to avoid serious degradation in output. On the Moon, no dust contamination is expected except due to nearby man-made disturbances and occasional meteorite impacts. Rocket plumes during landing and take-off and moving astronauts and their transport vehicles will create serious dust disturbance. The regolith particles due to the absence of air and the reduced gravity, will travel outward from the point of disturbance in parabolic trajectories more than 5 times as far and as high as on earth.

Some electrostatic charging of dust by the sun's light is also expected, and such charged particles will drift toward metal electrodes of opposite potential and tend to deposit upon them. The solar field will have very long conductors at exposed potentials of several hundred volts. It is likely that grounding lines will be needed around the perimeter of the field and along the conductors to keep dust away from active surfaces. This should not be difficult to arrange.

It seems clear that the photovoltaic field should be far enough away from the manned base and especially landing and launching pads, to be free of almost all dust sources. This is probably a distance of

several hundred meters, but the exact number must be calculated as closely as possible. Some cleaning of the cell surfaces by astronauts is possible either by manual brushing or by streams of compressed exhaust gasses captured from the manned base.

The low (1/6 Earth) gravity on the Moon and lack of vibration makes possible far simpler and lighter supporting structures for the solar panels than for Earth applications.

3.2.6 POWER CONDITIONING

The solar cell field can be wired in various parallel and series combinations to give almost any desired d.c. voltage and ampere output. Because failure rates of solar cell fields on Earth have been highest at the highest voltage components and because of lunar electrostatic dust accumulation it will be prudent to keep d.c. voltage output low and current high, even though this means heavier conductors around the panels. In our promising P-V option we suggest voltages at the field of not over ± 200 V d.c..

To regulate the raw power from the solar field it should be inverted to a.c. using solid-state inverters. These have recently been developed to a high point of efficiency and reliability. These solid-state devices also weigh much less than earlier ferro-magnetic techniques. Recent space power conditioning units have been built weighing 3 to 4 kg/kW.

The inverter output will be a constant a.c. voltage over large variations in solar field output voltage and this can be achieved without serious sacrifice of energy.

The exact design of the power conditioning and transmission system will depend upon many factors: the size, the location of the field relative to the base, the mode of panel positioning used (a,b or c in Figure 3.1), the schedule of the demands, and whatever energy storage system is used. An engineering trade-off for launch weight, costs and power efficiencies of various options will be needed when these factors are known.

The solar field will need enough energy storage to flatten out the solar supply cycle shown in Figure 3.1. Simple calculations show, however, that even to flatten out the cosine type curves of Figure 3.1 (b) would require a significant fraction of the full lunar night storage, which is a major problem.

It will therefore, be desirable to have full tracking, Figure 3.1 (a), or equilateral triangles, Figure 3.1 (c), to give nearly flat supply schedules and reasonable energy storage. It will also be important to arrange the schedules of the lunar base to cut down electrical loads in the early a.m. and late p.m. of the lunar day, as well as to cut the night load down to the smallest possible fraction of the 300 kW daytime load.

3.2.7 POWER TRANSMISSION

The solar field should probably be at least a 300 meters from the manned base or from manufacturing facilities where electricity is used. A three-phase transmission line consisting of three conductors at an increased a.c. voltage (such as 480 volts) with reduced current can reasonably be used. Transformers will then be needed to step the voltage up or down at the ends of the line. Components will be selected to correspond to space station power supplies for frequency compatibility.

A surprising finding is that if the conductors are buried under the lunar surface, which would be desirable for safety and convenience, they may overheat under full load due to the extremely low thermal conductivity of the lunar regolith measured in some Apollo samples. Therefore, unless further calculations show this will not happen, the conductors should be supported above the lunar surface by simple rods driven into the surface and cooled by radiation. Initial conductors should be bare aluminum in a flat strip cross-section, long dimension vertical, to minimize solar heat absorption and maximize radiation to space.

Since the conductors may be bare and at 480 volts a.c. or above, for safety of astronauts there should be some protective fence on each side of the line.

Transmission of power from the night-time source, wherever it is located, must be integrated with that from the solar field.

3.3 DESCRIPTION OF ONE PROMISING INITIAL SOLAR P-V SYSTEM

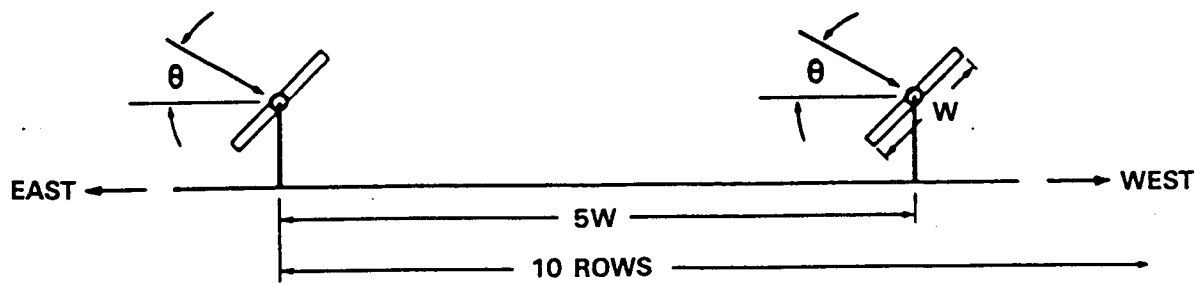
3.3.1 SYSTEM

We will now describe a specific solar P-V system to supply a steady 300kW of electric power. This system is feasible using presently proven technology provided energy storage can be solved.

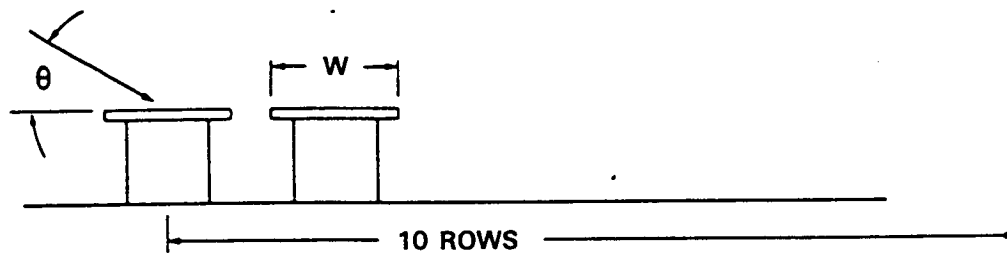
About 1,000,000 single crystal 75 mm x 75 mm x 0.25 mm silicon cells would be mounted on thin aluminum sheets supported by aluminum frames to form flat panels 2 m x 4 m in size. Cell efficiency would be $\geq 15\%$, panel efficiency $\geq 12\%$.

Cells would be fabricated into p-n junctions on Earth with anti-reflection coatings and with electrode connections to each cell made by evaporated metal films. Connecting conductors for all cells on the panel would be mounted on the ends and sides of each panel with flexible cables and plug connectors for interconnection of all panels.

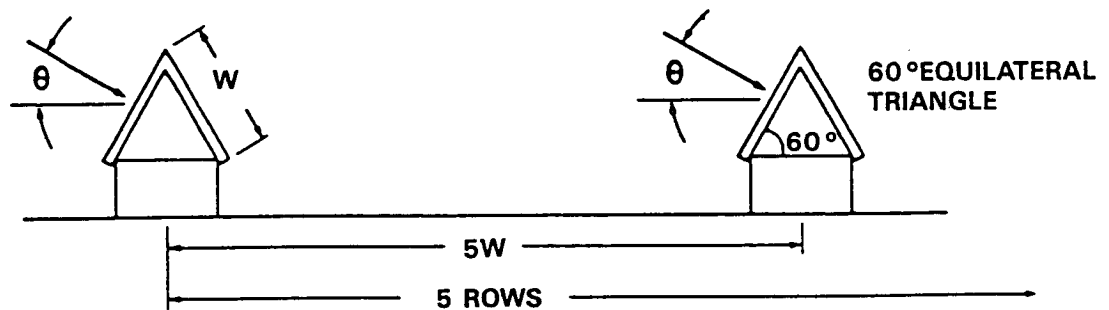
The 2m x 4m panels would make up the sides of equilateral triangles 2m on a side arranged in 56m long rows of 14 panels each, see Figure 3.2. All 672 cells along the row would be connected in series giving a peak output voltage of ± 200 d.c., and all twenty-four cells across the panel would be connected in parallel to give a peak output current of twenty-eight amperes from each row. Five rows in parallel would supply a peak output current of 140 amperes to the power conditioning unit. Rows would run north-south in groups of five



a. TRACKING



b. FIXED, HORIZONTAL



c. FIXED, TRIANGULAR

Figure 3.2. Details of Panel Arrangements of Figure 3.1

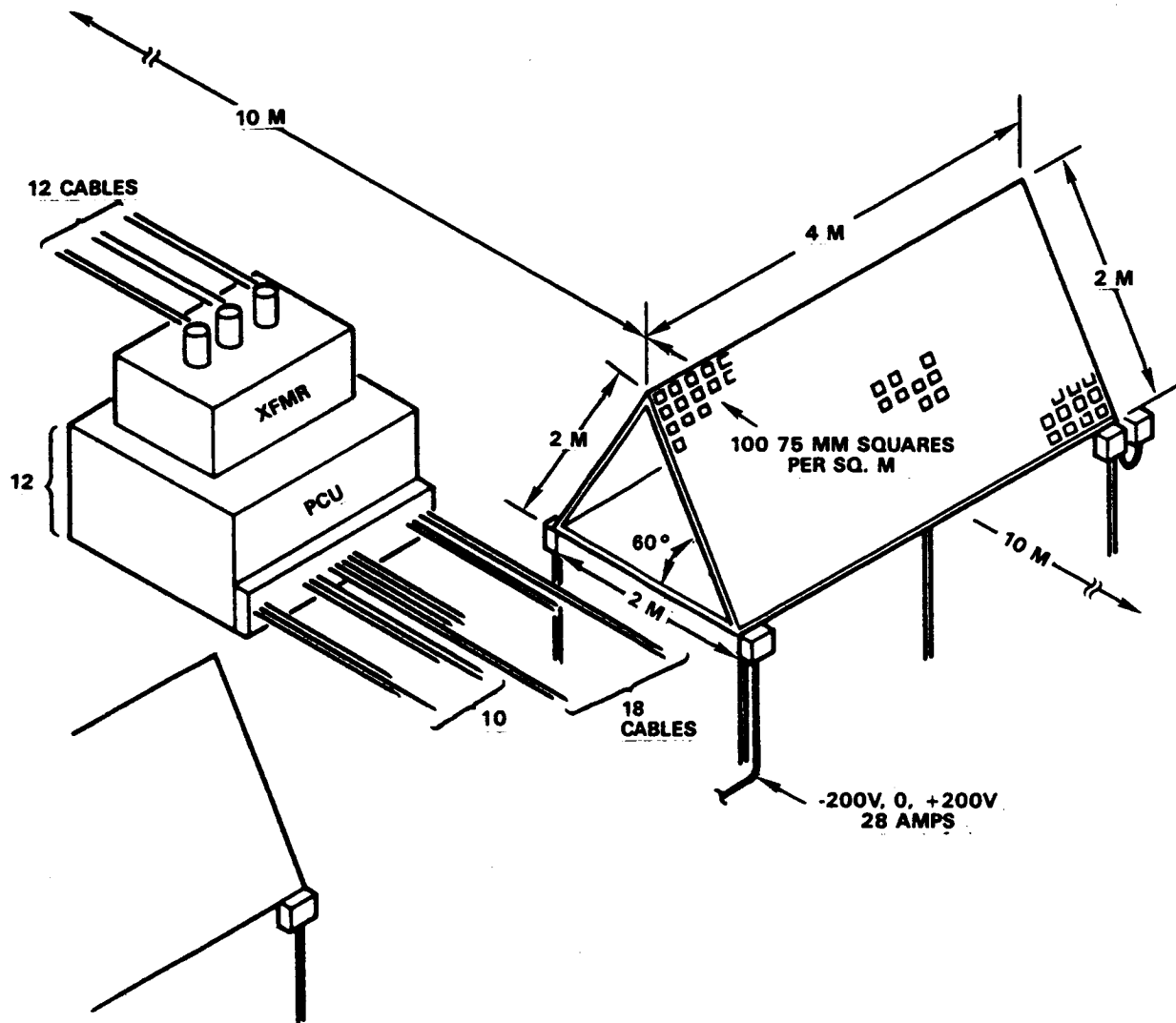


Figure 3.3. Details of Connections to Power Conditioning Unit for One 60 KW Power System Using Triangular Panel Arrangement

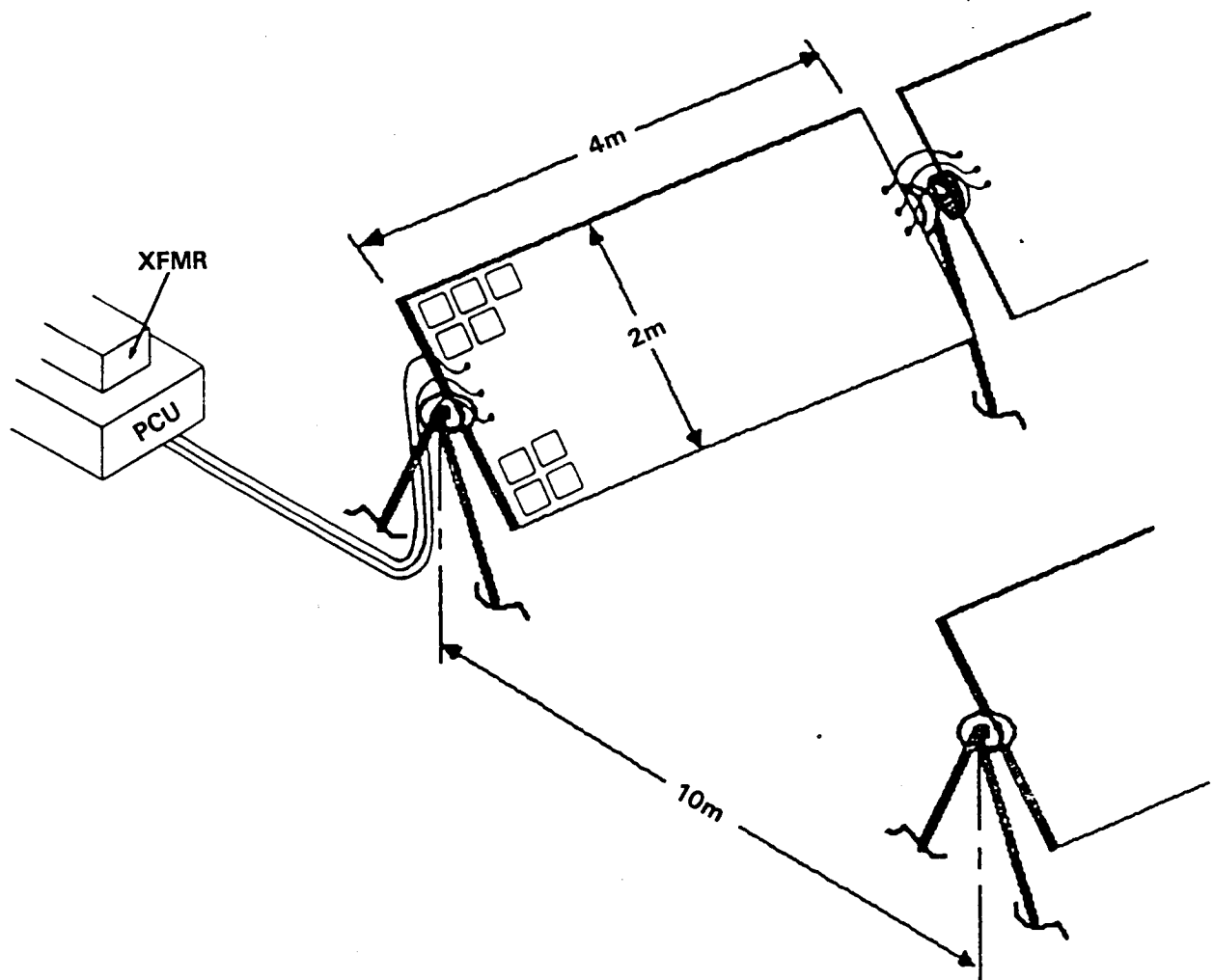
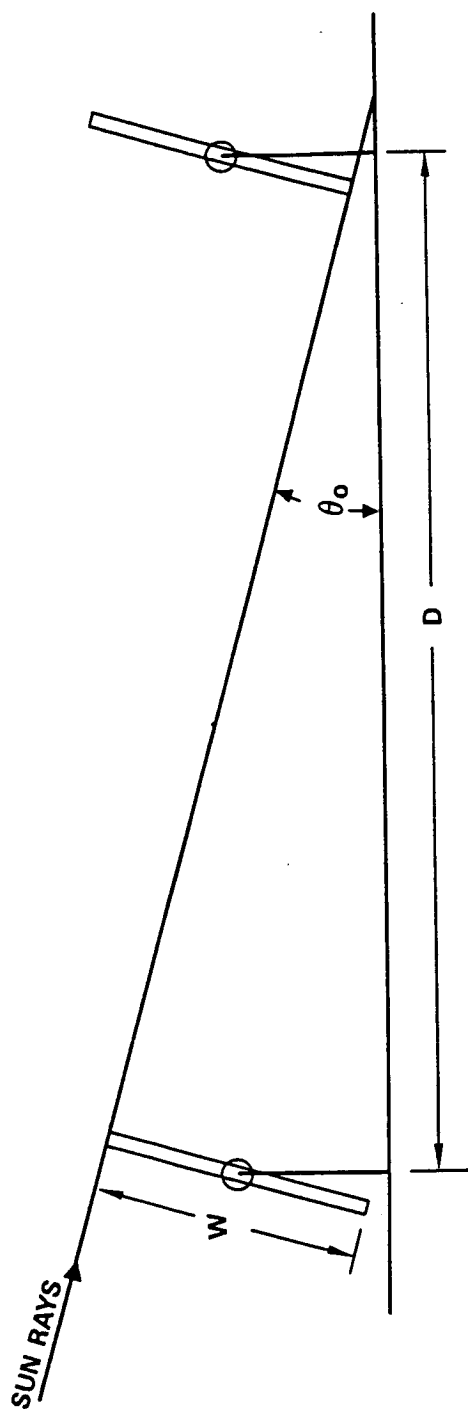
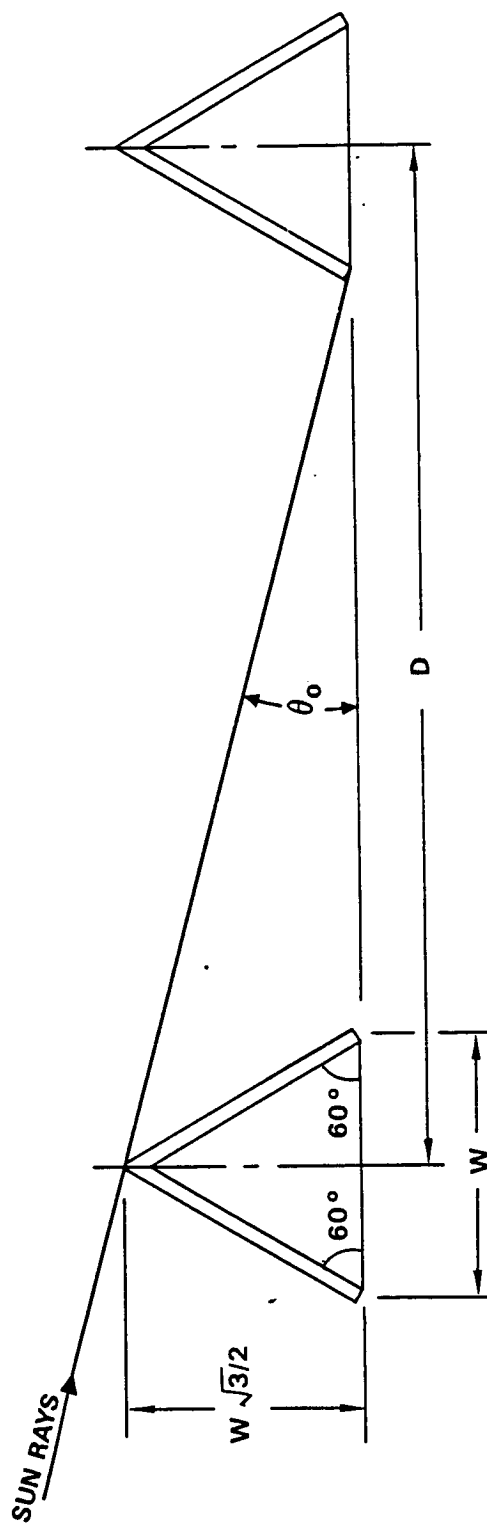


Figure 3.4. Detail of Tracking Panel Arrangement



a. TRACKING ARRANGEMENT. $\sin \theta_o \cong W/D$



c. TRIANGULAR ARRANGEMENT. $\tan \theta_o = \frac{W\sqrt{3}/2}{(D - W/2)}$

Figure 3.5. Details of Mutual Shadowing

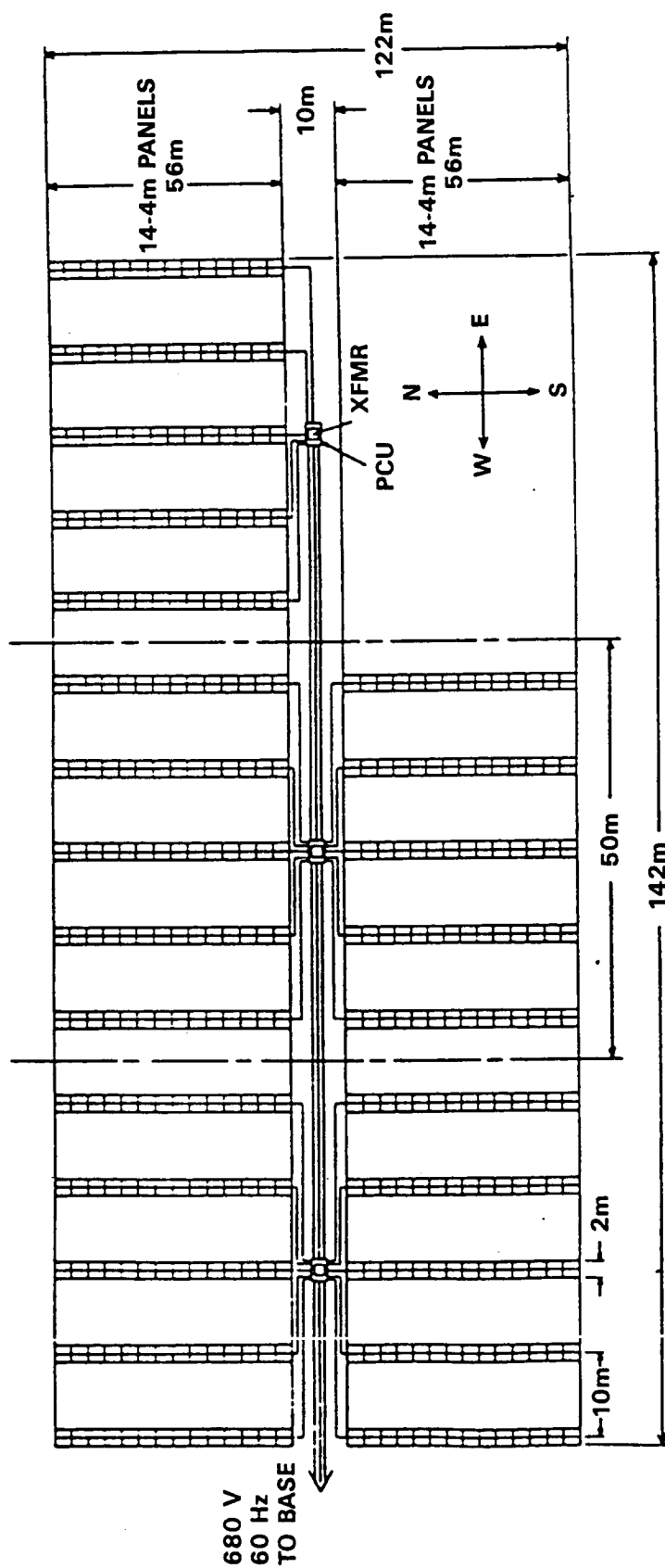


Figure 3.6. Plan View of 300 KW Solar Field After 5-60 KW Systems Have Been Assembled: Triangular Panel Arrangement

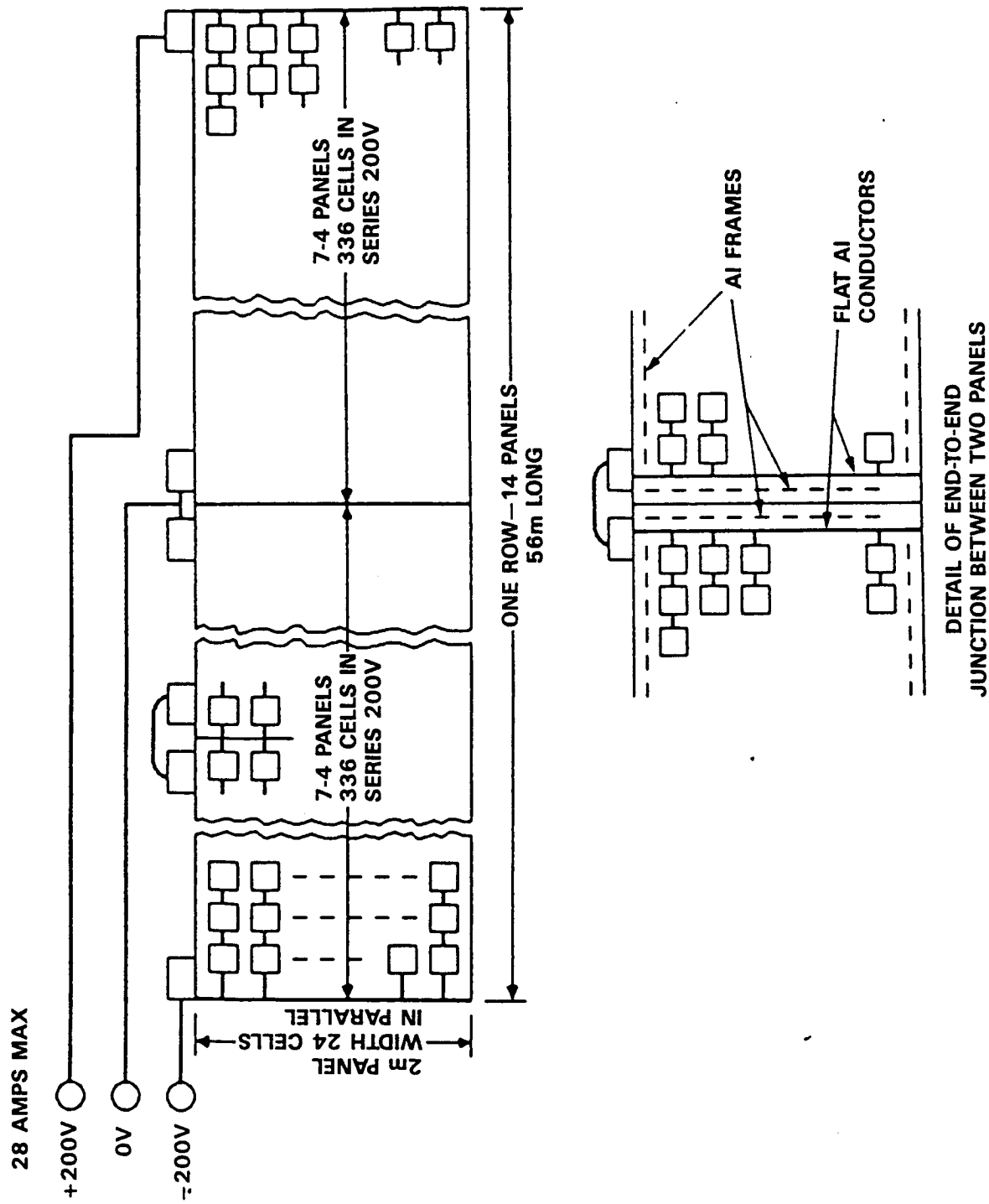


Figure 3.7. Details of Connections of One Side of One Row of Triangular Panel Arrangement. 3 Inch Square Cells

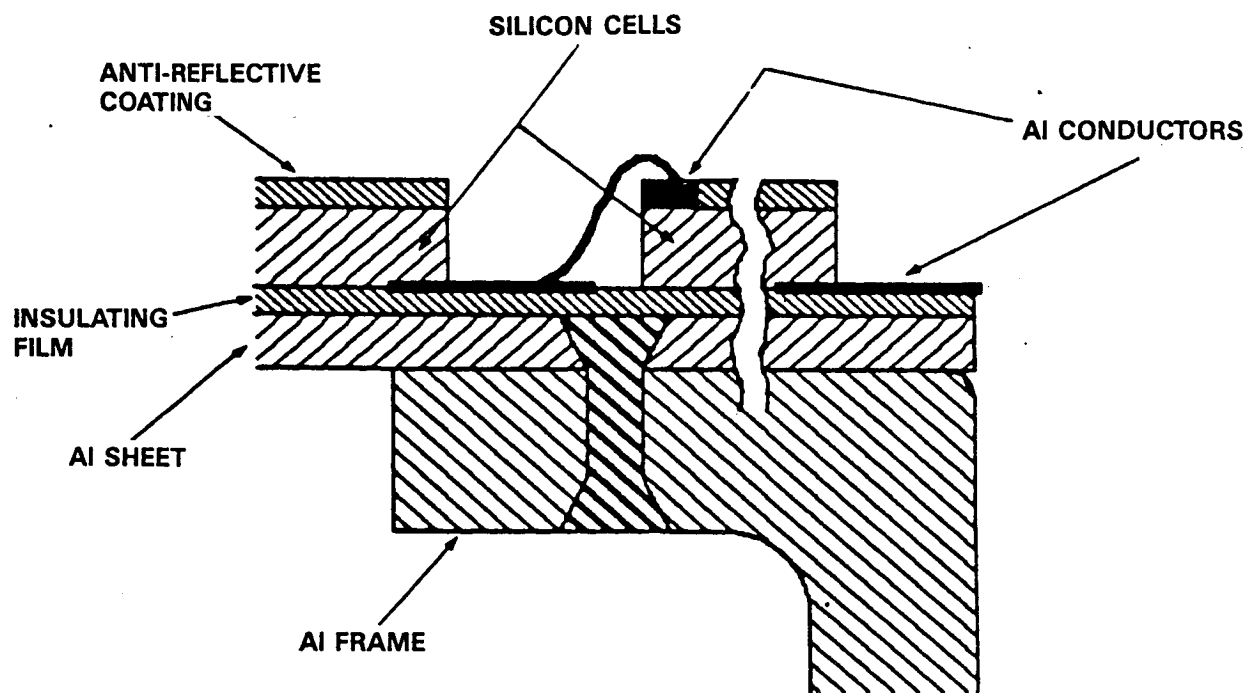


Figure 3.8. Detail of Solar Cells and Mounting

Table 3.1. "Values of Relative Solar Flux for three Panel Arrangement"

θ	D = 5W a) 10 PANELS TRACK	HORIZONTAL b) 10 PANELS FIXED	D = 5W 5 Δ ROWS c) 2 PANELS EACH
0°	0.1	0	0.0866
10.0°		0.187	0.468
11.3°	1.0		
30°	1.0	0.5	0.50
45°	1.0	0.707	0.483
60°	1.0	0.866	0.432
70°	1.0	0.94	0.470
80°	1.0	0.985	
90°	1.0	1.0	0.5

spaced apart along the east-west direction by 5 times one panel width or by 10 m. Each group of 5 rows would make up a 60 kW power source with its own power conditioning unit (PUC). As each new 60 kW system is brought up during the first year it would be positioned near the others till a 300 kW field is assembled. The equilateral triangular arrangement will yield a nearly flat output throughout the lunar day with an average flux of 47% of the total that could be available with perfect perpendicular tracking. The size of the total 300 kW solar field would be approximately 120 m x 150 m.

Panels would be unloaded from the lunar lander and transported to the solar field by astronauts using a small roving motorized crane. They would be mounted on the surface, after a minimum scraping and flattening of the site, using aluminum struts driven into the lunar soil. Panels would be electrically coupled to each other at installation by quality plug connectors. The interconnecting cables would then be deployed manually by astronauts.

The 3-phase transmission line between the solar field and the manned base, with transformers at either end, would be deployed using a lunar vehicle. All large current carrying conductors would be flat with long dimension vertical to radiate resistively generated heat. They could be supported a few meters above the surface on posts driven into the lunar soil .

To minimize electrostatic dust accumulation, the solar field will be separated from the manned base and the rocket landing-launching area by over 300 meters. Exposed potential on the panels will be kept low, to only plus or minus 200 volts d.c.. Around the periphery of the solar field, and perhaps above the apex of each triangular row of panels, grounding electrodes can be mounted to suppress electric fields.

3.3.1.1 THE ESTIMATED LAUNCH WEIGHTS OF ALL COMPONENTS OF THIS 60 kW SYSTEM ARE AS FOLLOWS:

Silicon Wafers	
(1,000,000 75 mm x 75 mm x 0.25 mm)	680 kg
Aluminum Sheet Under Cells	
(3600 m ² of 0.25 mm sheet)	635 kg
Aluminum Frames for Panels	
(25 mm and 12.5 mm angles)	635 kg
Conductors for all panels including busses and 3-phase transmission line 300 m long	91 kg
Power Conditioning Units	
(300 kW x 3 kg/kW)	91 kg
Transformer	<u>55 kg</u>
Total	2187 kg

3.4 AUGMENTATION OF SOLAR P-V SYSTEM BY LUNAR MATERIALS AND PROCESSING

Since the lunar base will be designed to grow in size (beyond the 300 kW level) and since a high priority will be the utilization of lunar materials for lunar-based processing for further space needs, we examine briefly how the initial P-V station described above can best be augmented.

We note first that the new P-V systems of different types from the original can be tied into the power network by suitable power conditioning units. This would allow bringing up and adding new more efficient Earth-built systems, or adding different and probably less efficient lunar built systems.

3.4.1 SOLAR CELLS

Silicon, the most likely choice of material for the original station brought from Earth, exists in great abundance in the lunar regolith.

Assuming this Si can be separated from its various sources such as SiO_2 using solar energy, the question remains, can new solar cells be made in large quantities on the Moon, and how would the cost of making them there compare with that of making them on Earth and transporting them to the Moon? At present, space qualified solar cells from Czochralski-grown silicon wafers cost about \$100/watt. An initial 300 kW field would then cost about \$20,000,000 in today's dollars to make on Earth. Launch weight of the panels with cells attached is only a few thousand kilograms, and volume is not excessive. The manufacture of high efficiency (15-22%) silicon cells is highly sophisticated and requires extreme purity of the source silicon and excellent control of minute quantities of dopant chemicals. It is unlikely that high efficiency cells can therefore be made on the Moon for many years.

Low efficiency silicon cells can be made by a variety of crystal growth techniques including polycrystalline or amorphous silicon films on insulating (ceramic) substrates. These processes are simpler, less sensitive to minute traces of impurities, and would be better contenders for lunar processing. Energy cost will be high - on the order of several electron volts per silicon atom (23 k calories/mole) to separate Si from SiO_2 , and several more to evaporate or sputter the silicon onto the substrate. Silicon can be grown in single crystal or polycrystalline form from the decomposition of silane, SiH_4 , at high temperatures. Some of the conducting connectors to the cells could be made from highly doped polycrystalline silicon films.

3.4.2 CERAMIC SUBSTANCES

The ceramic substrate under each cell and the entire 1.8 m x 3.6 m supporting panel, assumed to be aluminum from Earth in the initial installation, could be made from ceramic and thus, very possibly, by fusing components of the regolith.

3.4.3 METAL COMPONENTS

All cells must be connected by conductors to each other and to collecting wires around the panels, and all panels must be connected to power conditioning units and transformers.

Aluminum will be scarce and costly to produce on the Moon, as will copper, gold, silver and platinum, i.e., all the good electrical conductors. Iron is the only abundant lunar metal that could be separated easily and used for lunar manufacture. Its conductivity is about ten times poorer than that for aluminum and it is seldom used as a conductor on Earth because of its tendency to oxidize and form a resistive film. Nevertheless, it could be used on the Moon where no oxide is present. However, a whole new technology of making iron contacts to the silicon cells would have to be developed in an expensive vacuum environment development program on Earth before the technology could be transferred to the Moon.

The larger conductors between solar cells and the main bus bars, and the three-phase transmission line could be made with iron processed on the Moon where contact technology, using the larger cross-sections, are no problem. So also could frames for panels and any support structure needed to hold the panels above the lunar surface. The launch weight saved by making these components on the Moon could be a significant fraction, perhaps one-third to one-half of the total solar installation to be launched.

Iron forming processes would be fairly costly in energy. But, the ability to use iron for many other needed structures on the base and possibly for other space missions launched from the Moon would make its early availability very desirable.

3.4.4 POWER CONDITIONING UNITS AND TRANSFORMERS

Sophisticated solid-state power devices for the conditioning units would have to be made on Earth for many years. Transformers, on the other hand, could be made using lunar iron laminations.

3.4.5 CONCLUSIONS

Ceramic substrates and supporting panels, iron support frames, larger cross-section iron conductors, and possibly, low efficiency silicon polycrystalline or amorphous solar cells could be manufactured on the Moon to augment the initial solar power field.

3.5 COMPARATIVE PHOTOVOLTAIC APPROACHES

The preceding system design was based upon the 1986 technology of single crystal solar cells, manufactured by the Czochralski process. Some alternative approaches will now be evaluated against the criterion of system cost when delivered to the moon. The following conditions apply to this analysis:

- Transportation cost = \$6,600 per kg
- All alternative approaches are based upon silicon photocells.
- Power conditioning electronics will weigh 3 kg/kW
- Supporting aluminum framework will weigh 1.5 kg/kW.
- Calculations are for a 60 kW power module.

3.5.1 CZOCHRALSKI PROCESS SINGLE CRYSTAL SILICON.

- Acquisition cost of solar cells: \$100/watt
- Weight of silicon cells: 680 kg
- Weight of aluminum substrate: 635 kg
- Weight of peripheral equipment:
 - Supporting aluminum frames: $60 \times 10 = 600$ kg
 - Power transmission lines: $60 \times 1.5 = 90$ kg
 - Power conditioning electronics: $60 \times 3 = \underline{180}$ kg
 - Subtotal 870 kg
- Total weight per 60 kW = $870 + 635 + 680 = 2,185$
- Earth/lunar transportation cost = \$6,600/kg
- Transportation cost = $2,185 \times 6,600 = \$14,421,000$
- Acquisition cost = $60 \times 10^3 \times 100 = \$ \underline{6,000,000}$
- Total cost delivered to moon = \$20,421,000

3.5.2 SOVONICS STANDARD AMORPHOUS SILICON CELLS

The Sovonics company is manufacturing an amorphous silicon solar cell in a continuous, chemical vapor deposition process. These are deposited on an 0.127 mm stainless steel substrates. The thickness of silicon may be as small as one micron, therefore the substrate accounts for almost all of the weight. Modules approximately one square meter in size are being manufactured and marketed commercially. These modules are able to survive substantial damage, such as impact holes, and continue to deliver power. The cells have a conversion efficiency of 8% and currently cost \$5.75 per watt. Projected factors in the year 2000 era are 12% efficiency and \$1.00 per watt. Present manufacturing capacity is one megawatt per year.

Using a density of steel of 7.86 grams per cc, the weight per square meter of the amorphous cells is:

$$0.127 \times 10^{-1} \times 100 \times 100 \times 7.86 \quad 1 \times 1000 \text{ grams} = 1 \text{ kg/m}^2$$

The quantity of cells required will be based upon the following factors:

- Solar constant on the moon = 1.353 kW/sq. m
- The average daytime temperature of the solar cells in the lunar environment is 35° C and cell efficiency is degraded by 0.5% per degree above 20° C. Total degradation is (35-20)0.5 = 7.5%

The conversion efficiency as degraded by the temperature rise is obtained by: $8\% \times (1 - .075) = 7.4\%$

The required area, M for a 60 kW field is:

$$(1.353 \times 0.074)M = 60 \times 10^3$$

$$M \quad 6 \times 10^5 \text{ square meters}$$

- Total weight of solar cells = $6 \times 10^5 \times 1 = 6 \times 10^5 \text{kg} = 600\text{kg}$
 - Weight of peripheral equipment (from preceding case) = 870kg
- Total Weight = 1470kg

- Transportation cost = $1470 \times 6600 = \$9,702,000$
 - Acquisition cost = $(60 \times 10^3 \times 5.75) - 0.926 = \$ \underline{372,570}$
- Total \$10,074,570

3.5.3 SOVONICS ULTRA-LIGHT CELLS

In addition to their standard amorphous silicon solar cells, Sovonics manufactures an ultralight photo cell. Employing the same process as is used for the standard cell, these are deposited on a very thin plastic substrate. Their specific weight is 0.000417 kg/watt or 2400 watts per kg. The cost is \$100/watt. For a 60 kW power module:

Weight of solar cells = $0.000417 \times 60,000$	= 25 kg
Weight of peripheral equipment:	<u>600 kg</u>
Total weight:	625 kg

Transportation cost = 625×6600	= \$4,125,000
Acquisition cost = $60,000 \times 100$	= <u>\$6,000,000</u>
Total:	\$10,125,000

Summarizing the cost of a 60 kW module on the moon:

Single crystal silicon cells:	\$20,421,000
Sovonics standard process amorphous silicon:	\$10,074,570
Sovonics ultralight amorphous silicon:	\$10,125,000

This comparison is based upon technology and prices which are available today. There is every expectation that by the year 2000 the technology will have advanced to a point where the conversion efficiency of both single crystal and amorphous cells will have approximately doubled. It is also reasonable to expect that the acquisition cost will have been reduced by a factor of approximately five. these factors will make photovoltaic conversion an attractive candidate for providing electrical power for the lunar base.

Amorphous silicon is especially attractive because the manufacturing process appears to be adaptable to the lunar environment. Personnel at Sovonics judge that the hard vacuum of the moon would constitute a good environment for the chemical vapor deposition process. Raw materials are available, silicon dioxide being one of the most

abundant lunar compounds. Naturally an analysis of this approach in terms of cost effectiveness would have to be made. This would consider the weight of equipment which would be required for separation of the silicon dioxide from the lunar regolith, and of its refinement to a solar grade silicon. The next step is the production of silane, a silicon fluoride gas. This is decomposed by a glow discharge in the presence of hydrogen, resulting in the deposition of a silicon: fluorine: hydrogen alloy.

The weight of the equipment required for all these manufacturing steps must be estimated and its cost of transportation to the Moon computed. Energy requirements and their associated weights must also be estimated. The summation of these estimates must then be compared to the cost of production on Earth and transportation of finished modules to the Moon. The comparison must be done in light of the quantity of solar cells for which there is a lunar manufacturing potential. Naturally the larger the total quantity, the lower the cost per watt of lunar or terrestrial manufactured cells.

Production of all components of the power system must be evaluated in the same fashion. Little would be gained by a costly effort to manufacture solar cells in the lunar environment, if the supporting framework, power conditioning and power transmission components were still transported from Earth. This would require the ability to refine and work aluminum and to manufacture power transistors. While all these processes appear to be possible on the Moon at a time when the base has become rather large, it would appear that in the early years photovoltaic power systems will have to be manufactured on Earth and ferried to the Moon.

4.0 HEAT ENGINES

4.1 INTRODUCTION

NASA anticipates a return to the moon around the end of this century and the establishment of a permanent U.S. presence on the lunar surface early in the 21st century. This presence is projected to grow into a permanent settlement of 18-20 individuals by the year 2010.

This report presents the findings and conclusions of a study conducted by SDC and NASA contract NAS9-17359, Lunar Power Systems. It assumes an initial requirement for an uninterrupted supply of 60 kW of power which will be increased in 60 kW modules as power requirements grow, until power levels of 300 kW, one megawatt and eventually 10 megawatts are being generated.

For the stated requirements of electric power on the moon, there are two practical sources of primary energy: solar radiation and nuclear fission. Isotope-decay heat sources, often used in satellites and other small space craft, do not offer the scaling potential for the industrial-size power requirements of a permanent lunar colony.

Solar radiation can be converted into electricity by photovoltaic and thermoelectric processes and by thermodynamic or thermochemical systems, all of which are discussed in this section. Nuclear fission, i.e., the heat generated by a nuclear reactor can also be converted into electricity by thermoelectric or thermodynamic systems, essentially similar to those utilized for solar heat. Nuclear systems are already the subject of advanced design work at JPL and General Electric as part of NASA's SP-100 project, and will not be discussed here, except for pertinent comparisons with other systems.

A nuclear reactor has some inherent advantages: it functions day and night independently of the sun; its technology is well known and is industrially mature. But nuclear power may prove difficult if not impossible to use on the moon, for the same political and environmental reasons that have severely restricted its application here on earth. Even if enriched uranium, fast spectrum reactors of the SP-100 type are ultimately chosen as the best primary source for lunar power, solar radiation remains a technically viable candidate. It deserves careful consideration despite the system complications resulting from its availability during the lunar day only.

The systems considered fit well within the transport capabilities of the Orbital Transfer Vehicle (OTV) and of the Expendable Lunar Lander (ELL). They can be transported using the "Common Module," i.e., a cylindrical container 4.5 m in diameter and 11 m long; with a total mass, including contents, of 17.5 metric tons.

Potential candidates for solar/electric conversion are the Stirling, Brayton and Rankine engines, plus the Alkali Metal Thermoelectric Converter (AMTEC), which uses a thermochemical process. All of these heat engines can be constructed in modules with a wide range of output capability. All the above engines, as well as the solar-heat acquisition and waste-heat disposal systems are discussed and compared in pertinent sections of this report.

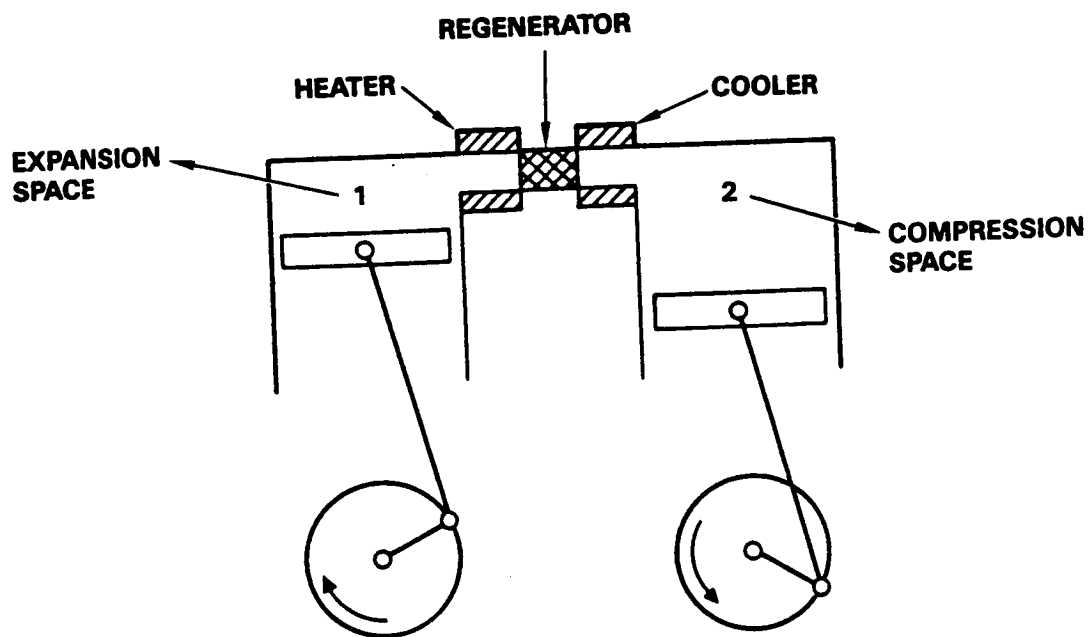
4.2 THE STIRLING ENGINE

The Stirling engine was invented in 1816 and enjoyed comparative success up to the early 1900's. However, the advent of the Otto and Diesel internal combustion engines led to a loss of interest in the further development of the Stirling engine. Recently, however, with the rapid advance of materials technology and the 1970 energy crisis, renewed attention has been devoted to

carefully refining of the Stirling engine design by well-known manufacturing corporations, both in the United States and in Europe. In its present state, the Stirling engine represents a mature primary power source with no unpredictable design or performance problems. A large number of engines for stationary and automotive applications have been built and tested in sizes up to 300 kW. Larger sizes have been proposed for marine applications. There is also a wealth of technical literature covering all aspects of the Stirling engine technology.

The thermodynamic cycle upon which the Stirling engine is based includes four distinct strokes or phases (Figure 4.1). Phase 1-2 is the isothermal compression, phase 2-3 is the constant volume heat addition, phase 3-4 is the isothermal expansion, and phase 4-1 is the constant volume heat rejection. The advantage of this cycle is the possibility of including a regenerator; by so doing, the ideal Stirling cycle has an efficiency equal to that of a Carnot cycle operating in the same temperature range. This may be demonstrated by considering the temperature-entropy diagram of Figure 4.1. The heat transfer to the working fluid between states 2 and 3, area 23ca2 is exactly equal to the heat transfer from the working fluid between states 4 and 1, area 14db1. Thus all Q_h takes place in isothermal expansion between state 3 and 4, and Q_l takes place in isothermal compression between states 1 and 2. Since all heat is supplied and rejected isothermally, the efficiency of this cycle will equal the efficiency of a Carnot cycle operating between the same temperatures.

Briefly stated, the difficulties in achieving an ideal Stirling cycle are primarily associated with heat transfer. It is difficult to achieve an isothermal compression or expansion in an engine operating at a reasonable speed, and there will be pressure drops in the regenerator and a temperature gradient between the two streams flowing through the regenerator. Reference 1 (G.T. Raeder and C. Hoopers "Stirling Engine") discusses these factors in great detail.



Kinematic Configuration for the Stirling Engine

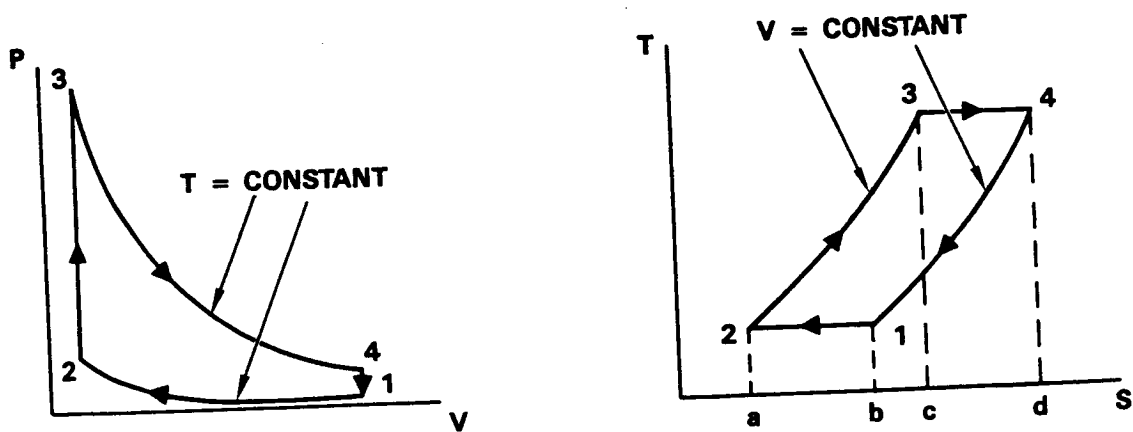


Figure 4.1. P-V and T-S Diagrams for the Stirling Engine

There are basically two types of Stirling engines, kinematic and free-piston. The kinematic type, illustrated in Figure 4.2, converts the reciprocating motion of the power piston to a steady rotating motion, by means of a crankshaft or similar arrangement. The free-piston type simply applies the oscillatory linear motion of the power piston to a coaxial extension of the piston rod, which can be configured with a linear alternator. This provides a higher potential efficiency, by eliminating the friction losses associated with the crankshaft.

The reciprocating power piston requires a good sliding seal to effectively prevent the passage of gas into the engine crankcase. Lubrication of both sliding pistons must be accomplished passively, or gas contamination will take place. Present seal life is now on the order of 4000 hours, but improvements are being made which may increase this life to 10,000 hours.

The free-piston engine largely alleviates the sealing problems of the kinematic engines, since the entire system can be hermetically sealed, with all engine components and the linear alternator integrally encased.

A variation of the free piston engine is the Harwell engine, developed at the Atomic Energy Research Establishment in Harwell, U.K. This design uses a metal diaphragm in place of the conventional power piston. This overcomes the sealing problem entirely; however, no scaling size prototypes of this engine have been built so far.

During the SP-100 program sponsored by NASA and DARPA, the Sunpower Corporation of Athens, Ohio, conducted a complete analysis and design of a 25 kW electric output free piston Stirling engine for application in a 100 kW spacecraft power module.

ORIGINAL PAGE IS
OF POOR QUALITY

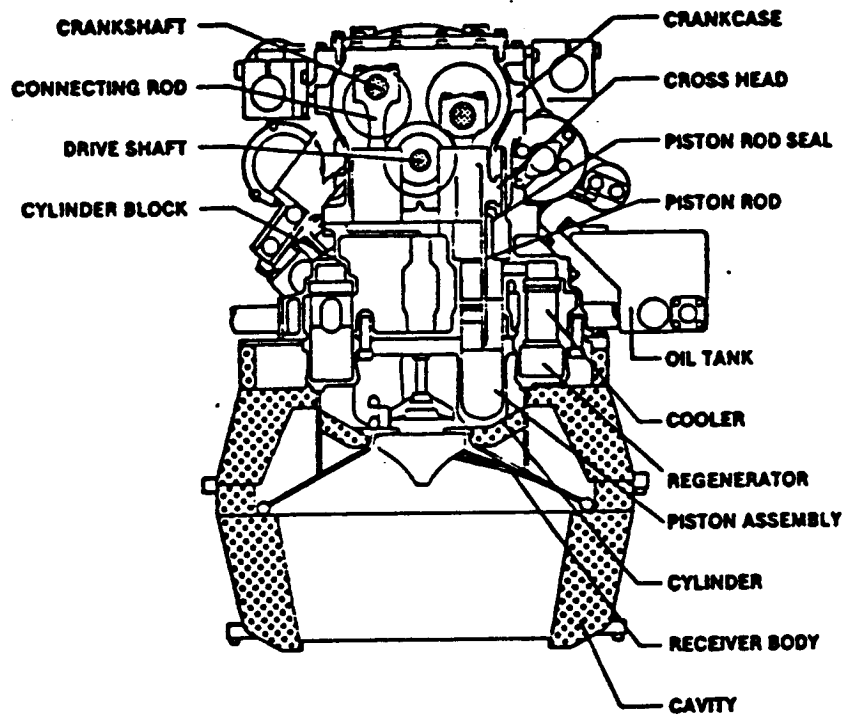


Figure 4.2. The 4-95 Solar Stirling Engine

C-2

A layout of this basic power module is shown in Figure 4.3. Overall system efficiency is 29% and Sunpower states that there are not specific problems with power levels twice that of the present system, i.e., up to 50 kW electric. Moreover, with new high-temperature materials and a temperature ratio of 3, an overall efficiency of 40 to 43% can be expected.

McDonnell Douglas has developed a solar power module incorporating an 11 meter solar collector, a 40 kW, 4 cylinder kinematic Stirling engine and an alternator with a constant output of 25 kW of electric power. One of these units has been in continuous operation for some time at the M-D facility in Huntington Beach, CA.

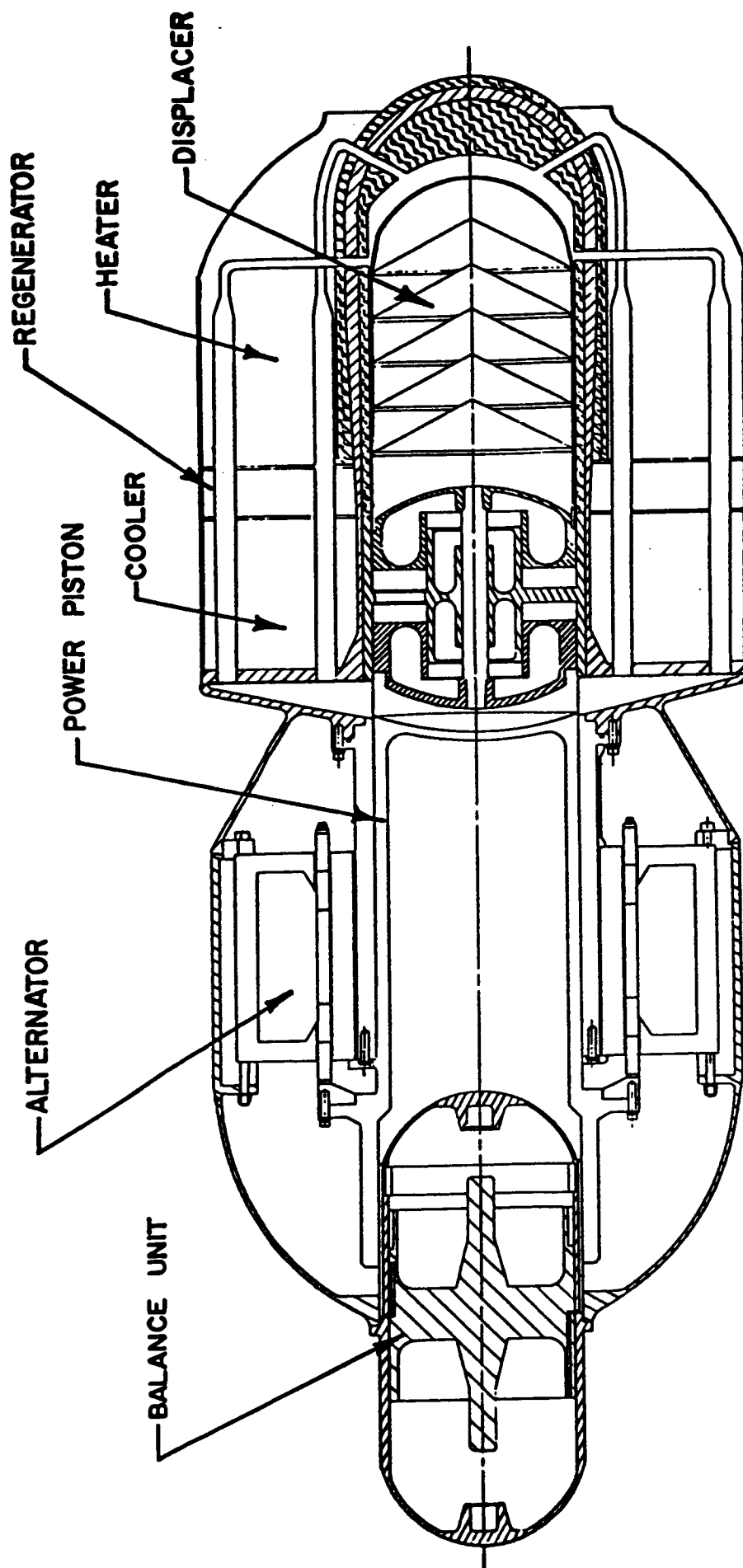
4.2.1 DETERMINATION OF THERMODYNAMIC EFFICIENCY

As previously noted the thermodynamic efficiency of the ideal Stirling cycle with perfect regeneration is equal to that of a Carnot cycle, operating between the same temperatures of source and sink.

$$\eta = \eta_{\text{Carnot}} = 1 - \frac{T_L}{T_H}$$

A schematic arrangement of an engine operating on the Stirling cycle and utilizing a regenerator is presented in Figure 4.4.

Since the ideal Stirling cycle cannot be achieved by a realistic engine, an attempt should be made to approximate the ideal conditions as closely as possible. The dead volume space, along with the flow losses associated with the working fluid, and heat transfer as a result of temperature gradients across finite boundaries will lead to irreversibilities that reduce the thermal efficiency of the cycle.



OVERALL LENGTH	1.25 M
MAXIMUM DIAMETER	.46 M
MASS	145 Kg

Figure 4.3. Space Power Module Showing Regenerator

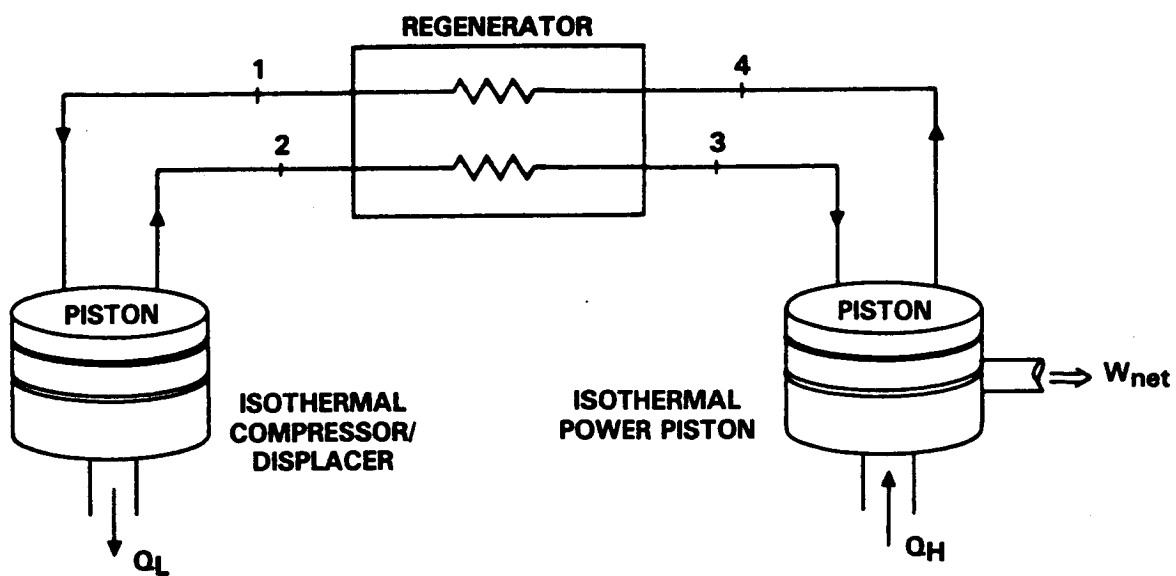


Figure 4.4. Schematic Diagram of Stirling Engine With Regenerator

An analysis of the first law of thermodynamics and of the process relationships of the Stirling cycle lead to an equation for the thermal efficiency as a function of regenerator efficiency, the ratio of volumes and source/sink temperatures. This relationship is given below.

$$\eta = \left(1 - \frac{T_L}{T_H}\right) \frac{\ln \frac{V_1}{V_2}}{\left[\frac{1-E}{K-1} \left(1 - \frac{T_L}{T_H}\right) + \ln \frac{V_1}{V_2}\right]}$$

For a perfect regenerator, $E=1$ and:

$$\eta = 1 - \frac{T_L}{T_H}$$

4.2.2 SOLAR STIRLING SYSTEMS

Electric power generation using paraboloidal dish concentrators and kinematic Stirling engines as energy conversion sub-systems has been under testing at several Southern California locations for the past few years. The high conversion efficiencies and reliability demonstrated by them warrant a close examination of these systems.

The United Stirling 4-95, four cylinder double acting Stirling engine has a maximum output of 25 kW in solar application and is compatible with an 11 meter diameter concentrator. The function of the pistons in a double-acting engine is twofold; they move the gas back and forth between the hot and cold sides, and transmit mechanical work to the drive shaft. The pistons are thermo-dynamically coordinated and each one operates simultaneously in two cycles; the hot upper surface of one piston is coordinated with the cold undersurface of the next piston, and so

on. Four to six cylinders, arranged in line or co-axially, are needed in order to optimize the efficiency of a Stirling module.

The highest accumulated hours of operation, with good results which have been obtained from testing of 36 Stirling engines give a total of 65,000 for the 36 engines and 11,000 for the longest operating single engine.

The high power/conversion unit efficiency (33%) of the Stirling engine, coupled with the excellent optical efficiency of the parabolic dish offer an attractive solar electric generating system.

4.2.3 THE MCDONNELL DOUGLAS SOLAR SYSTEM

McDonnell Douglas and United Stirling have designed and built a solar/electric module, which is currently in operation at McDonnell Douglas facilities in Huntington Beach (Figure 4.5). This module is self-contained and can generate 25 kW of electricity. The concentrator is composed of 82 mirrors (each of 1.1 m² area, 0.07 cm thickness), which concentrate the incident solar radiation onto the receiver of a Stirling engine located at the focal point. These mirrors, with a total reflective surface areas of 91 m², are aligned in a pattern which results in an optical efficiency of 80%. The conversion efficiency from solar to net electricity is 28% (@ solar insolation of 1000 W/m²) is shown in Figure 4.6.

4.2.4 OTHER STIRLING/SOLAR SYSTEMS

JPL and United Stirling have been testing an improved 4-95 solar Stirling engine in a parabolic dish system at Edwards Air Force Base since 1982. The electrical output from the system is 24 kW, with a 28% overall conversion efficiency from solar to

Figure 4.5

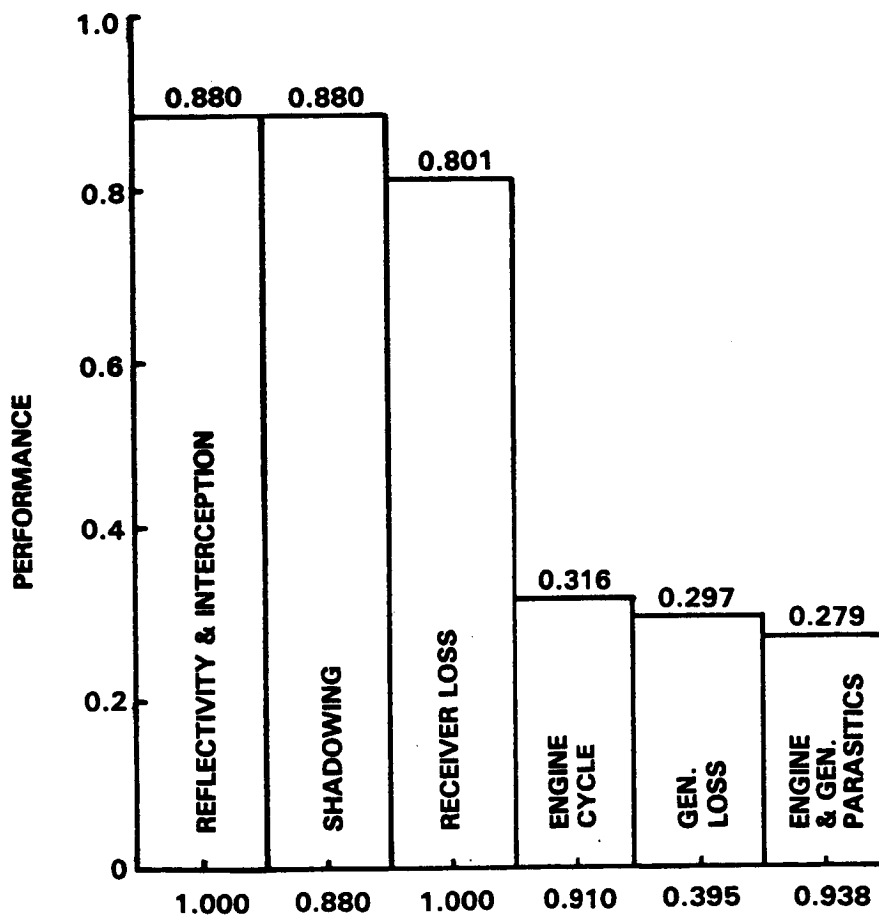


Figure 4.6 McDonnell Douglas/United Stirling System Conversion Efficiency

electricity. The performance of this system is presented in Figure 4.7 for a solar insolation of 1000 W/m^2 .

Advanco Corporation has designed, fabricated and tested a Solar/Stirling prototype (Vanguard, Figure 4.8), which is currently operational at the Southern California Edison's Santa Rosa sub-station. The Stirling engine/generator consists of a United Stirling model 4-95 solar engine and a Reliance model XE286T induction generator (Ref. 12). The power output is 25kWe with a solar insolation of 1000 W/m^2 . The overall solar to electric conversion efficiency is 27%. Each parabolic dish, with a net reflection area of 83 m^2 , consists of 328 back-silvered fusion glass mirrors, cold sagged and bonded to a spherically ground foam-glass substrate. These 5 cm thick, 0.28 m^2 (surface area) mirror facets have been individually mounted on 16 steel rack assemblies. Each solar concentrator can be controlled manually or automatically through the concentrator microprocessor control.

4.3 THE BRAYTON CYCLE ENGINE

The Brayton Cycle provides the basis for the gas turbine, an engine that has revolutionized aircraft technology and has enjoyed considerable success as stationary and marine power plant since 1950. Engines using a closed-loop derivation of the Brayton cycle have been in development since the early 1960s.

Significant milestones of the closed-loop Brayton Cycle include a 3 kWe proof-of-principle demonstrator built in 1962 and a 10.5 kWe power system that has operated in excess of 41,000 hours with no measurable degradation in performance. NASA published design requirements for reactor power systems for lunar exploration, incorporating a Brayton turbine for conversion of heat to electricity, as early as September 1967. A proposed design for a 40 kWe solar-powered system for the NASA space station program is

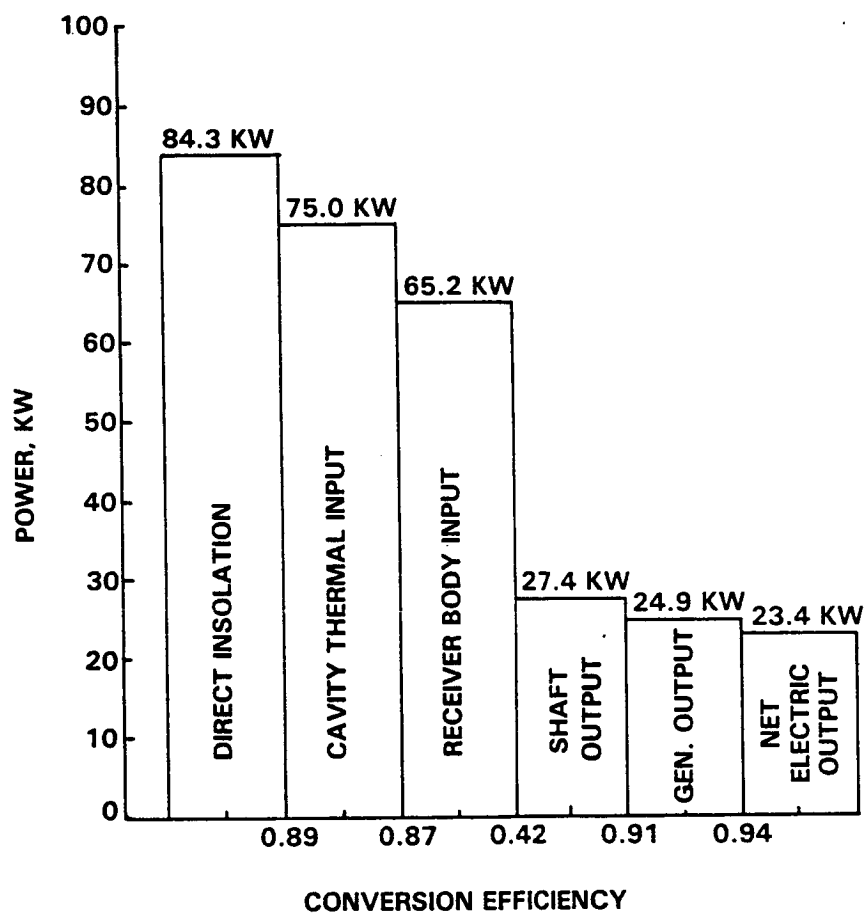


Figure 4.7. United Stirling/JPL Dish-Stirling System Performance

OVERALL MODULE FEATURES

DIAMETER: 11m (36 ft. 1 in.)

HEIGHT: 12m (39 ft. 4 in.)

WEIGHT: 7980 kg (17,560 lb.)

SYSTEM EFFICIENCY: 25.4%

ELECTRICAL POWER: 20.8 kW_e

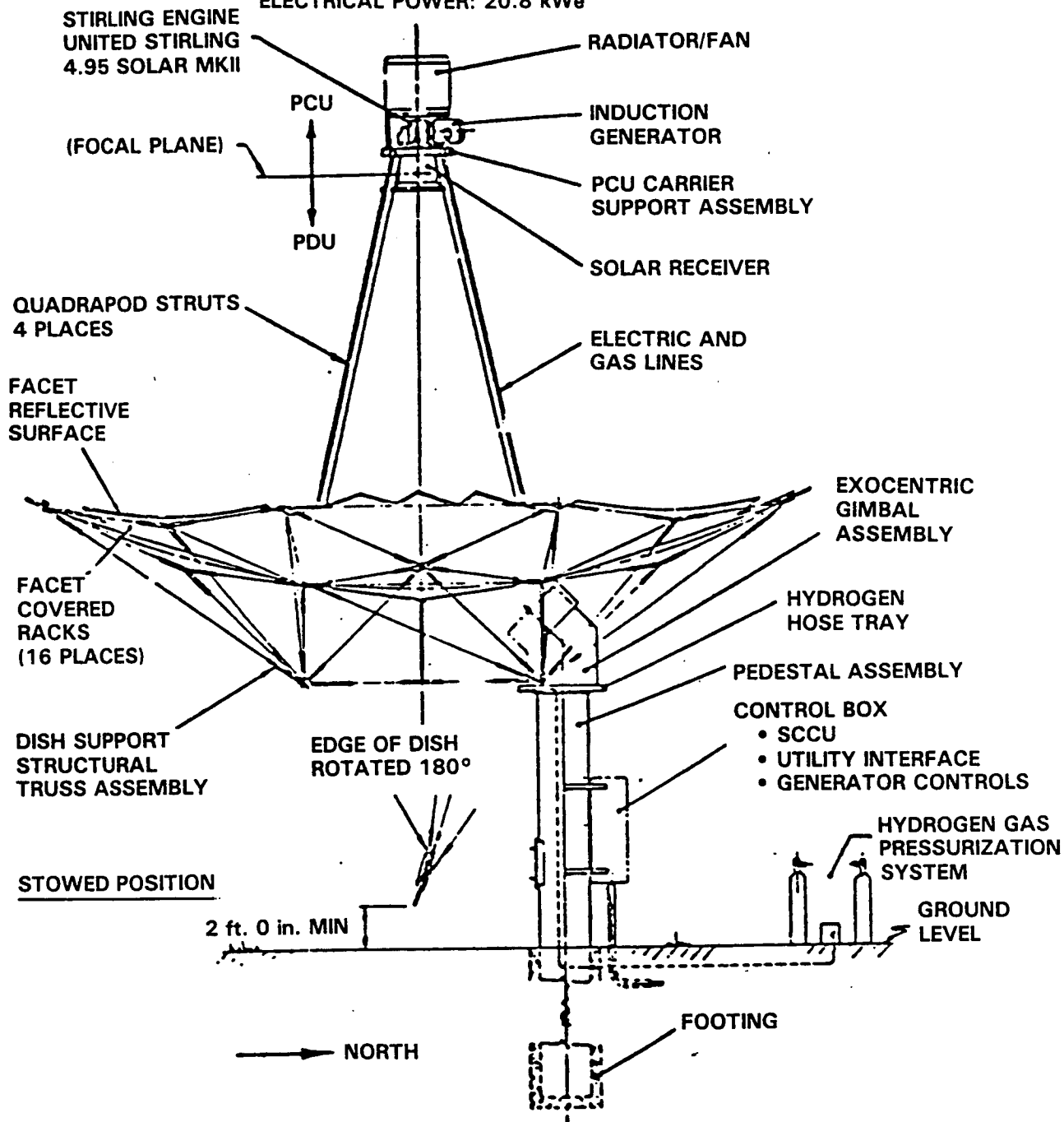


Figure 4.8. Advance Solar/Stirling System

now being developed by the Garrett Corporation in Phoenix. No other thermodynamic engine has attracted more serious attention in space circles for the generation of electric power in the substantial kW ranges.

The basic Brayton Cycle is shown schematically in Figure 4.9(a) and is defined in P-V diagram of Figure 4.9(b) and the T-S diagram of Figure 4.9(c). It consists of a compressor and turbine on a single shaft supported by hydrodynamic gas bearings. The working medium, generally hydrogen or helium, is compressed to P_2 in the compressor. The compressed gas enters a heat exchanger, where heat is transferred at constant pressure. The gas then expands against the turbine blades and flows to another heat exchanger, where heat will again be given up at constant pressure. The colder gas then flows back to the compressor, thus completing the cycle.

Present day Brayton engines always include a heat recuperator or regenerator in order to achieve high conversion efficiency, and the cycle then works as shown in Figure 4.10. Energy from an external heat source is used to heat the high pressure gas to the maximum cycle temperature. The gas then passes to the turbine to produce output power and drive the compressor. The turbine discharge gas is cooled first in the recuperator heat exchanger and then in the radiator, before being again introduced into the compressor. The low-pressure gas is compressed to the highest cycle pressure and is then heated at constant pressure in the recuperator, before passing through the heater, thus completing the closed loop. The recuperator recovers a significant portion of the turbine waste heat and therefore reduces the amount of heat that must be added to the system.

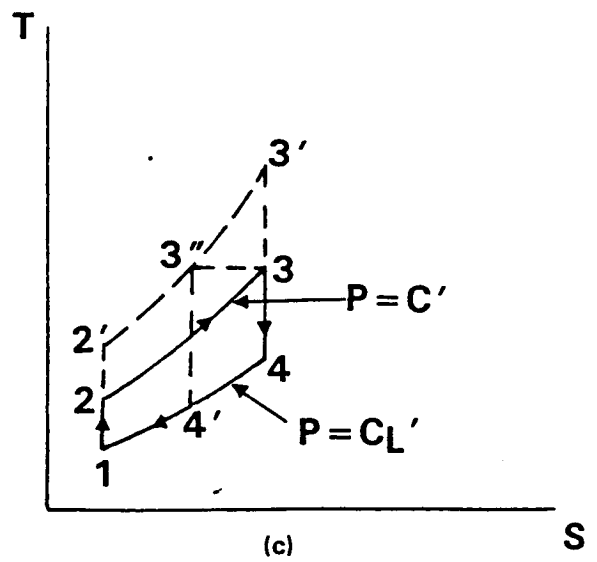
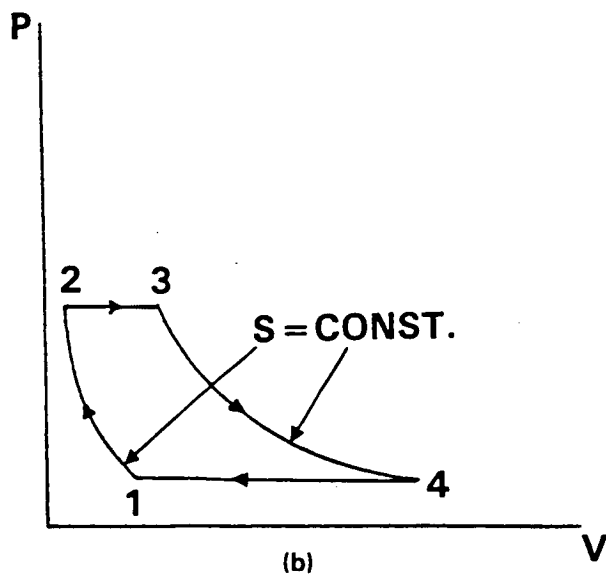
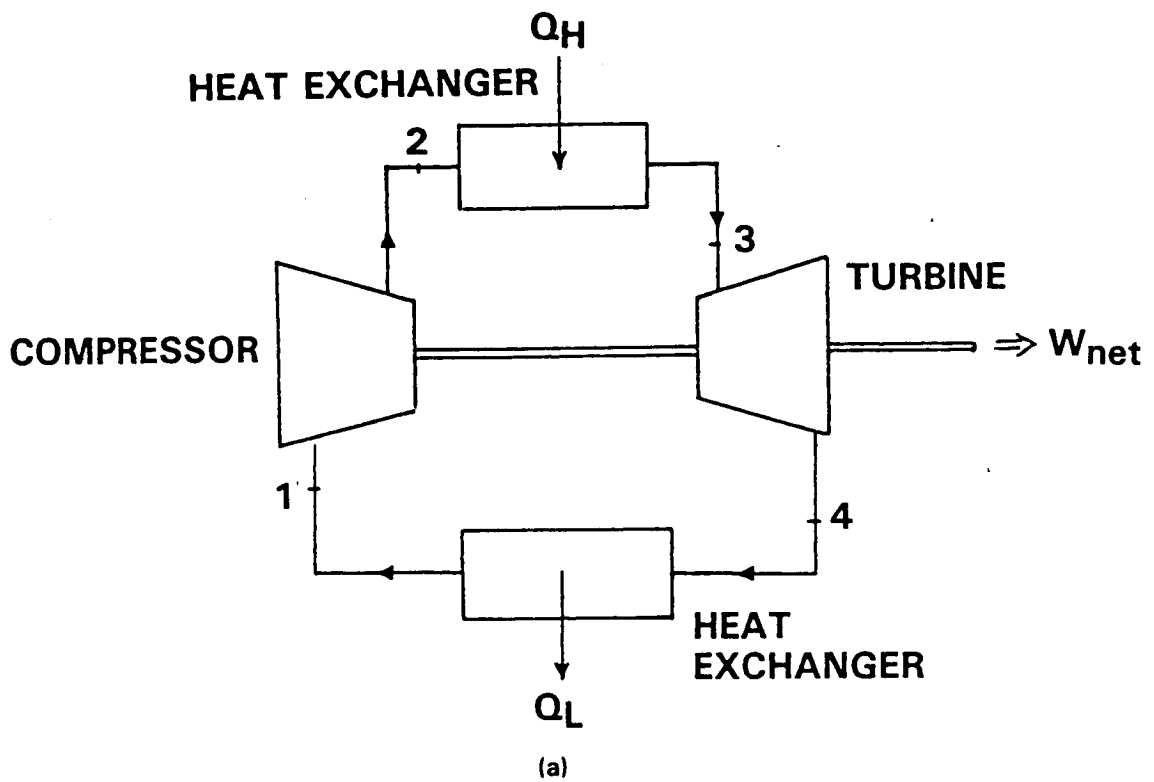
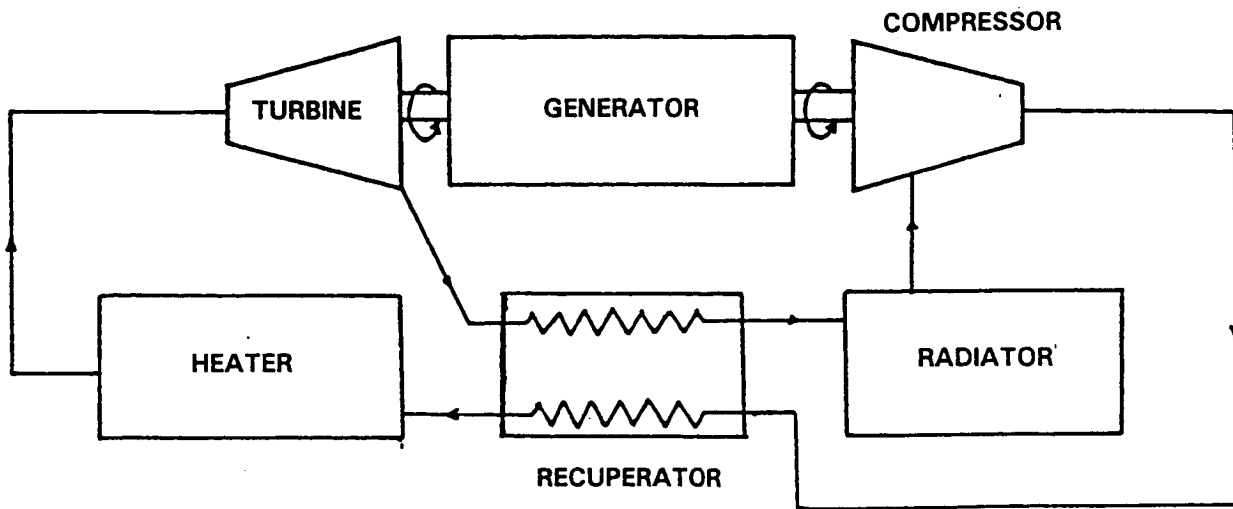


Figure 4.9. The Brayton Cycle



Schematic Diagram of Brayton Engine with Recuperator

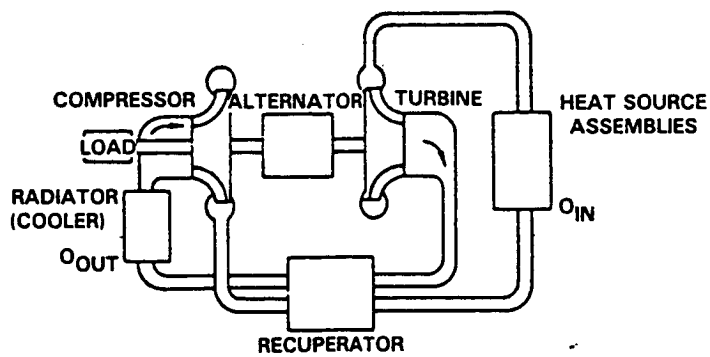


Figure 4.10. Closed Brayton Cycle with Heat Recuperator

The thermal efficiency of the Brayton Cycle is given by:

$$\eta = \left(1 - \frac{T_1}{T_2}\right) \left(1 - \frac{1}{(P_2/P_1)^{1-\frac{1}{K}}}\right)$$

The efficiency is therefore a function of the isentropic pressure ratio. From the T-S diagram of Figure 4.9, it is evident that increasing the pressure ratio will change the cycle from 12341 to 12'3'4'1. The latter cycle has a greater heat supply and rejects the same heat as the original cycle, and therefore it has a greater efficiency. The latter cycle also has a higher maximum temperature (T_3) than the original cycle (T_3). In an actual gas turbine the maximum temperature of the gas entering the turbine is limited by metallurgical considerations. The use of ceramics, however, can allow higher gas temperatures. If T_3 is fixed and the pressure ratio is increased, the resulting cycle 12'3"4"1 will have a higher efficiency than the original cycle.

The actual gas turbine engine differs from the ideal cycle primarily because of irreversibilities in the compressor and turbine, and because of pressure drop in the flow passages and heat exchanger. Thus the state points in a real Brayton Cycle are shown in Figure 4.11. One important feature of the Brayton Cycle is the large amount of compressor work compared to the turbine work. The over-all thermal efficiency of the cycle is very sensitive to the efficiencies of the compressor and turbine. If these efficiencies fall below 60%, all the work of the turbine will be required to drive the compressor and the over-all efficiency will be zero.

The efficiency of the Brayton Cycle is improved by introducing a heat recuperator as shown in Figure 4.10. The temperature difference between the hot, low pressure gas leaving the turbine and

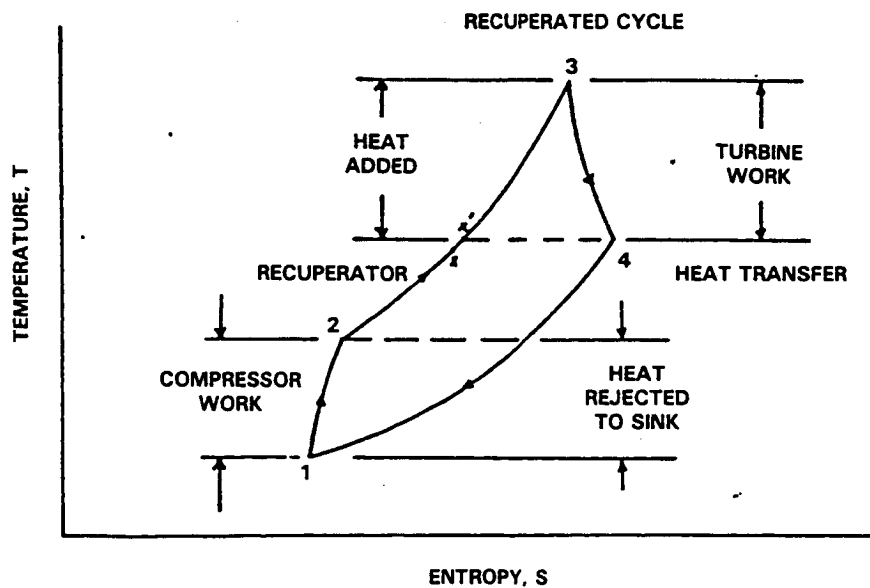
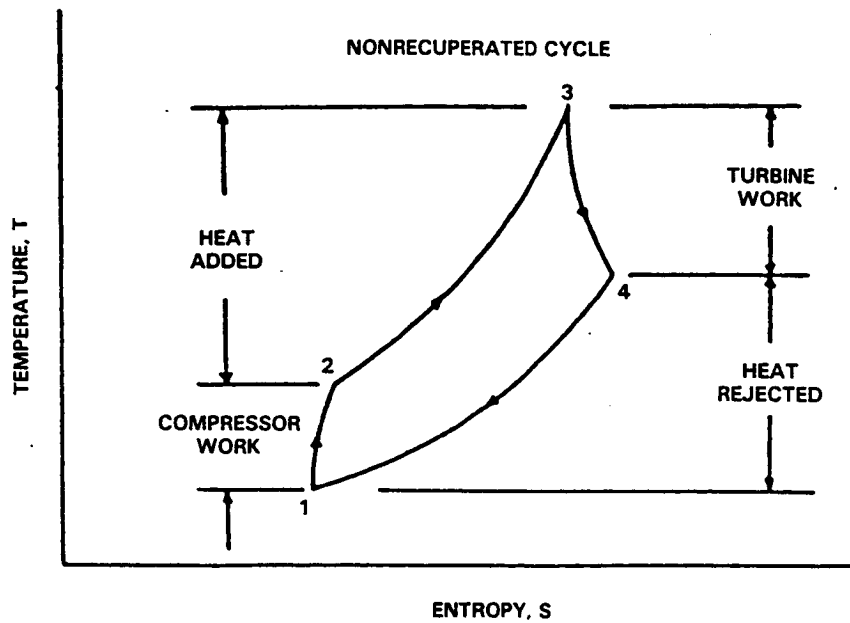


Figure 4.11. T-s Diagrams for Brayton Cycle With and Without Recuperator

the cold, high pressure gas leaving the compressor can be used to heat the latter. In an ideal recuperator, the temperature of the high-P gas equals the temperature of the low-P gas leaving the turbine. ($T_x = T_4$, Figure 4.11). In this case heat transfer from the external source is only required to increase the temperature from T_x to T_3 .

The efficiency of this cycle with heat recuperation is given by the equation below.

$$\eta = 1 - \frac{T_1}{T_3} \left(\frac{P_2}{P_1} \right)^{\left(\frac{K-1}{K} \right)}$$

Thus, for the ideal cycle with recuperator, the thermal efficiency depends not only on the pressure ratio, but also on the ratio of the minimum to maximum temperature.

The closed-cycle Brayton engine permits the use of highly efficient components. However, a low temperature radiator and low compressor inlet temperatures are required in order to obtain higher cycle efficiencies. High compressor and turbine efficiency, as well as an efficient recuperator are required for high thermal efficiencies. The recuperator permits recovery of a large portion of the cycle waste heat, correspondingly reducing the required heat input, as discussed before (see Figure 4.11). It also reduces the optimum compressor/turbine pressure ratio and increases the mass flow rate, leading to further increases in system efficiency.

4.4 THE RANKINE ENGINE

The Rankine cycle is depicted in Figure 4.12. The working medium is pumped in a reversible adiabatic process to state 2. Heat is

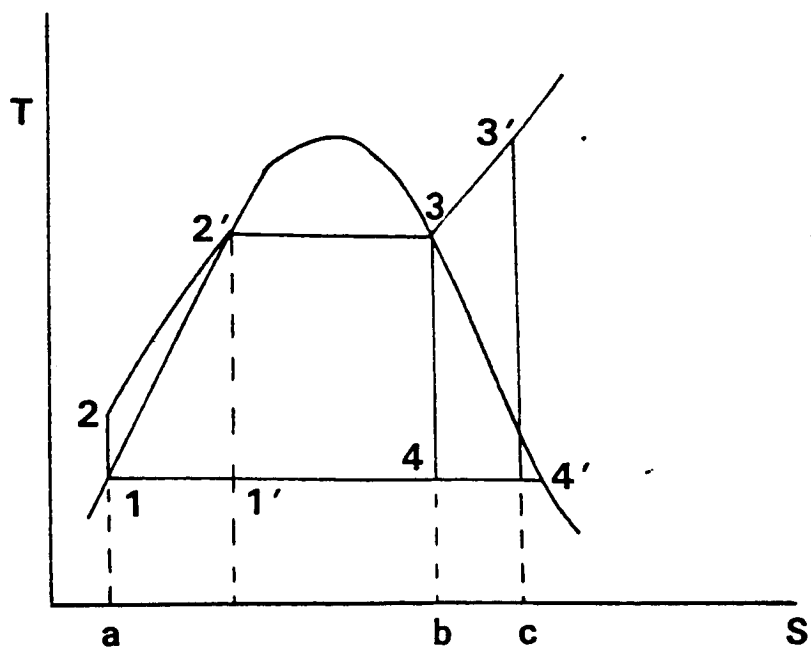
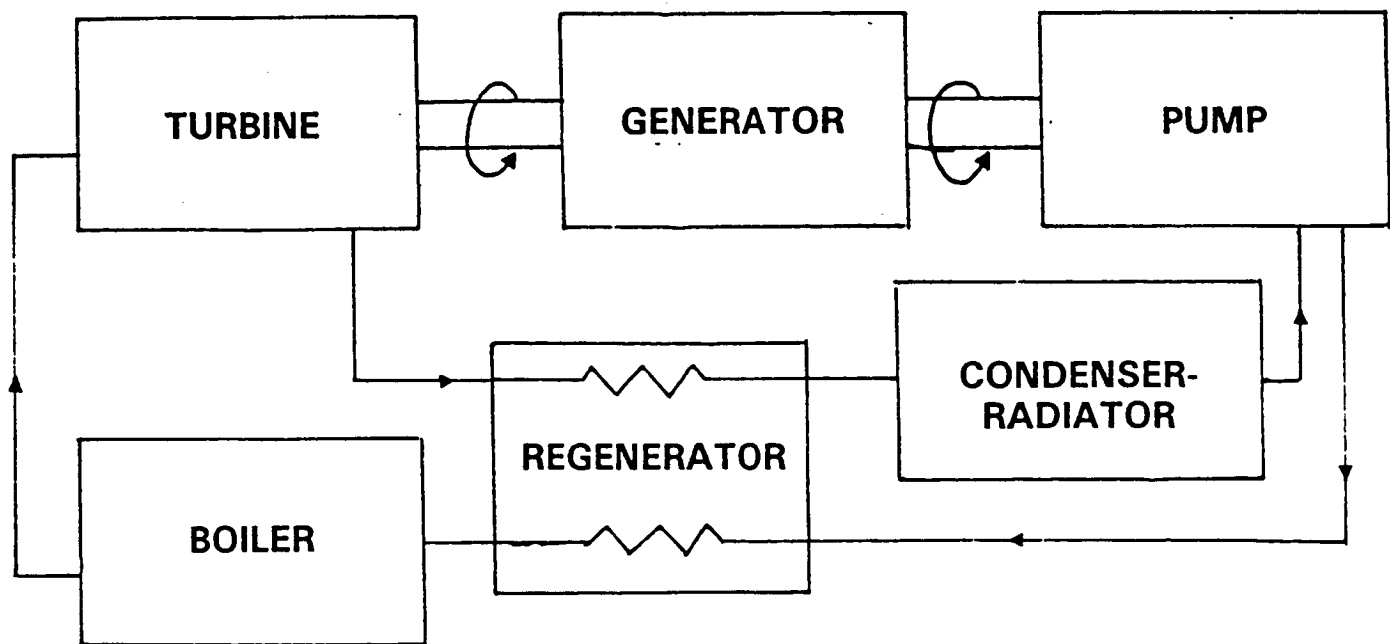


Figure 4.12. Schematic and T-S Diagram for Rankine Cycle

then added at constant pressure to vaporize or superheat the working fluid to state 3 (or 3'). Process 3-4 represents the reversed expansion in the turbine. The energy content of the gas at the turbine exhaust is dissipated by radiation until the gas is completely condensed to liquid. The liquid returns to the pump to complete the cycle. The efficiency of this cycle without superheat is given by:

$$\eta = \frac{W_{\text{net}}}{Q_H} \frac{\text{area } 122'341}{\text{area } a22'3ba}$$

The efficiency of the Rankine cycle depends on the average temperature at which heat is supplied and the average temperature at which heat is rejected. Increasing the former or decreasing the latter will result in a higher cycle efficiency. The ideal Rankine cycle has a lower efficiency than the corresponding Carnot cycle, since the average temperature between states 2 and 2' (Figure 4.12) is less than the temperature during evaporation. The regenerative and reheat cycles can be used respectively to increase the average temperature at which heat is supplied and to increase the pressure, while avoiding excessive moisture, in the low-pressure stages of the turbine, thus resulting in higher cycle efficiencies. Briefly stated, the Rankine cycle efficiency can be increased by lowering the exhaust pressure, increasing the pressure during heat addition, and by superheating the vapor.

The actual Rankine cycle, however, deviates from the ideal cycle because of frictional effects and heat transfer losses in the pipes, and losses associated with fluid flow through the turbine and pump.

The thermal efficiency of a Rankine cycle tends to decrease as the maximum temperature of the cycle approaches the critical

temperature of the working fluid. Therefore, a working fluid with a critical temperature higher than the maximum cycle temperature must be selected. Mercury and organic fluids are currently used in the Rankine cycle. The major advantage of organic fluids (Biphenyl) is the peculiar shape of the liquid/vapor phase region on the T-S diagram of Figure 4.13. The positive slope of the vapor line results in automatic superheating of the fluid during the power turbine expansion. Thus the turbine is always operated with superheated vapor, resulting in higher turbine and overall efficiencies with relatively low turbine inlet temperatures. Low turbine inlet temperature is the major attribute of organic Rankine systems. Mercury Rankine systems require a higher maximum cycle temperature than the temperature at which the greater portion of heat is added. Organic Rankine systems, especially without regeneration, lose some heat at a higher temperature than the temperature at which the majority of heat is rejected. Both conditions tend to reduce overall cycle efficiency.

4.5 THE AMTEC POWER PLANT

The Alkali Metal Thermoelectric Converter (AMTEC) is a comparatively recent device in the field of high efficiency, direct heat-to-electricity conversion. Although still in its preliminary development phase, both theoretical and experimental data indicate that it may indeed become the most promising system for lunar and space power applications within the next two decades.

Conceived in 1962 by J.T. Kummer and N. Weber at the Ford Motor Company Scientific Laboratory, it was patented in 1968, after Kummer and Weber conclusively demonstrated its feasibility in several experiments. Shortly after issuance of the patent, Weber began research on the new thermoelectric converter in collaboration with T. Cole and T.K. Hunt. At present, investigation of the AMTEC continues within groups at the Ford Motor Company,

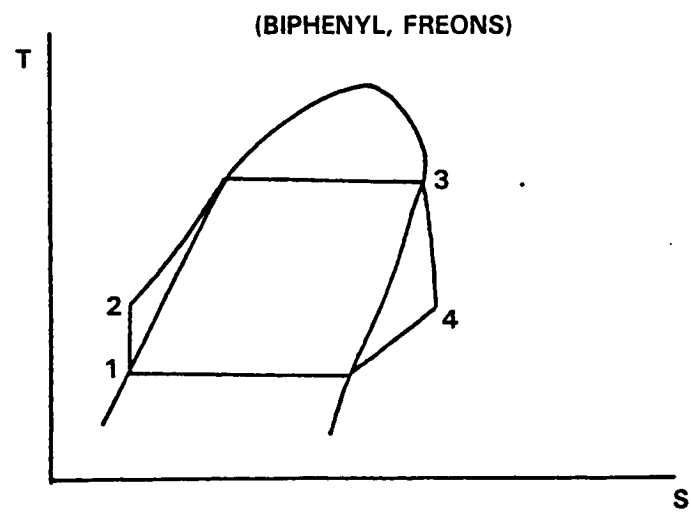
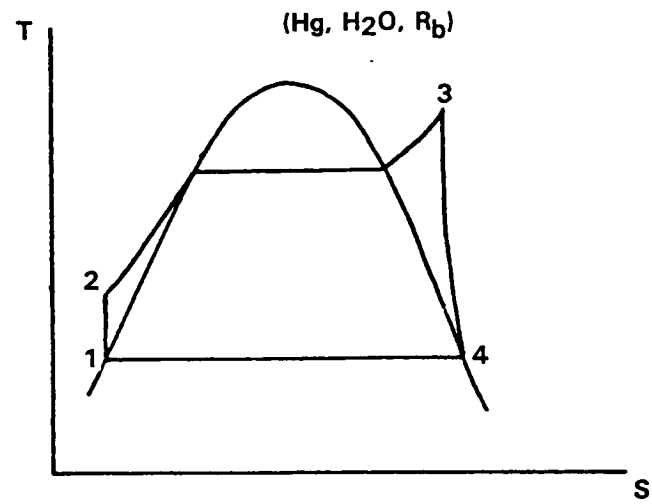


Figure 4.13. Rankine Cycle T-S Diagrams for Mercury and Organic Fluids

the Jet Propulsion Laboratory, the Sandia National Laboratory, Almax Industries, Ltd. of Canada, and by N. Weber at Cermatec.

Operation of the AMTEC derives from the unique sodium ion conducting properties of the Beta"-alumina solid electrolyte (BASE). An efficiency of 19% and a power density of 1 W/cm^2 have been demonstrated in laboratory devices, but calculations indicate that overall conversion efficiencies of 25-30%, or even higher, may be achieved with an optimized design. Concerning weight, even the primitive laboratory devices have achieved over 50 W/Kg and it is predictable that an advanced device would surpass 500 W/Kg. In addition, the AMTEC has no moving parts and its hot side temperature (900-1300°K) makes it compatible with nuclear reactors of the projected SP-100 type, or with advanced solar concentrator heat sources.

The operating cycle of the AMTEC is illustrated in Figure 4.14 and an assembly is shown in 4.15. A closed vessel is divided into a high temperature/pressure region in contact with the heat source, and a low temperature/pressure region in contact with a heat sink. These two regions are separated by a barrier of BASE, which has the electrolyte properties of ion conduction and electron insulation. The high temperature/pressure region contains liquid sodium at T_h , and the low temperature/pressure region contains mostly sodium vapor, plus a small amount of liquid sodium at T_l . Electrical leads make contact with a positive, porous electrode which covers the low temperature/pressure surface of the BASE, and with the high temperature liquid sodium, the negative electrode. When the circuit is closed, sodium ions are conducted through the BASE, due to the difference in vapor pressures (or chemical activity) across the BASE, while electrons flow to the porous electrode surface through the circuit load, thereby performing electrical work. A return line and an electromagnetic pump circulate the sodium working fluid through the AMTEC cycle.

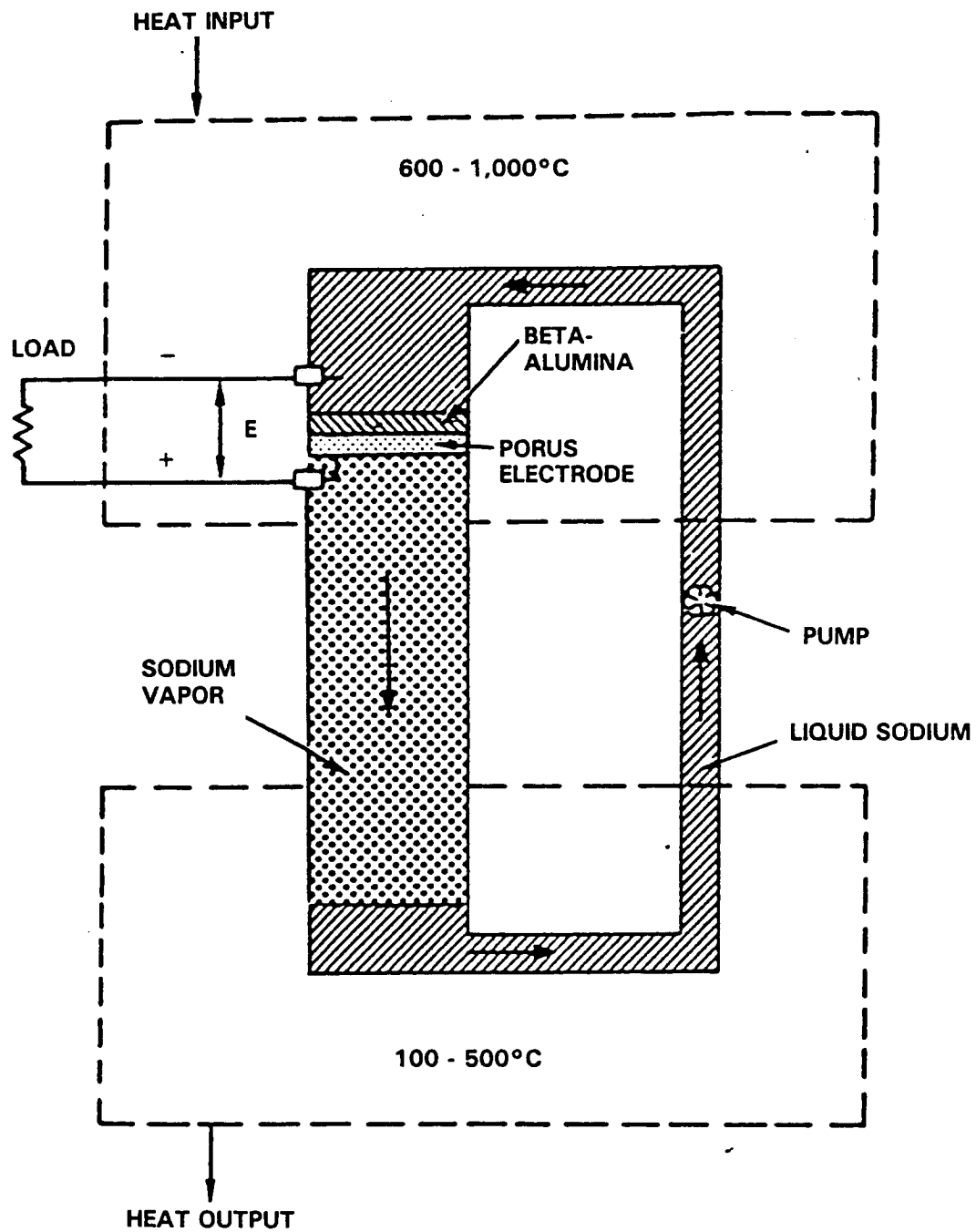


Figure 4.14. Thermodynamic Cycle of the AMTEC

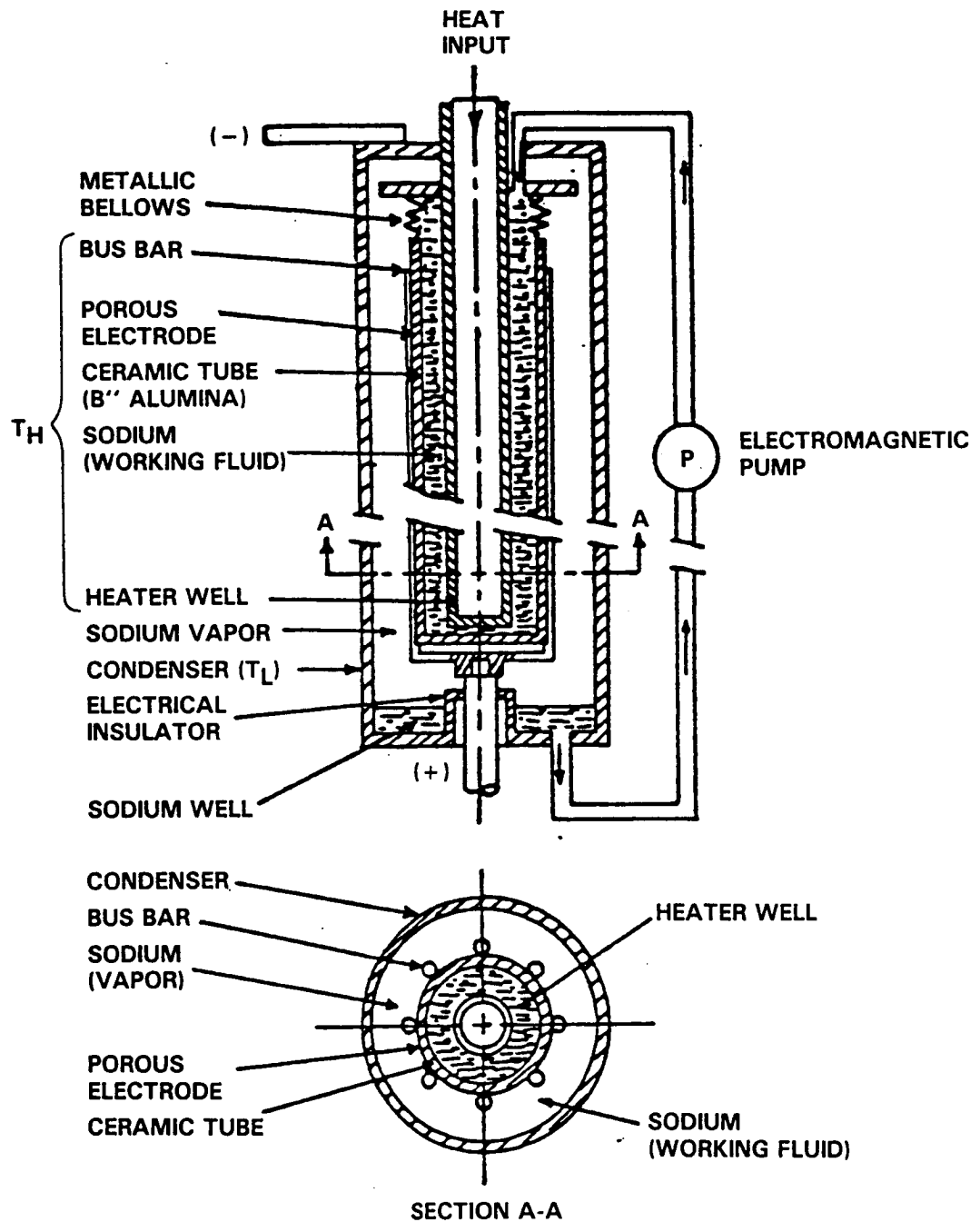


Figure 4.15. Schematic Diagram of the AMTEC Engine

Work on the AMTEC concept has to-date been focused on the development of a suitable electrode, with high power efficiency and long life and on production of suitable beta"-alumina electrolyte shapes. JPL has built a test cell for this purpose. Electrode compositions which had been studied include pure metals, alloys, cermets, oxides and borides. Thin film molybdenum and a cermet composed of a mixture of molybdenum and BASE powder appear at this point to be the most promising materials.

The molybdenum electrode is deposited as a porous thin film (1-3) usually by means of magnetron sputtering, on the outer surface of the tubular solid electrolyte. Alternatively beta/molybdenum electrodes are flame-sprayed at the same location. In the case of the thin film molybdenum electrode, power densities are initially very high (near the theoretical value) but the power output decays by a factor of three to five in the first 1000 hours of operation. For the cermet electrode, power densities are much lower initially, but have been observed to remain stable for up to 10,000 hours of operation (Hunt, 1983). Present research is directed mainly towards maintaining the high initial output of molybdenum electrodes after they have "matured," though some efforts are also being made to improve the initial power density of the cermet electrode. JPL has discovered that treating a "matured" molybdenum electrode with pure oxygen will restore 90% of the original output.

4.6 THE AMTEC SOLAR PLANT

Applications and design studies of the AMTEC have been rather limited. Subramian and Hunt (1982 and 1983) have studied the possibility of placing an AMTEC at the focus of a solar tracking parabolic dish. They concluded that the weight and cost of a 20 kW solar AMTEC system would be significantly lower than any other heat engine/generator combination being considered for

solar-to-electric conversion. Predicted efficiencies are near 30% in the AMTEC system and would reach 40% when a Rankine bottoming cycle is added. The Solar Energy group of the Sandia National Laboratories is now studying the integration of systems including the solar collector, the AMTEC and the heat rejection radiator. This group is also developing a device conceptually similar to the AMTEC but utilizing mercury as the working fluid.

An interesting possibility of using lunar materials in AMTEC systems is offered by the fact that the so-called KREEP minerals, which are common on the moon's surface, contain 6-7% by weight of potassium. According to N. Weber and other researchers, a beta"-alumina electrolyte with K instead of Na as a component of the crystal lattice is easy to produce and would permit the use of liquid potassium as a working fluid. This would probably also increase the high-performance life of molybdenum electrodes, since K is chemically less active than Na.

4.6.1 THE AMTEC-RANKINE COMBINED CYCLE

Experiments have shown that the efficiency of the AMTEC cycle is not sensitive to condenser temperature variations in the range of 100-500°K. Also, heat transfer from the condensing sodium liquid is very efficient (85-95%) at this temperature. These two facts lead to consideration of a combined AMTEC-Rankine cycle. This combination would have three to eight percent higher efficiency than either the advanced Brayton-Rankine combination or any Stirling engine.

The efficiencies of the near term and advanced AMTEC, as well as of the AMTEC-Rankine combined cycle are illustrated in Figure 4.16 as a function of receiver temperatures. The efficiency of this system reaches a maximum in the receiver temperature range of 1200-1300°K, with a condenser temperature of 500°K.

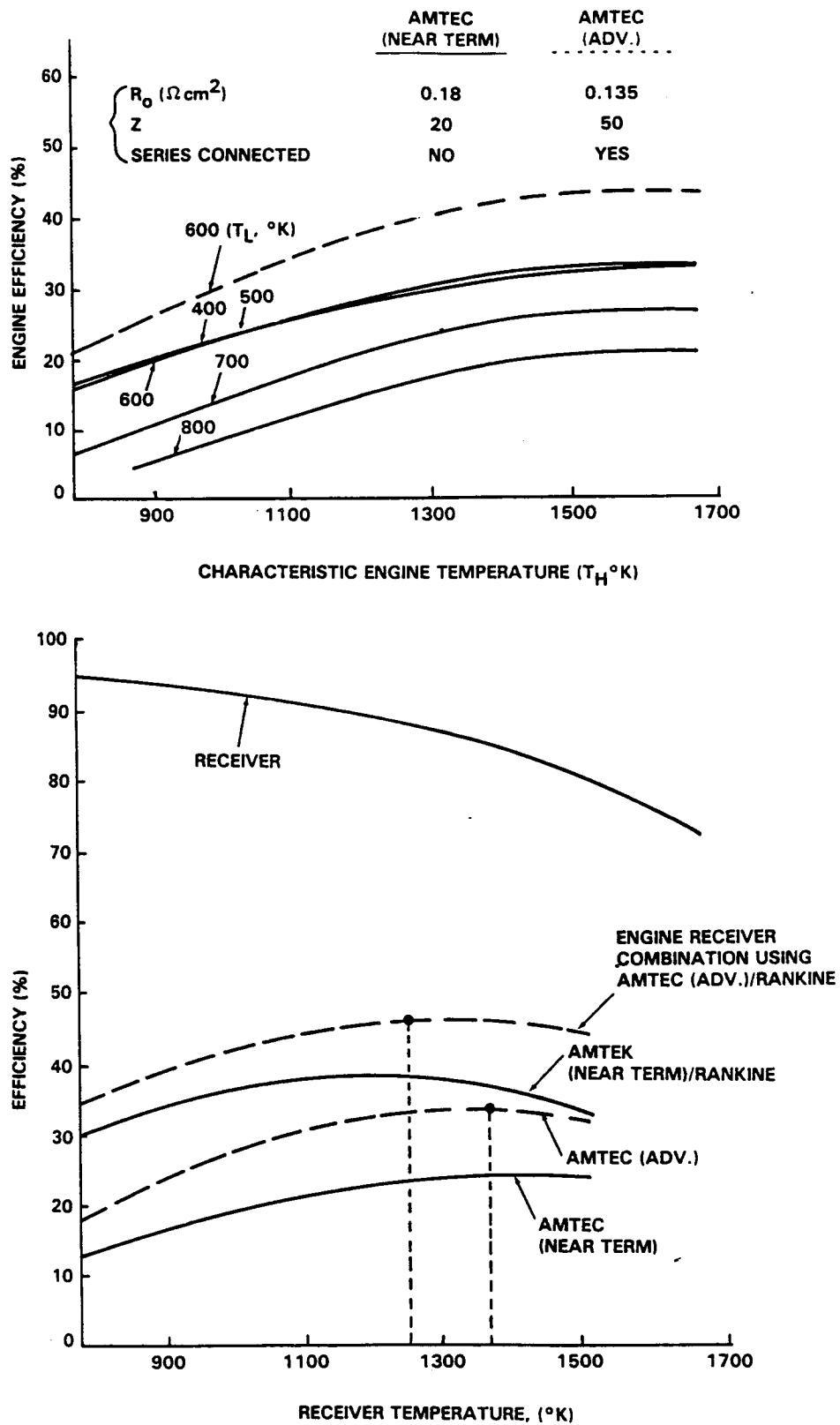


Figure 4.16. Top: AMTEC Efficiency vs. Engine Temperature
Bottom: AMTEC Receiver Combination and Receiver Efficiency vs. Receiver Temperature

Thus, an advanced AMTEC-Rankine system can achieve an overall heat-to-electricity conversion efficiency of around 41%. Moreover, storage of the thermal energy rejected by the AMTEC during the lunar day would permit operation of the Rankine engine during the lunar night.

Summing up, its high potential efficiency, low weight, low system pressures with no moving parts, high modularity and potentially long life are attractive features of the AMTEC, making it a promising candidate for application in a lunar power plant.

4.6.2 EFFICIENCY AND LOSS MECHANISMS

The ideal thermodynamic efficiency of the AMTEC cycle is 92% of the Carnot cycle efficiency (Ref. 4). The relationship below gives this efficiency, including major losses (Ref. 5).

$$\eta = \frac{W}{W + L + \Delta H + K (T_H - T_L) + \frac{\sigma}{Z} (T_H^4 - T_L^4)}$$

W is the work output, L is the latent heat of vaporization of Sodium, ΔH is the enthalpy change on heating Sodium from T_L to T_H , K is the thermal conductivity of the output leads, σ is the Stefan-Boltzmann constant, and Z is the radiation reduction factor. The radiative heat loss from the electrode to the condenser surface must be minimized in order to achieve higher device efficiencies. If the reflectivity of the electrolyte with a molybdenum coated porous electrode is 0.87, and that of a polished stainless steel condenser surface is 0.92, a value of 19 for the radiation reduction factor can be calculated (Ref.4). However, a film of condensing liquid sodium, with a reflectivity of 0.98 covers the condenser surface and results in higher Z values on the order of 56.7. Figure 4.17 (Ref.4) illustrates the

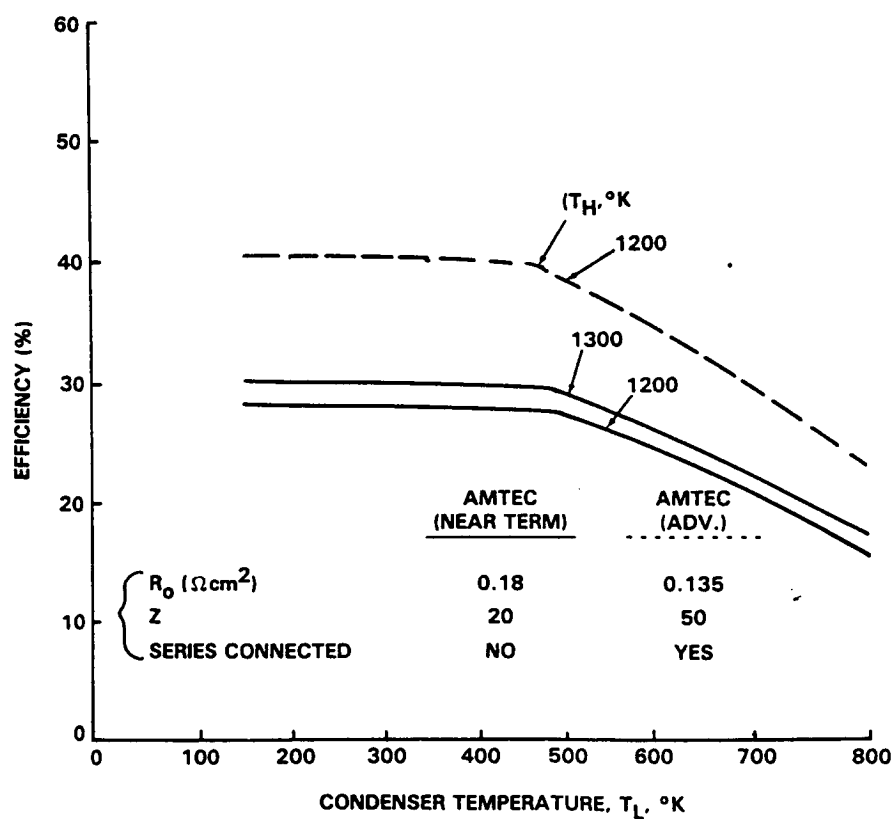
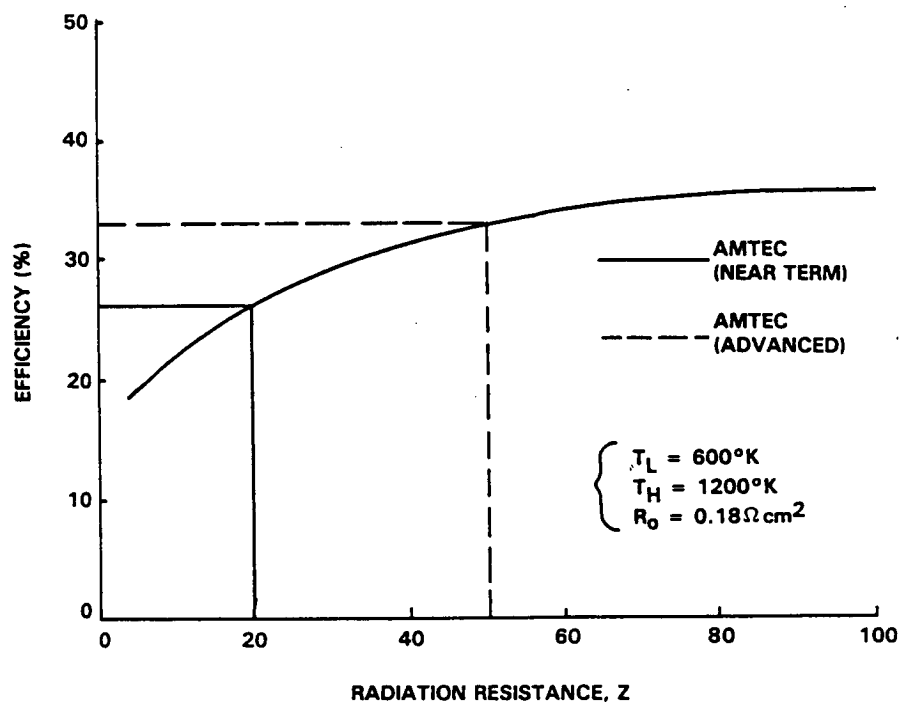


Figure 4.17. Top: AMTEC Efficiency as a Function of Radiation Resistance
Bottom: AMTEC Efficiency as a Function of Condenser Temperature

device efficiency of the AMTEC as a function of radiation resistance. A radiation shield between the electrode and the condenser will result in a reduction of radiation losses, but it will also lead to an increase in pressure at the porous electrode, and corresponding decrease in cell voltage. Another factor affecting the performance of the AMTEC is the internal resistance of the cell. Current values are on the order of 0.18 Ohm/cm², and future improvements are projected to reduce this value to around 0.135 Ohm/cm².

4.7 HEAT ACQUISITION AND WASTE HEAT REJECTION

A lunar power plant utilizing solar radiation as the primary energy source would require a heat acquisition and a waste-heat rejection system. The lunar day/night cycle and the large temperature differences between day and night (250°K) would also dictate the need for a reliable storage system.

The heat acquisition system, Figure 4.18, would typically include a solar concentrator, a cavity absorber and orientation mechanism. Waste heat rejection can take place in a conventional radiator or it can be effected by more sophisticated methods, such as the harenodynamic cooling and liquid droplet systems discussed later on.

Storage of thermal energy is conceptually simpler and more reliable than electric storage and leads logically to the possibility of utilizing a high temperature engine during the lunar day and a lower temperature engine during the lunar night.

Concentrated solar thermal radiation can result in source temperatures of over 1000°K. The concentrator can easily be controlled so as to follow the sun's course over the moon's sky. Solar energy is only limited by the 14-earth-day lunar cycle, the

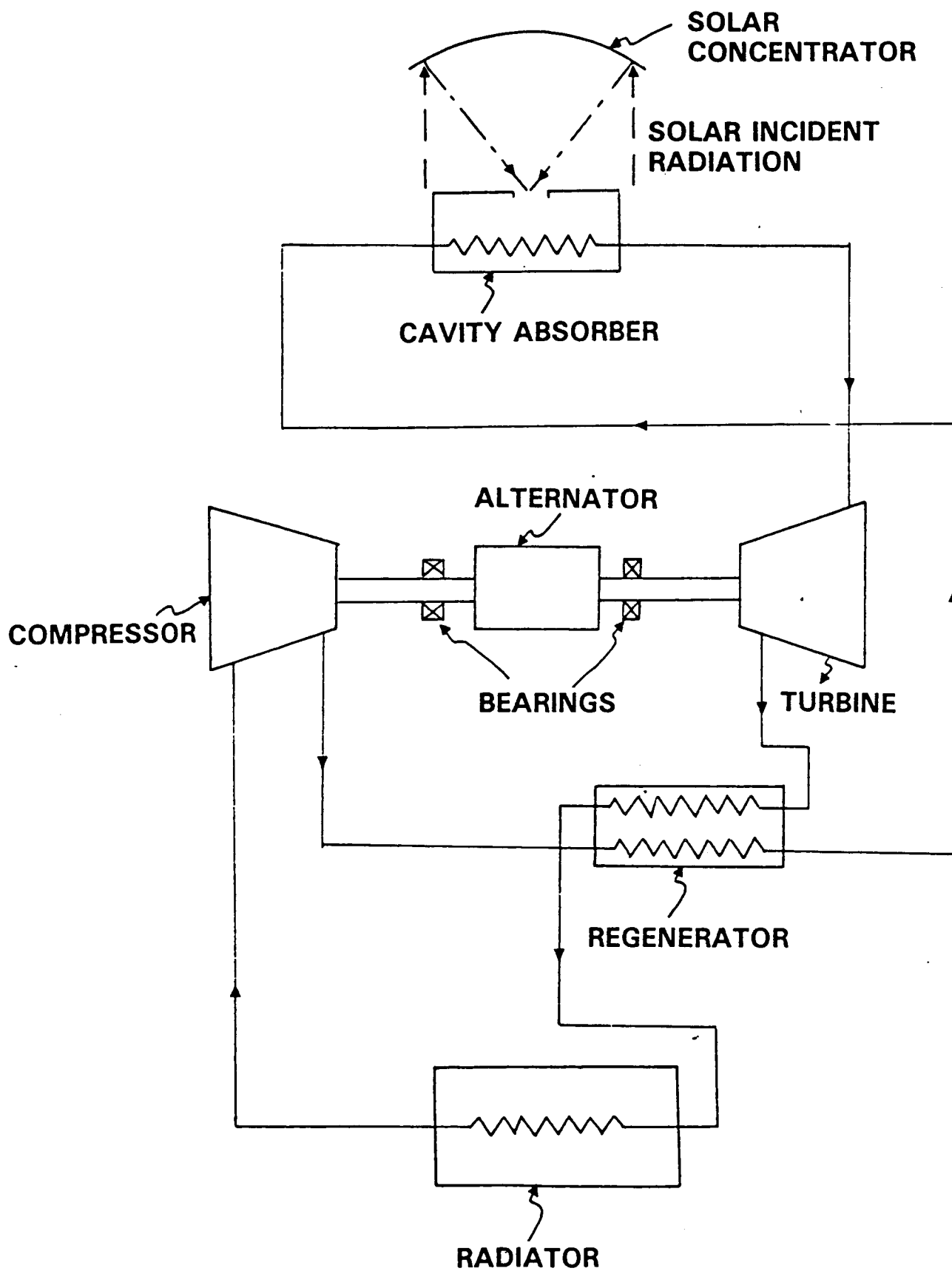


Figure 4.18. Schematic of the Energy Conversion System

variable incident sun angle and the insolation constant, approximated to be around 1353 W/m^2 .

Utilization of a heat engine for electric power generation leads to the problem of removing large amounts of waste heat from the cycle. Figure 4.19 demonstrates the amount of heat rejected by a 100 kW engine as a function of thermal efficiency. This figure shows the importance of increased thermal efficiencies and leads to important design considerations concerning the size and nature of the heat rejection device. A rough preliminary comparison of component efficiencies, thermodynamic efficiencies, and the size of heat rejection devices for Stirling, Brayton, Rankine and AMTEC systems is presented in Figure 4.18.

The radiator is potentially a relatively large portion of the closed cycle space power plant. The size and weight of the radiator varies inversely with the fourth power of its temperature. Therefore, at a given heat rejection rate, it is desirable to operate the radiator at as high a temperature as feasible. However, cycle efficiency decreases as the ratio of maximum cycle temperature to radiator temperature is reduced. Thus, an analysis to determine a minimum weight system must include a trade-off between cycle efficiency and radiator size as the minimum cycle temperature is varied. Preliminary radiation calculations, assuming 20% overall system efficiency and a gray radiator with emissivity of 0.8, heat rejection rate of 400 kW, and radiator effective temperature of 500°K , indicate that the area of the required radiator would be over 140 square meters.

4.8 THE SOLAR CONCENTRATOR

Concentration of incident solar radiation is essential for heat engine electric power generation on the moon. The type of concentrator used depends upon the power level of the system and

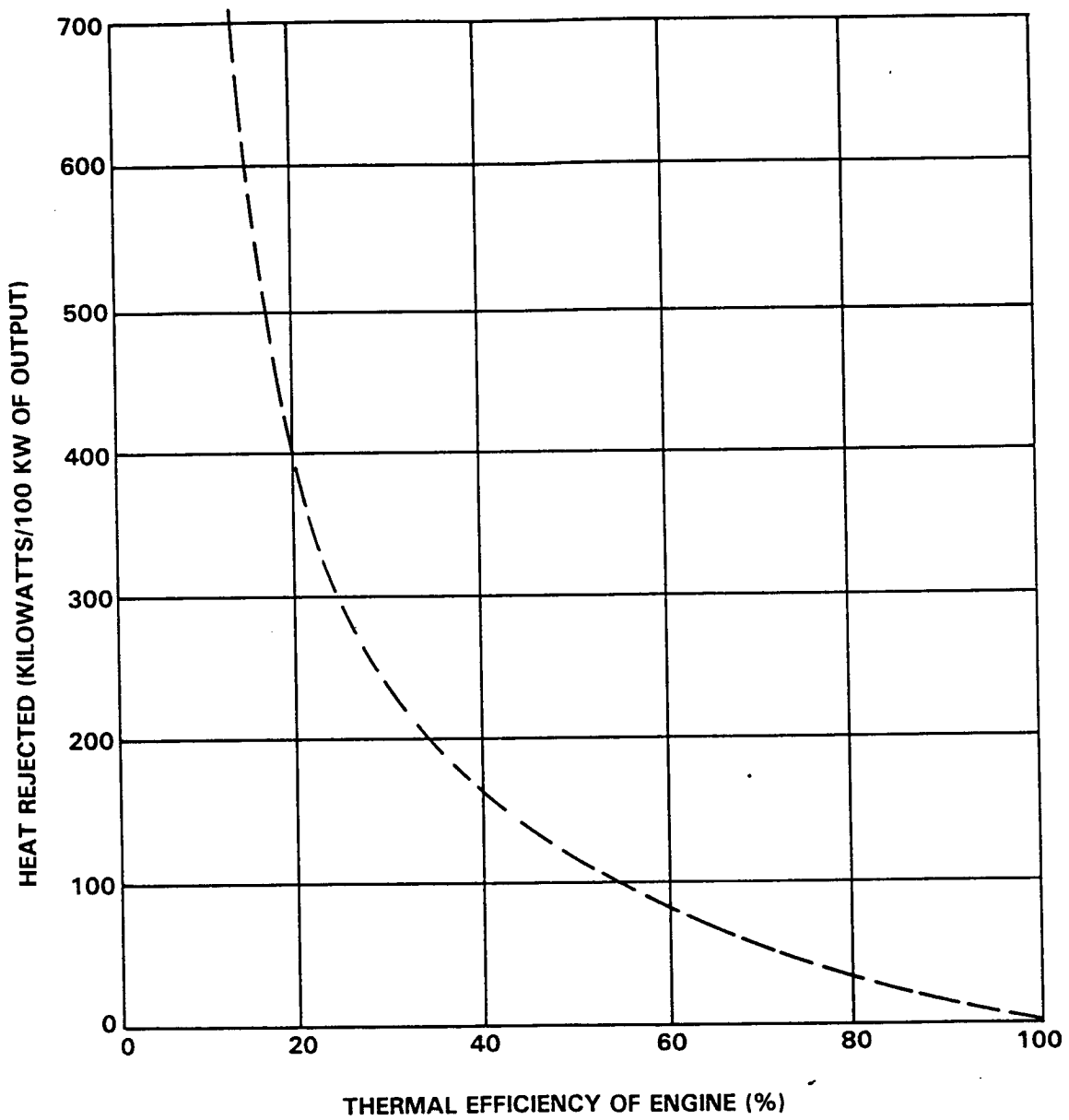


Figure 4.19. Heat Rejection from a 100 KW Engine as a Function of Thermal Efficiency

the temperature of the energy conversion device. A 2-D parabolic reflector and a 3-D paraboloidal mirror are prime candidates for solar energy concentrators. The latter has some advantages over the former because the concentration of solar energy into a small diameter cavity absorber is simpler than concentrating the same energy along a tube. Reradiation and reflection losses of the tubes will result in lower source temperatures than those achieved with a paraboloidal mirror.

Reference 10 presents an analysis of the parabolic reflector which will be briefly discussed here. The solar energy reaching the tube of the parabolic reflector is:

$$Q_m = G_{sc} B L_g N$$

G_{sc} is the solar constant, B is the width of the reflector, L_g is the length of the tube, and N is the number of parallel units (see Figure 4.20). However, due to the imperfect reflectivity of the mirror surface, geometric imperfections of the mirror, reradiation of the tube and reflection of direct solar energy from the tube, the amount of Q_m will be reduced. Defining the mirror efficiency as the ratio of net heat absorbed by the working fluid to the incident solar energy, the following relationship can be developed:

$$\eta_m = \rho_s \alpha_t F - \epsilon_T \sigma \pi T_t^4 \frac{D_o}{G_{sc} B}$$

Figure 4.21 illustrates that in order to obtain an efficiency of 70% or more, the ratio of tube diameter to mirror width (D_o/B) must be less than 0.01 and/or the tube temperature must be less than 555°K. Deposited copper oxide (Absorbitivity to solar radiation = 0.93, Emissivity = 0.11) on a highly polished surface, along with coating of the top three-quarters of the tube with a

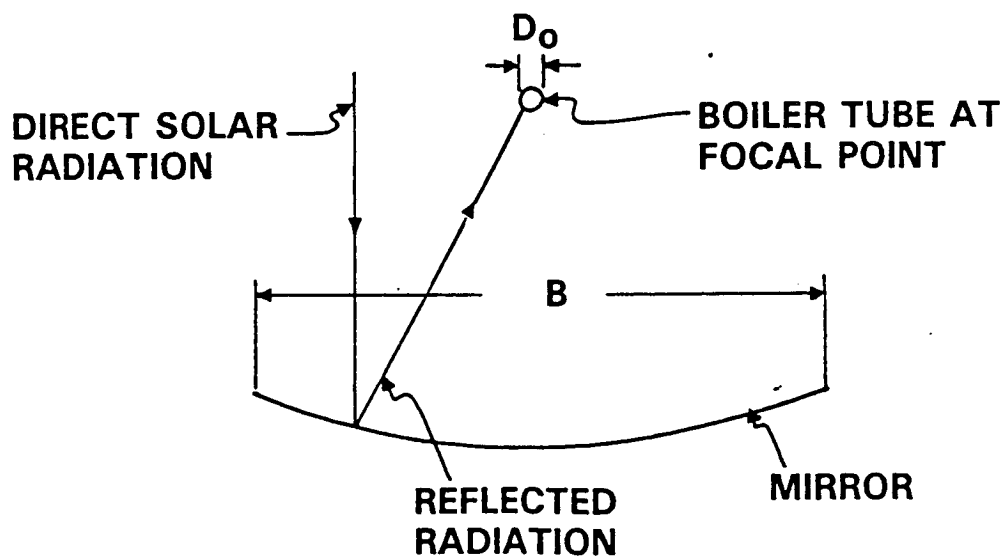
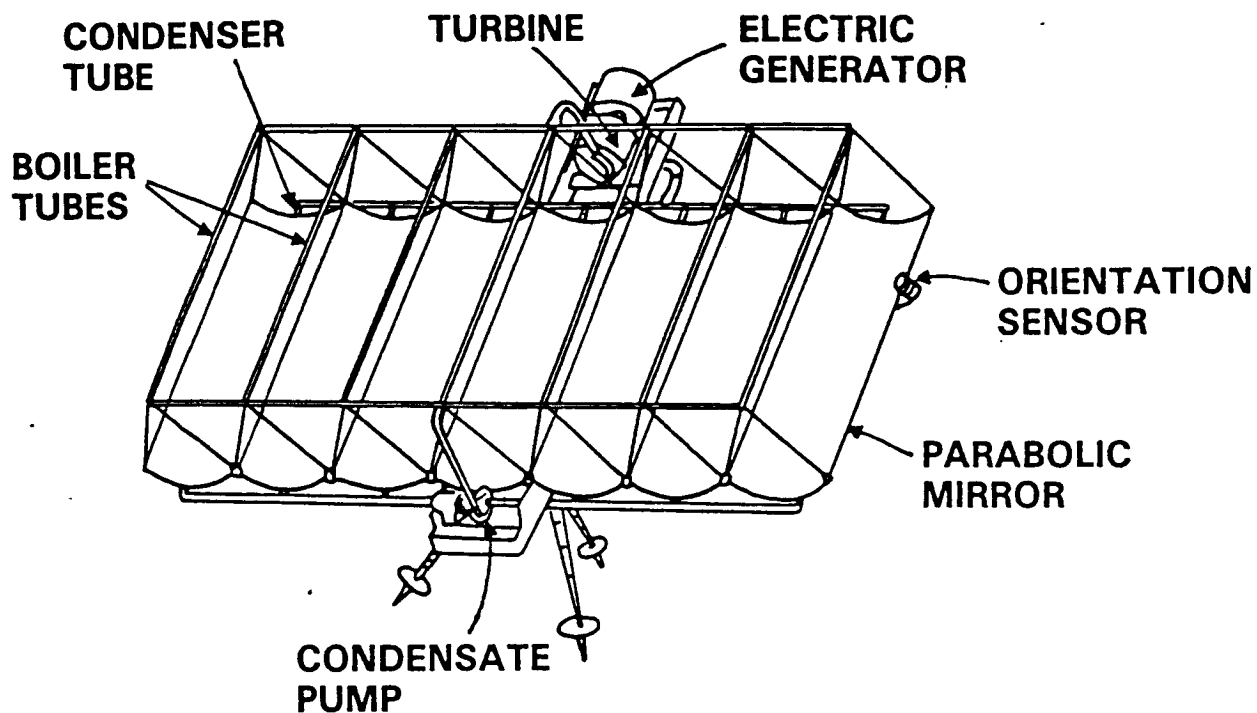


Figure 4.20. Solar Rankine Powerplant

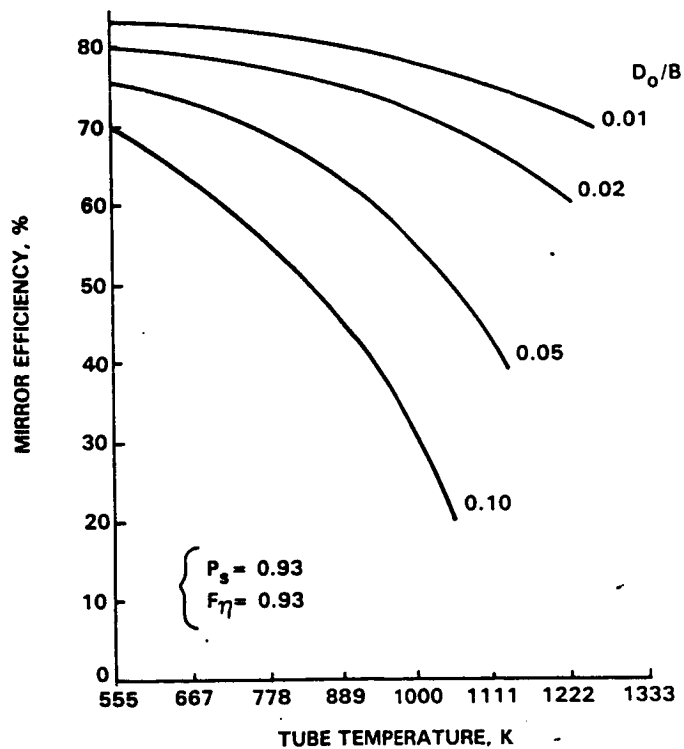
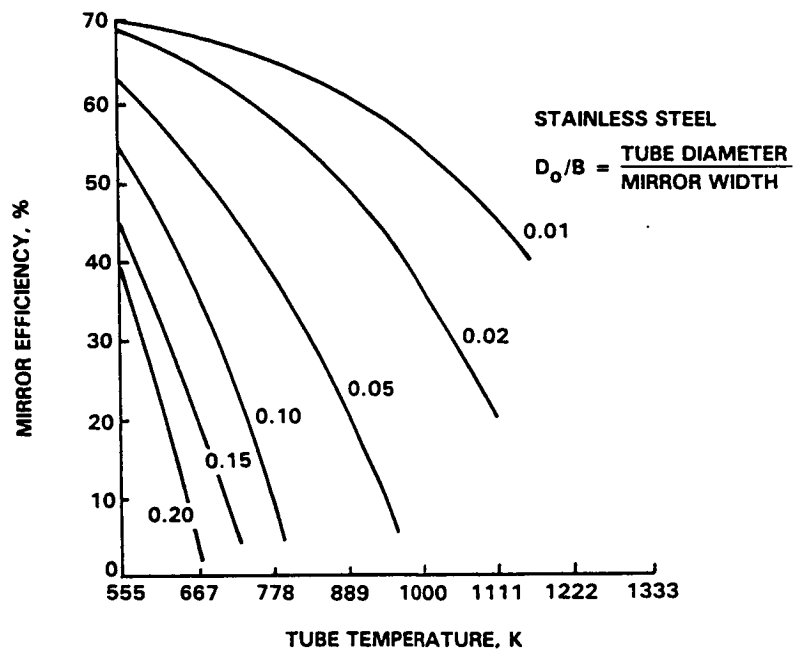


Figure 4.21. Top: Mirror Efficiency vs. Tube Temperature for Varying D_o/B
 Bottom: Mirror Efficiency vs. Tube Temperature for Varying D_o/B and Top 3/4 of Tube Silver Plated

low emissivity finish, results in improved efficiencies. However, at the high temperatures required for Stirling, Brayton or AMTEC engines, the paraboloidal mirror offers a more attractive alternative.

4.8.1 SOLAR CONCENTRATORS FOR SPACE APPLICATIONS

Previous studies (Ref. 13) have compared different types of solar concentrators with regard to unit weight, specific power, launch package volume, and operating temperatures of the energy conversion device. The concentrators considered include Fresnel, inflatable, inflatable-rigidized, one-piece, petal, and umbrella types.

The one-piece electroformed Nickel collectors, which closely approach the maximum theoretical concentrating ability, have unit weights of 4.39 to 4.88 Kg/m². The delivered energy per unit of collector weight is relatively low, but the absorber temperature is very high, (2222°K), compared to those of the light collectors. It also requires the largest packaged volume. The umbrella type collector has a low concentration ratio (25 to 400) and a temperature range of 55°K. The petal, Fresnel, inflatable and inflatable-rigidized fall in the concentration ratio range of 500 to 5000, which makes them suitable for temperature requirements in the 1000°K range. The inflatable has a very high ratio of delivered energy to collector weight (2645 W/Kg @ 1111°K, based on plastic weight only), while the petal model yields around 827 W/Kg. The inflatable paraboloidal concentrator gives relatively low concentrator and combined concentrator/absorber efficiencies near the concentration range of 1000 and temperatures of 1111°K. The unit weight for various types range from 0.146 Kg/m² for the inflatable to 2.25 Kg/m² for Fresnel. The inflatable-rigidized type concentrator has the most favorable packaged volume of any concentrator, especially in the larger

sizes. The inflatable-rigidized type provides moderate concentrator/absorber efficiencies, and a unit weight of 0.98 Kg/m² (Diameter less than 9.1 m). The following section provides a detailed analysis of the inflatable-rigidized concentrators.

4.8.2 INFLATABLE, FOAM-RIGIDIZED SOLAR CONCENTRATOR

An inflatable, foam-rigidized solar concentrator can be packaged in lightweight, small-volume units for launching and can be deployed as efficient, long-life energy collection subsystems for solar thermal power stations on the moon.

The advantages of inflatable, foam-rigidized concentrators are: 1) High deployed-to-packaged volumetric ratio, 2) low mass, 3) excellent potential for long-time, reliable, service-free operation in the lunar environment. Figure 4.22 illustrates the weights and packaged volumes for various diameters.

Before deployment, the foam-rigidized type of concentrator is completely flexible and can be efficiently folded and stowed. Two basic approaches to space rigidization of paraboloid concentrators exist (Ref. 12, 14, 18). The first uses a foam generator, which mixes the foam constituents and forces the foam through flow passages to cover the concentrator back surface. The second method uses a precoat material, which is applied to the concentrator back surface on the ground and subsequently hardens on exposure to the space environment. The latter method is preferred because of its simplicity.

A transparent overcoating applied to the reflecting surface changes the thermal emissivity of the surface and aids in temperature control. The radiation properties of two samples of vacuum-aluminized Mylar coated with silicon oxide are given in Reference 12. The samples were exposed to ultraviolet radiation

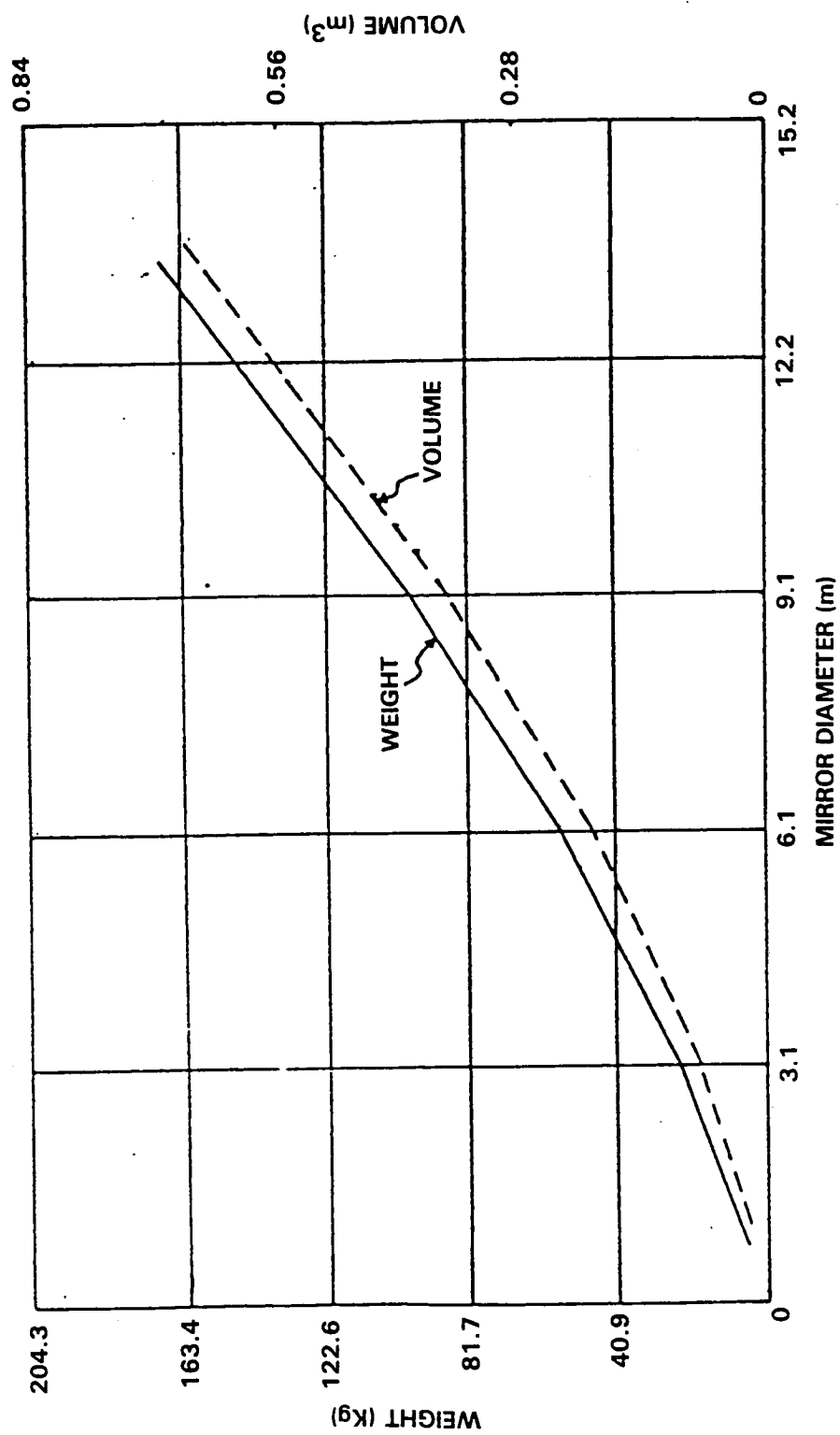


Figure 4.22. Weight and Packaged Volume of Inflatable, Foam-rigidized Concentrator as a Function of Mirror Diameter

in a vacuum and to elevated temperatures with no change in properties. The table below presents the radiation properties of coated Mylar.

<u>Specimen</u>	<u>Thickness, M</u>	<u>Solar Absorption</u>	<u>Emmittance</u>	<u>Ratio of</u>
A	1.63	0.252	0.438	0.575
B	1.00	0.253	0.148	1.71

4.8.3 PARABOLOIDAL DISH CONCENTRATORS

The paraboloidal dish-type concentrator, as illustrated in the previous sections, is the best suited concentrator for high temperature Stirling, Brayton or AMTEC engines. The concentrated solar radiation passes through the aperture of the receiver into its cavity, where the solar energy is absorbed and transmitted to the working fluid of the heat engine. Figure 4.23 illustrates a parabolic dish concentrator module.

There is a tradeoff between optical efficiency (ratio of energy passing through the aperture to energy incident on the concentrator) and geometric concentration ratio (ratio of aperture area to concentrator projected area) through the intercept factor (ratio of energy intercepted by the aperture to the energy incident on the infinite focal plane). Increasing the aperture size results in higher optical efficiency, but also increases radiation losses. In general, intercept factors greater than 0.9 are desirable for high-temperature receivers.

Figure 4.24 (Ref. 7) illustrates the fact that higher geometric concentration ratios are required, at increased receiver temperatures, to achieve reasonable collector (concentrator + receiver) performance. At high temperatures, small receiver apertures are desired to minimize the re-radiation losses.

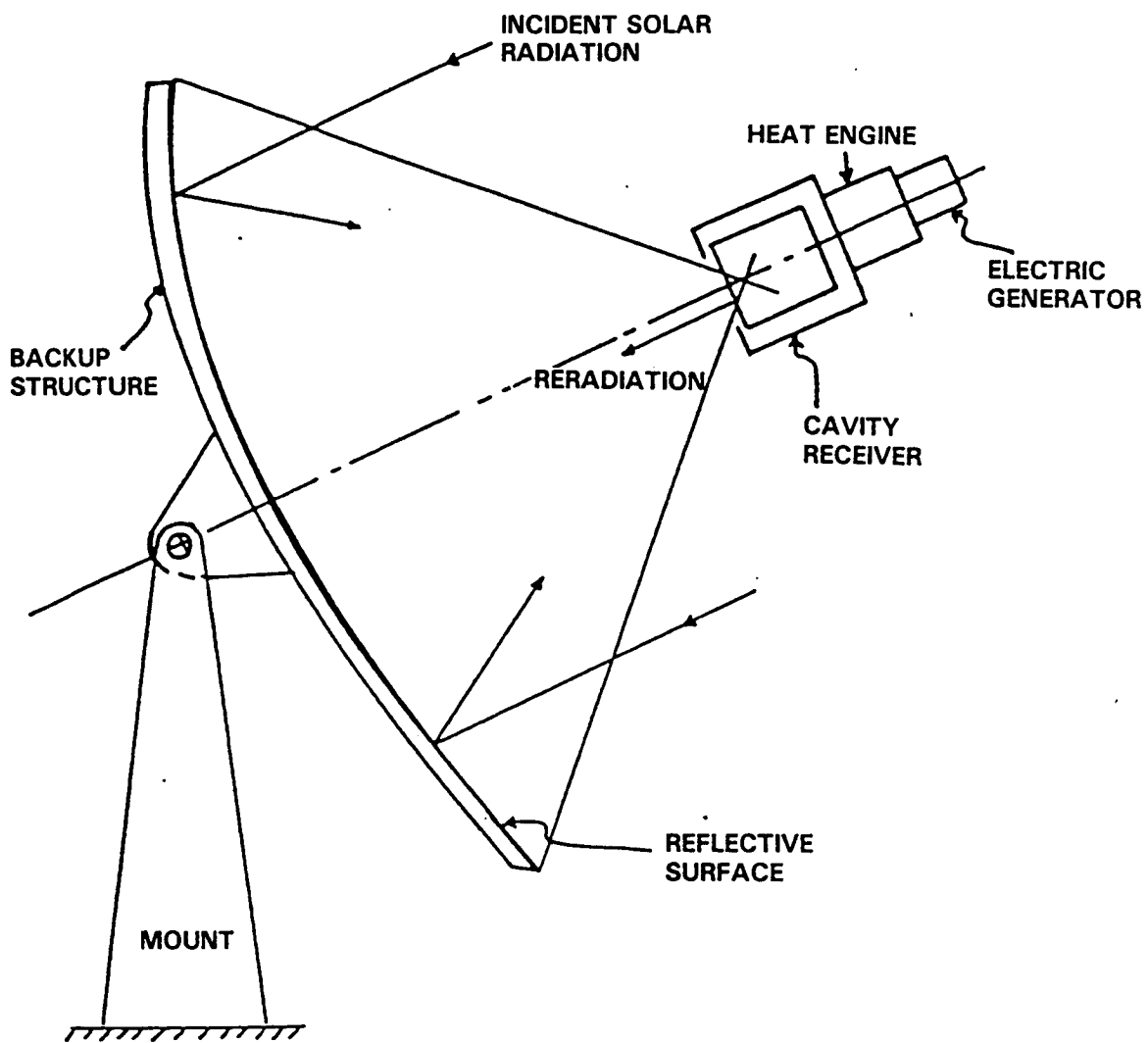


Figure 4.23. Schematic of Parabolic Dish Power Module

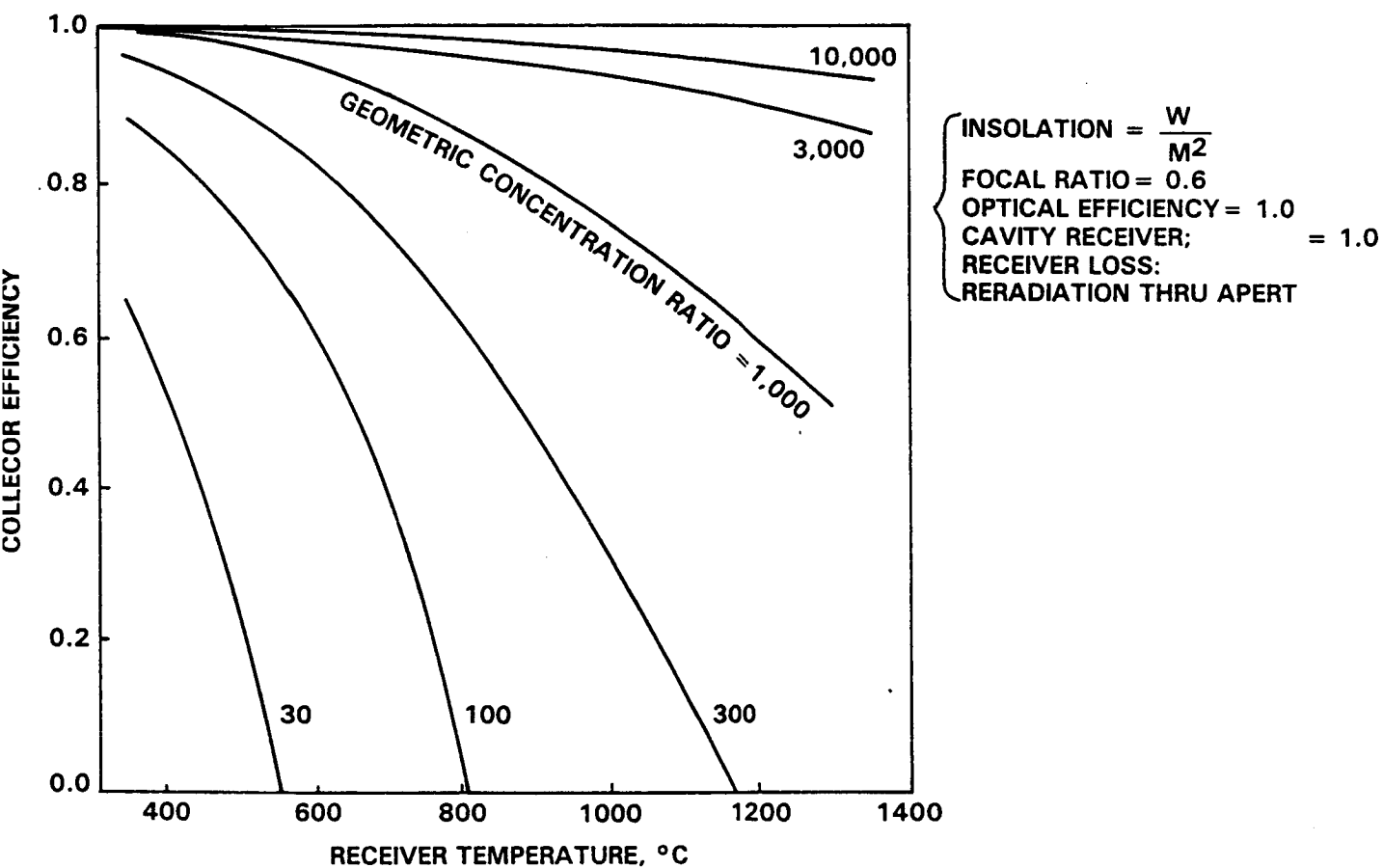


Figure 4.24. Effect of Geometric Concentration Ratio and Receiver Temperature on Collector and System Efficiency

Factors affecting the performance of a concentrator includes its geometrical configuration, critical thermo-optical properties, and tracking/pointing accuracy. Solar reflectance and specular-ity are fixed by mirror material selection. Surface degradation affects the reflectance properties of the mirror. Surface slope error is the most significant parameter governing the optical performance of the solar concentrator. This factor can be a result of surface waviness, imperfect alignment and slope errors due to manufacturing tolerances and structural deflections. Other design concepts such as the Cassegrain type, which uses a secondary mirror to reflect the concentrated radiation onto the receiver, may have some advantages for space applications and will be discussed in another section.

4.8.4 CONCENTRATORS, OPTICAL AND THERMAL CHARACTERISTICS

The Acurex Corporation has designed a high-flux, 12.2m dish with a thermal output of 96.5 KW (PDC-2, Ref. 15). The concentrator consists of a lightweight space-frame structure and 64 high accuracy reflective panels. The structurally efficient panels consist of cellular glass cores between thin back-silvered mirror glass on the front and unsilvered glass on the back. The table below presents the characteristics of the PDC-2.

Aperture Diameter, Meters	12.2
Focal Length to Aperture Diameter Ratio (f/D)	0.54
Receiver Aperture Diameter, Meters	0.25-0.38
Thermal Output Power, Kw	96.5
Solar Insolation (at lunar surface) Watts/m ²	1353
Design Life, Years	20

Figure 4.25 illustrates the PDC-2 concentrator.

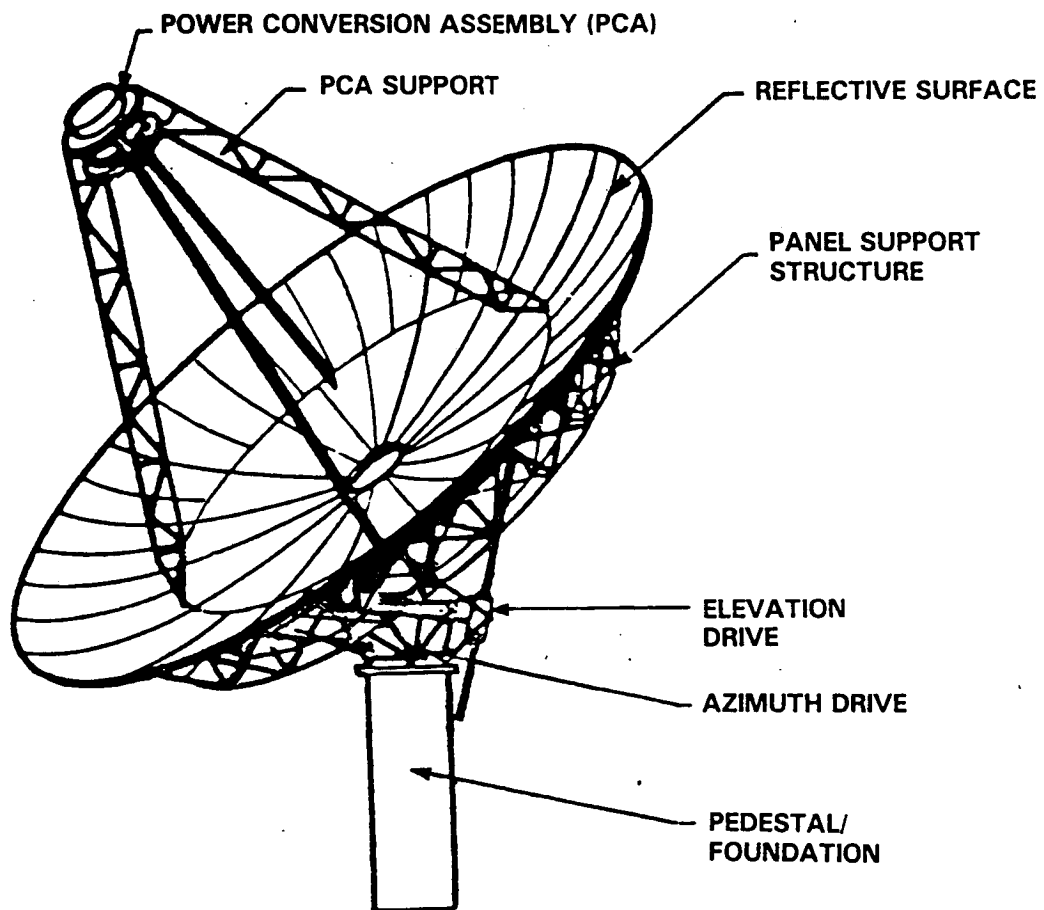


Figure 4.25. PDC-2 Solar Concentrator

Entech, Inc. has developed a point-focus Fresnel lens solar concentrator for high temperature solar thermal energy system applications (Ref. 16, Figure 4.26). The concentrator uses a transmittance-optimized refractive Fresnel lens as the optical element. The concentrator, which is suitable for high temperature engines, has a diameter of 11 m, and an overall collector (solar-to-thermal) efficiency of 71% at a receiver temperature of 1100°K, and a geometric concentration ratio of 1500. The table below summarizes its optical and thermal performance.

<u>OPTICAL PERFORMANCE</u>	<u>STIRLING-BRAYTON</u>	<u>RANKINE</u>
Geometric concentration ratio	1500	500
Lens transmittance	90%	90%
Receiver intercept factor	92%	99%
Blocking/Shading factor	94%	94%
Overall optical efficiency	78%	83%

THERMAL PERFORMANCE (at 800 W/m² Insolation)

Receiver cavity temperature, °K	1088	644
Receiver radiation thermal loss, KWth	5	2
Collector net output, KWth	54	61
Collector overall efficiency	71%	80%

Bomin/Solar has developed lightweight, foil-membrane mirrors, which are placed under a protective dome (Ref. 17). Plane mirror foil stretched over hollow, drum-shaped bodies, and a slight over or under-pressure inside the hollow body create a good approximation of a paraboloidal dish. Figure 4.27 (a) is a schematic illustration of this concentrator and Figure 4.27(b) is the optical flow diagram. Performance of this concentrator for mirrors of three meter and ten meter diameters is shown in Table 4.8.1.

Previous studies (Ref. 4) regarding auxiliary power generating systems for a large space laboratory, have compared different

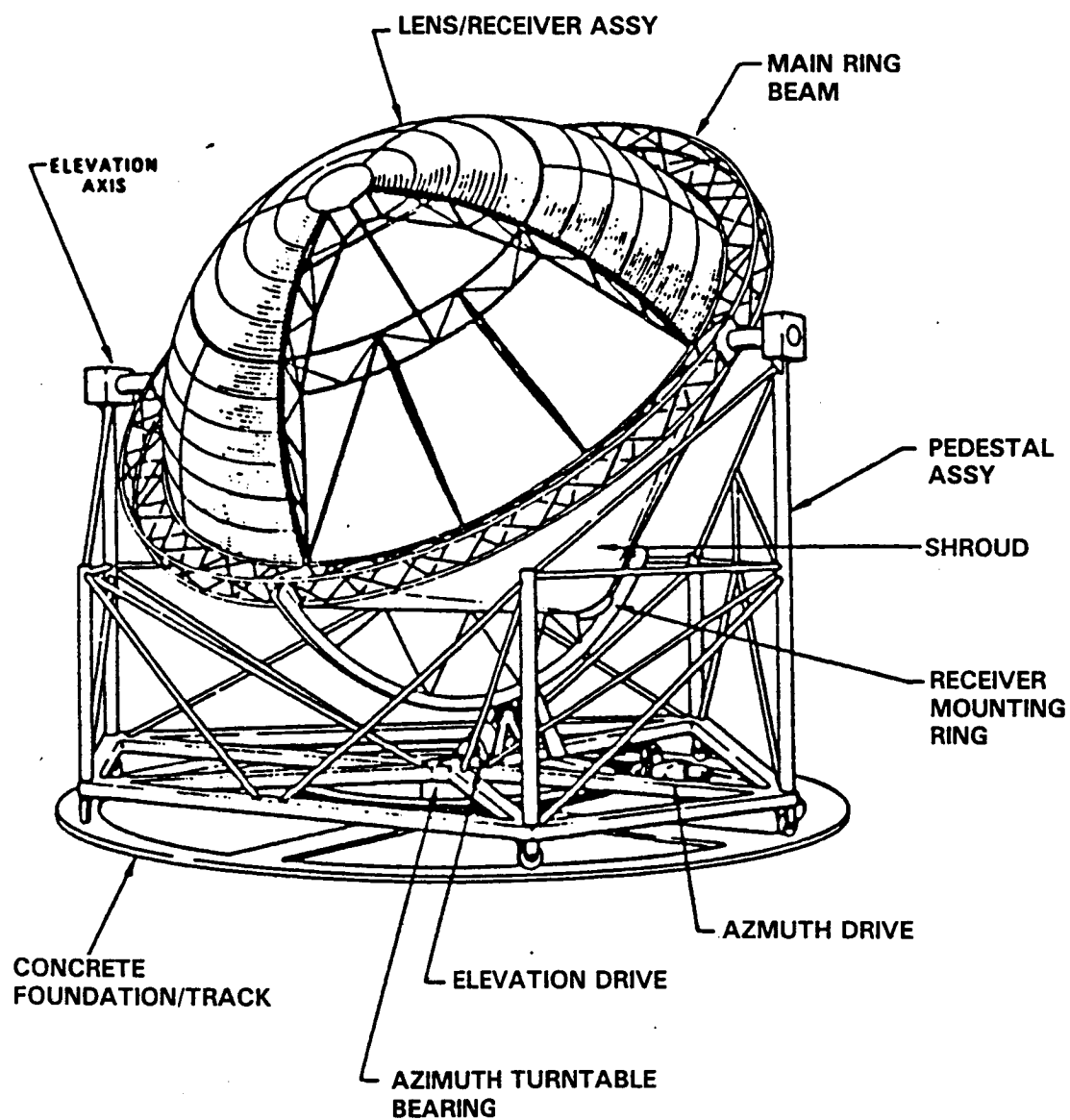
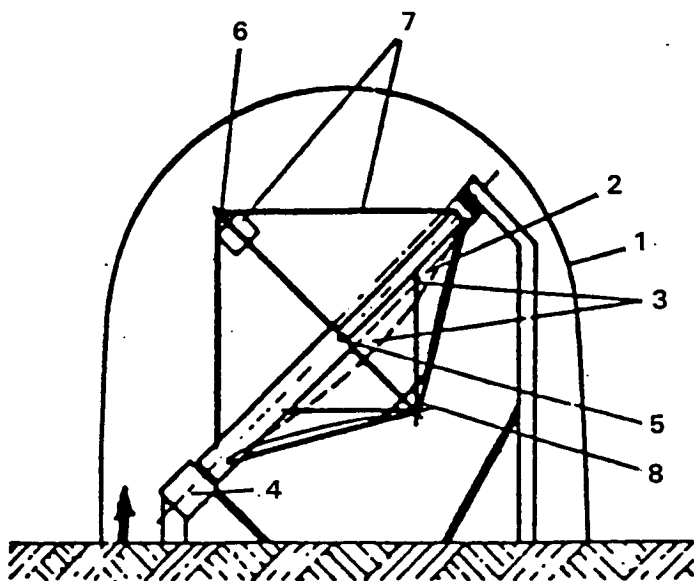


Figure 4.26. Point Focus Fresnel Lens Concentrator

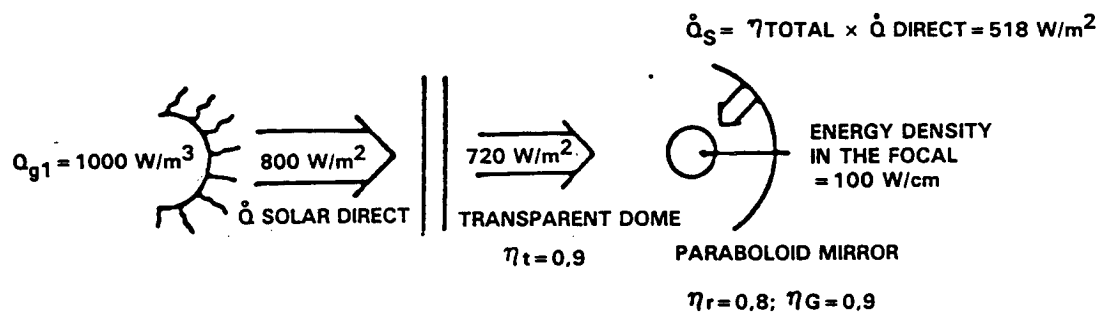


PROFILE THROUGH THE BACK

- 1 TRANSPARENT DOME
- 2 MIRROR FOIL
- 3 UNDERPRESSURE HOLLOW BODY
- 4 DAILY TRACKING AXIS
- 5 SEASONALLY TRACKING AXIS
- 6 TRACKING ELECTRONIC
- 7 UNDERPRESSURE SENSOR
- 8 RECEIVER AND ATTACHMENT

THE SYSTEM'S OPTICAL PERFORMANCE

(a)



$$\eta_{TOTAL} = \eta_t \times \eta_r \times \eta_G = 0.648$$

OPTICAL FLOW DIAGRAM

(b)

Figure 4.27. Bomin/Solar Concentrator

Table 4.8.1. TECHNICAL PERFORMANCE OF TWO PARABOLOIDAL SYSTEMS

Diameter of the mirror	3m	10m
Surface of the mirror	7.06 m ²	78.5 m ²
Weight of the mirror	approx. 200 kg	approx. 2000 kg
Weight of the protective dome approx.	200 kg	approx. 2000 kg
Material of mirror and cover	HOSTAFILON-ET	HOSTAFILON-ET
Focal length F: variable	1.5 m	5
Concentration factor C	<2000	<2000
Transparency t of protection cover	0.9	0.9
Reflectivity r of the mirror membrane	0.8	0.8
Performance factor G of the mirror	0.9	0.9
Optical efficiency of the mirror r x G	0.72	0.72
Thermal power in the hot spot (with 800 W/m ² direct insolation)	3.7 kW	40.7 kW
Efficiency ratio of the receiver	0.8	0.8
Efficiency ratio of the Stirling generator	0.3	0.3
Electric output of the Stirling engine	0.9 kW, AC	10 kW, AC
Thermal output (100°C) of the Stirling engine	1.75 kW	20 kW
kg material installed/kW output	approx. 450 kg	approx. 400 kg
kg material installed/kW + kW _{therm} output	approx. 150 kg	approx. 140 kg

solar dynamic systems on the basis of system mass, concentrator area, radiator area, and cost of different systems. The results for outputs of 27 and 40 kW are presented in the table below:

27 kW

<u>System</u>	<u>Mass, kg</u>	<u>Concentrator area, m²</u>	<u>Radiator area m²</u>
Stirling	3400	320	146
Brayton	2600	360	152
Rankine	2900	540	24

40 kW

Stirling	4700	465	215
Brayton	3100	520	220
Rankine	3750	770	35

Even though the Rankine engine offers minimum radiator area and low system mass, the moderate ratio of temperatures at which heat is added and rejected will reduce its efficiency and considerably increase the amount of heat rejection, and hence the radiator area, in the lunar environment.

The AMTEC engine is in its early stages of development and cannot be compared with equal detail. However, theoretical considerations indicate that a 40 kW system could have a mass of less than 1000 kg, with concentrator and radiator areas comparable to those of the Brayton engine.

4.9 SOLAR ABSORPTION

The solar absorber is an important component of the solar power-plant, since it links the concentrated solar radiation to the

heat engine. It is essential to increase the efficiency of the absorber and to reduce the losses. Due to the absence of free or forced convection, the primary loss mechanism is by radiative heat transfer. The factors contributing to the absorber efficiency include operating temperature, aperture size, capture geometry, absorptivity of the surfaces, emissivity of the surfaces, aperture radiation losses, heat exchanger characteristics, and insulation properties.

The cavity-type absorber is superior to flat plate and hemisphere receivers at high surface temperatures. The sun angle can be easily tracked and the solar radiation concentrated on the absorber. The cavity-absorber offers considerable design freedom because it has no intrinsic size limitations. The internal geometry of the cavity can be changed to achieve specific source temperatures. Flat plate and hemisphere absorbers radiate heat proportionally to their surface areas and do not enjoy the above advantages of cavity receivers. Also, large surface conductance between absorber walls and working fluid is required to transfer the heat from small available areas.

Proposed design improvements increase the efficiency into the over 90% range. While radiation losses are temperature dependent, the following analysis will aid in determining potential loss factors. The total power loss due to radiation can be written as:

$$R(\text{loss}) = \sigma F \epsilon T^4$$

A is the effective area, σ is the Stefan-Boltzmann constant, F is the geometrical view factor, ϵ is the effective emissivity, and T is the effective temperature. The aperture area is of prime importance in radiation losses. A decrease in aperture area will result in reduced radiation losses. A decrease in aperture area

will result in reduced radiation losses. However, this size is usually dictated by the concentrator optics. A trade-off study is required to maximize the flux received at the aperture while minimizing the radiation losses from the aperture.

The geometrical view factor out of the aperture must also be minimized. Cavity size, length to depth ratio, shape, and optical properties of the internal surface affect this analysis. These parameters will be discussed in the next section. The emissivity and absorptivity, usually fixed by material selection are also important factors and will be discussed. External optical methods such as a hyperbolic reflector can be incorporated into the absorber design in order to increase cavity input without requiring aperture enlargement. Table 4.1 represents receiver characteristics for selected Stirling, Brayton, and Rankine manufacturers.

4.9.1 DESIGN AND EFFICIENCY OF THE CAVITY ABSORBER

As mentioned before, the radiation losses from the cavity are primarily associated with reradiation from the opening since the surface of the receiver will be insulated, resulting in insignificant radiation losses from the surface. The geometrical view factor relationship for a cavity absorber (Figure 4.28) can be written as:

$$F_{11} + F_{12} = 1$$

The fraction of energy emitted by either surface and intercepted by the other can be written as:

$$B_{12} = \frac{F_{12} e_2}{1 - (1 - F_{12})(1 - e_1)} \text{ and } B_{21} = \frac{e_1}{1 - (1 - F_{12})(1 - e_1)}$$

Table 4.1 (Ref.7). Receiver Characteristics Summary of Select Manufacturers

ENGINE CYCLE	RANKINE		BRAYTON		STIRLING
	FORD	AiResearch	AiResearch	SANDERS	FAIRCHILD
MANUFACTURER					
WORKING FLUID	TOLUENE	STEAM	AIR	AIR	HELIUM
FLUID OUTLET TEMP., °K	675	980	1100	1650	1100
APERTURE DIA., cm	38	22.8	25.4	19.7	27.9
EFFICIENCY, %	70 to 90	80 to 92	70 to 80	up to 90	85 (est)
MAXIMUM PRESSURE MPa	5.5	14	0.25	0.7	14
MATERIAL	METAL	METAL	METAL	CERAMIC	METAL
BUFFER STORAGE	YES	NO	NO	YES	NO

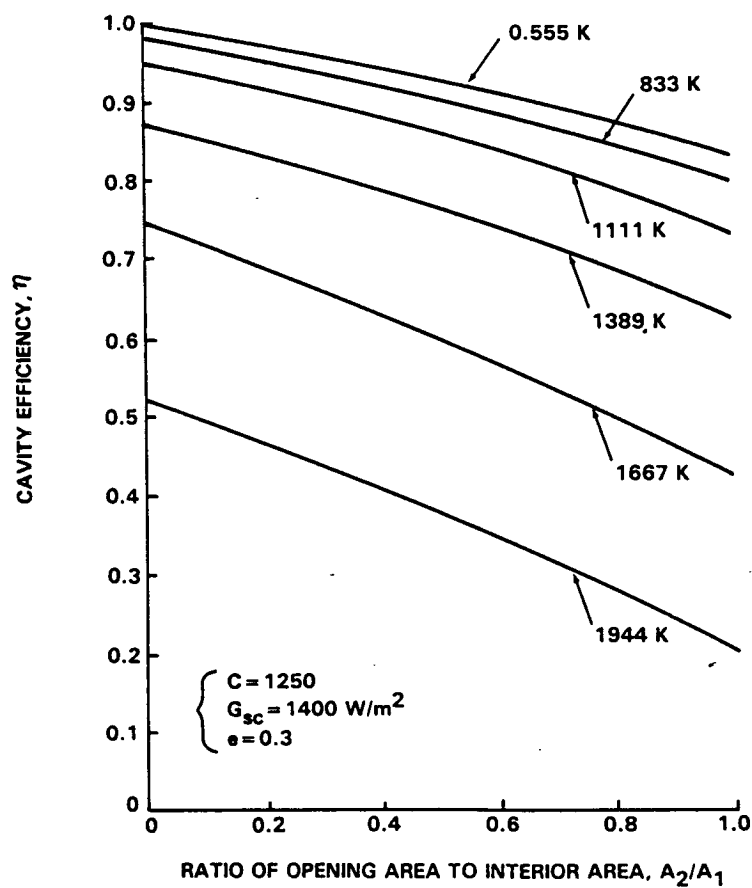
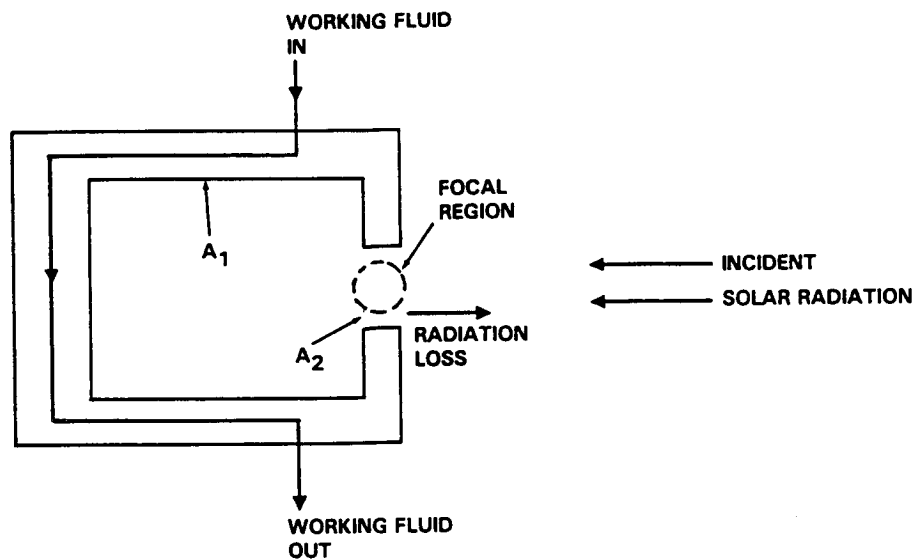


Figure 4.28. Schematic Representation of the Receiver System and Efficiency of the Cavity Absorber as a Function of the Area Ratio

To minimize losses by direct reflection as well as by reradiation, it is desirable to make F_{12} as small as possible. For values of F_{12} less than 0.06 the fraction of possible heat loss, as illustrated by Figure 4.31 is quite insensitive to variation in emissivity between 0.3 and 1.0. Figure 4.29 illustrates the solar radiation absorption capacity as a function of surface absorptivity for different values of F_{12} (Fraction of radiation passing directly out of opening after leaving surface by reflection).

The efficiency of the cavity receiver is defined as the fraction of incoming solar radiation available to heat the working fluid.

$$\eta = \frac{Q_s - Q_r}{Q_s}$$

Q_s is rate of solar radiation absorbed and Q_r is the rate of energy loss.

The cavity efficiency can now be written as: (For a detailed discussion see Ref. 9).

$$\eta = \frac{A_2 B_{21} (G_{sc} - A_1 B_{12} \sigma T_1^4)}{G_{sc} A_2 B_{21}}$$

The concentration factor C depends on the characteristics of the solar concentration system, which includes the accuracy, alignment, and surface characteristics of the reflector. These factors will be discussed in the Solar Concentrator section of this report. Figure 4.30 illustrates the efficiency of the cavity receiver as a function of the ratio of opening area to interior area for various temperatures. (For a paraboloidal mirror with $C=1250$ and a spherical cavity with a gray inner

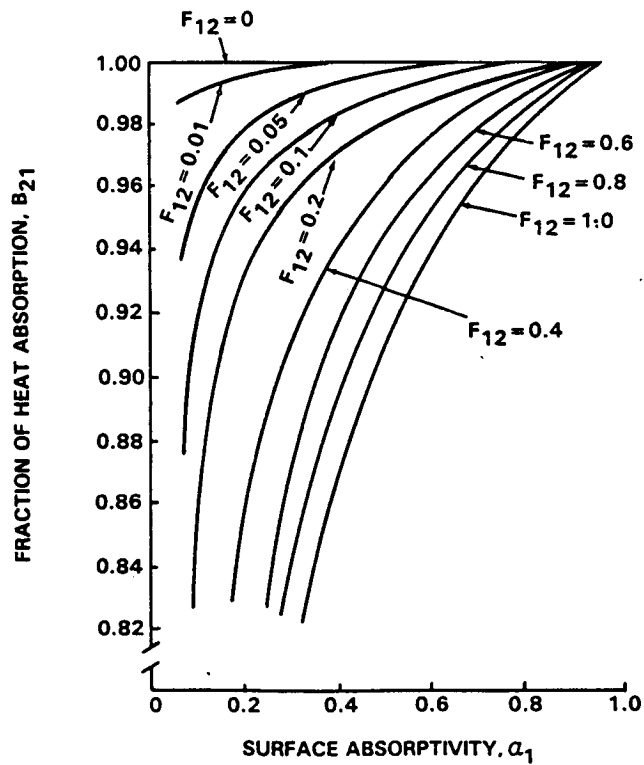
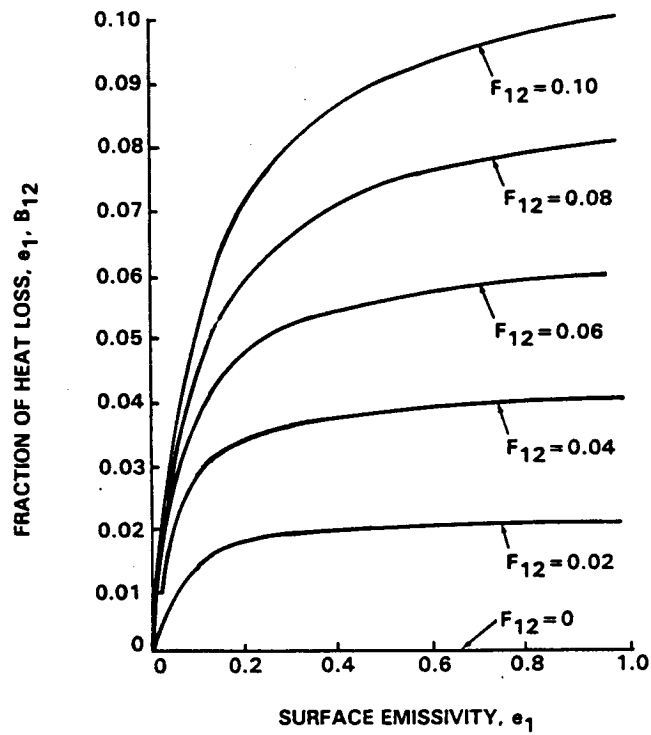


Figure 4.29. Radiation Heat Loss vs. Surface Emissivity and Solar Radiation Absorption Capacity vs. Surface Absorptivity

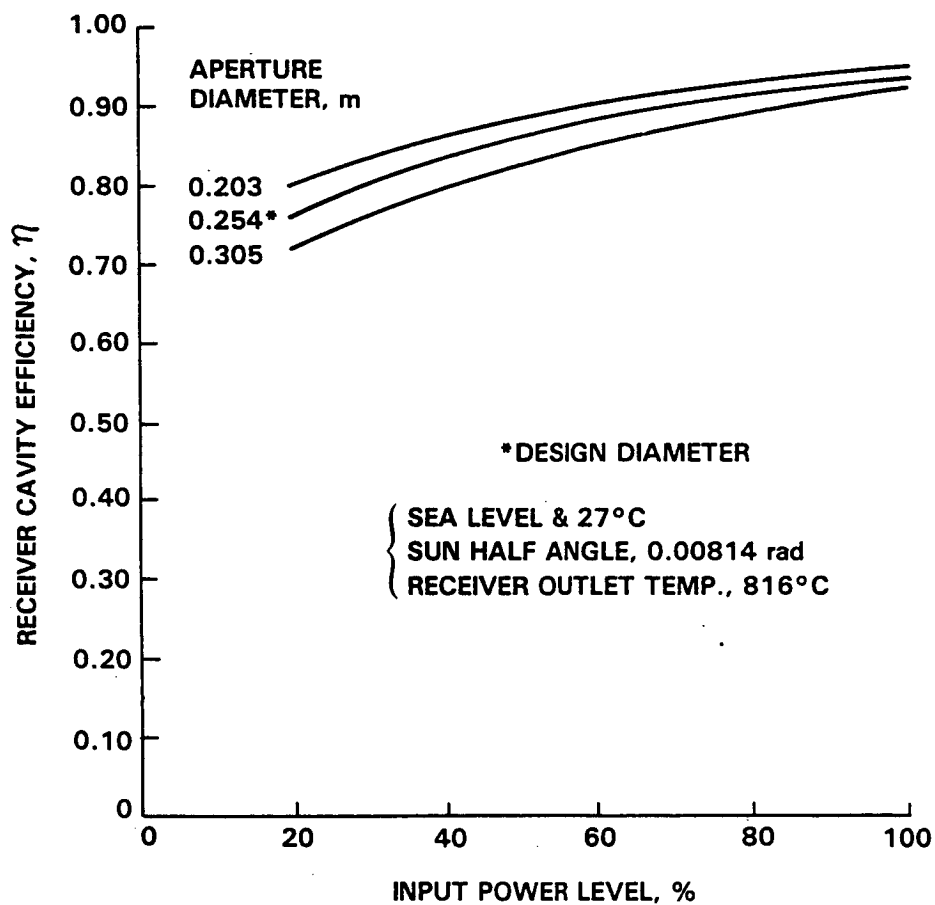


Figure 4.30. Brayton Solar Receiver Cavity Efficiency as a Function of Power Level

surface of 0.3 emissivity). The efficiency at $A_2/A_1 = 0$ corresponds to that of a black body cavity for which the efficiency equation reduces to:

$$\eta = 1 - \frac{\sigma T_1^4}{CG_{sc}}$$

Practically, non-uniform radiation over the interior of the cavity will result in hot spots. To avoid this, the cavity must be designed with a small value of F_{12} and material with a low surface absorptivity. Since the performance of the cavity is not a function of A_2 for $A_1 = 0.3$, the interior surface of the cavity should have an absorptivity of the order of 0.3 to minimize the differences in heat flux.

Finally, Figure 4.30 illustrates the efficiency for a solar Brayton receiver as a function of power level for conditions indicated on the figure. Theoretical cavity efficiency for thermal input energy is given for three aperture sizes, and the optimum aperture diameter has been marked.

4.10 THE HEAT REJECTION PROBLEM

Disposing of the waste heat is a greater problem in a lunar power plant than capturing the solar thermal energy. Several designs of conventional radiator systems have been proposed in connection with the SP-100 project and other space power systems.

A typical gas radiator for a 25 kWe Brayton power module would have an area of 126 m² and a mass of 1540 kg. This mass includes a 5 mm meteoroid protective armor, based on a 0.97 probability of not puncturing the gas radiator tubes during a 6 month storage period plus 10,000 hour operation. Such a radiator would not be

prohibitive in area or mass, assuming a turbine discharge temperature of 780°K , a heat sink temperature of 325°K and a compressor inlet temperature of 365°K .

However, there are two possible alternatives which appear technically attractive, albeit still requiring detailed system engineering: the Liquid Droplet Radiator (LDR) and the Harenodynamic Cooling System (HCS).

4.10.1 LIQUID DROPLET RADIATOR

The liquid droplet radiator (LDR) uses a recirculating free stream of liquid droplets to radiate waste heat from a thermal space power plant (Ref. 2). Using small droplets (diameter less than $100\text{ }\mu\text{m}$) of low vapor pressure liquids as the radiating element instead of the solid surface of the heat pipes, allows a much lighter heat rejection system accompanied by lower rejection temperatures resulting in higher overall conversion efficiencies.

As a preliminary comparison with advanced heat pipe radiators having a mass-to-area ratio of 7 Kg/m^2 , the liquid droplet sheet with a mass-to-area ratio of 0.007 Kg/m^2 (for lightweight oil, Dia. = $50\text{ }\mu\text{m}$) is 1000 times lighter (Ref. 2).

Even though the above comparison neglects the LDR fluid handling machinery, the advantages associated with the LDR include deployability, low mass-to-radiating area ratio (0.007 Kg/m^2 ; Ref. 3), and relatively low heat rejection temperatures (300°K).

4.10.2 PRINCIPLES OF OPERATION

As noted above, by using a sheet of recirculating droplets to radiate waste heat, the LDR can be made many times lighter than the most advanced heat pipes. The principle of the operation of

the LDR is based on a droplet generator and a droplet collector (Figure 4.31). The generator is a pressurized plenum with an array of nozzles to form liquid jets which break up into droplets via surface tension instability. Using an acoustic drive assists in the control of droplet size and spacing. The droplet collector re-forms the droplets into a continuum by centrifugal acceleration. Pumps are then used to transfer the liquid to the heat exchanger. The LDR system can adapt very well to the dish-solar thermal engines (4.31). Depending upon the power generating capacity of each dish module, 1 to 2 independent modules are required for a 60Kwe power module. This means that the modules can be operated in pairs in order to eliminate the need for a remotely-deployed collector and return piping. As illustrated in Figure 4.31, the liquid absorbs waste heat from the power conversion cycle of the left module, and is formed into a converging sheet of droplets which radiates heat as it travels to the collector of the right module. The liquid is collected and passes through the heat exchanger absorbing the heat from the working medium of the right module onto the collector of the left module to complete the cycle.

4.10.3 CANDIDATE FLUIDS FOR LDR

Vapor pressure and melting temperature are two deciding factors in choosing the working medium of the LDR system. High vapor pressure results in significant evaporation and high melting temperature causes fluid transport problems through the pipes. A vapor pressure of 10⁻⁷ mm Hg must be demonstrated if a fluid mass loss less than 20% over a 5-year period is desired (Ref. 3). The selected medium must also demonstrate stability under temperature cycling and radiation exposure, as well as good thermal conductivity.

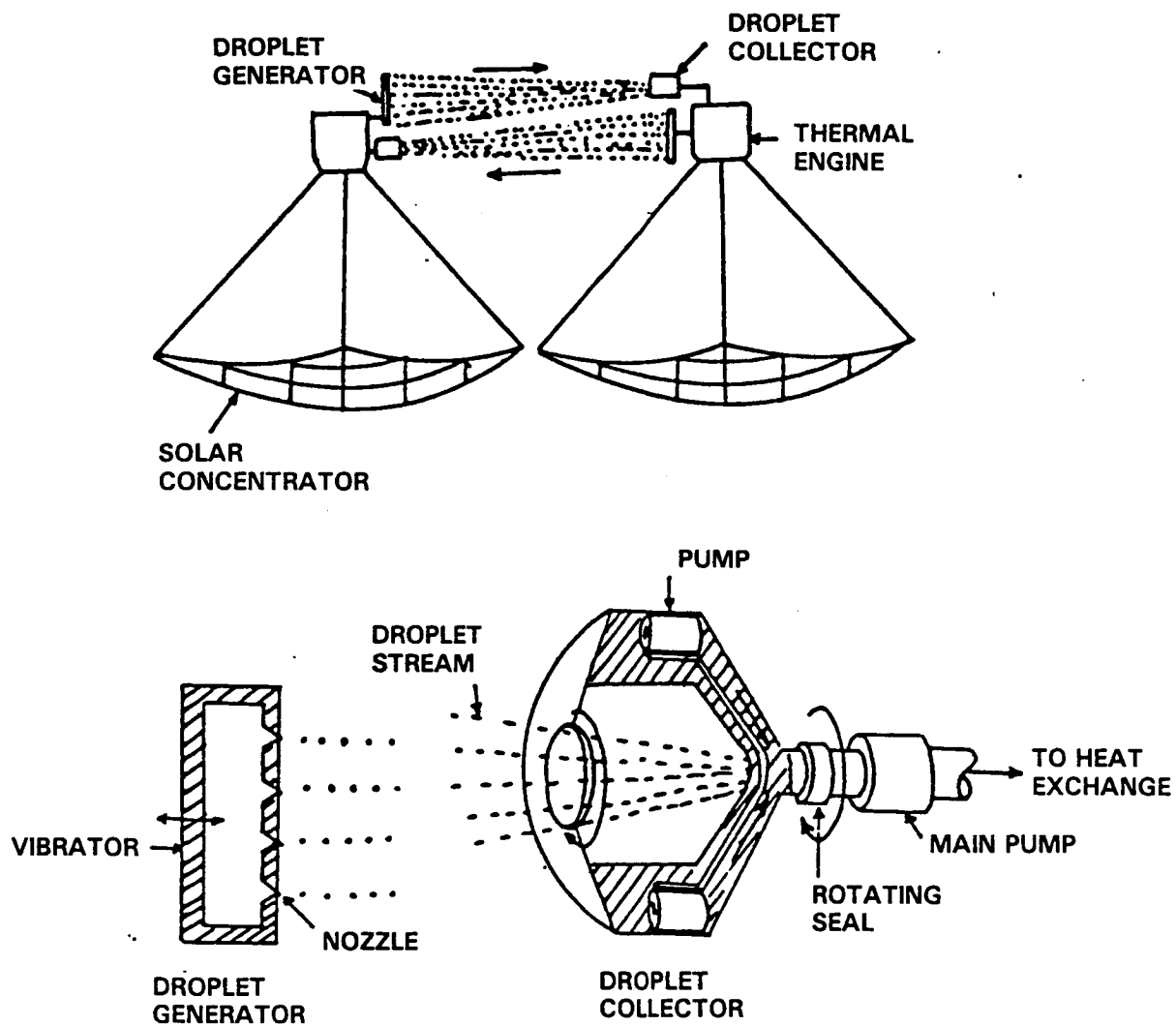


Figure 4.31. Top: Schematic of the Liquid Droplet Radiator System
Bottom: Liquid Droplet Radiator Components

Liquid metals appear to be good candidates for LDR working medium. Tin (melting temp. = 505°K) is an excellent medium for high temperature heat rejection since its vapor pressure is less than 10^{-7} mm Hg up to 1030°K . For heat rejection temperatures around 300°K , vacuum silicone oils are more suitable than liquid metals. Spectroscopic analysis of Dow 705 oil has indicated that fluid emissivity can reach 0.8. Figure 4.32 presents the operating temperature range for several working medium candidates.

The figure of merit in the above figure is emissivity/density, which for a given temperature, is almost proportional to the power/mass ratio. The emissivity of oils is assumed to be 0.8 and that of metals 0.1. Even though silicone oils have very low densities (0.8 g/cc^3), and superior radiation characteristics with respect to liquid metals, no oil with a suitably low vapor pressure above 400°K has been found yet.

4.10.4 BRAYTON CYCLE WITH LDR

Reference 3 presents a design study of a nuclear powered OTV, illustrated in Figure 4.33, using Brayton as the energy conversion cycle and the LDR as the heat rejection system. The table below demonstrates the Brayton cycle parameters.

Turbine Inlet Temperature:	1100°K
Maximum System Pressure:	11.5 atm
Heat Rejection Temperature:	$250\text{--}350^{\circ}\text{K}$, $T_e = 309^{\circ}\text{K}$
Compressor Efficiency:	0.8
Reactor Output Power:	8.7 MWe
Cycle Efficiency:	23.4%

The regenerator of the Brayton cycle was omitted from this analysis due to the low rejection temperature of the LDR system. The omission of the regenerator causes a slight decrease in cycle

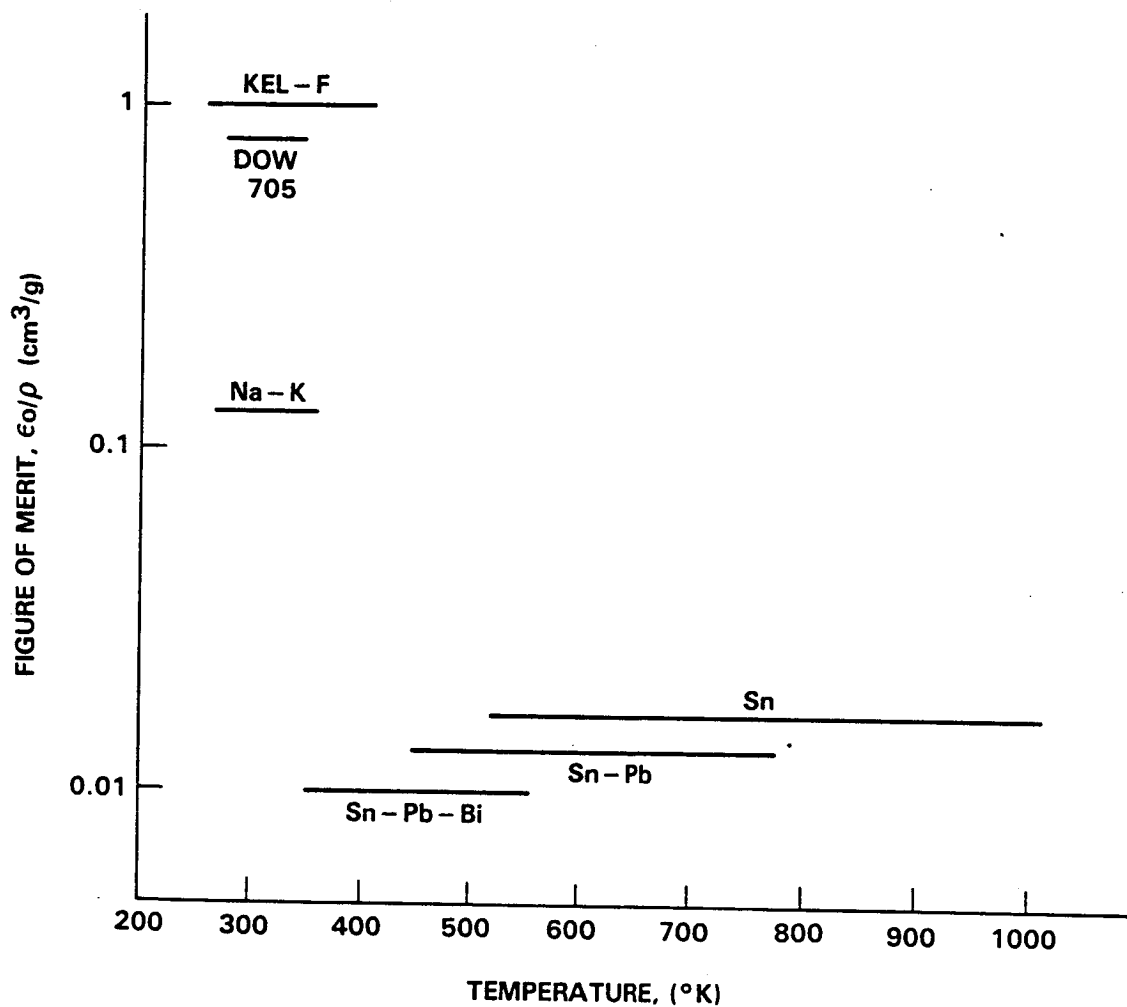


Figure 4.32. Operating Temperature Ranges for Candidate Radiator Fluids.
Figure of Merit is Roughly Proportional to Power/Mass

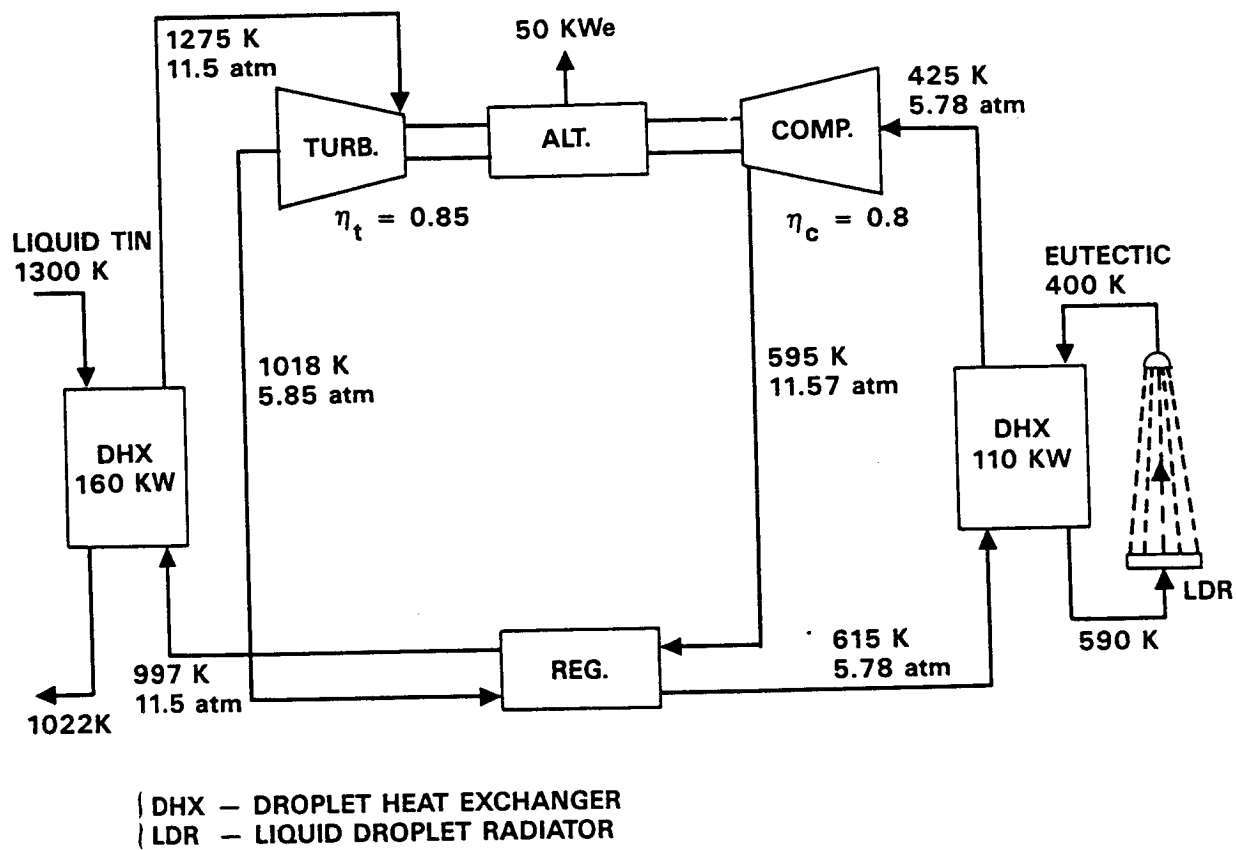


Figure 4.33. Application of Liquid Droplet Heat Exchanger and Liquid Droplet Radiator in a Brayton-Cycle Energy Conversion System

efficiency, however, the advantages of lower system weight and lower failure risk offset the former. The power to mass ratio of the LDR system was found to be 4.2 kW/Kg. High performance heat pipe radiators offer a power to mass ratio of about 0.07 kW/Kg. It is apparent that the LDR system provides a significant improvement in the performance of the power conversion system. The entire nuclear powered system has a system mass to power ratio of 1.9 Kg/kW.

4.10.5 RANKINE CYCLE WITH LDR

Reference 2 compares the performances of the LDR and heat pipes as the heat rejection systems of a 10 GW solar power satellite designed by Boeing. The Rankine cycle working medium is potassium with a maximum temperature of 1242°K and rejection temperature of 932°K. The cycle efficiency is about 19%. The radiator is comprised of NaK heat pipes. The power specific mass is about 0.20 Kg/kWrad, and the heat pipes constitute 50% of the radiator mass. The referenced study used an LDR system using Tin as the radiating medium droplet temperature of $T_0 = 932^\circ\text{K}$, and droplet collection temperature of $T_1 = 532^\circ\text{K}$. The effective radiator temperature can be calculated from the relations given below (Ref. 2):

$$T_e^4 = 3T_0^4/f^3 + f^2 + f \text{ where } f = T_0/T_1$$

Thus, the radiator effective temperature is calculated to be $T_e = 686^\circ\text{K}$. This leads to a power specific mass of 0.033 Kg/kWrad for the radiating sheet. Even though detailed design studies of LDR components are not available, estimates for the LDR machinery lead to a specific mass of 0.18 Kg/kWrad for the LDR system in this application. Even though this value is close to the specific mass offered by the heat pipe, reduced vulnerability to micrometeoroid damage and small transport packages of the LDR

makes it a much more attractive alternative. The mass of the radiating element of the LDR is 18% of the total heat-rejection system, while that of the heat pipe is 50%. This suggests that future efforts should focus on optimizing LDR component masses which will result in lower overall system mass and improved performance.

Decreasing the maximum droplet temperature from 932°K to 732°K, and keeping the droplet collection temperature constant, will result in an effective radiation temperature of $T_e = 619^\circ\text{K}$. The corresponding power specific mass for the LDR system will be 0.40 Kg/kWrad, while that of the heat pipe radiator will be 153 Kg/kWrad. The cycle performance will also improve to an estimated value of 30% for efficiency. This leads to a reduction of component masses and thermal stresses.

4.10.6 DIRECT CONTACT DROPLET HEAT EXCHANGER

A liquid droplet heat exchanger transfers heat efficiently between a gas and a liquid metal dispersed into droplets. Direct energy exchange between the mediums of different phase eliminates the materials related problems associated with conventional tube-type heat exchangers at elevated temperatures. The droplet heat exchanger offer large surface-to-volume ratios in a compact geometry, insignificant gas pressure drop, and very high effectiveness (0.90 - 0.95). A numerical analysis regarding the performance of two droplet heat exchangers and a liquid droplet radiator into a Brayton-cycle energy conversion system is presented in Ref. 14, and illustrated in Figure 4.33.

A mixture of 72% He and 28% Xe comprises the working gas of the Brayton cycle. This mixture is heated in the high temperature heat exchanger to 1275°K by molten Tin. The cycle efficiency is thus increased from 25% to 31% and leads to a 160 kWt required

for a power output of 50 kWe. A low-temperature heat exchanger, using droplets composed of a Tin-Lead-Bismuth eutectic (16% Sn, 52% Pb, 32% Bi by weight, melting temp. = 369°K), serves to transfer heat from the working gas and heat the droplets to 590°K. The eutectic is then pumped to the liquid droplet radiator at a mass flow rate of 3.5 Kg/sec in order to reject 110 kW of waste heat. The size and effectiveness of the high-temperature and low-temperature heat exchangers were respectively: 50 cm, dia. x 78 cm long, 0.92 - 31 cm dia. x 70 cm long, 0.89. Higher effectiveness can be achieved by reduction of the temperature difference between droplets and gas, as well as optimization of the mass flow rates.

4.10.7 STATUS OF TECHNOLOGY

It is apparent that a combination of liquid droplet heat exchanger and liquid droplet radiator offers significant advantages over conventional tube-type heat exchanger and heat pipe radiator for thermal management of a lunar powerplant. Even though these concepts are based on existing technology, no prototype testing in space environment has yet been conducted. Future research and development should focus on designing low-mass fluid handling systems for the LDR, since these machinery account for most of the heat rejection mass. Some of the technical problems facing the development of these concepts are: contamination of the radiator fluid, droplet charging, radiator orientation, manufacturing of the droplet generator, and materials compatibility.

4.11 HARENODYNAMIC COOLING

Harenodynamic cooling, a concept using the lunar sand as the cooling medium of the heat rejection system, a proposal of the late Kraft Ehricke, offers a unique and efficient approach to

waste heat rejection on the Moon (Ref. 1). The Harenodynamic cooling system is small, compact, and micrometeoroid resistant. Because of using materials already available on the Moon, its operation can be simple, inexpensive, and much more efficient than the current heat pipes.

4.11.1 PRINCIPLES OF OPERATION

The principle components of the Harenodynamic cooling system are: the convective heat exchange tube, cyclone separator mixer of sand and carrier gas, and cyclone injector. Figure 4.34 presents a schematic of the Harenodynamic cooling system. The fine sand at cryogenic temperatures, and pre-mixed with a carrier gas to prevent coagulation, is injected from a cyclone injector over the entire cross-section of the tube. Injecting the sand over the entire cross-section rather than from the walls, results in a maximized mixing rate and enhanced convective heat transfer rates between working fluid and sand particles. A cyclone separator is then used to remove the sand from the working fluid. Lunar gravity assists in collecting the sand underneath the separator and releasing it onto a feeder conveyor and a main conveyor. The large surface-to-volume ratio of the sand is then used for efficient radiative communication with the lunar environment. After the radiative exchange, the sand is returned to the sand depot, from where it can be recycled.

4.11.2 CONVECTIVE HEAT TRANSFER CONSIDERATIONS

The temperature of a mixture of sand and a working fluid gas is closely given by the following relationship, (For approximations used in deriving this equation see Ref. 1):

$$T_m = \frac{T_g}{r + T_g/T_s}$$

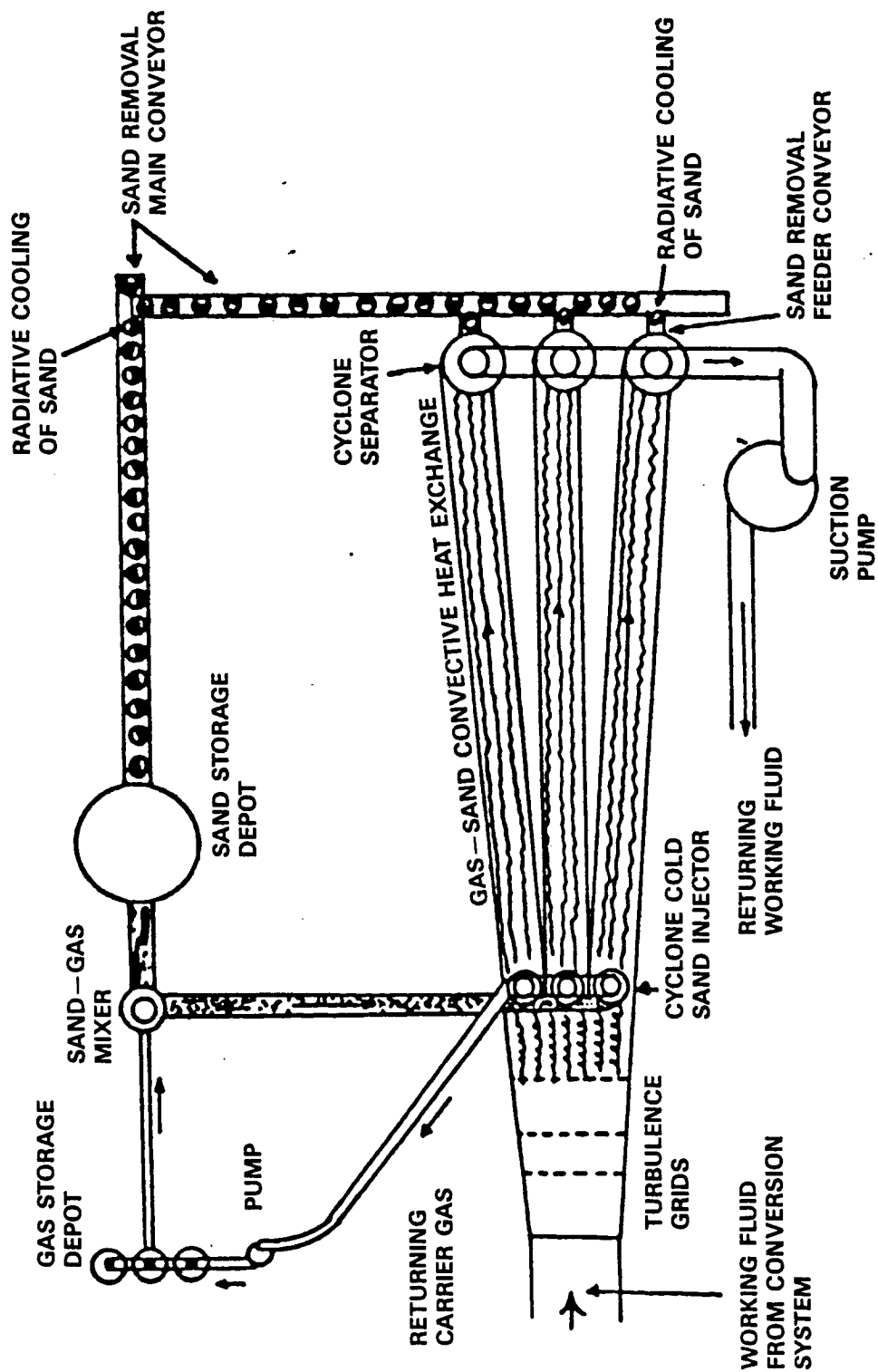


Figure 4.34. Schematic of Harenodynamic Cooling System

where T_g is the gas temperature, T_s is the sand temperature and r is the ratio of the sand mass to the gas mass: $r = m_g/m_s$. The above relation is independent of the working fluid, the carrier gas, and the mineral composition of the sand grains. Thus, the temperature of the mixture is a function of mixture ratio and the gas and sand temperatures at the beginning of the process. Figure 4.35 illustrates the temperature of the mixture as a function of the mixture ratio for varying initial working gas and sand temperatures (Ref. 1). Decreasing the sand temperature from 300°K to 170°K can reduce the amount of sand needed by up to 80%, depending upon the gas and mixture temperatures. This emphasizes the effectiveness of Harenodynamic cooling versus the conventional radiator, especially when the sand is at cryogenic temperatures. The Harenodynamic cooling system, unlike the conventional radiator, uses a high volume-to-surface ratio for heat exchange tubes, in order to increase the ratio of thermal energy absorbed-to-external surface (Q/A). Thus, the Harenodynamic cooling system does not require a mass optimization mass study.

4.11.3 HARENODYNAMIC COOLER VS. CONVENTIONAL RADIATOR

Reference 1 presents a detailed analysis of the performance of Harenodynamic cooling system. This section will emphasize the results of this analysis and compares it to the performance of a conventional radiator. Table below presents the important parameters of the Harenodynamic cooler.

Working gas:	Helium
Velocity:	20 m/s
Tube Diameter, d:	0.2 m
Time from injection to complete energy exchange/w Gas & Sand, t_m :	20 s

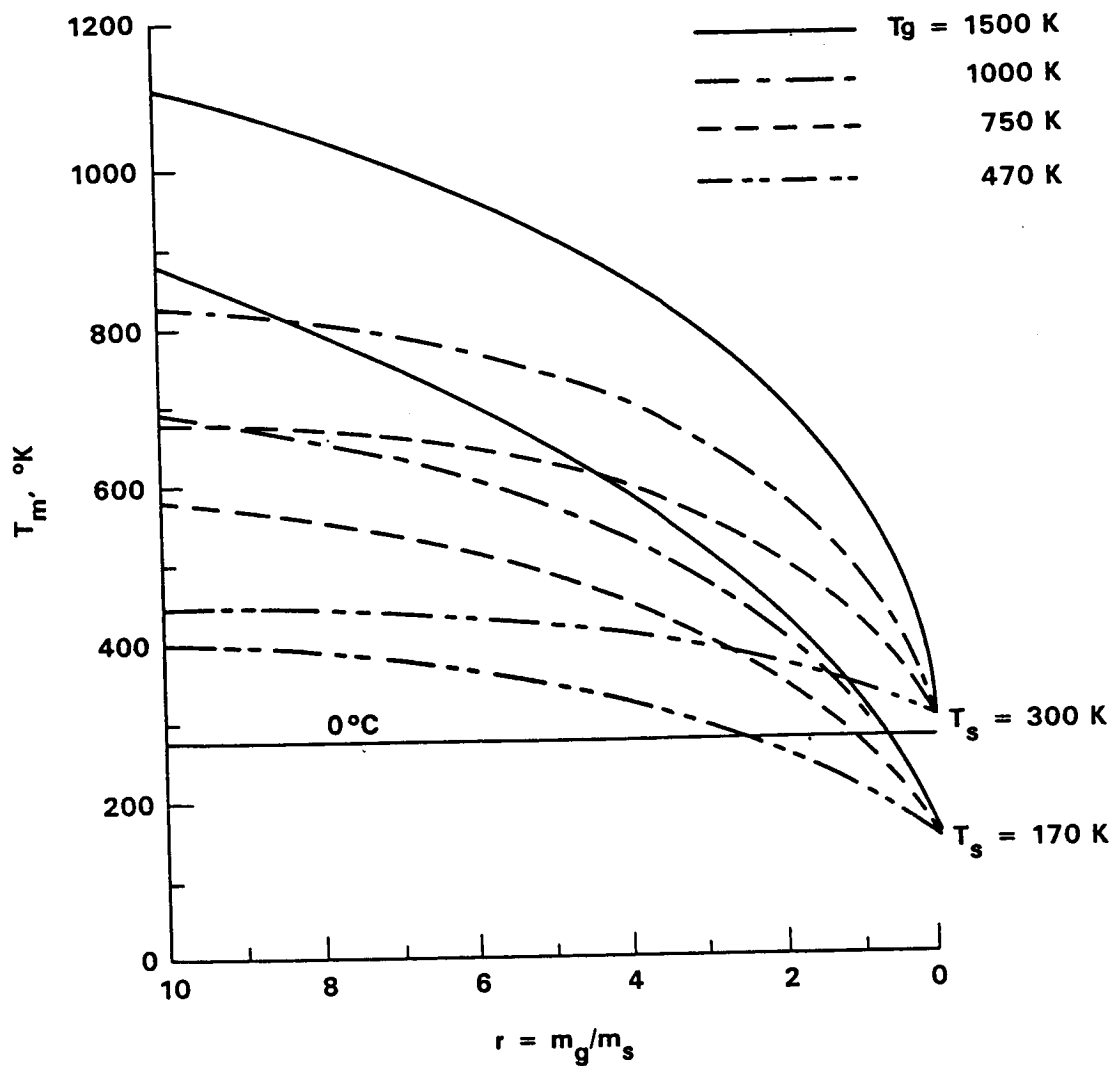


Figure 4.35. Temperature of the Gas Sand Mixture as Function of Mixture Ratio for Different Initial Temperatures of Gas and Sand

Sand Temp., T_s :	300°K
(or Sand Temp. 170 K & $r = 1.9$, $d = 0.53$)	
Gas Temperature, T_g :	770°K
Temperature of Mixture, T_m :	370°K
Power Output:	44kWt/m ²

Thus, a 400 m long Harenodynamic cooler is equivalent to a radiator capable of rejecting 43 kWt/m².

For a conventional radiator, the heat rejected at a radiator inlet temperature of T_2 is:

$$Q_r = \sigma \epsilon A_r T_2^4 = \sigma \epsilon A_r (1 - \eta_c)^4 T_1^4$$

Where A_r is radiating surface area, σ is the Stefan-Boltzmann constant, ϵ is the emissivity, T_1 is the inlet temperature of the gas into the conversion system, and η is the Carnot efficiency. The minimum radiating surface can be derived (see Ref. 1), and is given below:

$$\frac{A_r}{A_{\min}} = \frac{(1 - \eta_{c,\min})^4}{\frac{1}{\eta_s \eta_{c,\min}} - 1} \times \frac{\frac{1}{\eta_s \eta_c} - 1}{(1 - \eta_c)^4}$$

where η is the system conversion efficiency.

For $\eta_s = 0.5$, an increase in η_c to 0.44 ($T_H/T_L = 1.8$), results in doubling of the output power at the expense of 66% increase in radiating surface. However, further increase in Carnot efficiency by lowering the rejection temperature will not result in significant area-specific electric power increases. This leads to increasing of by raising the inlet gas temperature.

In the above analysis it was assumed that the radiator temperature remains constant throughout the radiative exchange process. However, the actual drop in radiator temperature will result in larger radiating surfaces than would be obtained from an isothermal radiator. According to Ref. 1, the actual radiating surface is about 4.3 times larger than that on an isothermal radiator.

For the same temperature ratio, the radiator (with an effective emissivity of 0.85) leads to an area-specific cooling performance of $Q_r/A_r = 0.444 \text{ kWt/m}^2$.

Comparing this value to that of the Harenodynamics cooler (43 kWt/m^2), demonstrates a two order of magnitude performance improvement for the Harenodynamic cooling system relative to the conventional radiator.

4.12 SUMMARY AND CONCLUSIONS

- 1) A solar energy power plant on the moon is feasible now with state-of-the-art commercial technology. However, since a lunar colony may only become a reality towards the end of the 20th century, and most likely during the first decade of the 21st, NASA should motivate research and development in new directions offering high technical promise. No scientific break-throughs are needed, but detailed design and prototype testing of these new systems would not only improve the all-around efficiency, reliability and cost effectiveness of a lunar power plant, but would also produce new technical solutions with useful industrial/military applications here on earth.
- 2) Problem areas concern mainly the energy storage and waste heat dissipation portions of the system. The energy storage problem can be completely by-passed, except for the minimal

amount needed for power smoothing, by locating the lunar power plant at or near either one of the lunar poles, where solar energy is continuously available. Otherwise, for a site at or near the lunar equator, an energy storage system will be required.

- 3) Solar energy is plentiful and easy to capture on the moon. Temperatures are limited by material constraints and not by the physics of heat acquisition systems. Heat dissipation in sufficient quantities to maintain an efficient thermal gradient can be achieved by conventional heat-pipe radiators, but a liquid droplet radiator (LDR) or a Harenodynamic cooler (HDC) offer smaller area, lower specific mass, higher power densities and much greater efficiency, especially with low outlet temperatures, where the performance of a conventional radiator degrades rapidly.
- 4) Solar thermodynamic systems are ready right now. The free piston Stirling engine designed by Sunpower, Inc., has an output of 25 kWe with an overall efficiency of 29% and a specific mass of 6 kg/kWe. A kinematic Stirling engine has been under testing at McDonnell-Douglas for more than 6000 hours, with solar-to-electricity conversion efficiency of 28% and a power output of 25 kWe.
- 5) The Alkali Metal Thermoelectric Converter (AMTEC), also known as the Sodium Heat Engine (SHE) is potentially the most attractive system with lightweight (0.25 to 0.5 kW/kg), no moving parts, high modularity, and a thermal-to-electric efficiency of 30%. An AMTEC/Rankine engine combination for high and low temperature operation would have an overall efficiency of 42%, with an inlet temperature of 1000°K. However, no scalable prototype has yet been built. Immediate development priorities are improvements of the porous molybdenum electrode and continued search for other suitable

electrode materials, including refractory metal oxydes (such as Ti, W, V, Zr oxydes) for possible application in a higher temperature AMTEC. Beta-alumina begins to creep at 1200°K and thus limits the possible power density. Most important, however, is the definition of parameters and construction of a 10kW AMTEC, as a prototype module for a lunar power plant. An AMTEC of this size is perfectly feasible with today's technology.

- 6) In 1986 dollars, transportation lost from the Earth to the Moon would be roughly \$6,600 per kg. A 60 kW advanced AMTEC module would have a mass, including an inflatable solar collector and a conventional heat-pipe radiator, of no more than 200 kg. This totals a transportation cost of \$13.2 million, which is not a prohibitive amount. Disassembled and properly packed for transportation, the entire module would fit in a cylindrical container measuring 4.5m diameter and 5m in length.
- 7) Solar cell, photovoltaic technology is progressing very rapidly in efficiency and lower manufacturing cost. By the year 2000, the corresponding figure of merit will have approximately doubled and will make a photovoltaic lunar planet substantially more attractive than it would be today.

REFERENCES

1. K.A. Ehricke, Space Global Co. "Harenodynamic Cooling: The Use of Lunar Sand as Cooling Medium." Acta Astronautical Vol. 11, No. 6, 1984
2. A.T. Mattick, A. Hertzberg, Univ. of Washington "The Liquid Droplet Radiator - An Ultralightweight Heat Rejection system for Efficient Energy Conversion In Space." Proc. of NASA Space Power - Int'l. Astronautical Federation, IAF, Rome, Italy 1981
3. G. Beals, J. Chin, J. Day, C. Gibson, K. Grevstad, G. Larson, D. Treiber, Univ. of Washington "A Lightweight Nuclear Powered OTV Utilizing A Liquid Droplet Radiator." Proc. of NASA Space Power, AIAA-83-1346 19th Joint Propulsion Conf. 1983
4. K. Subramaniam, T.K. Hunt, Ford Motor Co., "Solar Thermal/Electric Power Conversion Using the Sodium Heat Engine."
5. T.K. Hunt, N. Weber, Ford Motor Co., T. Cole, JPL "High Efficiency Thermoelectric Conversion with Beta-Alumina Electrolytes, The Sodium Heat Engine." Solid State Ionics 5, 1981
6. T. Cole, JPL "Thermoelectric Energy Conversion with Solid Electrolytes." Science, Vol. 221, 1983
7. C.P. Bankston, M. Shirbacheh, JPL "AMTEC: High Efficiency Static Conversion for Space Power." For NASA Manned Mars Mission Study Group, NASA/MSFC, 1985
8. C.P. Bankston, T. Cole, S.K. Khanna, A.P. Thakoor, JPL "Alkali Metal Thermoelectric Conversion (AMTEC) for Space Nuclear Power Systems, 1984

9. C.P. Bankston, T. Cole, R. Jones, R. Ewell, JPL "Experimental and System Studies of the Alkali Metal Thermoelectric Converter for Aerospace Power." J. of Energy, Vol. 7, No. 5, 1983
10. T. Cole, C.P. Bankston, JPL "Private Communication." 1985
11. H.G. Nelving, United Stirling AB, "Testing of the United Stirling 4-95 Solar Stirling Engine on Test Bed Concentrator." Proc. of the 5th Parabolic Dish Solar Thermal Power Prog. 1984
12. F.R. Livingston, JPL, "Stirling Module Development Overview." Proc. of the 5th Parabolic Dish Solar Thermal Power Prog. 1984
13. H.G. Nelving, United Stirling AB, D. Faller, McDonnell-Douglas "Private Communication." 1985
14. A.P. Buckner, A. Hertzberg, Univ. of Washington, "Direct Contact Heat Exchangers for Thermal Management in Space." Proc. of IECE 1982
15. R.C. Parish, NASA/JSC "Thermal Management Technology Status." Proc. of NASA Space Power 1984
16. R. Haslett, Grumman Aerospace Corp. "Space Station Thermal Control." Mechanical Engineering Dec. 1984
17. L. Morrison, Sunpower, Inc., "Private Communication." 1985
18. E.J. Roschke, W.A. Owen, W.A. Menard, T. Fujita, JPL "Trends in Concentrator, Receiver, and Storage Development for Terrestrial Applications." Proc. of NASA Space Power 1984

19. J.M. Bowyer, JPL "The kinematic Stirling engine as an energy conversion subsystem for paraboloidal dish solar thermal power plant." 1984
20. J.M. Bowyer, T. Fujita, B.C. Gajanana, JPL, 1982, "Comparison of advanced engines for parabolic dish solar thermal power plants."
21. D.G. Wilson, "Alternative Automobile Engines." Scientific American, 1978
22. A.D. Tonelli, T.C. Secord, Douglass Aircraft Co., Inc., 1964 "Auxiliary power generation system for a large space laboratory."
23. M.G. Coombs, L.W. Norman, AiResearch Manufacturing Co., "Application of the Brayton Cycle to nuclear electric space power systems." 1964
24. R.E. Barber, J.E. Mullaney, R.N. Bailey, Sundstrand Aviation, "Preliminary design analysis of solar powered, long duration space power systems for a power range of 1- to 25-kW." 1962
25. A. Pietsch, AiResearch Manufacturing Co., "Solar Brayton Cycle Power System Development." 1964
26. E.M. Knoernschild, "Power sources for use on the moon."
27. G.J. Van Wylen, R.E. Sonntag, University of Michigan, "Fundamentals of Classical Thermodynamics." 1978
28. K. Ya. Kondratyev, M.P. Federova, University of Leningrad, "Net radiation and its components for inclined surfaces on the moon."

SYMBOLS

T.....	Temperature
P.....	Pressure
V.....	Specific volume
s.....	Specific entropy
W.....	Work
Q.....	Heat transfer
R.....	Gas constant
η	Thermal efficiency
E.....	Regenerator effectiveness
K.....	Ratio of specific heats
C_p	Constant pressure specific heat
C_v	Constant volume specific heat
m.....	Mass
ρ	Viscosity of liquid

5.0 ENERGY STORAGE

5.1 INTRODUCTION

The most difficult engineering problem in the design of a solar conversion electrical power plant for the lunar environment is that of storing energy for the long lunar night. This problem could be avoided by the use of a small nuclear power-plant. This study has not considered nuclear sources for two reasons. The SP-100 satellite nuclear power program has progressed to a second phase contract, with a target date of 1992 for flight hardware and the requirement for power output has been increased from 100 to 300 watts. Nuclear power will therefore be an option for the lunar base when it is established. A second consideration for studying the feasibility of solar conversion methods rather than nuclear is that when the lunar base is established, political, environmental and possibly scientific pressure may deny the use of the nuclear option. Possibly a third consideration, having more aesthetic than engineering value is that there is a certain elegance in using the energy source which already exists at the lunar surface.

At the beginning of the study, all possible methods of storing energy were considered and after preliminary calculations, some were discarded and a more detailed study was done of batteries and fuel cells. Methods considered were:

- Fuel cells
- Batteries
- Thermal reservoirs
- Flywheels
- Capacitors
- Compressed Gas
- Gravitational
- Superconducting coils

These are all methods which have been employed at one time or another for various applications by the power utilities or space programs.

The difficulty in a satisfactory solution to this problem is a result of the length of the lunar night. The study has concentrated on concepts for 60 kilowatt modules, which can be ferried in on successive flights to build up to levels of 300 kW and eventually to the megawatt level. The lunar night is 336 hours long from sundown to sunup. One should not expect a significant output from the solar conversion fields for the last 10 of sun elevation before sundown nor the first 10 after sunup. One therefore has to consider a storage time of 375 hours. In order to supply 60 kW of power during this period, the energy storage subsystem must have a recoverable capacity of 22,500 kilowatt hours.

In section 5.2 the applicability of the hydrogen/oxygen fuel cell is considered and size and weight calculations are presented and are shown to be the best early era candidate. Batteries are one of the most mature forms of energy storage and in section 5.3 two advanced batteries are discussed. These are the sodium/sulfur battery and the aluminum/oxygen battery. Flywheels have been employed extensively as energy storage device for spacecraft and section 5.4 contains discussion and calculations for flywheels fabricated from several different materials. Thermal storage is a very good candidate and has some definite advantages, however, it is not considered practical to plan for its use until at least the third year of the base. This option is discussed more fully in section 5.5.

5.1.1 CAPACITOR STORAGE

Capacitors at first appeared to offer a practical solution to energy storage. Materials with a dielectric constant in the range of 7000 to 8000 which are now available make it practical to consider the manufacture of capacitors of one farad size. The energy stored in a capacitor is:

$$E = \frac{1}{2} CV^2 \text{ where}$$

E is in joules, C is in farads and V is in volts. If we have a one farad capacitor and charge it to 100 volts, we have stored

$$E = \frac{1}{2} \times 1 \times 100^2 = 5000 \text{ joules}$$

The factor for converting joules to watt hours is 2.778×10^{-4} .

$$E = 5000 \times 2.778 \times 10^{-4} = 1.389 \text{ Watt hrs.}$$

We require 22,500,000 watt hours of stored energy therefore it would require $22,500,000 \div 1.389$ or 16,198,704 one farad capacitors, clearly an impractical number to consider. The considerations of leakage discharge and the nonlinear voltage discharge curve would further compound the problem.

5.1.2 COMPRESSED GAS

There has been limited use by power utilities of large reservoirs of compressed gas as a method of energy storage for supplying peak power demands. Such installations exist in Illinois and in West Germany. In both areas advantage was taken of large caverns which remained from salt mines. This method was given no serious consideration because we know of no existing caverns on the moon. The absence of a gaseous lunar atmosphere would also make it difficult to supply a compression medium.

5.1.3 GRAVITATIONAL FIELDS

Storage of potential energy in a gravitational field is a frequently practiced method in the power utility industry where a water reservoir exists. During periods of light demand, excess

generating capacity is used to pump water from a lower to a higher reservoir. Then during periods of peak demand the water is released through hydraulic turbines for the generation of electricity. Of course the moon is lacking in water, however, some comparable scheme, employing lunar regolith could be devised. Something such as a large container of regolith could be elevated by a mechanism such as that employed in weight operated clocks. Elevation of the weight would be accomplished during the lunar day by excess electrical generating capacity. During the night its controlled descent could be used to turn a generator and generate electricity.

The density of regolith is approximately 3.5 grams/cc, Earth weight. Consider using weights which are one cubic meter in size and filled with regolith. The lunar weight of this mass will be:

$$\frac{3.5 \times 10^6}{6} = 583 \text{ kg}$$

6

Assume that the weight is elevated 100 meters. The stored potential energy is

$$583 \times 100 = 58,300 \text{ kg-M}$$

From Hudson's handbook the factor for conversion of kg-M to kW hr. is 0.522×10^{-7}

$$58,300 \times 0.522 \times 10^{-7} = 3.043 \times 10^{-3} \text{ kW hr.}$$

Since the storage requirement is for 22,500 Kw hr. it would require 7,394,019 such weights, neglecting efficiency factors. This is then seen to be a scheme which is conceptually attractive, but impractical from an engineering perspective.

5.2 FUEL CELLS

Fuel cells are a class of electrochemical energy storage devices, having some characteristics in common with primary batteries. Both depend upon a chemical reaction of their fuels in the presence of an electrolyte to release electrical energy. The

largest fuel cell installations use some form of hydrocarbon fuel and phosphoric acid or molten carbonate electrolytes. The Consolidated Edison Company is constructing a 4.8 megawatt power plant in New York City which will be used to augment rotating machinery power generation facilities during periods of peak loads.

The hydrocarbon class of fuel cell has little attraction for lunar base application because eventually one would like to plan for the use of locally available fuels and hydrocarbons have not been discovered on the moon. Hydrogen occurs in limited quantities on the moon, (but is expected to be fairly easily recoverable) while carbon exists only in trace quantities. The fuel cell which has good potential for lunar base usage is the alkaline electrolyte cell, using hydrogen and oxygen as fuel. This unit also depends upon the scarce lunar element hydrogen, however, closed cycle systems have been designed. Some leakage of hydrogen will doubtless occur even in a closed system, hydrogen being difficult to confine, however, it is the lightest consumable which one would have to transport from earth. Very early in the life of the lunar base, an oxygen plant is expected to be operational making that fuel element locally available.

The hydrogen/oxygen alkaline fuel cell has a long history of successful application to this country's manned space programs. Figure 5.2.1 shows the characteristics of hydrogen/oxygen fuel cells from the past and for those projected for the future. Characteristics of the Gemini, Apollo and Shuttle fuel cells are taken from the McGraw-Hill Handbook of Batteries and Fuel Cells. The characteristics of the STUDY cell are based upon a design study conducted by United Technologies for NASA Lewis Research Center which continues to sponsor research in fuel cell technology.

Figure 5.2.1. Progress in Hydrogen/Oxygen Fuel Cells

MISSION	AVERAGE POWER	FUEL CONSUMPTION	WEIGHT	POWER DENSITY
GEMINI	1 KW	400 GM/KW-HR	30 KG	30 KG/KW
APOLLO	1.42 KW	550 GM/KW-HR	110 KG	77 KG/KW
SHUTTLE	7 KW	446 GM/KW-HR	91 KG	13 KG/KW
STUDY	15 KW	426 GM/KW-HR	108 KG	11 KG/KW

For the lunar base application the POWER DENSITY column of figure 5.2.1 holds the most interest because it defines the weight of the fuel cell assembly alone and for a build-up of the lunar power system in 60 kW modules, lets us know how many of the basic fuel cell assemblies will be required. In the lunar base application, because of the 336 hour duration of lunar night, the mass of fuel required will greatly exceed that of the fuel cell assemblies.

The operational characteristics of an advanced fuel cell which could serve the needs of the lunar base are shown in Figure 5.2.2. Four such fuel cells will supply the required power level of 60 kW. It can be seen that the total weight of fuel cells which must be ferried to the lunar base is 1728 kg, a reasonable figure. The weight of fuel for the night will however, be much greater and for at least the first year of the base, will have to be ferried from Earth. The fuel cell systems will, however, be designed as closed cycle units, so that most of the fuel will be recoverable by the electrolysis of water, the end product of the fuel cell operation.

The quantity of fuel required can be calculated from the following formula:

$$\text{Mols of H}_2 = \frac{J \times A \times T_c \times N \times n \times 60}{96487 \times 2} \quad \text{where}$$

J = current density in amperes per square ft.

A = active area in square ft.

T_c = cycle time in minutes

N = number of cells in a stack

n = number of stacks

$$\text{Mols of O}_2 = \text{Mols of H}_2 \div 2$$

This formula was received from Mark Hoberecht of NASA Lewis Research Center in a private communication. (Although M-k-s units have been used consistently in this study, the above formula is used in the units in which it was provided).

Figure 5.2.2. Lunar Base Fuel Cells

AVERAGE POWER OUTPUT:	15 KW
CELLS PER STACK:	38
NUMBER OF STACKS:	4
WEIGHT PER STACK:	108 kg
OUTPUT VOLTAGE:	30 V DC
OVERALL EFFICIENCY:	50%
TOTAL FUEL CELL WEIGHT:	432 kg
CURRENT DENSITY:	= 0.534 A/cm²
CELL AREA	= 929 cm² (TOTAL)

**(BASED UPON DESIGN DATA IN REPORT NASA-CR-174802; FCR 6128
PREPARED FOR NASA LEWIS BY R.E. MARTIN, ET AL, UNITED
TECHNOLOGIES CORP.)**

Hoberecht has suggested that in the lunar time frame a current density of 500 amperes per square foot is possible. Using that figure and a cycle time of 375 hours and the data from Figure 5.2.2 the hydrogen weight is:

$$\begin{aligned} \text{Mols of H}_2 &= \frac{500 \times 1 \times (375 \times 60) \times 38 \times 4 \times 60}{96,487 \times 2} \\ &= 531,678 \end{aligned}$$

The mol weight of hydrogen is 2.02 grams, therefore the weight of hydrogen required is:

$$\text{H}_2 = 531,678 \times 2.02 = 1,073,989 \text{ grams}$$

This is rounded to 1,074 kg

The mols of oxygen required is:

$$\text{mols of O}_2 = \frac{531,678}{2} = 265,839$$

The mol weight of O₂ is 32 grams, so the weight of

$$\text{O}_2 = 265,839 \times 32 = 8,506,848 \text{ grams or approximately } 8,507 \text{ kg.}$$

The total required weight of fuel then, is 8507 + 1074 = 9581 kg. This compares to 1728 kg as the weight of the fuel cells themselves. 8507 kg is the weight of fuel which must be transported to the moon for one 60kW power plant. One would be inclined to want some contingency margin and to increase this figure to 10,000 kg. It appears that the most convenient transport arrangement would be to ship it as water. This would avoid the problem of handling liquified gases and the attendant insulation problems. This scheme would require that the water and the electrolysis plant be available at the beginning of lunar day and that the crew arrive at that time. There would, however be the same requirement for tankage as if the fuels were shipped as liquified gases, because the tanks would have to be on hand to hold the products of the electrolysis plant. It is necessary then to estimate the weight of tanks for holding liquid oxygen and liquid hydrogen. The weight of water was rounded up from 9581 kg to 10,000 kg, so that we are now dealing with 1120 kg of hydrogen and 8880 kg of oxygen.

From the Handbook of Chemistry and Physics, the density of liquid hydrogen is 0.070 grams/cc and its boiling point is -252.5 C. The factors for liquid oxygen are 1.149 grams/cc and -183.0 C. From these factors the volume of hydrogen is:

$$\frac{1,120,000 \text{ gm}}{0.070 \text{ gm/cc}} = 16,000,000 \text{ cc} = 16,000 \text{ liters}$$

The volume of oxygen is:

$$\frac{8,880,000 \text{ gm}}{1.149 \text{ gm/cc}} = 7,728,460 \text{ cc} = 7724 \text{ liters}$$

The tank for the associated volume of water is 10,000 liters, so that overall there is a requirement for three tanks on the moon. The tank characteristics will be based upon the assumption that both the hydrogen and oxygen will exist as a gas in equilibrium with the liquid at their critical temperatures and pressures. For hydrogen the critical temperature $T_c = 33 \text{ K}$ and critical pressure $p_c = 13 \text{ atmospheres}$. For oxygen the values are $T_c = 154.5 \text{ K}$ and $p_c = 50.5 \text{ atm}$. A tank length to diameter, $L/D = 4$ will be assumed. One atmosphere = $10,336 \text{ kg/m}^2$.

For the hydrogen tank which requires a capacity of 16 cubic meters,

$$\begin{aligned} \frac{\pi D^2}{4} \times L &= 16 & \text{and} & & L &= 4D \\ \frac{\pi D^2}{4} \times 4D &= 16 & & & D^3 &= 16/ \\ & & & & D &= 1.72 \\ & & & & L &= 6.88 \end{aligned}$$

Round these values to $D = 1.75$; $L = 7$

Assume the tanks to be fabricated from stainless steel, type 420, heat-treated. This material has a yield strength of 200,000 psi. The tanks will be designed for a stress of 150,000 psi or $10,568 \text{ kg/cm}^2$.

The stress in the wall of a pressurized cylinder is given by

$$S = pr/t, \text{ where } p \text{ is pressure}$$

r is radius of the cylinder

t is the wall thickness

The static pressure of the fluids in the hydrogen and oxygen tanks will be less than one atmosphere. It will therefore have little impact on the final answer and is neglected.

For the hydrogen tank,

$$S = 10.568 \times 10^7 \text{ kg/m}^2 = \frac{13 \times 10,336 \text{ kg/m}^2 \times 0.875 \text{ m}}{t}$$

$$t = \frac{0.134368 \times 10^6 \times 0.875}{10.568 \times 10^7} = 0.0011 \text{ m} = 0.11 \text{ cm}$$

The total volume of stainless steel for the cylinder is

$$\begin{aligned} V_C &= 2\pi r \times t \times L \\ &= 2\pi \times 0.875 \times 0.0011 \times 7 = 0.0428 \text{ m}^3 \end{aligned}$$

Assume the end closures to be hemispheres of the same thickness as the cylinder wall.

$$V_C = \frac{4\pi r_1^3}{3} - \frac{4\pi r_2^3}{3} = \frac{4\pi (0.875)^3}{3} - \frac{4\pi (0.875 - 0.0011)^3}{3} = 0.11 \text{ m}^3$$

$$\text{Total volume} = .0428 + .011 = 0.0538 \text{ m}^3$$

The density of this steel is 0.28 lb/in³ or

$$7,765 \text{ kg/m}^3. \text{ The tank weight will be } W = 0.0428 \times 7,765 = 332 \text{ kg}$$

A tank wall thickness of 1.1 mm will not be self-supporting when empty, and like the fuel tanks of the ATLAS booster will have to be pressurized when empty, to prevent collapse.

For the oxygen tank which requires a volume of 7.724 cubic meters, round to 8.0 m³. Use a length to diameter ratio of 4.

$$\text{Then } \frac{\pi D^2 \times L}{4} = 8 = \frac{\pi D^2 \times 4 D}{4} \text{ and}$$

$$D^3 = 8/\pi = 1.36; r = 0.68, L = 5.44$$

The critical pressure for oxygen is 50.5 atm. Stress in the cylinder wall will be:

$$s = 10.568 \times 10^7 \text{ kg/m}^2 = \frac{50.5 \times 10,336 \text{ kg/m}^2 \times 0.68}{t} \text{ and}$$

$$t = \frac{0.521968 \times 10^6 \times 0.68}{10,568 \times 10^7} = 0.0034 \text{ m} = 3.4 \text{ mm}$$

The volume of steel in the cylinder is

$$V_C = 2 \pi r \times t \times L = 2 \pi \times 0.68 \times 5.5 \times 0.0034 \\ = 0.08 \text{ m}^3 \text{ and } W = 0.08 \times 7,765 = 621 \text{ kg}$$

For the end closures

$$V_E = \frac{4 \pi (0.68)^3}{3} - \frac{4 \pi (0.068 - 0.0034)^3}{3} = 0.02 \text{ m}^3$$

$$W_E = 0.02 \times 7,765 = 155^3 \text{ kg}$$

$$\text{Total tank weight} = V_C + V_E = 621 + 155 = 776 \text{ kg}$$

The remaining tank element which will contribute significant weight to the fuel cell system is the water tank. Its weight is calculated as follows:

$$\text{Total weight of water} = 10,000 \text{ kg}$$

$$\text{Volume of water} = 10,000,000 \text{ cc} \\ = 10 \text{ m}^3$$

Let the water tank have a length to diameter ratio of 4

$$\frac{\pi D^2}{4} \times L = 10 = \frac{\pi D^2}{4} \times 4D \quad \text{and} \quad \begin{aligned} D^3 &= 10/\pi \\ D &= 1.47 \\ L &= 6 \text{ m} \end{aligned}$$

Assuming that the tank is oriented vertically, the pressure at the bottom of the tank due to the weight of the water is:

$$p = p_0 + \rho h, \text{ where } p_0 \text{ is atmospheric pressure,} \\ \rho \text{ is density of water and} \\ h \text{ is height of water column.}$$

In an Earth environment, the atmospheric pressure would be exactly balanced by the same pressure applied to the outside of the tank, however during ferry from Earth to Moon it will be assumed that the vapor pressure inside the tank is equivalent to one atmosphere and that there is no outside pressure to balance it. Therefore,

$$p = 10,359 \text{ kg/m}^2 + 1000 \text{ kg/m}^2 \times 6 \text{ m} \\ = 16,359 \text{ kg/m}^2$$

Assume that the water tank is made of the same stainless steel as the fuel tanks, and solve for tank wall thickness:

$$s = pr/t = 10.568 \times 10^7 \text{ kg/m}^2 = \frac{16,359 \times 0.75}{t}$$

$$t = \frac{16,359 \times 10^3 \times 0.75}{10,568 \times 10^7} = 1.161 \times 10^{-4} \text{ m}$$

$$= 0.1161 \text{ mm}$$

Although this solution satisfies the pressure conditioning of the water tank, a 0.1 millimeter wall thickness is considered too fragile for practical use. Therefore, an arbitrary increase to the 1.1 mm wall thickness of the hydrogen tank is taken. On that basis, the weight of the water tank is calculated:

The volume of steel is

$$V_C = 2(\pi) \times 0.75 \times 0.0011 \times 6$$

$$= 0.031 \text{ m}^3$$

For the end closures:

$$V_E = \frac{4(\pi)(0.75)^3}{3} - \frac{4(\pi)(0.75 - 0.0011)^3}{3}$$

$$= .0078$$

$$V = 0.031 + 0.0078 = 0.0388$$

$$W = 0.0388 \times 7,765 = 301 \text{ kg}$$

The third major component of the fuel cell system is the electrolyzer. In the study report: Electrochemical Energy Storage for an orbiting Space Station, by R.E. Martin, the design weight of the electrolysis cell system was 70% of the weight of the fuel cell system. Applying this factor to the lunar fuel cell system for a 60 kW power module we can estimate the total weight of the power system:

Fuel cell subsystem	-	1728 kg
Electrolysis subsystem	-	1210 kg
Reactants	-	9851 kg
Hydrogen tank	-	332 kg
Oxygen tank	-	776 kg
Water tank	-	<u>301 kg</u>
Total system weight		14,199 kg

The tank calculations were based upon a stress in the tanks due to the internal pressure of 75% of the yield strength of the material. It seems prudent to design for a greater safety factor to allow for accidents of overpressure which were not handled properly by safety values. If one arbitrarily doubles the thickness of the tank walls, doubling the tank weight, then the total system weight is:

Fuel cell subsystem	-	1728 kg
Electrolysis subsystem	-	1210 kg
Reactants	-	9851 kg
Hydrogen tank	-	664 kg
Oxygen tank	-	1552 kg
Water tank	-	<u>602 kg</u>
Total system weight		15,607 kg

This is an increase in total system weight of 10%, which is a reasonable price for the added safety factor.

The foregoing is not suggested as an optimum design for the fuel cell storage system, but provides a representative system weight which can be used as a basis for comparison to advanced battery systems.

5.3 ADVANCED BATTERIES

Batteries are probably the most extensively used methods of energy storage, aside from fuels, which are employed on earth. A large proportion of these are the lead/acid battery with which every automobile and many emergency back-up systems. The batteries which have been in common use on Earth, however do not have a high enough specific energy density to make them attractive for use at the lunar base. The total required weight for transport to the Moon would make them too expensive. Nevertheless, batteries are an attractive solution to the lunar base energy storage problem, because of their relative simplicity, reliability and for the secondary batteries, their ease of rechargeability.

During the energy crisis of the early 70s there was a reawakened interest in the development of new types of batteries which might be able to provide a practical source of energy for the propulsion of automobiles. Two of these show considerable promise and are potentially applicable to the lunar base. These are the sodium/sulfur battery, a secondary cell and the aluminum/oxygen battery, a primary cell.

5.3.1 THE SODIUM/SULPHUR CELL

The sodium sulphur battery is an invention of the Ford Motor Company. Active development programs exist at Ford, General Motors, General Electric, Hitachi and Brown-Boveri. Brown-Boveri in West Germany has the largest development program at the present time. Both they and Ford have experience in the use of the battery for the propulsion of automobiles. In this country funding for battery research and development has come from industry, from the Department of Energy and from the Air Force via Wright-Patterson AFB.

The sodium/sulphur battery is made up of reservoirs of sodium and sulphur, separated by a barrier of beta-alumina. The battery is normally operated at a temperature of about 350 C. At this temperature both the sodium and the sulphur are in the liquid phase and act as the electrodes of the battery. The beta-alumina serves as the electrolyte, providing a conduction path for positive ions and an insulating barrier for electrons, which flow through the load. The existence of this battery as a practical device is dependent on this solid-state electrolyte. The composition of choice today is identified as beta-double prime-alumina whose composition is by weight 90.4% Al_2O_3 , 8.85% Na_2O and 0.75% Li_2O . The resulting lattice structure provides the ionic conduction path for the positive sodium ions. The only domestic manufacturer is the Ceramtec Corporation in Salt Lake City.

Practical physical configurations for the battery have been extensively explored by the Aeronutronic Division of Ford Aerospace and Communications Corp. under contract to the Aero Propulsion Laboratory at Wright-Patterson AFB. The results of this work is documented in report AFWAL-TR-85-2078, entitled Sodium-Sulphur Satellite Battery Design Analysis by R.W. Minck, E.E. Ritchie and M.L. McClanahan. This report also contains detailed analyses of charge and discharge characteristics as well as information on reliability and manufacturability. The configuration of choice is the cylindrical cell which is illustrated in Figure 5.3.1.

Characteristics of the sodium/sulphur battery which make it a suitable candidate for use at the lunar base are: (1) a high specific energy, potentially 200 watt hours per kilogram for high ampere hour batteries; (2) a calendar life of approximately 10 years; a cycle life of approximately 2500; and flexible recharge characteristics.

A complication in the use of this battery at the lunar base arises from the fact that the highest specific energy is obtained in batteries of moderate ampere hour capacity and at a fairly high discharge rate. An example, taken from the data in the referenced report follows.

An energy density of 205 watt hours per kilogram is projected for a 40 ampere hour cell having an electrolyte diameter of 1.75 cm and a length to diameter ratio of 15, at a discharge current density of 0.3 amperes per cm^2 . The active electrolyte area is:

$$a = 2(\pi) \times \frac{1.75^2}{2} \times 15 = 144 \text{ cm}^2$$

Total cell current is:

$$A = 144 \times 0.3 = 43 \text{ amperes}$$

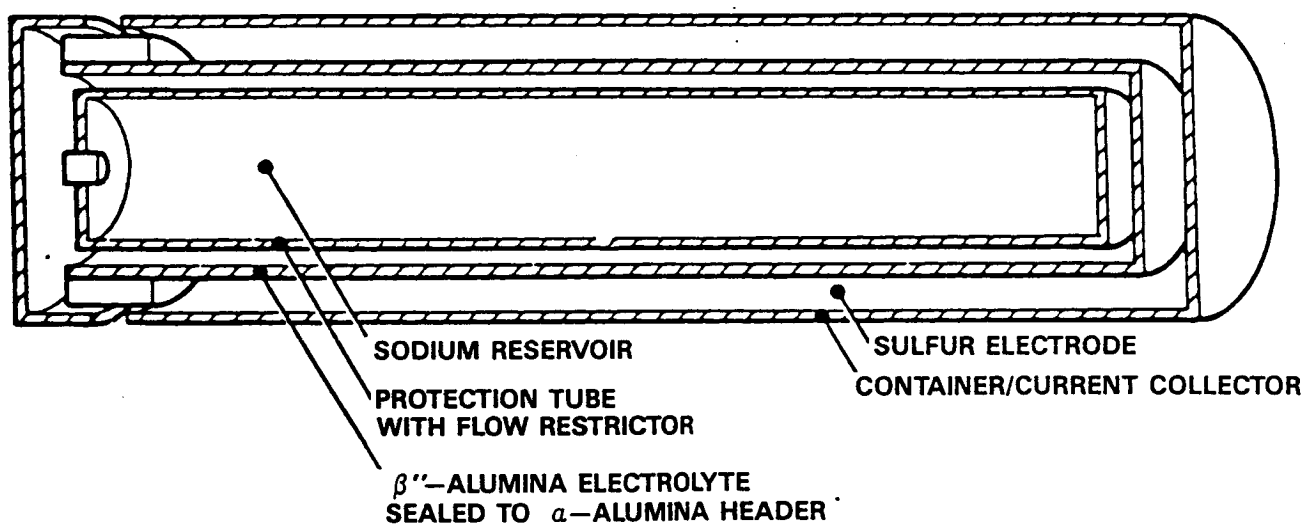


Figure 5.3.1. Sodium/Sulfur Battery, Single-Tube Cell Schematic

For a 40 ampere hour battery, the energy content will be depleted in less than an hour. Because of this a battery storage system based upon the sodium sulphur cell will require a fairly elaborate control subsystem for switching between banks of cells as their depletion condition is reached. It is possible to design and build such a control system, however, this adds to the complexity of the system and will result in a lower overall reliability.

In order to provide nighttime power for a 60 kW power system module, 22,500 kilowatt-hours of energy are required. At an energy density of 200 watt hours per kilogram, the weight of the batteries alone will be:

$$22,500 \div 0.2 = 112,500 \text{ kg}$$

This would have to be increased somewhat for the weight of the control subsystem. It can be seen from this analysis that although there is an appeal for the use of a battery resulting from its relative simplicity, weight-wise it is not competitive with the fuel cell system with its total launch weight of 15,600 kg.

5.3.2 THE ALUMINUM/OXYGEN BATTERY

The aluminum/oxygen battery is an advanced primary cell whose development, like that of the sodium/sulphur cell was inspired during the energy crisis by its potential for use in automotive propulsion. This is a primary battery and so requires a continual resupply of fuel. It is of interest because it has a high specific energy and because both fuels occur on the Moon. The fuels do not occur in free form but will require processing for recovery. An oxygen plant is reckoned to be one of the earliest lunar enterprises, with recovery probably being from ilmenite which has the lowest process energy input requirement. Aluminum processing will doubtless occur at some point in the life of the lunar base, however, it will not be one of the early processes.

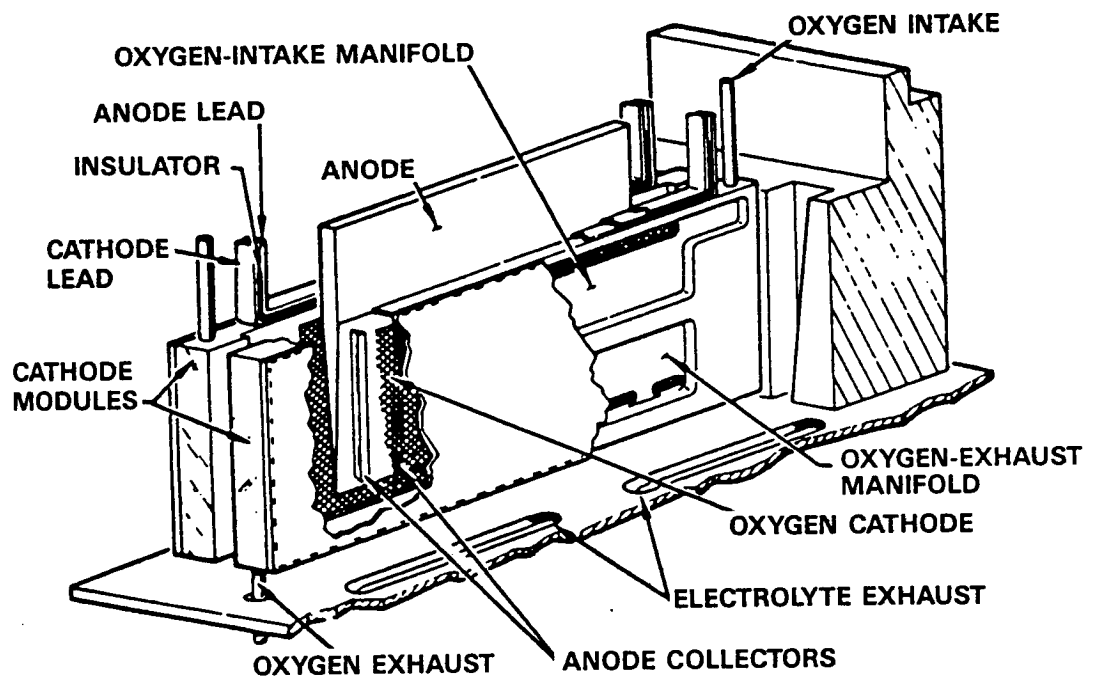
The principal sponsor of development work on the aluminum/oxygen battery has been Dr. Arturo Maimoni of the Lawrence Livermore National Laboratory working through the Department of energy. Work has been performed at Livermore, at ELTECH Systems Corporation and at Lockheed Palo Alto Research Laboratories. Dr. Maimoni's assessment of status is that the battery is in a very early stage of development but that sufficient progress has been made that one can be sure of having production units in time for use at the lunar base. The principal difficulty at the present time is funding for continued development. With the easing of crude oil prices and a more conservative use pattern for petroleum products, there is very little motivation today for research in alternate power sources.

A schematic of one configuration for the aluminum/oxygen battery is shown in Figure 5.3.2. The anode is an aluminum plate which is continuously consumed by the process in a reaction with gaseous oxygen. The fuel supply is renewed by adding aluminum plates as they are consumed and by a continuous flow of oxygen. The electrolyte is sodium hydroxide and the reaction product is caustic aluminate, $\text{NaAl}(\text{OH})_4$. A separate section of the battery decomposes the caustic aluminate into sodium hydroxide and aluminum trihydroxide. The latter precipitates as a solid which is similar to the feedstock used by the aluminum industry and can therefore be recycled.

The aluminum/oxygen battery is able to achieve a specific energy of 300 watt-hours per kilogram. Total weight requirement for a 60 kW power source for the 375 hour night is:

$$60 \times 10^3 \times 375 - 300 = 75,000 \text{ kg.}$$

When the lunar base is sufficiently mature to provide fuels for the aluminum air battery, the mass transported from Earth may be reduced by approximately 40%. In that circumstance the weight transported from Earth for a 60 kW power module would be 45,000 kg. Even in this case, batteries do not compete favorably with fuel cells.



WEDGE-SHAPED CELLS ARE FORMED BY POSITIONING TWO AIR-CATHODE CASSETTES AT AN ANGLE OF 3 TO 6 DEG. INDIVIDUAL CASSETTES CAN BE REMOVED AND REPLACED FOLLOWING ELECTRODE MALFUNCTION OR FAILURE

Figure 5.3.2. Aluminum/Oxygen Battery

5.4 SUMMARY OF BATTERY CHARACTERISTICS

Work continues toward the improvement of many different kinds of batteries and the current status of battery development has been summarized by Ralph J. Brodd of AMOCO Research Center in his report entitled "Advanced Batteries" published in CHEMTECH for October 1985. An excerpt from this report follows:

Battery Type	Energy Density Wh/kg	Cycle Life (cycles)	Efficiency (%)
Lead-Acid	42	800	75
Nickel-hydrogen	45	10,000	70
Nickel-zinc	60	400	70
Nickel-iron	54	1,100	60
Lithium-iron sulfide	95	900	70
Sodium-sulphur	200	2,500	80
Zinc-bromine	65	400	65
Zinc-chlorine	65	1,400	60
Aluminum-Oxygen	300	-	40
Iron-air	94	1,000	45
Lithium-iron sulfide	125	1,000	70
Zinc-air	100	250	50

5.4 THERMAL RESERVOIR STORAGE

Thermal storage does not offer an attractive option for energy storage in the early phase of the lunar base, because initially all power system components will have to be transported from earth and the weight of a thermal storage unit for 22,500 kW hrs. would be prohibitive. In the long-term however, this is expected to change. One of the earliest lunar manufacturing processes is expected to be the recovery of oxygen from ilmenite FeTiO_3 . A by-product of this process will be iron. Iron with a specific heat of $0.108 \text{ cal/gm}^\circ\text{C}$ and a thermal conductivity of $0.803 \text{ watts/cm}^\circ\text{C}$ will be a suitable material for a thermal reservoir. An appropriate quantity can be buried in an excavation in the regolith, the latter being an excellent thermal insulator.

A suitable transport medium for conducting thermal energy would be liquid sodium. The sodium could be heated by solar concentrators and pumped by electromagnetic pumps. The only moving part of such a system would be the liquid sodium. Such an energy storage system is far enough in the future of the lunar base that no engineering calculations were made in this study.

5.5 FLYWHEELS

5.5 INERTIA WHEELS

5.5.1 INTRODUCTION

The use of inertia wheels to store energy for a proposed lunar colony is examined. A review of strength of materials considerations indicates that high strength, low density composites represent the most attractive materials to use.

A review of the existing state-of-the-art in composite flywheel research and design produced two configurations worthy of further development and testing. One of these designs was proposed by General Electric's Space Systems Division and the other is proposed in the present study. The first minimizes overall weight (1280 Kg/wheel on earth) and maximizes energy density (155.0 Wh/Kg at burst) but makes little use of lunar materials (14% Glass). The second design maximizes the use of lunar materials (60% Glass) but is seen to have excessive weight (1810 Kg/wheel on Earth) and lower energy density (111.5 Wh/Kg at burst). 225 wheels of either configuration are estimated to be needed to supply the storage requirements of a 60 kW power module.

Terrestrial production of both designs could be feasible with respect to a 1992 need date if an accelerated program of research and development were undertaken. Lunar production of either design would require input of organic materials and, as such, would not be 100% self-sufficient.

Areas for further research are identified.

5.5.2 ADVANTAGES AND DISADVANTAGES OF FLYWHEELS

In considering inertia wheels as a candidate for a lunar colony's energy storage system the following advantages can be noted:

- Potential for high lifetime
- Potential for high energy density
- Potential for high power and voltage levels
- Latitude for thermal control is greater than that for batteries.
- Ready adaptability to "power module" approach
- No degradation in storage ability with age/cycles
- Variations in energy storage/discharge levels can be easily accommodated

Some of the immediately obvious disadvantages associated with inertia wheels include:

- Physical upper limit on energy density improvements
- Thermal limitations
- Need for maintenance (bearings motor/generator balancing, material integrity)
- Lack of adequate operational experience with advanced components (composite wheels, magnetic bearings, high voltage systems)

5.5.3 BASIC CONCEPTS

Appendix A presents the equations governing the distribution of circumferential and radial stresses in an isotropic rotating disk. For the solid disk and the annulus the circumferential stress level is always greater than the radial and, therefore, represents the governing design concern.

The theoretical maximum energy density (Wh/Kg) associated with an isotropic material is proportional to its yield stress divided by its density. Thus, a desirable material would be one of high yield strength and low density. (Note that this criterion is consistent with the need for minimizing the shuttle payload(s) associated with supplying material to a moon-based colony). To further minimize the flywheel mass the designer can take advantage of the need for greater strength in the circumferential direction than that of the radial direction. A well selected anisotropic material could meet the design requirements and result in lower mass than would an isotropic material.

In this light it is necessary to consider composite materials as well as more traditional materials. Table 5.5.1 presents an initial comparison of various metal and composite material properties. The values shown for maximum energy density correspond to an isotropic rotating disk of the given material. This should be considered as a relative figure of merit only. Appendix A contains the derivation of this quantity as well as a sample calculation. The data presented in Table 5.5.1 indicates a marked advantage of the composite materials over the traditional alloys in theoretical energy density. It is therefore felt that these materials deserve consideration in the present study.

Fused silica is typically used as optical waveguide material and, as such, has been the subject of much research from the point of

view of improving its tensile characteristics. After a survey of available literature of the subject T08 Fused Quartz was chosen to be the strongest available fused silicate. (A similar product, "Suprasil 2" has the same material properties. Both are available from Amersil, Inc., Sayreville, N.J.).

S-2 Glass, available from Owens-Corning Fiberglass, differs in chemical composition from the optical waveguide glasses. Fused quartz is made of silicon dioxide. The S-Glasses typically contain a significant fraction of aluminum and magnesium dioxide in addition to silicon dioxide.

Table 5.5.1 Material Properties

Material	Density (gm/cc)	Yield Stress (GN/m ²)	Burst Energy Density (Wh/kg)
Al 2024 T3	2.77	0.35	13.6
Al 7079 T6	2.7	0.46	18.7
Al-Boron	2.7	1.25	49.8
Graphite-Epoxy	1.7	1.0	63.2
Kevlar-Epoxy	1.35	1.5	119.7
T08 Fused Quartz Fiber	2.65	3.5	142.2
S-2 Glass Fiber	2.5	4.75	204.6
S-2 Glass Fiber/Epoxy Resin	2.08	1.79	92.7

Burst energy density is calculated for an isotropic disk

(Material properties were taken from (Bunsell, 1982), (Burdick, 1982), (Dimarcello, et.al., 1978), (Donnet, et.al., 1984), and (McMullen, 1984). Where values conflicted the most conservative set of data were taken).

5.5.4 OVERVIEW OF COMPOSITE INERTIA WHEEL TECHNOLOGY

In 1974 the Department of Energy (DOE) initiated a mechanical energy storage technology program having as its goal to develop by 1984 a viable composite flywheel with the following features:

- 88 Wh/Kg energy density at failure
- 44 to 55 Wh/Kg operational range
- 1 kWh storage capacity

In addition to the above, the need to develop an appropriate containment technology was recognized.

In parallel with the DOE effort NASA displayed an increased interest in composite flywheels as a potential Integrated Power and Attitude Control System (IPACS) for satellites and space stations. Combining energy storage and attitude control functions was (and still is) seen as an attractive weight reduction measure.

By virtue of their high energy storage density DOE selected two of the Phase 1 flywheel systems for additional research (Olszewski 1983). These two systems are summarized in Table 5.5.2 below.

Table 5.5.2 State-of-the-Art Composite Flywheel Performance

Manufacturer	Wheel Type	Material	Burst Energy Density (Wh/Kg)
General Electric	Disk/Ring	SG/G	68.0
Garrett AirResearch	Rim	K49/K29/SG	79.5

SG = S Glass
G = Graphite

K49 = Kevlar 49

K29 = Kevlar 29

Before evaluating the individual designs it is worthwhile to discuss the most popular composite flywheel designs.

5.5.2.1 MULTI-RING DESIGN

The multi-ring flywheel is composed of concentric rings that are assembled with interference fits. The radial pressure of the interference fitting serves to decrease radial tensile stresses during operation in addition to providing minor circumferential stress reduction. The rationale behind the multi-ring approach is that the rings are thin enough to maintain minimal radial stress levels and no stress is transmitted across the interfaces between rings.

5.5.2.2 RING/DISK DESIGN

The ring/disk design employs an inner disk around which a filament wound ring is interference fitted. The functions of the

ring include:

- High energy density operation
- Ring/disk interface pressure helps to reduce disk tensile and ring radial stresses
- Prevention of fraying and disk edge degradation
- Improvement of disk fatigue and creep problems
- Failure mode is circumferential ring burst instead of more severe disk rupture.

Advantages associated with this hybrid design include the fact that a higher energy density/unit volume can be achieved when compared to the multi-ring design, and it has a controlled failure mode.

5.5.3 THE GENERAL ELECTRIC COMPOSITE RING/DISK FLYWHEEL

The G.E. flywheel (Coppa, 1983) is composed of a glass/epoxy disk, a graphite fiber/epoxy matrix wound ring which is interference fitted over the disk, and an aluminum hub bonded elastomerically to the disk. The nominal energy storage capacities of the GE flywheels were 0.5 kWh (ultimate) and 0.25 kWh (operational). The operational energy density of the rotor was estimated to be 40 Wh/Kg. GE manufactured 14 such rotors which differed only in the type of epoxy resin used for the matrix material. Two rotors (H8 & H6) were subjected to ultimate speed burst testing and failed due to circumferential ring failure at 47,060 and 46,990 rpm (68.0 and 67.0 Wh/Kg, respectively). Rotor H8 successfully underwent 10,000 cycles of approximately 80% discharge. GE engineers developed analysis techniques and software to assist in the design and optimization of their hybrid rotor. Based on their experience and analysis the GE engineers concluded that future rotors should either be of the multi-ring variety or they should utilize a flexible (as opposed to a rigid) matrix material in the ring portion of a ring/disk rotor. The flexible matrix

ring material was found to be desirable because it would raise allowable radial strain levels high enough to eliminate radial fracture modes and permit thicker disks. Also recommended was the utilization of high strength fibers such as graphite or Kevlar to increase energy density.

5.5.4 GARRETT AIRESEARCH COMPOSITE RIM (SATCHWELL, 1979)

This flywheel was composed of a S-Glass/Kevlar49/Kevlar29 multi-ring rim mounted on a graphite composite spoked hub. The rim was made up of fifteen concentric rings of which the 2 inner ones were S Glass, the 5 middle ones were Kevlar 29, and the 8 outer ones were Kevlar 49 in an epoxy composite matrix. The rim was designed to become circular during operation and was not circular on assembly. Due to the sub-circular shape the fibers were subjected to bending stress while the rim is at rest. As the rim assumes its circular (operational) shape these bending stresses diminish.

The rim failed catastrophically after 2585 cycles at an energy storage density (65.4 Wh/Kg) that was 26% below design specifications. It is believed that this low performance was due to poor resin impregnation during fabrication. (Another possible explanation is that the bending load imposed on the fibers at rest may serve to weaken them over the long-term).

5.5.5 ADVANCED COMPOSITE FLYWHEEL CONCEPTS

Table 5.5.3 presents a summary of data pertaining to advanced composite flywheel designs found in the literature and one design proposed in the present study. The data presented are theoretical in that none of the proposed flywheels have actually been built or tested, however it should be noted that both GE and the Lord Corp. have acquired experience in composite flywheel design and analysis to add credibility to their proposed designs.

The proposed S2-Glass disk/fused quartz filament ring configuration represents an attractive concept for a lunar environment because it contains a higher percentage of silicon than the other two designs. It should be noted that the figures presented for the flywheel proposed in the present study are very approximate. A thorough analysis along the lines of (Genta 1984) is recommended.

In the discussion which follows rough estimates of the overall mass of material needed for the proposed lunar colony are presented. These estimates are based on simple "scale-up" analysis and do not attempt to address the potentially complex problems that might be encountered when transforming a design for a small (e.g. 5 kWh) wheel into one for a 100 kWh wheel. This data is summarized in Table 5.5.4 (Sample calculations are shown in Appendix B).

Table 5.5.4 Proposed Advanced Composite Flywheel Performance

Designer	Wheel Type	Material	Calculated Burst Energy Density (Wh/Kg)
General Electric	Disk/Ring	SG/G	155.0
Lord Corp.	Disk/Ring	SG/G	80.3
Present Study	Disk/Ring	S ₂ G/FQ	111.5

SG = S Glass

G = Graphite

FQ = T08 Fused Quartz

5.5.5.1 GE's ADVANCED COMPOSITE DISK/RING FLYWHEEL (COPPA, 1983)

A theoretical design for a space station size wheel (5.0 kWh) operational energy at 75% depth of discharge (DOD) produced specifications for high strain graphite fiber ring/glass epoxy disk rotor having a useful energy density of 79 Wh/kg. 100% operational speed is calculated to be 31,800 rpm.

As is shown in Appendix B, to supply the storage for a 60 kW power module would require 225 of these wheels weighing 1280 Kg. The wheel would have a thickness of 16.5 cm (5.2 In.) and a diameter of 2.97 m (117 in.). The useful energy per wheel would be approximately 100 kWh/wheel.

5.5.5.2 LORD CORPORATION'S DISK/RING FLYWHEEL (GUPTA, 1984)

This design is essentially a variation on the original GE disk/ring design (Table 5.5.2) in which the epoxy matrix in the ring is replaced with a urethane elastomer and a high strain carbon fiber is used in the ring.

Lord engineers claim that the following benefits result from their design:

- The ring could be made very thick
- The disk might be eliminated altogether and replaced with a metallic hub
- The maximum tensile stress occurs at the ring's outer diameter instead of at the ring/disk interface
- The problem of ring/disk separation is eliminated

Burst energy density for the flywheel was calculated to be 80.3 kWh/kg at a failure speed of 46,900 rpm. Assuming a maximum operation at 2/3 of burst energy (for consistency with G.E.'s data presented above) and 75% DOD this corresponds to a useful energy density of 40 kWh/Kg.

A 60 kW power module would require 225 of these wheels weighing 2520 Kg (5545 lbs on Earth) of which 24.5% would be S-2 Glass. The wheel would have a thickness of 25.4 cm (10 in) and a diameter of 2.8 m (111). The useful energy per wheel would be approximately 100 Wh/wheel.

5.5.5.3 PROPOSED S2-GLASS DISK/FUSED QUARTZ RING FLYWHEEL

This design is a variation on the Lord Corporation's disk/ring design discussed above in which the high strain carbon fiber in the ring is replaced with a zirconia induction furnace drawn, firepolished T08 Fused Quartz or Suprasil 2 optical waveguide quality fiber in an epoxy matrix. Burst energy density is calculated to be 111.5 Wh/Kg. Calculating the operational energy density in the same way as above results in a value of 55.8 Wh/Kg.

A 60 kW power module would require 225 of these wheels weighing 1810 Kg (3980 lbs on Earth) of which 60% would be "glass" (either S2-Glass or quartz fiber). The wheel would have a thickness of 25.4 cm (10 in.) and a diameter of 2.17 m (85.4 in.). The useful energy per wheel would be approximately 100 kWh/wheel.

5.5.5.4 COMPARISON OF ADVANCED FLYWHEEL DESIGNS

Criteria to consider in choosing a flywheel design for the lunar base include low overall mass for the initial installation, and maximum utilization of materials available on the moon for future expansion of the colony. As is evident from the data discussed above and presented in Table 5.5.4 none of the available designs readily meet these requirements.

Table 5.5.4 Approximate Advanced Composite Flywheel Material Requirements for Proposed Lunar Colony

Designer	Earth Weight per wheel (Kg)/(lb)	% "Glass"	Lunar Wt per Wheel (Kg)/(lb)
General Elec.	1280 (2815)	14.35	213 (470)
Lord Corp.	2520 (5545)	24.5	420 (925)
Present Study	1810 (3980)	60.0	300 (600)

Notes:

- Sample calculations in Appendix B.
- (1000 wheels) *(Mass/Wheel) = Total mass needed
- Mass/weight figures are for flywheel material only. Secondary/auxiliary systems are not included.
- % "Glass": either S2-Glass or Fused Quartz
- Energy storage per wheel = 100 kWh.

All three designs involve the use of organic resins which pose as yet unresolved questions in the lunar environment. (See the manufacturing and environmental sections of the current study).

For purposes of comparison the designs are scaled in terms of 100 kWh wheels of which 225 would be required. Questions of bearings, motor/generators, control and other secondary systems have not yet been examined though it is safe to say that they will comprise at least an additional 10% of the total wheel weight.

Due to the large difference in gravity forces any terrestrial testing and trouble-shooting may still leave unanswered questions about the complete system operation in the lunar environment. The prospect of installing, "shaking down", and operating 225 of these somewhat massive flywheel systems is troubling for such a critical application.

From the standpoint of transport, handling, and energy density the G.E. design appears to offer the most promise. Additional research is required to resolve questions of scale-up, bearing, and secondary systems, manufacture, and (perhaps automated) installation.

The system proposed in the present study is worthy of more research because of its high silicon utilization. Research efforts are needed to design and test prototypes, as well as improve the strength characteristic of the fused silicon fibers.

One possible scenario would be to use a version of the G.E. design for the initial installation while concurrently developing the 60% "glass" design for future expansion of the colony.

5.5.6 ENVIRONMENTAL CONSIDERATIONS

Environmental considerations for a lunar installation include:

- Temperature variations,
- Radiation,
- Vacuum conditions, and
- Meteorites.

All of the above will impact the choice and design of a lunar based energy storage system. These factors are discussed briefly below for the flywheel systems evaluated previously.

5.5.6.1 TEMPERATURE VARIATIONS AND RADIATION

Temperature (as well as radiation) variations on the lunar surface must be considered in design. Large temperature swings occur on the lunar surface between night and day. Typical resin matrix materials used in composite laminates are discussed in (Bunsell, 1982). The epoxy resins which are used in all three of the advanced flywheel designs proposed above are generally rated to an upper limit of 150 C. The lower limits are not discussed but at extremely low temperatures brittleness could conceivably become a problem. If fused quartz fibers are used they will also require protection from high temperatures. As discussed in (Kao, 1977) the time to failure of a silica fiber decreases exponentially with increasing temperature. The effect of extremely low temperatures is not known at the present time. In general thermal gradients across the composite material are not desirable due to the possibility of causing internal strains between the matrix and fiber materials. Isolation from the extreme lunar surface thermal conditions is clearly necessary. This isolation could come in the form of a simple airplane hanger-like shielding or from locating the flywheels underground. (In addition to protection from the thermal environment there will be a need for frictional heat rejection from the inertia wheel system that is not addressed in the present report). Ultra-violet radiation can degrade the stability and material properties of epoxy and silicon resins (as well as Kevlar). Radiation shielding will therefore be necessary.

5.5.6.2 VACUUM CONSIDERATIONS

A point of principal importance in the manufacture of composite laminates using resin matrix requires is that of "curing". Moisture absorption during manufacture requires subsequent dispersion. As discussed in (Dorey, 1982) attaining equilibrium can be a long-term process during which a danger exists from the formation of internal stresses and voids. The effect of a vacuum environment on composite matrix materials is one that still requires investigation. It is anticipated that serious outgas problems will require sealing any exposed material in a highly effective manner.

5.5.6.3 METEORITES

Clearly the possibility of meteorites hitting critical rotating equipment requires addressing. It is felt that any isolation from the lunar thermal cycles should also provide protection from meteorites.

5.5.6.4 OTHER ENVIRONMENTAL CONSIDERATIONS

The three flywheel designs discussed in the present report will fail in the circumferential ring burst mode which is least catastrophic of the flywheel failure modes. This mode of failure is characterized by shredding of the outer ring. It is presumed that a control system would be used to detect this sort of imbalance and stop the wheel. A well designed array of flywheel modules could conceivably reduce or eliminate the need for containment though the occasional presence of astronauts suggests that the problem be more thoroughly investigated.

5.5.7 MANUFACTURING: TERRESTRIAL AND LUNAR CONSIDERATIONS

5.5.7.1 TERRESTRIAL CONSIDERATIONS

In general terms the 1992 state-of-the-art requirement for lunar colony systems does not pose any problems that a program of continued research and accelerated development could not resolve. From a materials standpoint much work has been and continues to be done in advanced research and product development. Composite materials have become standard fare in aerospace applications and they are gaining increasing importance in the marine and automobile industries. Production of high-strength optical fibers has been developed towards the end of developing underwater and other long distance communications applications. Techniques for producing high-strength optical waveguides typically involve firepolishing initial rod or tubular glass stock with an oxyhydrogen torch after which the fibers are drawn in a carbon dioxide laser or zirconia induction furnace

(Runk, 1977). (The latter technique provides the strongest fibers). The principal manufacturing concerns have to do with the assurance of high quality materials. Meeting these concerns is not seen to be insurmountable.

5.5.7.2 LUNAR CONSIDERATIONS

None of the flywheels discussed in the present study are completely composed of materials available on the moon. The presence of organic polymer resins in each design illustrates the need for non-lunar materials. Specifically, the most important non-lunar material that would be needed is carbon as an ingredient in the resins and, possibly, for fiber production. Carbon could be provided by the Earth or through mining of asteroids. The possibility of using inorganic polymers was examined (Lee, 1979) in which their general undesirability for use in high stress environments was discussed. Much research in the field of inorganic polymer science would be required before they could be considered for use in composite laminates. If organic polymers are to be used in a lunar application the question of where to produce the resins would deserve attention. The raw material could conceivably be transported to the Moon (or a nearby station) for subsequent resin production if it were considered viable. The principal elements needed for the production of glass (S2-Glass or fused quartz) exist on the moon. A scheme developed to produce fiberglass as a byproduct of aluminum production is discussed in (Ho, 1979). This type of technique could presumably be adapted to produce the glasses needed for composite fibers. Glass fiber manufacture requires temperatures above 1500 C concentrated upon relatively small areas. Questions of how to provide and control this heat would need in-depth examination if these materials are to be produced on the moon.

5.5.8 CONCLUSIONS

In the interest of minimum weight and maximum strength and energy density non-metallic composite materials show the most promise.

Specifically: graphite/epoxy, S2-Glass/expoxy, and fused quartz offer the most favorable characteristics. Lunar production of these composites would not be 100% self-sufficient. The most promising candidate flywheel is the General Electric disk/ring. This flywheel was proposed to store 5 kWh of useful energy and, as such, would require a significant effort to be scaled up to store more energy. The G.E. flywheel would require a significant input of organic materials as it contains only 14% glass.

It is estimated that 225 of these wheels each weighing 1200 Kg (terrestrial) would be required for a 60 kW power module.

The other design recommended for additional research and development involves an S2-Glass fiber/epoxy disk around which a fused quartz fiber/epoxy laminate ring would be wound. This design maximizes the use of lunar material (60% glasses) but results in a higher weight (1810 Kg terrestrial) and lower energy density than the G.E. design. One-thousand of these wheels would be needed.

Both designs will fail in the least dangerous circumferential ring burst mode. Some form of containment or isolation is, nevertheless, considered necessary to insure protection of humans against catastrophic wheel failure. Either configuration would require protection from radiation in addition to isolation from extreme lunar surface temperature swings. Effective sealing of resins against outgassing would probably be necessary as well as protection against meteors.

A 1992 date for technology readiness does not appear to pose any insurmountable problems. The G.E. design would require less development effort than that proposed in the present study because of its similarity to flywheels that have already been developed and tested.

5.5.8.1 AREAS FOR FUTURE INVESTIGATIONS

The following topics would require research and development efforts to meet the 1992 technology readiness deadline:

- Flywheel design and scale-up studies with special emphasis on increasing energy density and minimizing weight.
- Analysis of the effects of the lunar environment on epoxy resin materials.
- Development of high efficiency, low weight auxiliary systems for control and energy conversion.
- Development of high quality terrestrial manufacturing capability.
- Research into long-range extra-terrestrial and lunar manufacturing techniques.

6.0 LUNAR MATERIALS

6.1 INTRODUCTION

In the build-up of a permanent lunar base, there is clearly a desire to employ locally available materials where that can be done at a cost saving, relative to importing material from earth. In most of the processes which would be employed for refining lunar materials, there will be a need, initially to import processing machinery and materials from earth. The overall analysis has to consider this cost with respect to the total amount of lunar material which will be produced over the lifetime of the equipment, in order to know whether lunar production is cost effective. One can anticipate that the conclusion for lunar produced oxygen is that it is cost effective, because the quantity produced will be large.

When considering the use of lunar materials in an electrical power system, the range of options will be very limited in the early phase of the base, and is probably restricted to those materials which can be used for thermal energy storage or fuels. In the field of photovoltaics there appears to be no prospect of early lunar manufacture. The process which appears to be most favorable for the lunar environment is the chemical vapor deposition method of manufacturing amorphous silicon cells. The hard vacuum of the moon may provide a more favorable situation than that of earth. Silicon dioxide is plentiful on the moon, however, in order to be useful for solar cells, it must first be refined to solar grade silicon and then silane gas, SiH_4 made from that. Although fairly early use may be made of silicon compounds for structural purposes, refinement first of metallurgical grade and then to solar grade silicon presents an order of difficulty whose solution is not justified in the first few years of the base.

For the manufacture of any of the components of heat engines, either metalworking or precision ceramic fabrication or both. The materials are there, principally in the form of oxides, however, their refinement in the early phase of the base is unlikely. Working fluids and fuel offer a better prospect for early supply from lunar materials.

Either helium or hydrogen is used as the working fluid for the Stirling and Brayton engines and both these elements may be fairly easily recoverable in quantities which are adequate to make up leakage in closed cycle engines. The working fluid for the sodium heat engine is liquid sodium which occurs in small quantities on the moon.

Some method of storing energy for the lunar night is a requirement of a manned lunar base if power is not supplied by a nuclear plant. A procedure which has been used on earth is to store the energy thermally in either molten potassium chloride or sodium chloride. The following sections explore the prospects for obtaining these compounds from lunar materials.

6.2 OVERVIEW

The vast majority of materials returned from the Moon are significantly depleted in sodium (Na), chlorine (Cl), and potassium (K) relative to solar and terrestrial abundances (1,2). The absence of any potential for water-based hydrothermal processes limits the possibilities for concentrated mineral deposits familiar to the mining industry on Earth. Those limited enrichments of Na, Cl, and K that are known to exist on the Moon are conceptually analogous in many ways to low-grade disseminated gold and copper deposits on Earth.

The known potential resources for Na, Cl, and K on the Moon consist of volcanic glasses that contain on the order of 0.3 wt.% Na and 0.01 wt.% Cl (proportion in leachable grain surface deposits) and of so-called KREEP materials (rich in potassium, rare earth elements and phosphorous) that contain on the order of 0.6 wt.% K and 0.6 wt.% Na. The volcanic glasses form well-defined and naturally concentrated deposits up to 50m thick around most of the outer portions of the Serenitatis Basin. The KREEP materials are present in various petrographic forms dispersed in the regolith, regolith breccias, and impact breccias at several Apollo landing sites. KREEP material, however, appears to be most concentrated in regolith over areas around the Imbrium Basin traditionally mapped as the "Fra Mauro" formation. The most promising general location for a lunar base that would have immediate access to both extensive deposits of volcanic glass and KREEP-bearing Fra Mauro materials is near the crater Sulpicius Gallus. At this location, the orange/red soil deposits associated with the southwestern rim of the Serenitatis Basin are in contact with the Fra Mauro formation. Gamma-ray geochemical surveys from lunar orbit strongly suggest that the Fra Mauro near Sulpicius Gallus contains significant amounts of KREEP materials.

6.3 PYROCLASTIC GLASSES (CHLORINE)

A variety of volcanic glasses and/or devitrified glasses of original pyroclastic deposition have been identified as a component of lunar soils or observed as in situ deposits on the lunar surface (3,4). Those volcanic glasses of immediate potential significance to the development of chlorine resources for lunar base power operations are (a) Apollo 17 orange glasses and their black devitrified equivalents (studied and sampled at the Apollo 17 landing

site in the Valley of Taurus-Littrow) which are widespread near the southeastern and eastern margins of the Serenitatis Basin (5), (b) stratified orange and red deposits (observed and photographed from orbit by the Apollo 17 crew (which are widespread near the southern and southwestern margins of the Serenitatis Basin (4,6), and (c) Apollo 15 green glasses (sampled at the Apollo 15 landing site near Hadley Rille) which may be widespread near the eastern margins of the Imbrium Basin (3), and (d) various glass beads found in small concentrations in mare regolith from the Apollo 11,12,15 and 16 landing sites (7).

The physical, chemical and geological characteristics of these materials support the literature consensus that they formed during lava fountaining caused by the separation of a volatile phase as highly mafic magmas neared the lunar surface (3). The presence of unusually high concentrations of volatile elements, including Cl and other halogens, deposited on the surfaces of individual glass spheres (7,8,9,10,11 and Tables 6.1, 6.2, 6.3, 6.4) indicates that portions of this evolved volatile phase condensed on those spheres after quenching in the lunar vacuum and before deposition on the lunar surface (10). It is these condensates that represent an easily mined and beneficiated potential resource base for Cl as well as other materials.

The Apollo 17 orange soil is the best studied of the lunar volcanic glasses, and those studies can be extrapolated to extensive deposits of orange, red and black soils, i.e., pyroclastic volcanic glasses and their devitrified equivalents, that have been delineated around the margins of the Serenitatis Basin (4,6). The Apollo 15 green glasses may be of similar potential, however, their areal extent and thickness has not been precisely determined. The mapping of the distribution of green glasses around Imbrium could possibly be accomplished through study of the

TABLE 6.1 MAJOR ELEMENT COMPOSITIONS OF MARE VOLCANIC GLASSES

Group	Apollo 11 Green	Apollo 14 Green A	Apollo 14 Green B	Apollo 14 VLT	Apollo 15 Green A	Apollo 15 Green C	Apollo 15 Green D	Apollo 15 Green E	Apollo 16 Green
SiO ₂	43.7 ± .1	44.1 ± .2	44.8 ± .2	46.0 ± .4	45.5 ± .1	48.0 ± .3	45.1 ± .1	45.2 ± .1	43.9 ± .1
TiO ₂	0.57 ± .08	0.97 ± .07	0.45 ± .05	0.55 ± .03	0.38 ± .03	0.26 ± .03	0.41 ± .03	0.43 ± .03	0.39 ± .03
Al ₂ O ₃	7.96 ± .17	6.71 ± .08	7.14 ± .13	9.30 ± .01	7.75 ± .09	7.74 ± .09	7.43 ± .11	7.44 ± .09	7.83 ± .06
Cr ₂ O ₃	0.46 ± .03	0.56 ± .02	0.54 ± .04	0.58 ± .03	0.56 ± .03	0.57 ± .02	0.55 ± .03	0.54 ± .02	0.39 ± .03
FeO	21.5 ± .2	23.1 ± .3	19.8 ± .2	18.2 ± .1	19.7 ± .1	16.5 ± .3	20.3 ± .1	19.8 ± .2	21.9 ± .1
MnO	n.d.	0.28 ± .04	0.24 ± .03	0.21 ± .02	0.22 ± .03	0.19 ± .02	0.22 ± .03	0.22 ± .03	0.24 ± .05
MgO	17.0 ± .2	16.6 ± .1	19.1 ± .1	15.9 ± .1	17.2 ± .1	18.2 ± .1	17.6 ± .2	18.3 ± .2	16.9 ± .1
CaO	8.44 ± .07	7.94 ± .2	8.03 ± .09	9.24 ± .16	8.65 ± .05	8.57 ± .05	8.43 ± .09	8.15 ± .06	8.44 ± .06
Na ₂ O	n.d.	<0.07	0.06 ± .03	0.11 ± .02	n.d.	n.d.	n.d.	n.d.	n.d.
K ₂ O	n.d.	<0.06	0.03 ± .01	0.07 ± .01	n.d.	n.d.	n.d.	n.d.	n.d.
#fragments	24	11	6	4	173	8	160	16	7
reference	(1)	(2, 5)	(2, 5)	(2, 5)	(3)	(3)	(3)	(3)	(4)

Array	Apollo 14 Yellow	Apollo 11 Orange	Apollo 15 Orange	Apollo 17 Orange	Apollo 14 Orange	Apollo 14 Red	Apollo 14 Black	Apollo 17 VLT	Apollo 15 Yellow	Apollo 15 Red A
SiO ₂	40.8 ± .1	37.3 ± .2	37.9 ± .1	38.5 ± .2	39.2 ± .2	33.4	34.0 ± .5	45.3	42.9 ± .2	35.6 ± .1
TiO ₂	4.58 ± .07	10.0 ± .1	9.12 ± .08	9.12 ± .08	12.5 ± .1	16.4	16.4 ± .3	0.66	3.48 ± .05	13.8 ± .0
Al ₂ O ₃	6.16 ± .04	5.68 ± .18	5.63 ± .14	5.79 ± .10	5.69 ± .07	4.60	4.6 ± .3	9.60	8.30 ± .11	7.15 ± .04
Cr ₂ O ₃	0.41 ± .02	0.63 ± .03	0.65 ± .01	0.69 ± .03	0.86 ± .08	0.84	0.92 ± .06	0.40	0.59 ± .04	0.77 ± .03
FeO	24.7 ± .2	23.7 ± .3	23.7 ± .3	22.9 ± .2	22.2 ± .2	23.9	24.5 ± .6	19.6	22.1 ± .2	21.9 ± .1
MnO	0.30 ± .01	n.d.	n.d.	n.d.	0.31 ± .03	0.30	0.31 ± .03	0.26	0.27 ± .04	0.25 ± .04
MgO	14.8 ± .2	14.3 ± .2	14.9 ± .3	14.9 ± .3	14.5 ± .1	13.0	13.3 ± .5	15.0	13.5 ± .1	12.1 ± .1
CaO	7.74 ± .09	7.62 ± .08	7.41 ± .11	7.40 ± .09	7.04 ± .05	6.27	6.9 ± .2	9.40	8.50 ± .06	7.89 ± .08
Na ₂ O	0.42 ± .02	0.31 ± .07	0.36 ± .09	0.38 ± .05	0.28 ± .09	0.05	0.23 ± .08	0.27	0.45 ± .04	0.49 ± .02
K ₂ O	0.10 ± .02	n.d.	n.d.	n.d.	0.29 ± .10	0.12	0.16 ± .05	0.04	n.d.	0.12 ± .02
#fragments	3	75	6	140	4	22	22	2	11	3
reference	(5)	(1)	•	•	(5, 6)	(7)	(5, 6)	(8)	(9)	(10)

[1]	Delano (1981a)	[6]	Delano (1981d)	*	unpublished data
[2]	Delano (1981b)	[7]	Marvin and Walker (1978)		
[3]	Delano (1979)	[8]	Warner et al. (1979)		
[4]	Delano and Rudowski (1980)	[9]	Delano (1980a)		
[5]	Delano (1981c)	[10]	Delano (1980b)		

TABLE 6.2 74220 SPHERES 5 (COUNTS x 10 IN 5 SEC)

Mass	1	2	3	4	5	6	7	8	9	10	11	12	13	14
82 ZnO	0.36	0.50	0.84	1.7	2.6	2.4	2.3	2.1	2.0	1.9	2.0	2.1	1.8	1.8
80	0.7	1.2	2.4	4.8	7.2	8.9	8.5	8.2	9.9	10.3	16.2	10.1	9.8	10
69 Ga	1.7	6	24	62	53	40	31	24	22	18	16	14	12	10.7
66 Zn	6.6	7.5	17	47	74	40	66	62	56	50	48	46	42	386
64 TiO	36	58	113	285	442	480	473	470	487	440	425	410	390	386
60 Ni	1.3	1.9	3.8	8.2	11	13	14	14.6	16	15	14	14	14	14
56 Fe	130	260	570	1100	1450	1660	1880	1970	2200	2020	2100	2200	2070	2100
48 Ti	21	95	160	160	640	716	769	504	712	536	590	680	670	590
46 Ti	8.8		79	79	103		106	96	108	100	100	101	101	97
40 Ca	430	240	1300	3060	1260	3100	3900	2260	980	1970	2600	3140	3016	3140
39 K	320	683			2236	1700	1370	1106	980	822	670	730	722	680
35 Cl	0.66	0.71	0.57	0.60	0.70	0.54	0.57	0.45	0.43	0.40	0.38	0.40	0.37	0.37
34 S	0.03	0.11	0.26	0.46	0.38	0.27	0.22	0.22	0.21	0.17	0.18	0.15	0.13	0.17
32 S+O ₂	0.5	0.6	5.3	10.7	7.9	5.9	4.7	4.1	3.6	3.2	3.1	2.96	3.0	2.9
30 Si	11	9.4	59	171	205	183	155	137	126	113	112	105	108	104
24 Mg	175	140		210	752	840	1350	2242	1800	1300	1061	1660	1800	1550
23 Na	910	1200		2860	4400	4130	3430	2700	2300	1440	1700	1780	1640	1500
20 Ca ²⁺	18	30		40	170	270	260	270	270	168	225	220	130	197
19 F	0.9	3.1	7.3		9.3	7.0	5.5	4.4	3.6	3.0	2.8	2.3	2.1	1.9
16 O	5.4	8	17	20	37	34	31	29	27	25	26	24	24	23
7 Li	0.37				0.84		1.40	1.46	0.56	0.43		0.57	0.34	0.23

The data are taken in order from mass 82.80.69—7 and then over again. Each cycle takes ~5 min. The count rate for major elements from the glass steadily increase but the count rate for Zn, Ga, K, Cl, S, Na, and F reach their highest values in cycles 4 or 5 (20–30 min) and then decrease. In those cases where there is a molecular ion interference from the glass the count rate remains high. The initial rise in count rate (cycles 1, 2, and 3) is caused by sputtering through the carbon coat.

TABLE 6.3 CONCENTRATIONS OF 17 ELEMENTS IN SIZE FRACTIONS OF ORANGE GLASS FINES SAMPLES 74220 AND IN TEACH. ETCH and RESIDUE FRACTIONS OF THE 500–62 μm EXCEPT Na, Ca, Cr, Mn, Fe IN mg/g

Fraction	Na	Ca	Sc	Cr	Mn	Fe	Co	Ni	La	Ce	Sm	Eu	Yb	Lu	Hf	Ta	Th
Bulk	2.03	46	37	5.03	2.13	185	68	110 \pm 45	5.4	19	5.2	1.70	4.1	0.50	5.4	0.90	0.61
500–62 μm , leach*	0.008	1.25	1.00	1.36	0.57	5.3	2.4	3.6 \pm 1.2	0.35	0.9	0.29	0.050	0.16	0.023	0.16	0.021	0.022
500–62 μm , etch*	0.20	0.94	0.18	4.56	2.43	19.9	6.7	8.9 \pm 2.1	0.16	0.2	0.06	0.019	0.05	0.007	0.65	0.112	0.094
500–62 μm , res.*	1.53	46	35	4.46	1.80	163	60	71 \pm 35	5.2	19	5.3	1.60	3.7	0.51	5.0	0.75	0.58
500–62 μm , total	1.82	48	36	5.05	2.10	188	69	83 \pm 40	5.6	20	5.6	1.67	3.9	0.54	5.8	0.86	0.70
62–20 μm	1.82	46	36	4.87	1.97	182	62	160 \pm 40	5.4	19	5.5	1.65	3.6	0.49	5.7	0.90	0.62
20–0.1 μm	2.40	48	40	5.40	1.95	200	72	35 \pm 30	6.5	20	6.2	1.93	4.4	0.65	6.3	1.02	0.64
500–62 μm , res.†	1.72	52	39	5.02	2.03	184	68	80 \pm 40	5.9	21	6.0	1.8	4.2	0.57	5.6	0.85	0.65
500–62 μm , 1 + et	2.58	21	25	5.30	2.68	225	81	112 \pm 30	3.6	9.7	3.1	0.62	1.9	0.27	7.2	1.19	1.04

*Data listed as weight fraction of entire 500–62 μm separate.

†Measured concentration in residue

TABLE 6.4 SOURCE OF SUBLIMATES AN APOLLO 15 GREEN AND APOLLO 17 ORANGE GLASS SAMPLES SUMMARY OF VOLATILE AND CHALCOPHILE TRACE ELEMENTS

	Ni	Cu	Zn	Ga	Ge	Ag	Cd	Ir	Au	Ti	Pb	Bi	S	Se	Te	F	Cl	Br	I	C
	ppm	ppm	ppm	ppm	ppb	ppb	ppb	ppb	ppb	ppb	ppm	ppb	ppm	ppb	ppb	ppm	ppm	ppb	ppb	ppm
15300	250 (d)		31 (d)	4.6 (d)	370 (d)		59 (d)	6.6 (d)	2 (d)		2.1 (m)		600 (v)							110 (v)
15401	185 (b)	6.8 (b)	65 (b)	4.7 (b)	248 (p)	61 (p)	102 (p)	2.3 (p)	1 (p)	5 (p)		1 (p)	440 (v)	231 (p)	16 (p)	7 (c)		75 (p)		29 (v)
			52 (p)	7 (c)	192 (p)	59 (p)	79 (p)	1.9 (p)		4.4 (p)				182 (p)	18 (p)			74 (p)		
15431	180 (b)	6.0 (b)	55 (b)	4.7 (b)	263 (c)		240 (c)	2.5 (c)	3 (c)				550 (v)							35 (v)
	215 (c)			4.4 (c)	203 (a)		237 (a)	4.5 (a)	1.6 (a)											
	202 (a)		37 (a)	5.3 (a)																
Green glass surface	171 (a)		113 (a)	10.8 (a)	665 (a)		678 (a)	1.2 (a)	5.4 (a)											
Interior			1.6 (a)	2.9 (a)	12.3 (a)		7.6 (a)	0.3 (a)	0.05 (a)											
15426	170 (b)	3.5 (b)	80 (p)	4.7 (b)	196 (p)	39 (p)	183 (p)	0.4 (p)		6.9 (p)	1.25 (u)	2.4 (p)	340 (v)	174 (p)	16 (p)			136 (p)		21 (v)
Typical A15 soil	285 (b)		14 (b)	4.3 (d)	470 (d)	6.5 (p)	41 (d)	8.9 (d)	7.2 (d)	1.5 (p)	1.95 (u)	2.7 (p)	800 (v)	162 (p)	7 (p)	60 (w)	20 (w)	120 (p)		140 (v)
Typical A15 basalt	70 (p)		10 (p)		270 (p)			5.6 (p)	2 (p)	0.2 (p)		0.1 (p)	590 (v)	123 (p)	6 (p)	55 (w)	2 (w)	8 (p)		12 (v)
			1.4 (d)	3.4 (d)	20 (d)	1 (p)	1.6 (d)	0.07 (d)	0.15 (d)											
74220 bulk	67 (m)	26 (l)	292 (l)	16.5 (r)	250 (m)		320 (m)	0.81 (p)	0.02 (p)	20 (m)	2.5 (l)	1.4 (m)	560 (n)	640 (m)	62 (p)	102 (l)	103 (l)	1500 (l)	14 (l)	5 (c)
	85 (l)	25 (r)	253 (l)										750 (n)			61 (l)	72 (l)	420 (l)	13 (l)	
74240 and	75 (l)	28 (l)	270 (r)	13.4 (r)	155 (m)	25 (m)	210 (m)	2.8 (m)	1 (m)	9.1 (m)	2 (l)	0.7 (m)		340 (m)	24 (m)	230 (l)	59 (l)	800 (l)	13 (l)	55 (v)
74241	64 (m)	21 (r)	83 (l)	10 (l)	210 (r)			7.9 (r)	2.6 (r)							210 (r)		610 (m)		
	82 (r)		37 (l)																	
74260 and	126 (l)	21.6 (h)	86 (m)	16 (h)									1000 (n)							45 (v)
74261	99 (f)	32 (l)	109 (f)	10 (l)																
74001	68 (m)		35 (l)																	
			148 (m)		105 (m)	72 (m)	25 (m)	0.02 (m)	0.7 (m)	4 (m)	1 (l)	0.7 (m)		350 (m)	38 (m)	<2 (l)	40 (l)	180 (l)	6 (l)	
Typical A17 soil	160 (f)	7 (h)	27 (m)	4 (h)	190 (m)	10 (m)	32 (m)	5 (m)	1.7 (m)	1.3 (m)	1.2 (l)	0.5 (m)	1000 (n)	250 (m)	10 (m)	40 (l)	20 (l)	210 (m)	3 (l)	120 (m)
	200 (l)	5 (l)	41 (f)																	
Typical A17 basalt	113 (m)		20 (l)																	
Carbonaceous chondrites	11,000	130	303 (s)	10 (s)	31,200 (s)	182 (s)	639 (s)	574 (s)	152 (s)	45 (s)	2.9	130	62,000	19,500 (s)	3,040 (s)	190	260	1,760 (s)	300	35,000
Cd																				

(a) Chou et al. (1975), (b) Taylor et al. (1973), (c) Chou et al. (1974), (d) Baedeker et al. (1973), (e) Varretta et al. (1972), (f) Rhodes et al. (1974), (g) Brunfeld et al. (1974a), (h) Brunfeld et al. (1974b), (i) Brunfeld et al. (1974c), (j) Brunfeld et al. (1974d), (k) Nunn et al. (1974), (l) Jovanovic and Reed (1974), (m) Jovanovic and Reed (1974), (n) Gibson and Moore (1974), (o) Moore et al. (1974), (p) Gnanapathy et al. (1973), (q) Wicks et al. (1973), (r) Kranebuhl et al. (1973), (s) Barnes et al. (1973), (t) Moore (1973), (u) Moore (1974), (v) Moore (1974), (w) Jovanovic and Reed (1973).

prime color film exposed from orbit during the Apollo 15, 16 and 17 missions, as there are strong indications that such glasses are associated with a light blue-gray annulus around the southeastern edge of the Imbrium Basin (6).

The volatile condensates on the surfaces of glass spheres that make up the orange soil include about 0.01% Na(10) (versus about 0.2%-0.4% in bulk samples) (7,10) and about 0.01% Cl(8). There are various theories on how these elements are bound on the surface as well as conflicting reports of the ease of leaching the Cl and other halogens from these surfaces (10,11), however, it would seem that such Cl leaching for commercial purposes is an easily resolved problem. Na may be a useful by-product of such leaching. Once overburden is removed from deposits of stratified orange and related solid, continuous surface mining techniques should be possible that would provide a steady stream of material into the "leach" plant. From the leach plant, the raw leachate could move through a process of selective precipitation. The potential leaching and precipitation processes will be discussed as a separate report.

6.4 KREEP MATERIAL (SODIUM AND POTASSIUM)

The principal known potential resource base for sodium and potassium on the moon are silicate-dominated materials referred to as KREEP (12), that is, material rich in potassium (K), rare earth elements (REE), and phosphorous (P) relative to other lunar rocks and soils. The maximum measured concentrations of Na₂O and K₂O KREEP are 1.0 and 1.1 wt.%, respectively, and are known to range downward to about 0.4 and 0.1 wt.%, respectively (13 and Tables 6.5, 6.6, 6.7). Likely general values for Na₂O and K₂O are 0.64 and 0.69 wt.% (14). Crystalline and /or glassy silicate materials rich in KREEP components were first recognized in

TABLE 6.5 COMPOSITION OF THE KREEP COMPONENTS
AND BEST ESTIMATES OF THE CONCENTRATION
OF 50 ELEMENTS

Element	Laul et al. [1972]	Laul and Schmitt [1973]	Boynton et al. [1975]	This Work	Uncertainty*	References†
Li, µg/g	56	c	3, 8, 9, 10
Na, mg/g	7.4‡	=	=	6.4	a	1, 2, 10
Mg, mg/g	...	48	=	64	a	1, 2, 5, 9, 10
Al, mg/g	101‡	=	=	88	a	1, 5, 6, 10
Si, mg/g	224	a	5, 8, 10
K, mg/g	7.5‡	=	=	6.9	a	1, 10
P, mg/g	3.4	c	5, 8
S, mg/g	1.1	d	5, 7
Ca, mg/g	75‡	=	=	68	b	1, 5, 9, 10
Sc, µg/g	25	20	=	23	b	1, 4, 10
Ti, mg/g	9.6‡	=	10	=	b	1, 6, 10
V, µg/g	50	45	=	43	b	1, 6, 9
Cr, mg/g	1.30	1.03	=	1.30	b	1, 10
Mn, mg/g	1.39	0.93	=	1.08	b	1, 10
Fe, mg/g	70‡	=	78	82	a	1, 6, 10
Co, µg/g	35	=	=	33	c	1, 4, 6, 9, 10
Ni, µg/g	...	200	28	20	d	1
Cu, g/g	20	d	9, 10
Zn, µg/g	4.5	3.6	d	1, 10
Ga, µg/g	9.0	7.5	a	1, 4, 9, 10
Ge, ng/g	40	=	d	1
Rb, µg/g	22	c	1, 2, 5, 9, 10
Sr, µg/g	200	b	2, 5, 9, 10
Y, µg/g	300	b	5, 9
Zr, µg/g	800	1100	...	1700	b	1, 5
Nb, µg/g	80	c	5, 10
Ru, ng/g	0.5	d	1
Cd, ng/g	16	15	d	1
In, ng/g	2.6	1.2	d	1
Cs, µg/g	2.0	c	1, 10
Ba, µg/g	1100	=	=	1200	a	1, 5, 6, 8, 9, 10
La, µg/g	108	110	=	=	a	1, 2, 4, 6, 10
Ce, µg/g	297	300	=	270	a	1, 2, 4, 5, 6, 8, 10
Nd, µg/g	...	180	...	=	a	1, 2, 4, 5, 8, 10
Sm, µg/g	49	=	=	=	a	1, 2, 4, 5, 6, 8, 10
Eu, µg/g	3.2	3.0	=	=	b	1, 2, 4, 5, 6, 10
Gd, µg/g	57	b	4, 5, 8, 10
Tb, µg/g	10	=	=	=	a	1, 4, 6, 10
Dy, µg/g	...	60	=	65	a	1, 4, 10
Ho, µg/g	14	b	4, 10
Er, µg/g	39	b	2, 4, 5, 8, 10
Yb, µg/g	39	=	=	36	a	1, 2, 4, 5, 6, 8, 10
Lu, µg/g	5.7	5.0	=	=	a	1, 2, 4, 6, 8, 10
Hf, µg/g	36	32	=	37	a	1, 4, 8, 10
Ta, µg/g	3.9	4.0	=	=	a	1, 6, 10
W, µg/g	2.0	c	10
Ir, ng/g	...	4	0.1	=	d	1
Au, ng/g	...	1.4	0.2	0.1	d	1
Th, µg/g	19	=	=	18	a	1, 5, 6, 10
U, µg/g	6	5	=	=	a	1, 5, 6, 10

An equals sign indicates acceptance of a previously estimated value.

*The estimated uncertainties in composition of a hypothetical Apollo 14 rock containing 49 µg/g Sm: a, ±3.5–6%; b, ±6–10%; c, ±10–17%; and d, ±>17%.

†1, Warren et al. [1978b]; 2, Hubbard et al. [1970]; 3, Eugster [1971]; 4, Helmke et al. [1972]; 5, Hubbard et al. [1972]; 6, Laul et al. [1972]; 7, Moore et al. [1972]; 8, Philpotts et al. [1972]; 9, Rose et al. [1972]; and 10, Wänke et al. [1972].

‡Hubbard and Gast [1971] value.

||Meyer and Hubbard [1970] value.

ORIGINAL PAGE IS
OF POOR QUALITY

TABLE 6.6 CHEMICAL ANALYSIS OF KREEP BASALTS AND RELATED MATERIALS

References	Oceanic Tholeiitic Basalt	"Point B"	Apollo 12 KREEP Glass	KREEP composition 1972	Small particles	Apollo 12 KREEP Muscovite	Apollo 16 VMA Basalt	Apollo 16 KREEP Basalt	Ignorant Basalt	Apollo 17 North	Apollo 17 Breccia
	(1)	(2)	12033.971A	DARK	14310	12382	62295 (4)	62235	62275	76315	76315
SiO ₂	49.3	49.1	48.2	48.13	49.2	52.9	48.73	47.05	48.3	48.3	48.3
TiO ₂	1.5	2.6	2.6	1.90	1.24	2.1	2.23	1.19	0.6	1.53	1.50
Al ₂ O ₃	17.0	15.9	15.5	17.49	20.1	17.8	14.77	18.88	17.33	17.83	18.14
FeO	8.8	9.26	10.6	11.01	8.36	8.6	10.55	9.45	7.91	9.14	8.95
MgO	7.2	9.19	7.7	10.72	2.47	7.5	11.17	10.16	11.83	12.39	12.02
CaO	11.7	12.1	10.9	7.99	12.3	9.9	11.78	10.59	12.03	11.4	11.32
Na ₂ O	2.7	0.69	0.61	0.88	0.63	0.7	0.96	0.42	0.44	0.69	0.60
K ₂ O	0.16	0.67	1.1	0.63	0.49	0.6	0.57	0.33	0.32	0.27	0.26
P ₂ O ₅	0.16		0.8	0.90	0.34	0.6	0.55	0.39	0.3	0.30	0.29
ppm											
Li	9	98.7	44	44	20	26	27.2	20.1	18.5	19.3	14.6
Ba	8.60	1207	1162	1030	617	750	187	445	492	337	359
Rb	1.05			16.3	12.8	15.3	4.59	9.80	9.32	7.32	5.86
Th	0.18			17.2	11.36			8.56	9.4	5.55	
U	0.10			4.5	3.22	3.5	3.1	2.34	2.57	1.45	1.52
Ce	7.58	265	267	250	144	197	312	113	125	93.7	131
Ce:Eu	7.28	45	79	77	67	76	79	60	75	65	83
Ce:Yb	3.08		7.76	8.3	7.83	8.03	8.48	8.89	8.17	7.44	7.73
Cr	297	2180	1300	1230	1230	2400	775	1477	2350	1300	1437
Ni	97		20	20	64		215	348	580	438	260
ppb											
As		0.99	-0.1	4.3	0.033	0.033	3.10	10.2	0.045	10.5	3.4
Au		1.5	-0.1	10.5	0.026	0.0132	3.38	11.6	0.023	6.45	5.9
Ir											

(a) Engel *et al.*, 1965; (b) Philpotts *et al.*, 1969; (c) Tatumoto *et al.*, 1972a; (d) Walker *et al.*, 1971; (e) Meyer *et al.*, 1971; (f) Hubbard and Gast, 1971; (g) Morgan *et al.*, 1972; (h) Schonfeld and Meyer, 1972; (i) Powell *et al.*, 1973; (j) Helms *et al.*, 1973; (k) Meyer, 1972; (l) Meyer, 1972; (m) Hubbard *et al.*, 1973; (n) Morgan *et al.*, 1973b; (o) Dowty *et al.*, 1976; (p) Gros *et al.*, 1976; (q) O'Keefe *et al.*, 1978; (r) Rhodes and Hubbard, 1979; (s) Hubbard *et al.*, 1974; (t) Krähenbühl *et al.*, 1973; (u) Sioeser *et al.*, 1974; (v) Blanchard *et al.*, 1975; (w) Rhodes *et al.*, 1974; (x) Morgan *et al.*, 1974.

Footnotes: (1) Terrestrial; (2) Peritectic in olivine-anorthite-alica pseudoternary phase diagram; (3) Estimated component used in chemical mixing model; (4) Very High Alumina Basalt—not a KREEP basalt.

TABLE 6.7 CHEMICAL ANALYSIS OF FRA MAURO BASALT (GLASSES)

	Apollo 14 Type B	Apollo 14 Type C	Apollo 14 Type D	Apollo 15 Low K	Apollo 15 Moderate K	Apollo 15 High K
SiO ₂	47.3	48.2	51.6	46.6	49.6	53.3
TiO ₂	1.9	2.2	1.8	1.2	1.4	2.1
Al ₂ O ₃	17.0	17.1	16.9	18.8	17.6	15.6
FeO	10.6	10.5	11.0	9.7	9.5	10.2
MgO	10.2	7.6	4.7	11.0	9.0	5.8
CaO	10.5	10.9	10.9	11.6	10.8	9.6
Na ₂ O	0.6	0.8	0.8	0.4	0.7	1.0
K ₂ O	0.5	0.6	0.8	0.1	0.5	1.1
R ₂ O	(a)	(a)	(a)	(b)	(b)	(b)

(a) Apollo Soil Survey, 1971; (b) Reid *et al.*, 1972.

ORIGINAL PAGE IS
OF POOR QUALITY

breccia in the Apollo 12 regolith (15). Such materials probably had been thrown into that area of the moon by the impact that created the crater Copernicus (16). However, the "type" locality for KREEP-rich material is the Apollo 14 landing site where it appears to be associated with the Fra Mauro formation (17), an extensive deposit of ejecta that surrounds the Imbrium Basin. Gamma-ray geochemical surveys that sense the thorium also concentrated in KREEP material support the correlation of KREEP with the Fra Mauro formation (18).

6.5 POTENTIAL RESOURCES

The KREEP materials in Fra Mauro are mixed extensively with low-Na and low-K anorthositic breccia derived from the dominant lunar curstal rocks excavated by the Imbrium event. It is not yet clear what techniques can be used to develop KREEP concentrates from the already pulverized Fra Mauro regolith, however, both density and magnetic contrasts probably exist relative to other regolith components (13). There is some natural enrichment of Na and K in the fine-grained fractions of all lunar regolith (19). This issue should be pursued through direct studies of Apollo 14 regolith samples. Once the nature of probable KREEP concentrates is defined, the best processes for Na and/or K extraction can be investigated.

6.6 RESOURCE DEVELOPMENT

The high concentration of orange and red pyroclastic glasses in the Sulpicius Gallus formation (4,20) and the presence of KREEP materials in the regolith over the Fra Mauro formation in the same general region of the moon (18) suggest strongly that a lunar power station, utilizing Cl and Na and/or K derived from these two resource bases, should be located near the contact between the two

formations near the southwest edge of the Serenitatis Basin.

POSSIBLE FUTURE SUBTASKS

1. Chlorine leach and extraction process options with respect to orange glass.
2. KREEP material concentration process options with respect to Fra Mauro regolith
3. Photogeologic study of the distribution of green glass deposits.
4. Literature study of chlorine-rich highland rocks to determine quantitative importance (21).
5. Power station site selection options.

7.0 Processing of Lunar Materials

7.1 Possible Methods for Extraction of Sodium from Lunar KREEP Materials

This report introduces several methods which may be applicable to the extraction of sodium from lunar KREEP (potassium (E), Rare Earth Elements and Phosphorous) materials. Chemical, electrical, radiation and vaporization methods are considered.

In KREEP materials, Na may be found both in various types of crystalline feldspars and in melt inclusions [1]. For the purposes of this report it is assumed that the bulk of the Na is contained in the high silicate melt inclusions. The structure and composition of these melt inclusions is assumed to be predominantly that of a silicate glass containing oxides of Al, K, Fe, Ca and Na. The compositional analysis used as a basis for this report [1] is:

<u>OXIDE</u>	<u>WEIGHT PERCENT</u>
SiO_2	75
Al_2O_3	12.5
K_2O	7
FeO	1.5
CaO	1.5
Na_2O	.75

Other oxides which may be significant but which were assumed to be present in concentrations less than 0.75 wt% and were therefore not considered in this report are MgO , TiO_2 , P_2O_5 , and MnO .

In pure silicate glass (vitreous silica - SiO_2), covalent SiO_4 tetrahedra are connected at random orientations by sharing each O (called "bridging") between two tetrahedra. Compounds that link up in this way to form the amorphous solid continua of a glass are

called network formers. K, Na, Ca, and Al are added to this network as oxides; K_2O (potash), Na_2O (soda), CaO (lime) and Al_2O_3 (alumina).

When K_2O or Na_2O are added to vitreous silica, the oxygen in the oxide displaces one of the bridging oxygens in the silica by connecting to one of the Si bonds. This creates two non-bridging oxygens (NBOs) to which the alkali metal atoms attach themselves ionically. Compounds such as these are called network modifiers; they soften and open the silicate structure by breaking covalent bonds and creating ionically bonded NBOs. The strength and melting point (mp) of the glass are inversely proportional to the alkali ion concentration.

Lime is also typically a network modifier in silicate glasses. When CaO is added to the SiO_2 structure, two NBOs are formed and the divalent Ca^{2+} bonds ionically to both of them. Although CaO also softens the SiO_2 network, it does so to a lesser extent than the alkali ions due both to its ionic linking character between two NBOs and to the fact that it blocks the motion of alkali ions through the network [2]. In high concentrations (CaO) 40 mol%, the so-called "invert glasses"), Ca becomes a network former and has the effect of strengthening the glassy material [3].

The effect of transition metal oxides, such as FeO , depends on the ionization state of the metal. Iron was not specifically studied for this report but is assumed to be divalent and therefore similar to Ca in physical and chemical properties in glass [4].

Alumina is intermediate; it can either act as a network former or a network modifier [2], dependent on the composition of the glass. In alkali silicate glasses, each Al_2O_3 enters the network by using two NBOs to create two AlO_4 tetrahedra. This can continue until all of the NBOs are taken up (number of Al atoms = number of Na + K atoms or $Al/(Na+K) = 1$). Up until this point,

Al_2O_3 acts as a network former. When $\text{Al}/(\text{Na}+\text{K}) = 1$ the glass is composed of SiO_4 and AlO_4 tetrahedra. What becomes of any additional Al_2O_3 is less clear. It has been suggested that for every three new AlO_4 tetrahedra that are formed, one Al^{3+} goes into a higher coordination state to neutralize the charges [5]. Thus, the alumina can act as a network modifier also. As might be expected, the viscosity and strength of the glass increase sharply with an increase in Al_2O_3 concentration up to the point where $(\text{Al}.\text{Na}+\text{K})=1$. However, both strength and viscosity (and mp) continue to increase slightly as $\text{Al}/(\text{Na}+\text{K})$ becomes greater than one. Thus it appears that despite the low concentrations of Na, K, Fe, and Ca likely to be found in lunar KREEP glasses, the alumina present will have the effect of strengthening the material and raising its mp significantly.

7.1.1 CHEMICAL PROCESSES

Two chemical processes are commonly used to break down silicate glasses: etching and leaching. Etching is a first-order reaction that destroys the silicate network by hydration and dissolution. For example, $2x\text{NaOH} + (\text{SiO}_2)_x \rightarrow x\text{Na}_2\text{SiO}_3 + x\text{H}_2\text{O}$. Leaching is a diffusion-controlled process involving the exchange of H^+ in solution for alkali ions present in the glass. For example,



Combined etching and leaching reactions are also known. In fact, almost every etching or leaching reaction is actually a combination of etching and leaching. A leaching front begins at the surface with H^+ Na^+ (or K^+) exchange. The alkalis removed from the glass then participate in alkali attack on the silicate network [4]. These reactions are often referred to generically in the literature as leaching, regardless of the degree of leaching or etching. The most common reagent for the combined reaction is water.

In general, alkali attack reaction rates are several orders of magnitude greater than acid attack reaction rates. However, both of these attack mechanisms are strongly dependent on a number of conditions:

Surface Chemistry: The rate of chemical attack in glasses depends on conditions at the surface of the material. Alkali silicate glasses tend to have different compositions near exposed surfaces than the bulk composition due to weathering. In addition, chemical attack processes themselves deplete reactive element concentrations as they proceed, and also tend to form inert layers of reaction by-products. Thus, chemical attack processes proceed quite slowly and even under enhanced reaction conditions may provide significant ion depletion to a depth on the order of several microns [6].

Bulk Composition: The ultimate composition of glassy materials strongly affects their reactivity. The presence of Al and Fe reduces the rate of chemical attack [4]. Ca is often added to silicate glasses to improve chemical durability [2], and attack rates are generally dependent upon alkali ion concentration [4].

Reagent pH: As might be expected, chemical attack reaction rates depend on the reactivity of the attack solution. As the reaction proceeds, the solution is continuously made less effective as the reaction itself neutralizes its pH near the surface. The combined leach-etch reaction may be made self sustaining but is unacceptably slow for production scenarios.

Temperature: As is true of most reactions, these chemical attack mechanisms are dependent on temperature. All of these reactions proceed more rapidly with increasing temperature. For leaching reactions, the temperature dependence is logarithmic (via the Arrhenius equation).

Diffusion: Diffusion processes can often be shown to follow a relation of the form: $\text{rate} = D_0 \exp\left(\frac{\Delta E}{RT}\right) \frac{\partial c}{\partial t}$ where ΔE is the activation energy for diffusion, c is concentration, R is the gas constant, T is absolute temperature, t is time and D_0 is a diffusion constant [7]. Under ideal reaction conditions at a given temperature, etching rate decreases linearly with time and leaching (diffusion controlled) decreases as $\log(\text{time})$. For real reactions, however, E increases as the surface concentration decreases. It may be that some percentage of the Na^+ in the silicate network are in sufficiently deep potential energy wells that they are essentially immobile short of total glass dissolution. (This may include most of the sodium in KREEP materials). Leaching processes can also be carried out using gaseous reagents.

Compounds containing SO_2 , SO_3 , Cl and F as well as water vapor have been used in this fashion [8,9]. An enhanced leaching process involves bubbling the reagent through molten glass material (transpiration). These processes are also diffusion-controlled and are subject to the same limitations as those using liquid reagents. However, the structural limitations of ionic motion in solid glass are overcome and the reactions proceed much more quickly (note that T is in the exponential term in the rate equation) and completely (the mechanical problems of inert layer build-up and local reagent depletion are eliminated).

Detailed research and technical information is available regarding chemical processes due to the glass manufacturing industry which uses such processes in the manufacture of all types of silicate glasses especially in processes known as "fluxing" and "fining".

7.1.2 ELECTRICAL PROCESSES

Electrical conductivity in silicate glasses is ionic. Since Na^+ and Li^+ are the only common ionic species with any appreciable mobility in the silicate network at low temperatures due to their size, sodium is likely to be responsible for any conductivity in KREEP glasses. CaO and Al_2O_3 increase electrical resistivity of solid glasses [4], presumably by reducing Na^+ mobility. The presence of K_2O also reduces conductivity due to a little-understood occurrence known as the "mixed alkali effect". Due to this effect the conductivity of the glass is reduced when a mixture of certain alkalis is present from the conductivity when any one of the alkalis is present alone [2].

Electrolysis and polarization are associated with conductivity in glasses and may be applicable to sodium extraction processes.

In electrolytic processes [10], it is essential to provide a supply of ions at the anode to replace the Na^+ that migrate away due to the electric field. Various salts (NaNO_3 , LiNO_3 , NaCl) and water have been used for this purpose. It has been shown that it is possible to remove a large fraction, but, significantly, not all, of the Na^+ in a glass by replacing them with certain appropriate ions [2].

Ionic conduction by vacancy migration in crystals is well understood. Ions can be conducted through a crystal without benefit of an electrolyte since the ions skip from vacancy to vacancy and each ion that leaves the crystal creates a new vacancy for subsequent ions. In solid form, glasses have very high resistivities (typically 10^7 - 10^{18} Ωcm). Presumably this is due to the lack of regular vacancies. However, the resistivity of silicate glasses drops rapidly (in fact, exponentially) with temperature [2]. It appears that since both the activation energy required for an alkali ion to jump from site to site is

reduced and the average kinetic energy of those ions is increased with increasing temperature, it may be possible to induce direct conduction merely by polarizing KREEP glass at high temperature. The alkalis could be collected at the cathode and with proper enhancements, O_2 might be collected at the anode.

Extraction of sodium from silicate glasses by electrical methods has not been a topic of much practical interest to date. However, the electrical properties of silicate glasses have been studied extensively and technological information is available from industry and research documents regarding glass insulators.

7.1.3 RADIATION METHODS

The behavior of silicate glasses under exposure to high-energy radiation is a relatively new and incomplete field. Radiations which have been studied include light particles (electrons, positrons, and electromagnetic and gamma radiations), heavy particles (neutrons, protons, deuterons and d-particles) and heavier ions (Ar^4 , Xe , N^{+2}) [4,11,12]. Of particular interest are studies of electron and ion irradiation.

When an alkali silicate glass at $200^\circ C$ or greater, is bombarded with high-energy electrons, the NBOs in the silicate structure are released and combine to form molecular O_2 . The O_2 is sufficiently stable that it is not re-absorbed by the dangling Si bonds which then, presumably, connect to other NBOs. The O_2 eventually forms bubbles in the silicate structure. The alkali ions that formed the NBOs in the first place are forced to migrate to maintain local charge neutrality. Many of these ions are released at the surface [12].

Implantation of cations in the surface of alkali silicate glasses has the effect of damaging the SiO_2 structure by milling the surface and directly releasing the alkali cations. Although K^+ ions are large and heavy, they are also loosely bound and are preferentially ejected. The resulting surface deficit drive the

movement of other alkali ions toward the surface. The rate of ion release depends on the energy and rate of implantation. By a "knock-on" atom effect, alkalis are released to a greater depth than the depth of the actual ion implantation. Alkalis have been virtually depleted to depths near 0.5 micron by this method [11].

Although this area of study is relatively new, much research is currently being carried out by nuclear scientists. The primary motivation for these studies involves the use of silicate glass containers for nuclear waste disposal.

7.1.4 VAPORIZATION METHODS

Sodium may be released from silicate glasses directly as a vapor either by heating the glass to a molten state or by entirely vaporizing the material. Appreciable alkali depletion rates occur over silicate glass melts in the composition ranges commonly found in glass manufacturing ($\text{Na} > 10\text{wt}\%$). Nonetheless, these rates are unacceptably slow for production and silicate glass manufacturing industry invariably uses chemical reagents to enhance the process [see references listed under Chemical Methods above]. Furthermore, geologists who have studied sodium vaporization in order to determine if this is the cause of the relative depletion of Na in lunar materials have found vaporization rates that are unacceptably low for a production scenario. For example, Gooding, et al found that it took 16.4 hours at 1200°C in vacuum to reduce the Na content of a terrestrial basalt (B2) to that of a lunar basalt (12022) [13].

A number of studies have been done to determine the feasibility of direct total vaporization of lunar materials for resource materials extraction [14,15]. Briefly, the process involves vaporization of the raw material by intense heating followed by fractional distillation, magnetic and/or electronic separation processes. The lunar hard vacuum is used to drive the separation

process. It is estimated that such a process would require 7100 kWh/ton of raw material, 2/3 of which could be obtained by direct solar heating. Optimum vaporization temperature is estimated to be 3000°C [16].

Information regarding vaporization over the melt can be found in research due to the glass manufacturing industry. Direct vaporization methods are fairly limited to extraterrestrial materials processing research (see the references).

7.1.5 OTHER METHODS

Many other processes may be attractive for the separation of sodium from KREEP glasses. Some technologies which deserve mention but which were not studied for this report are:

Gel glasses: Many types of glass can be made into a gel for processing [17]. Control of composition and ease of handling at low temperatures are some advantages.

Phase separation: Under certain conditions, the various components of silicate glasses can form immiscible liquid phases [18]. This might be an efficient way to concentrate sodium for extraction.

Stress enhancement: It should be mentioned that the release of alkalis from solid glasses by any of the above methods is enhanced by application of a stress field [19].

7.1.6 DISCUSSION

Although chemical processes are well known and documented, several difficulties with their application in the lunar environment come to mind:

1. For these chemical processes, an excess of reagent must always be provided in order for the reaction to proceed. If sodium is the primary intended product, it is clear that unless abundant reagents can be found in the lunar environment, it will be more economical to import the sodium directly rather than to import a greater mass of reagent as well as processing equipment.

2. Chemical processing equipment for the lunar environment will be particularly complicated and maintenance intensive. The reagents that have a significant effect on silicate glasses also have significant effects on most containment vessels. For the low-temperature processes, preliminary crushing and grinding will be necessary to expose fresh surfaces for chemical attack. Once the process is under way, the reagent will have to be agitated and continuously replenished. For the high-temperature (molten glass) processes, substantial heat must be provided due to the high mp of aluminosilicate networks and provisions must be made for bubbling, molten material transfer, caustic vapor collection and so on. In addition, at high temperatures, most metals and metalloids (including carbon) preferentially ionize and enter the silicate network, making most containments temporary at best.
3. All of these processes generate large quantities of chemical wastes. Most, if not all of these wastes could be recycled and re-used, but recycling processes will also require special handling, materials and energy.
4. The end product of these processes is not pure sodium but either NaOH or a salt. Again, more equipment is necessary to separate Na from these compounds. This can be accomplished relatively simply by electrolysis but the other products remain highly reactive and will require special treatment.

Electrical processes involving electrolytes suffer from the same disadvantages as chemical processes. If sufficient sodium could be released by polarization at high temperatures, this would eliminate many of the complicated and dangerous chemical processes but mechanical agitation would still likely be necessary, as would containment of molten glass. In addition, electrodes decay and would have to be imported.

Irradiation processes have some advantages in that the machinery is mostly non-mechanical and requires no atmosphere. The metal ions are released directly and can be separated electromagnetically. In addition, electron bombardment produces another useful resource, O_2 . However, these processes are energy intensive and ion implantation requires a source of ions; also probably imported.

Vaporization from the melt suffers the same difficulties as the chemical processes and electrolysis for a very marginal production rate. However, this is worth considering if the material is going to be melted for some other use. Direct vaporization has several advantages for the lunar environment. No process reagents need to be imported, the lunar hard vacuum is used to advantage and the end products are relatively pure. However, this process is very energy-intensive and will require much development of new technology.

A tentative conclusion at this very preliminary stage is that, given the scarcity of sodium in the lunar environment and the condition in which it is found, it seems unlikely to emerge as a primary lunar resource. However, sodium does exist in the lunar environment and might be an important secondary resource, co-produced with some other, more expedient, material.

7.1.7 SUGGESTIONS FOR FURTHER DEVELOPMENT

Several areas were not covered in this report which should be investigated before any firm conclusions are drawn:

High iron melt inclusions: The high-silicate melt inclusions are intermixed in KREEP materials with high-iron melt inclusions with order-of-magnitude weight percent analysis: SiO_2 - 38%; FeO - 31%; CaO - 11%; MgO - 6%; TiO_2 - 6%; Al_2O_3 - 4%; with K_2O , Na_2O , MnO , and Cr_2O_3 each less than 0.5% [1]. The melt inclusions are in the micron-millimeter size range. Separation of the two melt inclusion types must be considered.

Effect of iron: FeO is a substantial component of the high-silicate melt inclusions. It was not explicitly included in this report. Glass engineering literature contains less about transition metal oxides in silicate glasses than about the alkali oxides since the transition metals are primarily used for color. Fe should exist in reduced form in KREEP glasses as Fe^{2+} and should therefore have physical properties similar to Ca^{2+} .

Crystalline materials: A substantial amount of the sodium present in KREEP may be included in the crystalline materials. For example, sodium is about 8.8 wt% in albite. The ultimate compositional analysis of KREEP materials is necessary to determine if the crystalline forms are reasonable resource bases and new process considerations will be necessary if they are.

REFERENCES

1. Roedder, E. and Weiblen, P.W.; PETROGRAPHIC FEATURES AND PETROLOGIC SIGNIFICANCE OF MELT INCLUSIONS IN APOLLO 14 AND 15 ROCKS Proceedings of the Third Lunar Science Conference, Geochim Cosmochim Acta, Vol. 1, p251-79, 1972.
2. Holloway, D.G.; THE PHYSICAL PROPERTIES OF GLASS Wykeham Publications, London, 1973
3. Shelby, J.E.; FORMATION AND PROPERTIES OF CALCIUM ALUMINOSILICATE GLASSES J Pm Ceram Soc v68 n3 Mar 1985 p155-8
4. McLellan, G.W. and Shand E.B.; GLASS ENGINEERING HANDBOOK McGraw-Hill, New York 1984.
5. Day, D.E. and Rindone, G.E.; PROPERTIES OF SODA ALUMINOSILICATE GLASSES I J Am Ceram Soc v45 n10 p489-96
6. Das, C.R.; CHEMICAL DURABILITY OF SODIUM SILICATE GLASSES CONTAINING Al_2O_3 AND ZrO_2 J Am Ceram Soc v64 n4 Apr 1981 p188-93
7. Barrett, C.R., Nix, W.D., and Tetelman, A.S.; THE PRINCIPLES OF ENGINEERING MATERIALS Prentice-Hall, Englewood Cliffs, NJ 1973
8. Sanders, D.M., Wilke, M.E., Hurwitz, S. and Haller, W.K.; ROLE OF WATER VAPOR AND SULFUR COMPOUNDS IN SODIUM VAPORIZATION DURING GLASS MELTING J Am Ceram Soc v64 n7 Jul 1981 p399-404
9. Brow, R.K. and LaCourse, W.C.; FLUORINE TREATMENTS OF SODA-LIME SILICATE GLASS SURFACES J Am Ceram Soc v66 n8 Aug 1983 pC123-4

10. Doremus, R.H., Babinec, A., D'Angelo, K., Doody, M., Lanford, W.A., and Burman, C.; ELECTROLYSIS OF SODA-LIME SILICATE GLASS IN WATER J Am Ceram Soc v67 n7 July 84 p476-49
11. Arnold, G.W.; ALKALI DEPLETION AND ION BEAM MIXING IN GLASSES Nucl Instr Meth Phys Res B 1984 p516-20
12. DeNatale, J.F. and Howitt, D.G.; A MECHANISM FOR RADIATION DAMAGE IN SILICATE GLASSES Nucl Instr Meth Phys Res B 1984 p489-97.
13. Gooding, J.L. and Muenow, D.W.; ACTIVATED RELEASE OF ALKALIS DURING THE VESICULATION OF MOLTEN BASALTS UNDER HIGH VACUUM: IMPLICATIONS FOR LUNAR VOLCANISM Geochim Cosmochim v40 1976 p675-86.
14. Carrol, W.F. (ed); RESEARCH ON THE USE OF SPACE RESOURCES NASA JPL publication 83-86 1983
15. Steurer, W.H.; EXTRATERRESTRIAL MATERIALS PROCESSING NASA JPL publication 82-41 1982
16. Singer, B. LUNAR OXYGEN PRODUCTION unpublished, by personal communication, 1986.
17. See, for example, Brinker et al SOL GEL GLASS: I,II,III in J Non Cryst Solids v72 n2-3, July 1985; p345 p369.
18. Mazurin, O.V. and Porai-Koshits, E.A.; PHASE SEPARATION IN GLASS North-Holland, Amsterdam 1984.
19. Nogami, M. and Tomozawa, M.; EFFECT OF STRESS ON WATER DIFFUSION IN SILICA GLASS J Am Ceram Soc v67 n2 Feb 1984 p151-54

7.2 POSSIBLE METHODS OF LUNAR OXYGEN PRODUCTION

7.2.1 INTRODUCTION

As a propellant and as a fundamental constituent of any life support environment, oxygen is the single most valuable commodity available in lunar resources (Carroll, 1983). Lunar escape velocity (2.4 km/s) is substantially less than the earth's (11.2 km/s). Coupled with the virtually frictionless lunar "atmosphere", access to space from the lunar surface is about 22 times more energy efficient than lifting objects into space from the Earth's surface (Waldron et al., 1980). Generation and transport of oxygen from the lunar surface is, therefore, energetically and economically attractive for refueling earth orbiting space stations of the near future and for potential missions to other regions of our solar system in the next century.

This section identifies and summarizes methods for obtaining oxygen from lunar materials which have been recently reported, or are presently under investigation. Process schemes, availability of lunar resources, energy requirements, and feasibility of each potential method, along with pertinent bibliographies, have been assembled. A brief outline of these methods is presented here:

1) HYDROGEN REDUCTION OF LUNAR ILMENITE

Ilmenite feedstock electrostatically concentrated from bulk lunar regolith is reacted with hydrogen gas at about 1000°C, producing water upon reduction. Water is then passed through a high temperature - solid state electrolysis cell and dissociated into recyclable hydrogen and recoverable oxygen.

2) CARBOTHERMAL REDUCTION OF ILMENITE

Ilmenite feedstock electrostatically concentrated from bulk lunar regolith is melted along with carbon yielding an iron-titanium slag and CO vapor. CO vapor can be dissociated by solid state electrolysis to recover oxygen and recyclable carbon. If iron production is desired, additional catalysis and cracking of hydrocarbon compounds yields water which can, upon electrolysis, yield oxygen as well.

3) MAGMA ELECTROLYSIS/ELECTROWINNING OF MOLTEN LUNAR

MATERIAL

Molten salt electrolysis cells can be designed such that lunar material will yield oxygen gas at the anode while metalbearing cations are reduced at the cathode. Performance of the electrolyte is enhanced via the use of various fluxing agents (electrowinning); however, proper cell design will allow for oxygen production from molten bulk lunar regolith (magma electrolysis).

4) VAPOR PHASE REDUCTION

Intense heating of lunar regolith particles by an RF induction coil, or in a solar furnace will volatilize, dissociate, and/or ionize constituent metal oxides and generate a partial pressure of about 200 torr. If dissociation takes place in a chamber open to the hard lunar vacuum (10^{-14} torr) through an orifice, the vapor will rapidly be drawn toward the orifice. Vapor separation/fractional distillation can be used to condense metal species from the vapor leaving oxygen as the sole component for recovery. At sufficient temperature (8000° - $10,000^{\circ}$ C) ionization of metals in the vapor is nearly complete, whereas oxygen remains neutral; as the vapor (plasma) travels toward the vacuum orifice metal species are collected on charged plates, leaving a stream of pure oxygen for recovery.

5) LIBERATION OF OXYGEN USING FLUORINE

Fluorine may be used to liberate oxygen directly from bulk lunar regolith; however, the oxygen product must be purified using potassium iodide. HF acid leaching of lunar regolith yields water which can be electrolyzed to recover oxygen. Complex processing is necessary to recover and recycle fluorine in either process.

CONCLUSIONS

Feasibility comparisons of the above methods reveals that hydrogen reduction of ilmenite and vapor phase reduction of bulk lunar regolith appear to be the most attractive processes for further study. The ultimate choice of which method to implement will depend on critical and accurate assessment of the energy required to facilitate each process, including trade-offs involving possible import of raw materials from earth. Future research efforts should be directed toward utilization of solar energy for process heat, experimental testing of the vapor phase reduction techniques, development of durable solid state electrolysis cells, and detailed comparison of the energy and materials requirements of potential oxygen production options and intra-option alternatives.

7.2.2 ILMENITE REDUCTION

7.2.2.1 Process Outline: Hydrogen Reduction

Continuous fluxing of ilmenite with hydrogen vapor at or above 900 C will initiate reaction (1) below. Electrolysis of the product H_2O will yield oxygen and hydrogen (reaction 2), the latter can be recycled for use on fresh ilmenite feedstock

(Gibson and Knudsen, 1985; Downs, 1971):



electrolysis

The process scheme of Gibson and Knudsen (1985) is outlined diagrammatically in Figure 7.2.1. In their scheme, cold ilmenite feedstock is introduced to a preheated reactor bed where hot H_2 recycled from the electrolysis cell is introduced. Preheated feed is then introduced to the main reactor bed where heat is supplied to bring the feed up to reaction temperature of about 1000 C (Downs, 1971, Williams, 1985; Gibson and Knudsen, 1985). Reaction (1) is endothermic ($\Delta H = +9.7$ kcal/gm-mole 00 C) and reversible, thus equilibrium conversion of H_2 to H_2O is temperature dependent. At 900° C, Per-pass conversion of H_2 does not exceed 7.4% (Fig. 2, Gibson and Knudsen, 1985; Williams, 1985).

Spent solids are removed from the main reactor bed and facilitate heating of incoming H_2 from the recycling circuit (Fig. 7.2.1). It is suggested that electrolysis of product H_2O (reaction 1) take place at or near reaction temperature (Gibson and Knudsen, 1985). Vapor phase electrolysis using a solid-state electrolyte has been experimentally investigated by Weissbart et al. (1969) who produced O_2 from mixtures of CO , CO_2 , and H_2O . Details of this process are discussed below (see solid state electrolysis). Unreacted H_2 from the main reactor bed is cycled through the electrolysis cell along with H_2O . The counter current gas-solid flow design outlined above will additionally reduce energy requirements by conserving and recycling heat along with hydrogen vapor (Gibson and Knudsen, 1985).

ORIGINAL PAGE IS
OF POOR QUALITY

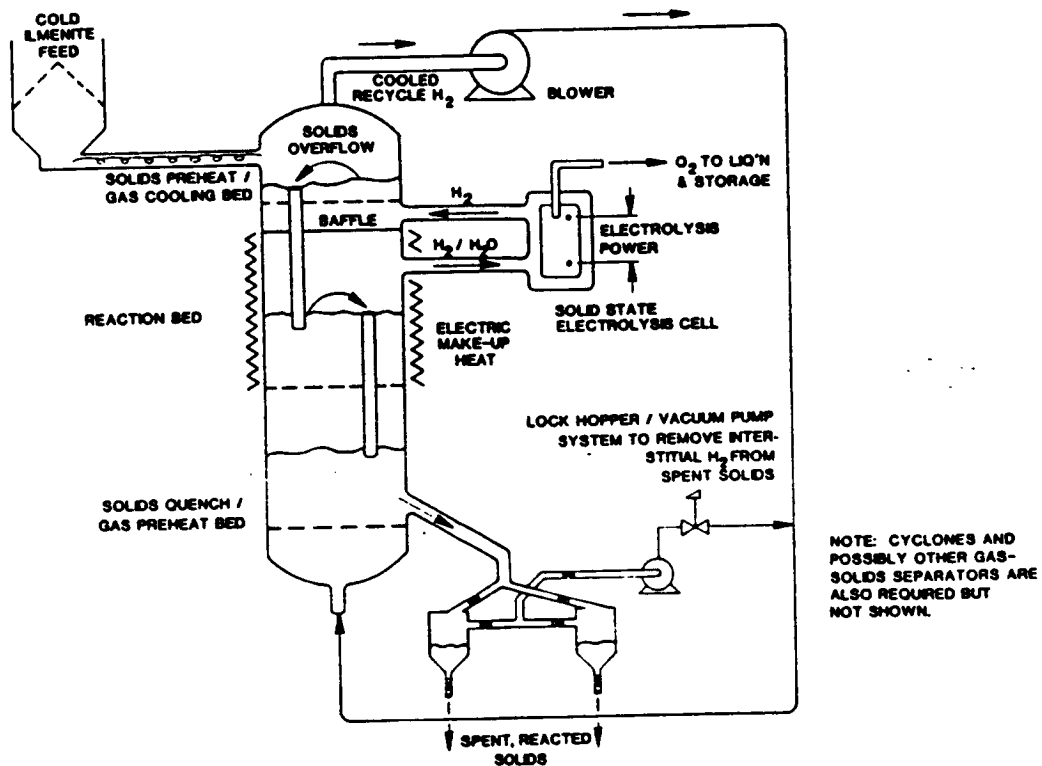


Figure 7.2.1 Continuous counter-current gas/fluid bed reactor for ilmenite reduction and oxygen extraction (After Gibson and Knudsen, 1985)

Williams (1985) performed preliminary experimental tests on lunar simulant ilmenite aimed at estimating increases in prepass conversion rates of H_2 by using cold traps to condense H_2O above a reaction bed. His study indicates that enhancements are not substantial for non-equilibrium continuous flow processes such as outlined above and that the lunar simulant ilmenite contained enough sulfides to produce H_2S , which significantly attacked the electrolysis cell membrane. Since lunar ilmenite contains sulfides as well, this could be a serious barrier to lunar implementation of the hydrogen reduction process (Williams, 1985).

7.2.2.2 LUNAR RESOURCES AS RAW MATERIALS

Lunar Regolith: General Characteristics

The chemistry, mineralogy, and petrology of lunar regolith have been summarized by Heiden (1975) and Papike et al. (1982); only a cursory review is given here. Additionally, a thorough review of lunar materials as potential resources is given by Criswell and Waldron (1982).

Lunar regolith consists of unconsolidated debris locally derived from mare basalt or highland anorthosite bedrock and forms a nearly complete groundcover up to several meters in depth (Papike et al., 1982). Regolith soils derived from lunar highlands are petrologically and chemically distinct from those derived from lunar maria because extensive lateral transport appears to be negligible (i.e. beyond several meters), while vertical mixing and cycling of local bedrock is important (Papike et al., 1982; Labotka et al., 1980). Regolith forms largely by comminution of local bedrock lithologies due to (micro)meteorite impacts (Mendell and McKay, 1975; Papike et al., 1982; Pillinger, 1979; DesMarais et al., 1974). However, constructional processes of

agglutinate formation via impact melting and welding of regolith fines is also important (Pillinger, 1979; Des Marais et al., 1974). Most lunar soil exists in a state of dynamic equilibrium between comminution and agglutination; abundance and composition of agglutinate particles is a measure of lunar soil maturity (DesMarais et al., 1972, 1974a; Laul et al., 1984; Taylor et al., 1979). The < 10 μm fraction of lunar regolith is consistently enriched in Al_2O_3 , CaO , Na_2O , K_2O , Th, and LREE (the so-called KREEP component) and depleted in MgO , FeO , MnO , and Sc due to rapid comminution of KREEP enriched feldspar and mesostasis relative to pyroxene and olivine in the regolith (Papike et al., 1982). McKay and Williams (1979) indicate that ilmenite contents also systematically increase in finer grain size fractions in mare-derived regolith soils.

General processes of lunar sedimentology have been reviewed by Lindsay (1976; 1975), however, detailed analysis of stratigraphy brought to light by Apollo drill cores, indicates that extremely complex cycles of accumulation, mixing, and maturation are to be expected (Laul, et al., 1979). Detailed petrographic and chemical descriptions of virtually every lunar regolith sample appear in *The Handbook of Lunar Soils* edited by Morris et al. (1983). Lunar regolith generally contains between 0.30 and 4.2 wt. % TiO_2 , however, regolith derived predominantly from Ti-rich lunar maria (basaltic in composition) can contain up to 7.5-8.5 wt. % TiO_2 (Papike et al., 1982; McKay and Williams, 1979). Virtually all TiO_2 in lunar regolith is found in ilmenite.

ILMENITE (FeTiO_3) OCCURENCE

A relatively pure feedstock consisting of > 90% ilmenite is necessary to insure significant H_2O production from reaction (1). Lunar regolith is a desirable source for ilmenite because it is already comminuted and should be easily obtained by surface mining methods. Modal ilmenite abundances in lunar regolith range from about 1 to 10% and average about 5.0% (Papike et al.,

1982; McKay and Williams, 1979). McKay and Williams (1979) indicate that finer grain size fractions of lunar regolith are slightly enriched in modal ilmenite relative to bulk regolith. McKay and Williams (1979) identified the Apollo 11 and Apollo 17 mare basalts as containing the highest modal ilmenite contents of any known lunar material at 14.5 and 20.4%, respectively.

Curiously, regolith developed adjacent to these basalt localities is, however, not significantly enriched in ilmenite relative to the average lunar regolith (McKay and Williams, 1979). Remote sensing studies of mare basalt types suggests that Apollo 11 and 17
basalts
probably

represent lunar maximum TiO_2 contents (Pieters et al., 1976; Pieters, 1978; McKay and Williams, 1979). The probability that near-surface high grade ilmenite "ore deposits" exist is low unless ilmenite settling within relatively thick cooling units of basaltic magma has formed ilmenite rich segregation layers.

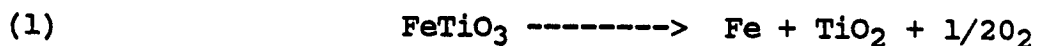
EXTRACTION OF ILMENITE

Agosto (1985) suggests a two stage process for concentrating ilmenite from a bulk lunar regolith feedstock: Stage 1 involves magnetic separation of agglutinate and other highly ferromagnetic particles from the regolith. Stage 2 involves electrostatic separation of ilmenite from the nonferromagnetic regolith. Multistage, multipass electrostatic separation of ilmenite should easily yield concentrates of 90+ % ilmenite. Agosto's (1983, 1985) experiments do not, however, fully duplicate hard-vacuum or low gravity lunar conditions, both of which are expected to affect the mechanics of ilmenite separation. Methods and problems associated with mining the bulk lunar regolith for further processing are discussed by Podnieks and Roepke (1985) and Gertsch (1983).

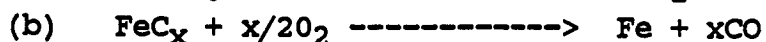
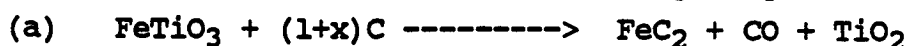
7.2.2.3 CARBOTHERMAL REDUCTION OF ILMENITE

Process Outline

The overall process chemistry of the carbothermal scheme of Cutler and Krag (1985) is similar to that devised by Rosenberg et al. (1965) as follows:

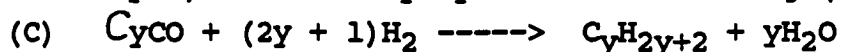


The process can be divided into the following stages:

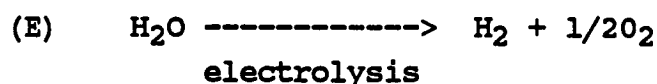


Feed stock and carbonaceous reductant are heated until melting, reduction, and slag-metal separation take place (Step a) followed by Fe decarburization (Step b).

The Carbonaceous reductant (Step a) can be recycled carbon from this process in addition to contributions from organic-rich garbage, etc.. Carbon recycling and H₂O production are facilitated through forming hydrocarbon waxes (Fischer-Tropsch synthesis; Step C) followed by hydrocarbon cracking (Step D):



Water derived from Step D can be converted to oxygen and hydrogen by solid state electrolysis (Weissbart et al., 1969):



An outline of the process scheme appears in Fig. 7.2.2.

A valuable by-product of carbothermal ilmenite reduction is steel, however, the importance of oxygen production far outweighs steel production during initial establishment of a lunar base (Carrol, 1983) so that refinement of Fe (reaction b) may not be immediately necessary (however, this step does enhance carbon recovery and recycling in the process). Reaction Step A is similar to reactions proposed for lunar production of Ti, Mg, Al, and Fe by Rao et al. (1978) in that CO is a product. Rao, et al. (1978) suggests three methods of oxygen production from CO gas: 1) Catalysis yielding CO₂ for photosynthetic O₂ production, 2) Fischer-Tropsch synthesis (reaction c above), or 3) solid state electrolysis of CO₂ produced by catalysis of CO (Weissbart et al., 1969; Erstfield and Williams, 1979). Since solid state electrolysis is suggested by Gibson and Knudsen (1985) to break down water in the hydrogen reduction scheme outlined above and appears useful in decomposing CO and CO₂, a brief outline of solid state electrolysis follows.

SOLID STATE ELECTROLYSIS

High-temperature vapor-phase electrolysis of CO + CO₂ + H₂O mixtures can be performed using a solid oxide electrolyte

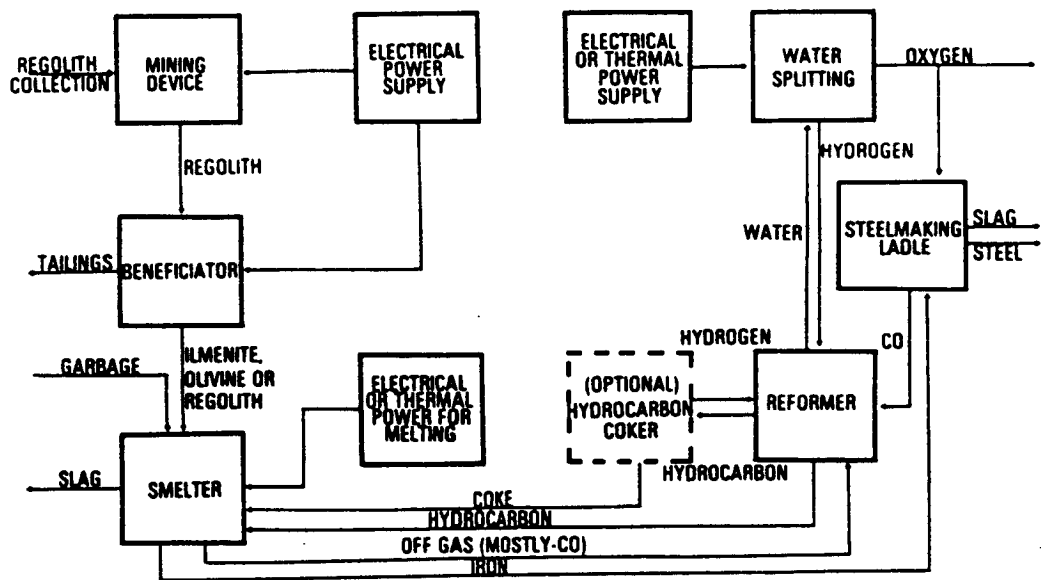


Figure 7.2.2 Flow diagram of the carbothermal oxygen production plant
(After Cutler and Krag, 1985)

permeable to O_2 - ions only (Weissbart et al., 1969; Erstfield and Williams, 1979; Steurer, 1982; Fig. 7.2.3). The only experimental study of oxygen yields using solid state electrolysis was carried out by Weissbart, et al. (1969). In addition, a detailed theoretical assessment is given by Erstfield and Williams (1979). Both Weissbart, et al. (1969) and Erstfield and Williams (1979) favored CaO-stabilized zirconia as the preferred electrolyte, used in conjunction with platinum plated electrodes. Erstfield and Williams (1979) were particularly interested in high temperature recovery of oxygen from CO and CO_2 by-products of Rao, et al's. (1979) lunar anorthite carbochlorination process and from water derived from hydrogen reduction of lunar ilmenite. They concluded that electrolytic recovery of oxygen from CO, CO_2 , and H_2O should be an effective means of oxygen production. Cutler and Krag (1985) and Erstfield and Williams (1979) suggest that further research and development, particularly on reaction kinetics and resistance of electrolyte to chemical deterioration, are necessary before solid state electrolysis could be implemented.

LUNAR RESOURCES AS RAW MATERIALS

Ilmenite

Ilmenite must be concentrated to 90% by mode for use in reduction by reaction a. Electrostatic separation appears to be a promising method of ilmenite beneficiation from lunar soil as outlined above for hydrogen reduction.

Carbon

The occurrence of carbon in lunar soils is similar to that of hydrogen discussed above. Hodges (1976) indicates that about 8 tons of carbon is implanted into lunar regolith each year by the solar wind. In order to account for measured abundances of

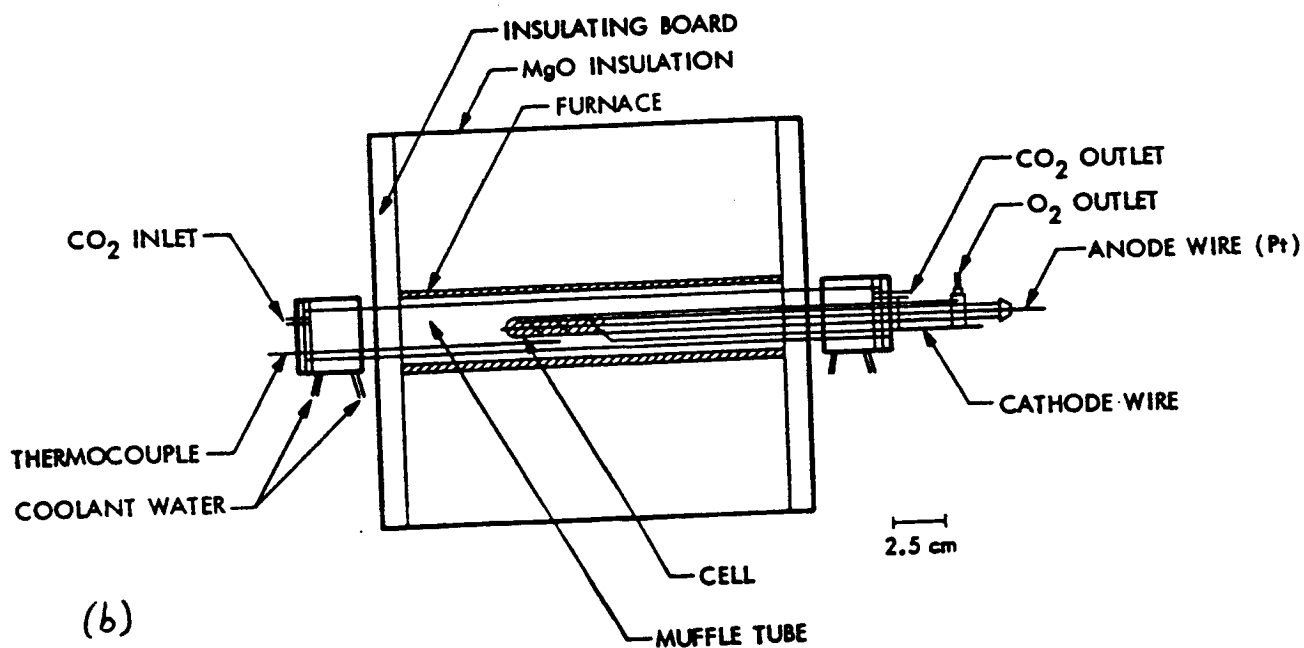
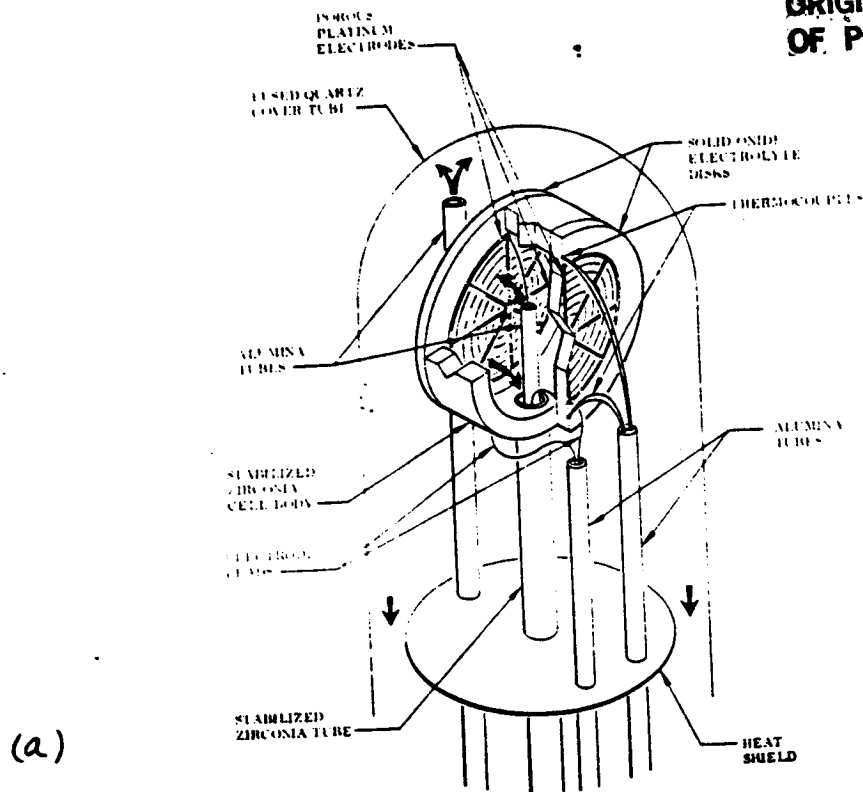


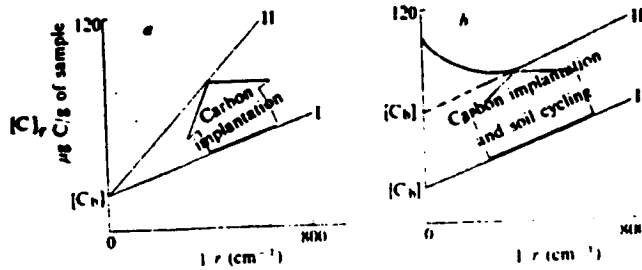
Figure 7.2.3 Solid-state electrolysis cells: (a) from Weissbart et al. (1969), (b) from Steurer (1982)

carbon in lunar soils, carbon influx must be balanced by escape from the lunar soil due to spallation and sputtering effects of incoming solar wind and meteoritic bombardment (Hodges, 1976; Blanford et al., 1985). Thus, some carbon, along with hydrogen may reside in permanently shaded areas of the lunar poles where it may have condensed from the lunar daytime "atmosphere" created by volatile escape. Additionally, volatile (H,C,N,He) rich ejecta layers may have been produced by cometary impacts (Gibson and Moore, 1973; Schultz and Srnka, 1979).

Experimental studies of carbon release from different size fractions of lunar soil (DesMarais et al., 1972, 1973, 1974a, 1974b) have demonstrated that the rate of carbon (and hydrogen) accumulation is slow compared to the rate of reworking of lunar soils. Carbon (and hydrogen) contents of lunar solid increase over time due to solar wind input and soil cycling (Fig. 7.2.4). Carbon is most abundant in mature soils generally characterized by high agglutinate abundances (DesMarais et al., 1973). Pyrolysis and combustion studies reveal that mature lunar soils commonly may contain 70-150 ppm carbon which is released in gasses of CO_2 , CO , and CH_4 by heating (DesMarais et al., 1972, 1973a, 1973b). Heating may be the most effective method of carbon extraction for lunar materials; it is the only method for which experimental data on carbon recovery exist.

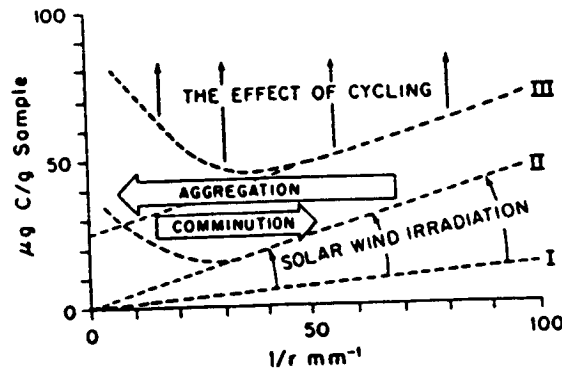
ENERGY REQUIREMENTS

Cutler and Krag (1985) made a rough estimate of energy consumption per ton of oxygen produced (Table 7.2.1). The overall energy budget is at least several megawatts/ton of oxygen (Table 7.2.1) with electrolysis of product water accounting for nearly half the consumption. The energy requirement would be slightly reduced if iron processing is eliminated from consideration. Energy efficient recovery may be slightly enhanced by electrolyzing both CO and H_2O as discussed above. Cutler and Krag (1985) indicate that the energy budget outlined



(a)

a. Hypothetical plots of $[C]$ against $1/r$ for a lunar soil where the rate of carbon accumulation exceeds the rate of soil cycling. In this case, the bulk carbon component $[C_0]$ represents indigenous lunar carbon in both an immature (I) and mature soil (II). The greater carbon content of the mature soil derives from its greater surface concentration, S_c . b. Hypothetical plots of $[C]$ against $1/r$ for a lunar soil where the rate of soil cycling exceeds the rate of carbon accumulation. For the young soil (I) which has just arrived at cyclic equilibrium, $[C_0]$ represents the indigenous lunar carbon component. For the more mature soil (II), $[C_0]'$ represents the indigenous lunar carbon component plus extralunar carbon which has been added to the bulk carbon component by recycling of agglutinates. The upswing in the solid line for larger particle sizes is due to the presence of agglutinates with a high carbon content. The dashed line represents an extrapolation of the $3S_c/f$ slope to determine the bulk carbon concentration $[C_0]'$.



(b)

Schematic carbon concentrations of sieved lunar fines. Carbon is implanted into particle surfaces by solar wind, and is then redistributed in the soil by the processes of aggregation and comminution. As a result, the sequence of curves I, II, and III represents the evolution of the carbon concentration as the soil proceeds towards maturity.

Figure 7.2.4 Schematic plots of carbon concentration vs. grain size showing the effects of reworking and regolith maturation on the abundance of solar wind species in the regolith: (a) After DesMarais et al. 1972 (b) After Des Marais et al. (1974a)

in Table 7.2.1 would constitute the lion's share of total energy required for all other lunar base functions. This budget (Table 7.2.1) does not, however, include the energy expended during mining and beneficiation of lunar regolith. If ilmenite, carbon, and hydrogen are to be concentrated and extracted from the regolith, overall energy consumption would rise considerably. The task remains to compare this cost with that of direct importation of hydrogen or carbon.

TABLE 7.2.1

ENERGY AND POWER REQUIREMENTS PER TON OF PRODUCT OXYGEN	
Process Step	
Energy (GJ)	
Reduce 3.68 tons of iron (75% efficiency)	12
.1	
Heat to melt 3.68 tons of iron (500kWh/ton)	6
.6	
Heat content of 4.25 tons of slag (470kWh/ton)	7
.2	
Heat content of off gas (1350 oC effective heating)	8
.0	
Energy to electrolyze water (60% efficiency)	28
.9	
Energy to liquify oxygen	5
.4	
Total energy consumption, carbothermal process	68
.2	
Total power requirement for 1000 tons of O ₂ per year (100% duty cycle)	2
.16 MW	
Nuclear power plant capacity (90% duty cycle)	2
.40 MW	
Solar power plant capacity (40% duty cycle)	5
.40 MW	
Methane reductant, no heat regeneration.	
Data scaled from that presented by Rosenberg et al.	
(1965f) for a 12,000 lb/mon oxygen production facility	
without heat pumping. Power was assumed to scale	
linearly.	

FEASIBILITY

Pro

- (1) Carbon reacts completely in a single pass and extracts more oxygen from ilmenite per-pass than does hydrogen on a mass per cycle basis (C extracts 1.25x its mass, H extracts 0.4-0.9x its mass).
- (2) Makeup carbon may be available from a variety of sources such as garbage or scrap.
- (3) Ilmenite smelters, electrolysis, and hydrocarbon reforming and cracking are terrestrially proven processes.
- (4) Hydrocarbons are easier to handle than pure hydrogen.
- (5) Molten slag may provide a suitable method of storing heat energy.

Con

- (1) It may become difficult to operate an ilmenite smelter in a continuous mode; batch processing may be necessary and very costly. Handling of molten slag could prove difficult.
- (2) Carbon deposits can build up and become difficult to remove resulting in inefficient processing.
- (3) Research into the kinetics of carbothermal ilmenite reduction under lunar conditions is incomplete.
- (4) Carbon and hydrogen abundances in lunar regolith are low. If implementation of the carbothermal scheme depends on lunar production of these reagents, very large tonnages of regolith would have to be processed.

REFERENCES

- Agosto, W.N. (1985) Electrostatic concentration of lunar soil minerals. In: Mendell, W.W. (ed) Lunar bases and space activities of the 21st century. Lunar Planet Sci Inst. Houston, TX. pp 453-464
- Blanford, G.E., Borgesen P., Maurette, M., Moller, W., Monart, B. (1985) Hydrogen and water desorption on the moon: approximate, on-line simulations. In: Mendell, W.W. (ed) Lunar bases and space activities of the 21st century. Lunar Planet Sci. Inst. Houston, TX pp. 603-609.
- Carroll, W.F. (ed) (1983) Research on the use of space resources. JPL pub 83-86. Pasadena, CA 325 pp
- Carter, J.L. (1985) Lunar regolith fines: a source of hydrogen. In: Mendell, W.W. (ed) Lunar bases and space activities of the 21st century. Lunar Planet Sci Inst., Houston, TX pp 571-581
- Cutler, A.H. and Krag, P. (1985) A carbothermal scheme for lunar oxygen production. In: Mendell, W.W. (ed), Lunar bases and space activities of the 21st century. Lunar and Planetary Institute. Houston, TX pp 559-570.
- DesMarais, D.J., Hayes, J.M., Meinschein, W.G. (1974a) The distribution in lunar soil of hydrogen released by pyrolysis. Proc. Lunar Planet Sci Conf. 5: 1811-1822
- DesMarais, D.J., Hayes, J.M., Meinschein, W.G. (1974b) The distribution i lunar soil of carbon released by pyrolysis. Proc Lunar Sci Conf. 4:1543-1558

- DesMarais, D.J., Hayes, J.M., Meinschein, W.G. (1973) Accumulation of carbon in lunar soils. *Nature Phys Sci* 246: 65-68.
- DesMarais, D.J., Hayes, J.M., Meinschein, W.G. (1972) Pyrolysis study of carbon in lunar fines and rocks. In: *The Apollo 15 lunar samples*. Lunar Sci Inst., Houston, TX pp 294-297
- Downs, W.R. (1971) Oxygen and water from lunar surface material. NASA TM-X 58061. NASA JSC, Houston, TX
- Erstfield, T.E., Williams, R.J. (1979) High temperature electrolytic recovery of oxygen from gaseous effluents from carbochlorination of lunar anorthite and the hydrogenation of ilmenite: A theoretical study. NASA TM58214. NASA JSC. Houston, TX 51pp
- Gibson, E.K., Moore, G.W. (1973) Volatile-rich lunar soil: evidence of a possible cometary impact. *Science* 179:69-71.
- Hodges, Jr., R.R. (1976) The escape of solar wind carbon from the moon. *Proc Lunar Planet Sci Conf* 7:493-500
- Pillinger, C.T. (1979) Solar-wind exposure effects in the lunar soil. *Rep Progress Phys.* 42: 897-961
- Rao, D.B., Chowdery, U.V., Erstfield, T.E., Williams, R.J., Chang, Y.A. (1979) Extraction Processes for the production of aluminum, titanium, iron, magnesium, and oxygen from nonterrestrial sources. In: Billingham, J., Gilbreath, W., Gosset, B., O'Leary (eds) *Space resources and space settlements*. NASA SP-428. NASA Washington, D.C. pp 257-274

- Rosenberg, S.D., Gutler, G.A., and Miller, F.E. (1965)
Manufacture of oxygen from lunar materials. Annals of New
York Academy of Science. 1106, pp 1106-1122
- Schultz, P.H., Srnka, L.J. (1980) Cometary collisions on the moon
and Mercury. Nature 284: 22-26
- Steurer, W.H. (ed) (1982) Extraterrestrial Materials Processing.
JPL pub 82-41. Pasadena, CA. 147 pp
- Weissbart, J., Smart, W., Wydeven, T. (1969) Oxygen reclamation
from carbon dioxide using a solid oxide electrolyte.
Aerospace Medicine 40: 136-140.

7.3 POSSIBLE METHODS OF HYDROGEN PRODUCTION

Hydrogen Occurrence

Hydrogen is the most abundant element in the solar wind (Table 7.1). Since the lunar regolith has been bombarded by solar wind, in addition to micrometeorites, for considerable lengths of time, regolith components are enriched in solar wind species H, He, C, and N (Pillinger, 1979; DesMarais et al., 1972; 1973; 1974; Becker, 1980; Criswell and Waldron, 1982). Lunar rocks and particles are comminuted by micrometeorite impacts and to a much lesser extent by solar wind erosion, however, micrometeorite impacts can also weld and aggregate fine particles together forming agglutinates. Over time, comminution may be balanced by agglutination and a mean "steady-state" particle size may attain (Pillinger, 1979; DesMarais et al., 1973).

Lunar soil maturity reflects the degree of comminution, reworking, and agglutination (Pillinger, 1979; DesMarais et al., 1973). The reworking rate of lunar soils by micrometeorite impacts is high relative to the influx of solar wind species so that mature lunar soils should contain higher abundances of solar wind species than immature soils or pristine bedrock (DesMarais, 1973). Bulk lunar regolith contains between 10 and 100 ppm hydrogen (Steurer, 1982). However, Carter (1985) and Bustin (1984) have shown that indeed the finest grain-size fractions of lunar soils contain the largest hydrogen abundances; this reflects the surface correlated abundance of solar wind species. Most solar wind species are trapped $<200 \text{ \AA}$ from grain surfaces (Pillinger, 1979; Carter, 1985). Since surface area/volume is larger for smaller grains, this is the more enriched fraction with respect to hydrogen. Bustin, et al. (1984) found that roughly 63% of the hydrogen in a typical lunar soil is bound in the finest 23% of that soil. This result agrees well with theoretical calculations (Carter, 1985). This

unique physical property may allow for effective separation and beneficiation of hydrogen from lunar regolith fines.

Blanford et al. (1985) and Hodges (1976) indicate that incoming solar wind hydrogen (and carbon) must be balanced by escape of these species into a lunar "atmosphere" as abundances characteristic of mature regolith soils do not account for the annual solar wind input. Bombardment by incoming solar wind may cause spallation or sputtering of hydrogen and/or carbon from lunar soil during the lunar day. An important implication of these studies is that hydrogen and/or carbon may exist at the lunar poles where substantial condensation of these gases could occur in environments permanently isolated or shadowed from further solar wind bombardment (Hodges, 1976). However, no direct or indirect confirmation of near-polar concentrations of volatile elements was provided by Apollo samples of regolith cold traps (Schmitt personal comments, 1986). Identification and physical description of this potential hydrogen resource should be considered an important enterprise of future lunar exploration (Carrol, 1983). Additionally, the possibility of unusually volatile rich deposits comprising regolith horizons due to cometary or meteor (carbonaceous chondrite) impacts has been discussed by Gibson and Moore (1973) and Schultz and Srnka (1980). Should such deposits exist, they may be candidates for hydrogen extraction.

EXTRACTION OF HYDROGEN

Direct Heating

About 80% of the hydrogen content of Lunar soil is released below 600 C during experimental heating at rates of 4 C/min. (Carter, 1985; Gibson and Johnson, 1971; Gibson and Moore, 1972). Hydrogen should be recovered easily with only moderate thermal input in this manner. However, significant extraction per unit

volume of raw material is only possible if lunar regolith is beneficiated to include only a fine (<20 micron) fraction.

Vibratory screening can remove the fraction of particles >100 micron. The < 20 micron fraction can then be separated by gaseous classification using turboscreening (Carter, 1985). Much experimental work is desired utilizing lunar simulants under lunar conditions. The necessary tonnages of regolith which must be processed are very high. For example, assuming the following: 1) An average abundance of 100 ppm hydrogen, 2) 63% of hydrogen residing in the <20 micron fraction, 3) 81% recovery of hydrogen during heating of concentrate, and 4) 23 wt.% of the lunar regolith residing in the <20 micron fraction, a minimum of 19,596 tons of lunar regolith fines must be processed to yield 4,507 tons of concentrate which when heated would yield a single ton of hydrogen (Carter, 1985). This is equivalent to 51% of the total hydrogen present in non-beneficiated regolith fines.

Microwave Energy

Lunar regolith could be heated in situ using microwave energy supplied by a mobile microwave transmitter. Controlled heating via microwaves may be less time consuming and require less energy than other heating methods such as in situ direct solar heating which is impractical because intense heating could lead to melting of the upper surface and retention of volatiles in the substrate (Tucker et al., 1985).

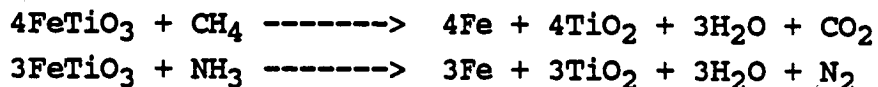
Collection of molecular hydrogen generated in situ will be a difficult technical hurdle, however, any hydrogen evolved as water could easily be collected and condensed. To date no microwave extraction research has been done on lunar samples, nor have indigenous lunar conditions been thoroughly considered (Tucker et al., 1985).

Microbial Extraction

White and Hirsch (1985) suggest that lunar base economics could be substantially improved if bacteria which may be necessary to aid in recycling organic waste can also be used to extract hydrogen from regolith fines. A three stage process is envisioned whereby anaerobic and photosynthetic production of hydrogen occurs while all organic waste produced by the lunar population could be fermented much as is done on Earth. Transportation of microbes is not a problem, however, potential toxic concentrations of some elements in lunar regolith fines could inhibit the use of many potential bacterial strains. Additionally, the suggested feedstock for microbial "reactors" is beneficiated (<20 micron) lunar regolith fines which probably implies use of unrealistic masses of raw material (see Direct Heating discussion above).

Transportation of Hydrogen

It is very likely, given the tonnages of regolith fines which must be processed owing to the low abundance of hydrogen, that importation of hydrogen will be necessitated (Freidlander, 1985). Liquified gases will be the most convenient form of transport. Well known methods exist for recovery of hydrogen from both methane (CH₄) and ammonia (NH₃). Either methane or ammonia could be used directly in the reduction of ilmenite (Freidlander, 1985):



Weight penalties exist for transporting hydrogen as methane or ammonia, however, shipping pure liquid hydrogen would require larger (costlier) shipping vessels than either methane or ammonia. Additionally, the higher boiling points of methane and ammonia relative to pure hydrogen mean less boil-off and waste (Freidlander, 1985).

Energy Requirements

Although power consumption estimates are unavailable for many of the steps outlined above, a discussion of the relative energy requirements for each step is given here. Within the Hydrogen reactor process itself (Fig. 7.2.1), the reactor furnace and electrolysis cell are expected to use an order of magnitude more energy than peripheral equipment (pumps, blowers, cyclones, etc.; Gibson and Knudsen 1985; Williams, 1985). It is difficult at this time to estimate the energy requirements of mining and beneficiating lunar regolith, however, if both ilmenite and hydrogen are to be extracted, beneficiation could conceivably approach the process reactor in energy consumption. Use of solar energy to heat the main reactor (Fig. 7.2.1) could significantly reduce consumption of electrical power from a lunar generating station (Cutler and Krag, 1985).

FEASIBILITY

Pro

- (1) Use of hydrogen as a reductant facilitates efficient recycling of unused hydrogen and process heat (Fig. 1; Gibson and Knudsen, 1985).
- (2) Ilmenite exists as a proven lunar resource; it can be mined and concentrated from lunar regolith with relative ease (Agosto, 1985).
- (3) Counter current gas-solid flow reactor technology has been proven in terrestrial application; its extension to extraterrestrial processes can be based on known system performance.
- (4) The process chemistry is straightforward and occurs in a solid state, rather than in aqueous solutions.

(5) Hydrogen is a much "cleaner" reducing agent than carbon or carbon compounds which could lead to undesirable carbon deposits.

Con

The most serious obstacles to implementing the hydrogen reduction scheme of Gibson and Knudsen (1985) are given below.

(1) Thermodynamic limitations on oxygen yield are manifest by low per-pass conversion of H_2 to H_2O .

(2) The low abundance of hydrogen in lunar regolith would necessitate processing of extremely large quantities of regolith. Costly importation of hydrogen may therefore be necessary (Freidlander, 1985).

(3) Experimental studies on lunar simulant ilmenite indicates that H_2S by-product vapor will cause deterioration of system components; this problem must be overcome before lunar implementation (Williams, 1985).

(4) Solid state electrolytic production of oxygen is required; much research and development is desired before lunar implementation (Erstfield and Williams, 1979).

REFERENCES

- Agosto, W.N. (1985) Electrostatic concentration of lunar soil minerals. In: Mendell, W.W. (ed) Lunar bases and space activities of the 21st century. Lunar Planet Sci Inst. Houston, TX. pp 453-464
- Agosto, W.N. (1983) Electrostatic separation of binary comminuted mineral mixtures. In: Space manufacturing 1983, Advances in the astronautical sciences. Amer Astronaut Soc AAS 83-231 pp 315-334
- Becker, R.H. (1980) Light elements in lunar soils revisited: carbon, nitrogen, hydrogen and helium. Proc Lunar Planet Sci Conf 11: 1743-1762
- Blanford, G.E., Borgesen P., Maurette, M., Moller, W., Monart, B. (1985) Hydrogen and water desorption on the moon: approximate, on-line simulations. In: Mendell, W.W. (ed) Lunar bases and space activities of the 21st century. Lunar Planet Sci. Inst. Houston, TX pp. 603-609.
- Bustin, R., Kotra, R.K., Gibson, E.K., Nace, G.A., McKay, D.S. (1984) Hydrogen abundances in lunar soils. (abs) In: Lunar and Planetary Science XV. Lunar Planet Inst., Houston, TX pp. 112-113
- Carroll, W.F. (ed) (1983) Research on the use of space resources. JPL pub 83-86. Pasadena, CA 325 pp
- Carter, J.L. (1985) Lunar regolith fines: a source of hydrogen. In: Mendell, W.W. (ed) Lunar bases and space activities of the 21st century. Lunar Planet Sci Inst., Houston, TX pp 571-581

- Criswell, D.R., Waldron, R.D. (1982) Lunar utilization, In: O'Leary, B. (ed) Space industrialization II. CRC press. Boca Raton, FL pp 1-53.
- Cutler, A.H. and Krag, P. (1985) A carbothermal scheme for lunar oxygen production. In: Mendell, W.W. (ed), Lunar bases and space activities of the 21st century. Lunar and Planetary Institute. Houston, TX pp 559-570.
- DesMarais, D.J., Hayes, J.M., Meinschein, W.G. (1974a) The distribution in lunar soil of hydrogen released by pyrolysis. Proc. Lunar Planet Sci Conf. 5: 1811-1822
- DesMarais, D.J., Hayes, J.M., Meinschein, W.G. (1974b) The distribution i lunar soil of carbon released by pyrolysis. Proc Lunar Sci Conf. 4:1543-1558
- DesMarais, D.J., Hayes, J.M., Meinschein, W.G. (1973) Accumulation of carbon in lunar soils. Nature Phys Sci 246: 65-68.
- DesMarais, D.J., Hayes, J.M., Meinschein, W.G. (1972) Pyrolysis study of carbon in lunar fines and rocks. In: The Apollo 15 lunar samples. Lunar Sci Inst., Houston, TX pp 294-297
- Downs, W.R. (1971) Oxygen and water from lunar surface material. NASA TM-X 58061. NASA JSC, Houston, TX
- Erstfield, T.E., Williams, R.J. (1979) High temperature electrolytic recovery of oxygen from gaseous effluents from carbochlorination of lunar anorthite and the hydrogenation of ilmenite: A theoretical study. NASA TM58214. NASA JSC. Houston, TX 51pp
- Freidlander, H.N. (1985) An analysis of alternate hydrogen sources for lunar manufacture. In: Mendell, W.W. (ed) Lunar bases and space activities of the 21st century. Lunar Planet Sci Inst., Houston, TX pp 611-618.

- Gertsch, R.E. (1983) A method for mining lunar soil. In: O'Neil (ed) Space manufacturing 1983. Am Astronautical Soc., San Diego, CA pp 337-346.
- Gibson, E.K., Moore, G.W. (1973) Volatile-rich lunar soil: evidence of a possible cometary impact. Science 179:69-71.
- Gibson, E.K., Moore, G.W. (1973) Volatile-rich lunar soil: evidence of a possible cometary impact. Science 179:69-71.
- Gibson, M.A. and Knudsen, C.W. (1985) Lunar oxygen production from ilmenite. In: Mendell, W.W. (ed) Lunar bases and space activities of the 21st century. Lunar Planet Sci Inst., Houston, TX pp 543-550.
- Gibson, E.K., Moore, G.W. (1972) Inorganic gas release and thermal analysis study of Apollo 14 and 15 soils. Proc Lunar Planet Sci Conf 3: 2029-2040
- Gibson, E.K., Johnson, S.M. (1971) Thermal analysis-inorganic gas release studies of lunar samples. Proce Lunar Planet Sci Conf 2: 1381-1396
- Heiken, G. (1975) Petrology of lunar soils. Rev Geophys Space Phys 13: 567-587
- Hodges, Jr., R.R. (1976) The escape of solar wind carbon from the moon. Proc Lunar Planet Sci Conf 7:493-500
- Labotka, T.C., Kempa, M.J., White, C., Papike, J.J., Laul, J.C. (1980) The lunar regolith: Comparative petrology of the Apollo sites. Proc Lunar Planet Sci Conf. 11: 1285-1305

- Laul, J.C., Smith, M.R., Papike, J.J., Simon, S.B. (1984) Agglutinates as recorders of regolith evolution: application to the Apollo 17 drill core. Proc 15th Lunar Planet Sci Conf. J Geophys Res 89: C161-C170
- Lindsay, J.F. (1976) Lunar stratigraphy and sedimentology. Elsevier, New York. 320 pp
- Lindsay, J.F. (1975) A steady-state model for the lunar soil. Bull Geol Soc Am 86 1661-1670.
- McKay, D.S., Williams, R.J. (1979) A geologic assessment of potential lunar ores. In: O'Neil, G.K. (ed) Space resources and space settlements. NASA SP-428. NASA Wash., DC pp 243-255
- Mendell, W.W., McKay, D.S. (1975) A lunar soil evolution model. The Moon 13: 285-292
- Morris, R.V., Lauer, H.V., Jr., Gose, W.A. (1979) Characterization and depositional and evolutionary history of the Apollo 17 deep drill core. Proc Lunar Planet Sci Conf. 10: 1141-1158
- Morris, R.V., Score, R., Dardano, C., Heiken, G. (1983) Handbook of Lunar soils. NASA Planetary Mat Branch Pub 67. NASA JSC, Houston, TX pp913
- Papike, J.J., Simon, B., Laul, J.C. (1982) The lunar regolith: Chemistry, mineralogy, and petrology. Rev Geophys Space Phys 20: 761-826
- Pieters, C.M. (1978) Mare basalt types on the front side of the moon. Proc Lunar Planet Sci Conf. 9: 2825-2849

- Pieters, C.M., McCord, T.B., (1976) Characterization of mare basalt types: I. A remote sensing study using reflection spectroscopy of surface soils. Proc Lunar Planet Sci Conf 7: 2677-2690
- Pillinger, C.T. (1979) Solar-wind exposure effects in the lunar soil. Rep Progress Phys. 42: 897-961
- Podnieks, E.R., Roepke, W.W. (1985) Mining for lunar base support. In: Mendell, W.W. (ed) Lunar bases and space activities of the 21st century. Lunar Planet Sci Inst., Houston, TX pp
- Schultz, P.H., Srnka, L.J. (1980) Cometary collisions on the moon and Mercury. Nature 284: 22-26
- Steurer, W.H. (ed) (1982) Extraterrestrial Materials Processing. JPL pub 82-41. Pasadena, CA. 147 pp
- Taylor, G.J., Warner, R.D., Keil, K.K. (1979) Stratigraphy and depositional history of the Apollo 17 drill core. Proc Lunar Planet Sci Conf 10: 1159-1184
- Tucker, D.S., Vaniman, D.T., Anderson, J.L., Clinard, F.W., Jr., Feber, R.C., Frost, H.M., Meek, T.T., Wallace, T.C. (1985) Hydrogen recovery from extraterrestrial materials using microwave energy. In: Mendell, W.W. (ed) Lunar bases and space activities of the 21st century. Lunar Planet Sci Inst., Houston, TX pp 583-590
- Weissbart, J., Smart, W., Wydeven, T. (1969) Oxygen reclamation from carbon dioxide using a solid oxide electrolyte. Aerospace Medicine 40: 136-140.

White, D.C. and Hirsch, P. (1985) Microbial extraction of hydrogen from lunar dust. In: Mendell, W.W. (ed) Lunar bases and space activities of the 21st century. Lunar Sci Inst. Houston, TX pp 591-602

Williams, R.J. (1985) Oxygen extraction from lunar materials: an experimental test of an ilmenite reduction process. In: Mendell, W.W. (ed) Lunar bases and space activities of the 21st century. Lunar Planet Sci Inst., Houston, TX pp 551-558

7.4 ELECTROLYSIS OF MOLTEN LUNAR MATERIALS

Overview

Molten-salt electrolysis can in theory be performed using lunar regolith material as an electrolyte. Oxygen bearing anions within the electrolyte are discharged (oxidized) at an anode, producing O_2 gas which can be collected (Downs, 1970; Kesterke, 1971; Steurer, 1982; Carroll, 1983). Reduction of metal-bearing cations occurs at the cathode leading to deposition of metals on the cathode as dendrites or low-melting alloys. Theoretically, silicate ions discharging at the cathode could also release O_2 gas (Kesterke, 1971).

Distinction must be made between electrowinning and magma electrolysis (Carroll, 1983). In electrowinning processes, a flux is added in sufficient quantity to enhance conductivity, reduce viscosity, and to reduce the melting temperature of the electrolyte (Carroll, 1983; Kesterke, 1971; Downs, 1971). In order to overcome the burden of importing fluxing agents and anode material, Carroll, (1983) suggests magma electrolysis using raw lunar regolith (basalt) alone as an electrolyte with a relatively non-consumable anode.

7.5 ELECTROWINNING OF OXYGEN

Process Outline

Kesterke (1971) experimentally investigated electrowinning of lunar regolith simulant (basaltic scoria) as a means of oxygen production. Kesterke's apparatus is shown in Figure 7.5.1. A boron nitride crucible was used as a refractory container for the electrolyte. An arc-welder supplied AC current to a resistor for cell heating; operation temperature was 650 C in a vacuum of 10^{-2} torr, while a silicon rectifier supplied DC current for electrolysis.

Fluxing materials had to be used to promote fluidity and electrical conductivity of the molten minerals. As an example, the electrolysis of TiO_2 takes place as follows:

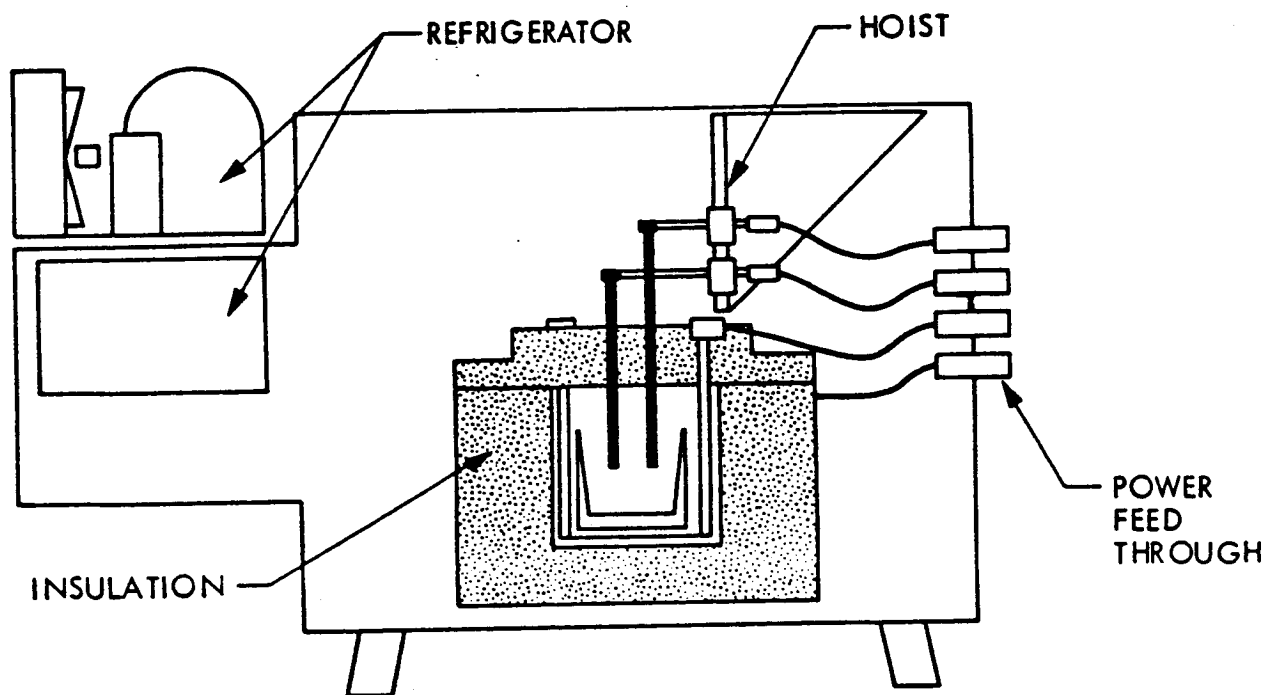
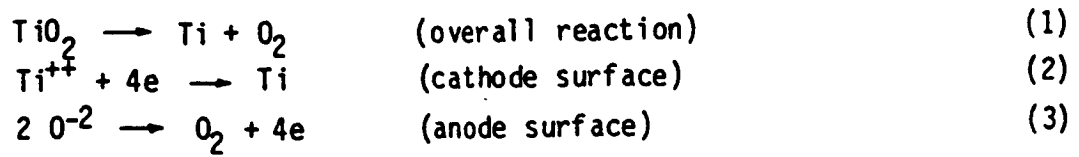


Figure 7.5.1 Electrolytic Cell used by Kesterke (1971).
(After Steurer, 1982)

As an analog to lunar material, a terrestrial scoria (vesicular basalt) was chosen as an appropriate silicate-bearing electrolyte. Due to high viscosity and low conductivity, electrolysis could not be performed effectively without introduction of a flux to the silicate electrolyte bath. Various fluoride, oxide, borate, and phosphate fluxes were evaluated experimentally. Lithium fluoride provide the best improvement in conductivity. However, silicate-fluoride melts are highly corrosive; performance of refractory electrode materials was evaluated. Iridium was found best for use as the anode and silica carbide was best for the cathode. These materials were found to work well for an electrolyte of the following composition: 69.4% BaF_2 + 5.6% LiF + 25% Scoria.

Improvement in O_2 production was obtained by changing initial electrolyte bath composition to: 48.5% BaF_2 + 16.5% LiF + 35% Scoria. This change from the above composition did not affect conduction significantly. Increasing anode surface area from 0.45 in^2 to 0.85 in^2 also improved O_2 output. Examining cathode deposits vs. remaining electrolyte after running the experiments, demonstrated that SiO_2 was not substantially reduced and remained largely in the electrolyte.

Downs (1971) and Jaret, et al. (1980) suggested the use of sodium hydroxide and sodium fluoride compounds (cryolite) as a fluxing agent to facilitate oxygen production from anorthite rich lunar regolith. Similar processes have been used terrestrially in electrowinning of aluminum (Downs, 1971; Jaret, et al., 1980; Rao, et al., 1979).

Oppenheim and Tabor (1972) suggest that solar energy might be used to bring the electrolyte up to near-melting temperature. This would substantially reduce the amount of electrical energy input required for any lunar electrolysis.

FEASIBILITY

Pro

- (1) No processing of lunar regolith is necessary.
- (2) Use of solar energy could allow for electrowinning to be carried out with minimal electrical energy input.

Con

- (1) The most serious problem identified by Kesterke (1971) is cell performance over extended periods of time due to gradual deterioration in both the electrolyte and the electrical cell. There is a gradual increase in electrical resistance in the melt over time due to early electrowinning of easily reduced oxides followed by electrowinning from more stable SiO_2 ; this leads to decreased O_2 production over time unless the electrolyte can be reconstituted continuously.
- (2) The solution to the above problem is to frequently renew the electrolyte bath. Mechanically this is not a problem; however, this would require large amounts of flux as a resource (recovery of flux from spent electrolyte is ruled out as being prohibitively expensive). Unless deposits of suitable flux can be located on the lunar surface, installation of a molten-salt type reactor is probably prohibitive in cost (Kesterke, 1971; Carroll, 1983).
- (3) Anode, cathode, and container deterioration are likely to be major drawbacks (Carroll, 1983; Cutler, 1985).

REFERENCES

- Carroll, W.F. (ed) (1983) Research on the use of space resources. JPL pub. 83:36. Pasadena, CA
- Cutler, A.H., Krag, P. (1985) A carbothermal scheme for lunar oxygen production. In: Mendell, W.W. (ed) Lunar bases and space activities of the 21st century. Lunar Planet Inst., Houston, TX. pp 559-569.
- Downs, W.R. (1971) Oxygen and water from lunar-surface material. NASA TM X-58061. NASA JSC, Houston, TX 21 pp.
- Jarrett, N., Das, S.K., Haupin, W.E. (1980) Extraction of oxygen and metals from lunar ores. Space Solar Power Rev. 1:281-287
- Kesterke, D.G. (1971) Electrowinning of oxygen from silicate rocks. U.S. Bureau of Mines Report of Investigations 7587. Reno, NV. 12 pp
- Oppenheim, M.J., Tabor, H. (1972) Oxygen from electrolyzed lunar rocks: a discussion of the energetics. In: Ordway, F.I. (ed) Advances in Space Science and Technology. Academic Press. New York. 11: 233-247
- Steurer, W.H. (1982) Extraterrestrial materials processing. JPL pub. 82-41. Pasadena, CA

7.6 MAGMA ELECTROLYSIS

Process Outline

Carroll (1983) indicates that molten basalt (used as a lunar analog) alone is conductive enough to sustain electrolysis without addition of any fluxing agent. Magma electrolysis, however, may be hindered by (1) kinetic blocks to reduction of particular species (Al_2O_3 and SiO_2), and (2) semiconduction, which acts as a parasitic process competing for electrical energy input with ionic conduction which facilitates transport of metal species and oxygen. Experiments were carried out using an Mo crucible as a cathode and an Mo anode rod (Fig. 7.6.1). Conduction across a mock basalt magma was measured at 1550°C and an input current of $1.25\text{A}/\text{cm}^2$; semiconduction appears not to be a significant problem. Electrolytic efficiency (energy supplied/energy used to electrolyze the magma) was found to be $>95\%$ (Carroll, 1983). Iron was produced at the cathode (container) and could cause deterioration in conduction over time and damage the container. Unfortunately, oxygen yields at the anode were not quantified.

FEASIBILITY

Pro

- (1) The most attractive aspect of magma electrolysis is the lack of need for any flux material. Lunar regolith could be melted without preprocessing.
- (2) As suggested above, solar heating to near-melting temperatures could substantially save electrical energy consumption (Oppenheim and Tabor, 1972).

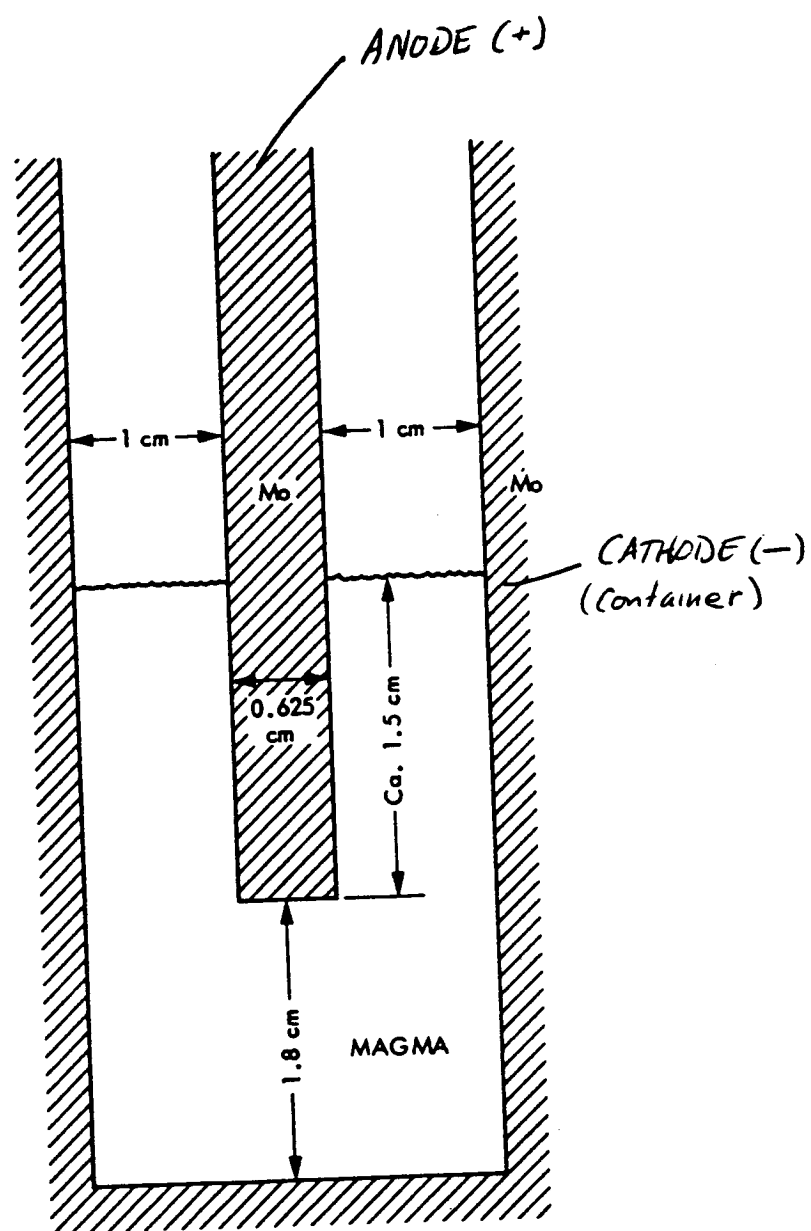


Figure 7.6.1 Electrolysis cell from Carroll (1983).

Con

- (1) Significant problems exist in terms of finding refractory anode and cathode (container) materials sufficiently resistant to the magma bath and any precipitates at the cathode (Carroll, 1983).
- (2) Melting of regolith will require larger thermal inputs than for similar electrowinning techniques which employ fluxes.

REFERENCES

- Carroll, W.F. (ed) (1983) Research on the use of space resources. JPL pub. 83:36. Pasadena, CA
- Downs, W.R. (1971) Oxygen and water from lunar-surface material. NASA TM X-58061. NASA JSC, Houston, TX 21 pp.
- Jarrett, N., Das, S.K., Haupin, W.E. (1980) Extraction of oxygen and metals from lunar ores. Space Solar Power Rev. 1:281-287
- Kesterke, D.G. (1971) Electrowinning of oxygen from silicate rocks. U.S. Bureau of Mines Report of Investigations 7587. Reno, NV. 12 pp
- Oppenheim, M.J., Tabor, H. (1972) Oxygen from electrolyzed lunar rocks: a discussion of the energetics. In: Ordway, F.I. (ed) Advances in Space Science and Technology. Academic Press. New York. 11: 233-247
- Steurer, W.H. (1982) Extraterrestrial materials processing. JPL pub. 82-41. Pasadena, CA

7.7 VAPOR PHASE REDUCTION

Overview

Vapor phase reduction refers to processes by which metal and/or oxygen can be extracted from vaporized, dissociated or ionized raw materials (Steurer, 1982; Carroll, 1983). These processes would rely on the lunar hard vacuum to draw vapor through various types of extraction and collection devices. The dissociated or ionized vapor is produced by intense heating of finely powdered raw oxide material such as lunar regolith. A group of scientists at the Jet Propulsion Laboratory (JPL) outlined four prospective vapor phase reduction processes (Steurer, 1982):

- (1) Vapor separation/fractional distillation
- (2) Ionization/electrostatic vapor deposition
- (3) Ionization/electromagnetic recovery
- (4) Selective ionization

Due to high energy requirements necessary to maintain an ionized vapor, further theoretical and experimental investigation was confined to the vapor separation and selective ionization processes (Carroll, 1983). Details of these two processes are outlined below, brief summaries of all four processes appear in Steurer (1982).

7.8 VAPOR SEPARATION

Process Outline

The apparatus used in vapor separation is conceptually outlined in Figures 7.8.1 and 7.8.2. Finely granulated raw material oxides (lunar regolith) are either passed through an induction coil heater or deposited in a solar furnace reaction vessel where vaporization and dissociation take place and oxygen is released.

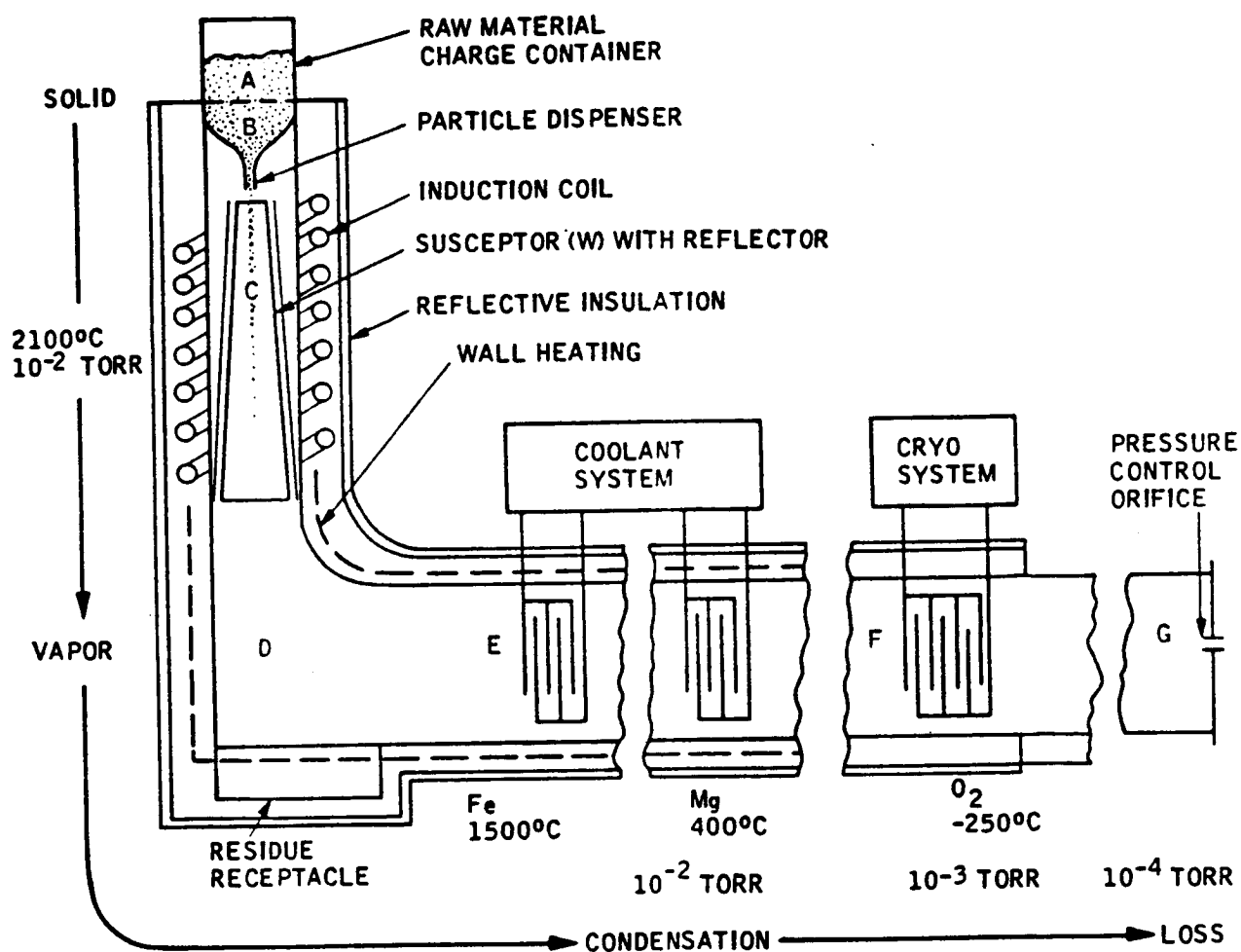


Figure VI-17 Vapor-Phase Reduction: Recovery of Metals and Oxygen by Fractional Distillation. (Conceptual)

Figure 7.8.1 Vapor separation apparatus (After Steurer, 1982).

ORIGINAL PAGE IS
OF POOR QUALITY

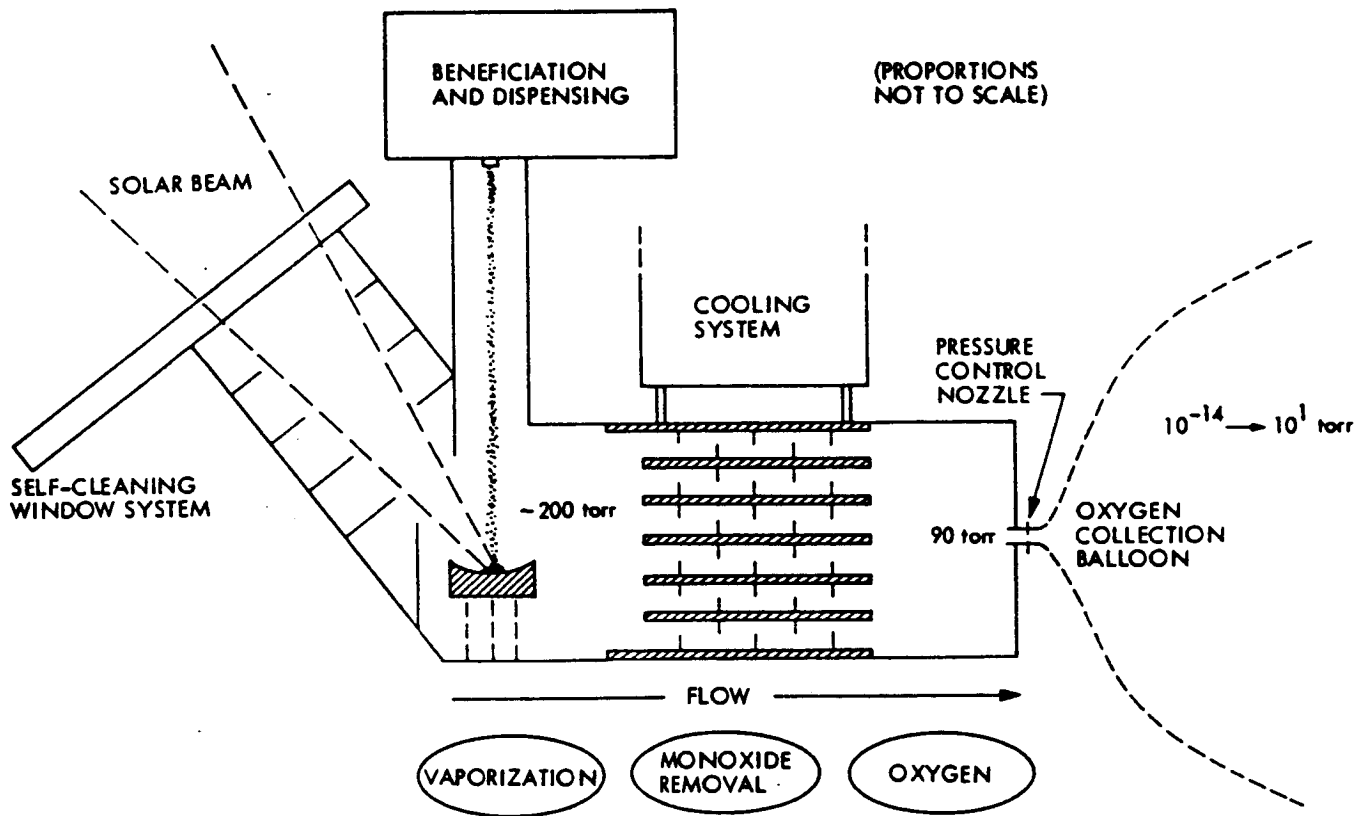


Figure 7.8.2 Vapor separation apparatus (After Carroll, 1983).

A pressure of some 200 torr is maintained in the chamber where dissociation takes place and the system is open to the lunar hard vacuum of 10^{-14} torr through a control orifice. The extreme pressure differential causes the dissociated vapor to travel rapidly toward the orifice. The dissociated vapor travels through a labyrinth of cooling plates where metal monoxides are condensed at various temperatures. Oxygen can then be collected either by a final condensation step (Steurer, 1982) or filling a balloon against the lunar vacuum (Carroll, 1983; Figs. 7.8.1 and 7.8.2). If solar furnace heating is utilized in the vaporization step, the optimal operation temperature is 3000° K (Carroll, 1983).

Theoretical research has been conducted on (1) degree of dissociation of single oxides as a function of temperature, (2) oxygen yield, (3) composition of vapor using basalt as a lunar simulant raw material, and (4) energy requirements.

Significant results (Carroll, 1983) are: (1) Dissociation of oxides and the partial pressure of free oxygen generated is substantial at temperatures $>2500^{\circ}$ K, (2) Oxygen yield is insensitive to temperature above 2000° K and the oxygen yield of FeO is zero, therefore, removal of Fe-rich particles by magnetic or electrostatic separation prior to vaporization would increase the yield of oxygen per volume of raw material, (3) maximum oxygen yields are expected to be about 24% from the original raw material mass, and (4) oxygen may be cooled prior to liquification by radiating heat into space. Temporary storage of oxygen in a balloon may be desirable.

Lunar Resources

Finely comminuted lunar regolith can be used directly as a feedstock. Techniques of mining lunar regolith are reviewed by Podnieks and Roepke (1985). Magnetic separation of the FeO

bearing (ferromagnetic) fraction from the regolith would slightly enhance oxygen yields.

Energy Requirements

Thermodynamic calculations indicate that 4.8 kcal/g or 5100 kWh/ton is a rough figure for energy required to vaporize the raw oxide material (Carroll, 1983). A conservative estimate of 2000 kWh/ton (of raw material) is suggested to operate the cooling/condensation recovery phase, bringing the total energy requirement to about 7100 kWh/ton of raw material. At the suggested oxygen recovery rate of 24%, this converts to about 30,000 kWh/ton of oxygen produced. Furthermore, it is estimated that 2/3 of the power could be provided by direct solar heating, necessitating production of about 10,000 kWh/ton electrically (Carroll, 1983).

Feasibility

Pro

- (1) Perhaps the most attractive aspect of any vapor separation technique lies in the fact that no import of raw materials is required. Lunar regolith can be used directly as a feedstock.
- (2) Oxygen yields are superior relative to other processes.
- (3) The process can be turned on and off without substantial warm-up or warm-down times.

Con

- (1) The major drawback is the relatively high energy consumption.

(2) Vapor separation is a relatively low pressure process; which translates into a necessarily high throughput of feedstock to insure adequate recovery of oxygen.

(3) Vapor phase reduction processes will be difficult to test terrestrially due to the need of a substantial hard vacuum.

(4) Maximum oxygen yields require removal of FeO-bearing material from the lunar regolith.

7.9 SELECTIVE IONIZATION

Process Outline

If the vaporization step in the separation process above is carried out at high temperatures (4000° – 8000° K) the resulting dissociated vapor will be a highly charged ionic vapor or plasma. It has been experimentally determined that at discrete temperatures between 4000° – 8000° K, metal species in a thermal plasma are much more highly ionized than oxygen (Fig. 7.9.1; Steurer, 1982; Carroll, 1983). If such a plasma is drawn through an apparatus as shown in Figs. 7.9.2 and 7.9.3 (utilizing the same pressure differential with lunar vacuum as for vapor separation above), positively charged metal species and electrons should be attracted to the negatively and positively charged electrostatic plates and separated from the neutral oxygen in the plasma.

High temperature vaporization and ionization can be achieved by electron beam gun, arc-discharge, RF induction, and laser beam techniques (Steurer, 1982). The RF induction heating appears most promising as a proven and energy efficient technique. Theoretical assessment was made of the following aspect of selective ionization: (1) encountered species as a function of plasma temperature, (2) degree of ionization, (3) expected oxygen yield, and (4) energy requirements. The following significant results were obtained (Carroll, 1983):

(1) Although interfering effects exist within the plasma (common ion effects, etc.), theoretical calculations (Fig. 7.9.4) indicate that oxygen does indeed remain effectively neutral relative to the most abundant metal species in lunar soil,

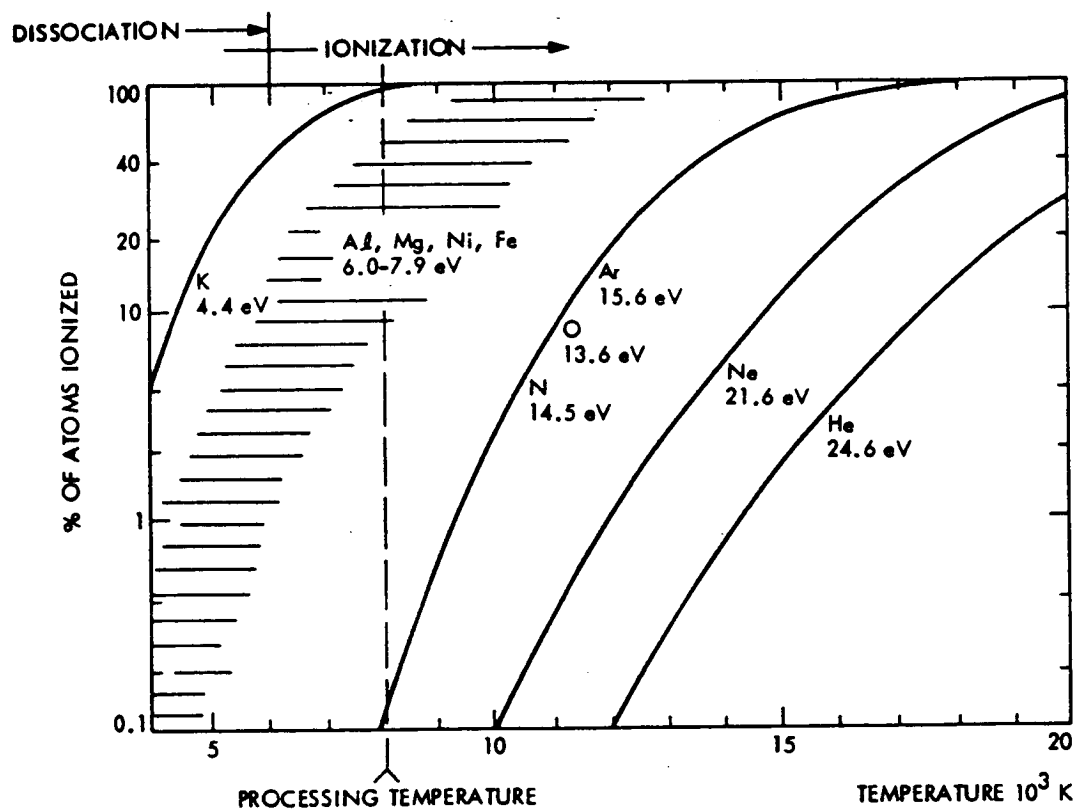


Figure 7.9.1 Ionization potential of elements as a function of temperature (After Carroll, 1983)

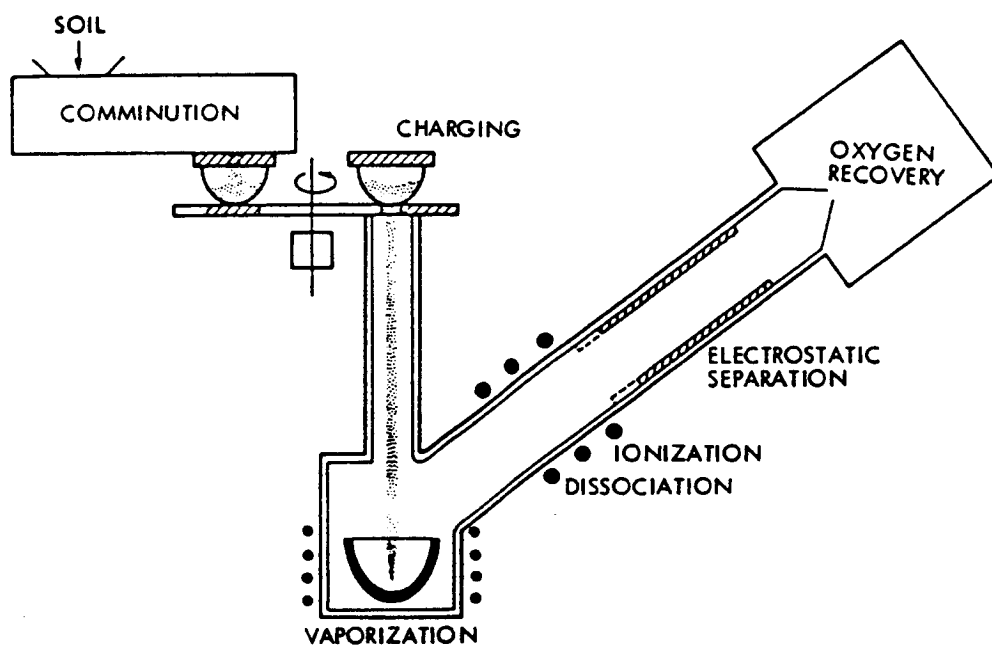


Figure 7.9.2 Apparatus for selective ionization processing.
(After Carroll, 1983, see Fig. 11 for detail).

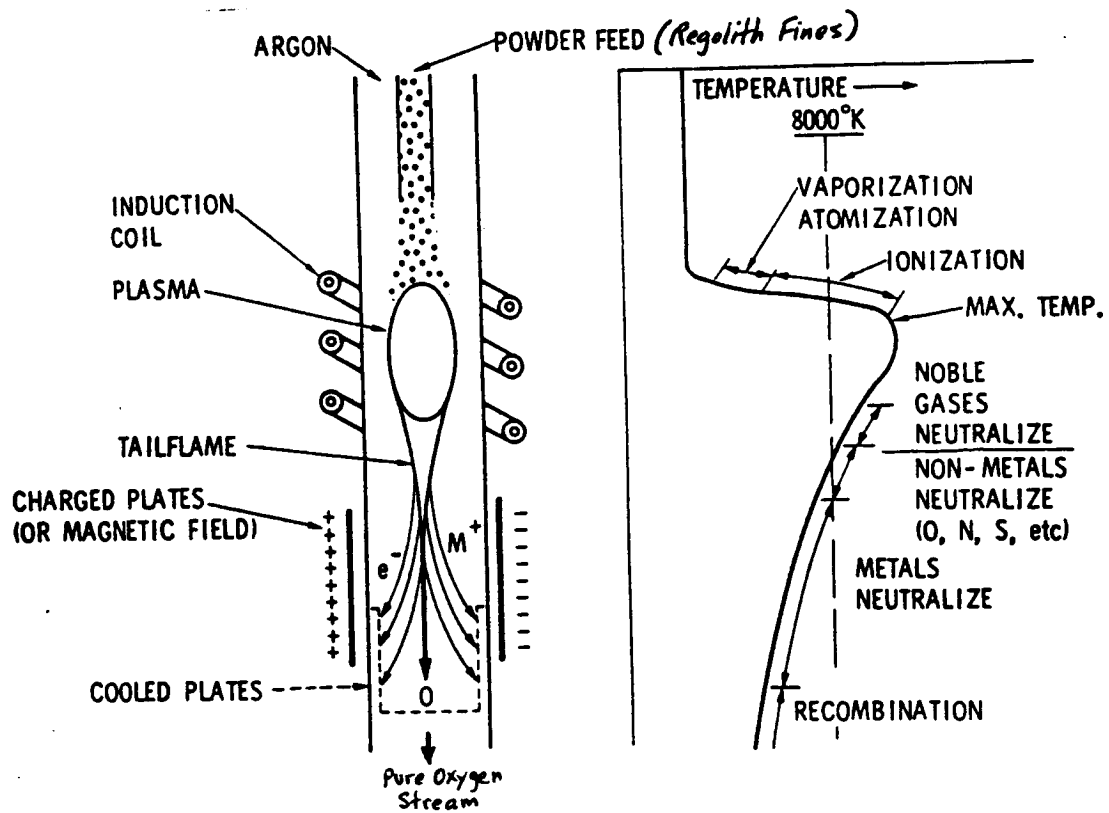


Figure 7.9.3 Schematic summary of the details of the selective ionization process (After Steurer, 1982).

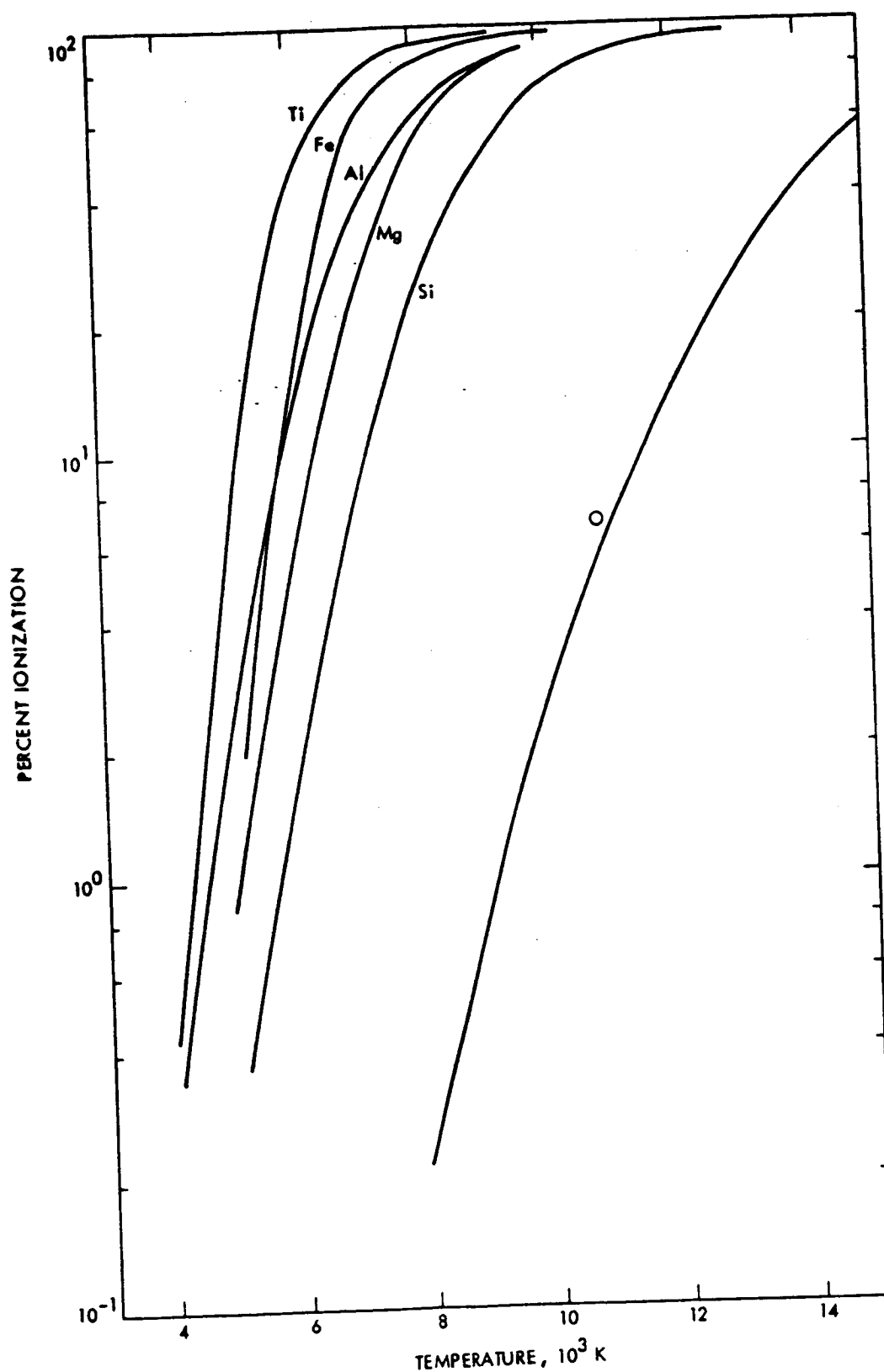


Figure 7.9.4 Theoretically calculated percent ionization of metals and oxygen as a function of temperature (After Carroll, 1983)

(2) Based on the above data (Fig. 7.9.3) at 8000°K ionization is about 65% (ion/atom in total plasma) and oxygen yield is 28% relative to the initial mass of raw lunar soil. At 10,000°K and 90% ionization, oxygen can be recovered at about 39% efficiency.

Energy Requirements

Thermodynamic calculations suggest that about 6000 kWh/ton is required for vaporization, while 5500 kWh/ton is required to bring the vapor into thermal equilibrium at 10,000°K. Additional energy of about 450 kWh/ton is required to maintain voltage across the electrostatic plates. At 90% yield, these figures sum to 13,300 kWh/ton required for oxygen-metal separation. If energy is lost at a 10% rate, and oxygen yield is 39%, about 34,500 kWh/ton of raw material is required if oxygen is the only product of interest (metals could be recovered as well at a cost of higher overall energy consumption; Carroll, 1983).

Feasibility

The advantages and disadvantages are comparable to those suggested for vapor separation above. In addition:

Pro

Selective ionization is an extremely efficient process which yields a very pure oxygen product.

Con

Energy consumption is somewhat greater than that suggested for vapor separation above.

REFERENCES

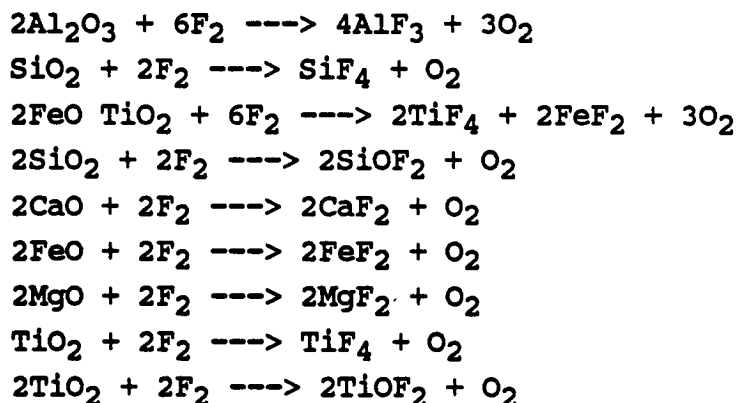
- Carroll, W.F. (ed) (1983) Research on the use of space resources.
JPL pub. 83:36. Pasadena, CA
- Podnieks, E.R., Roepke, W.W. (1985) Mining for lunar base support. In: Mendell, W.W. (ed) Lunar bases and space activities of the 21st century. Lunar Planet Inst., Houston, TX pp 445-452
- Steurer, W.H. (1982) Extraterrestrial materials processing. JPL pub. 82-41. Pasadena, CA

7.10 OXYGEN LIBERATION USING FLUORINE

Direct Fluorine Liberation of Oxygen

Downs (1971; 1973) suggested the use of pure fluorine to liberate oxygen from bulk lunar regolith. Fluorine displaces and liberates oxygen from virtually all metal oxides at temperatures between 25° and 800° C. Optimum reaction conditions attain at about 500° C and 760 torr; under these conditions oxyfluorides should not form and fluorine exchange should be complete (Downs, 1971; 1973). Reactions of interest are given in Table 7.10.1.

TABLE 7.10.1 Equations of fluorine reaction with lunar regolith derived oxides (After Downs, 1973)



Downs (1971) indicates that reaction of 42.5 kg of fluorine with 45.4 kg of regolith will yield 19.1 kg of oxygen under the conditions outlined above. Due to the economics of transport, fluorine, of course, must be recycled. Metal fluorides produced (reactions in Table 7.10.1) can be reacted with potassium vapor at conditions of 100-280 torr and 800°-850° C to yield KF liquid and metal species. Liquid KF can then be electrolyzed; both K and F derived from electrolysis can be recycled. Oxygen derived from the reactions in Table 7.10.1 must be purified. Downs (1971) suggests passing the product vapors (which will contain mainly O₂ with minor F₂) through a bed of potassium iodide to facilitate the following reaction:



Product KF can be electrolyzed (as above) so that K, I and F from this reaction are recycled (Downs, 1971). The overall process scheme is patented (Downs, 1973) and is schematically represented in Fig. 7.10.1.

HF Acid Leaching of Lunar Regolith

Low temperature, hydrochemical conversion of lunar regolith oxides to fluorides and fluorosilicates can be accomplished using HF acid leaching (Waldron, et al, 1980). Pertinent reactions are summarized in Table 7.10.2.:

Table 7.10.2 HF acid leach process equations
(after Waldron et.al,1980)

1. $xMO SiO_2 + (4 + 2x) HF = xMF_2 + SiF_4 (aq) + (2 + x) H_2O$
 - 1'. $xMO SiO_2 + (5 + 2x) HF = xMF_2 + HSiF_3 (aq) + (2 + x) H_2O$
 2. $SiF_4 (aq) + nH_2O = SiF_4 (v) + nH_2O (v)$
 - 2'. $HSiF_3 (aq) + nH_2O = SiF_4 (v) + HF (aq) + nH_2O (v)$
 3. $(1-y) [SiF_4 (v) + 4H_2O = Si (OH)_4 + 4HF]$
 - 3a. $(1-y) [SiF_4 (v) + 2H_2O = SiO_2 + 4HF]$
 4. $(1-y'-z) [xMF_2 + xH_2O = xMO + 2xHF]$
 5. $y [SiF_4 + 4Na = Si + 4NaF]$
 6. $y' [xMF_2 + 2xNa = xM + 2xNaF]$
 7. $z [xMF_2 + xSiF_4 (aq) = xMSiF_6 (aq)]$
 8. $z [xMSiF_6 (aq) + H_2O + \text{electrical energy} = (x/2)O_2 + xM + xH_2SiF_6]$
 - 8a. $z [xMSiF_6 (aq) + M'SO_3R^* = xM'SiF_6 (aq) + xMSO_3R^*]$
 9. $m NaF + mR^*OH = mNaOH + mR^*F$
 - 9a. $m NaF + (m/2) Ca (OH)_2 = mNaOH + (m/w) CaF_2$
 10. $m NaOH + \text{electrical energy} = mNa + (m/2)O_2 + (m/2)H_2O$
 11. $(1-y) [Si (OH)_4 = SiO_2 + 2H_2O]$
- R* = ion exchange resin
 $m = 4y + 2xy'$

The fluorine replacement reactions (1 and 1' in Table 7.10.2) produce water which can be electrolyzed to recover oxygen and hydrogen. Silica is removed by vaporizing and drawing off the SiF_4 product and metal species are separated by a variety of solution, precipitation, ion exchange, electrolysis, and NaOH reduction techniques (Waldron et al., 1980). A flow chart of the various processes proposed in HF acid leaching is depicted in Figure 7.10.1.

Waldron, et al., (1980) were concerned mainly with space station recovery of metals and metal alloys rather than oxygen. However, in light of the importance of oxygen production, the HF acid leach process outlined above could be streamlined to include only those processes capable of producing oxygen. Reactions 1 and 1' (Table 7.10.2) yield water which can be directly electrolyzed to produce oxygen and hydrogen. To insure recovery and recycling of valuable fluorine, SiF_4 would necessarily be treated by hydrolysis and fractional distillation (reactions 2, 2', 3, and 3a, Table 7.10.2; Fig. 7.10.2). Hydrogen produced from the electrolysis of water could be effectively combined with this fluorine completing the recycling circuit. Processes involved with HF acid leaching of lunar materials are yet under active investigation (Waldron, 1983; Waldron, 1985 as reported in Cutler and Krag, 1985).

Lunar Resources

Fluorine abundances range from about 40 ppm in bulk lunar regolith to about 300 ppm in some mare basalts (Criswell and Waldron, 1982). Goldberg, et al., (1976) have demonstrated that fluorine common to Apollo 15 green glass and Apollo 17 orange glass particle surfaces is of lunar (rather than solar wind or extralunar) origin; it was probably deposited on glass particle surfaces and on surfaces lining vesicles as a result of degassing of lunar (basalt) magmas. Surface coatings of the orange and

ORIGINAL PAGE IS
OF POOR QUALITY

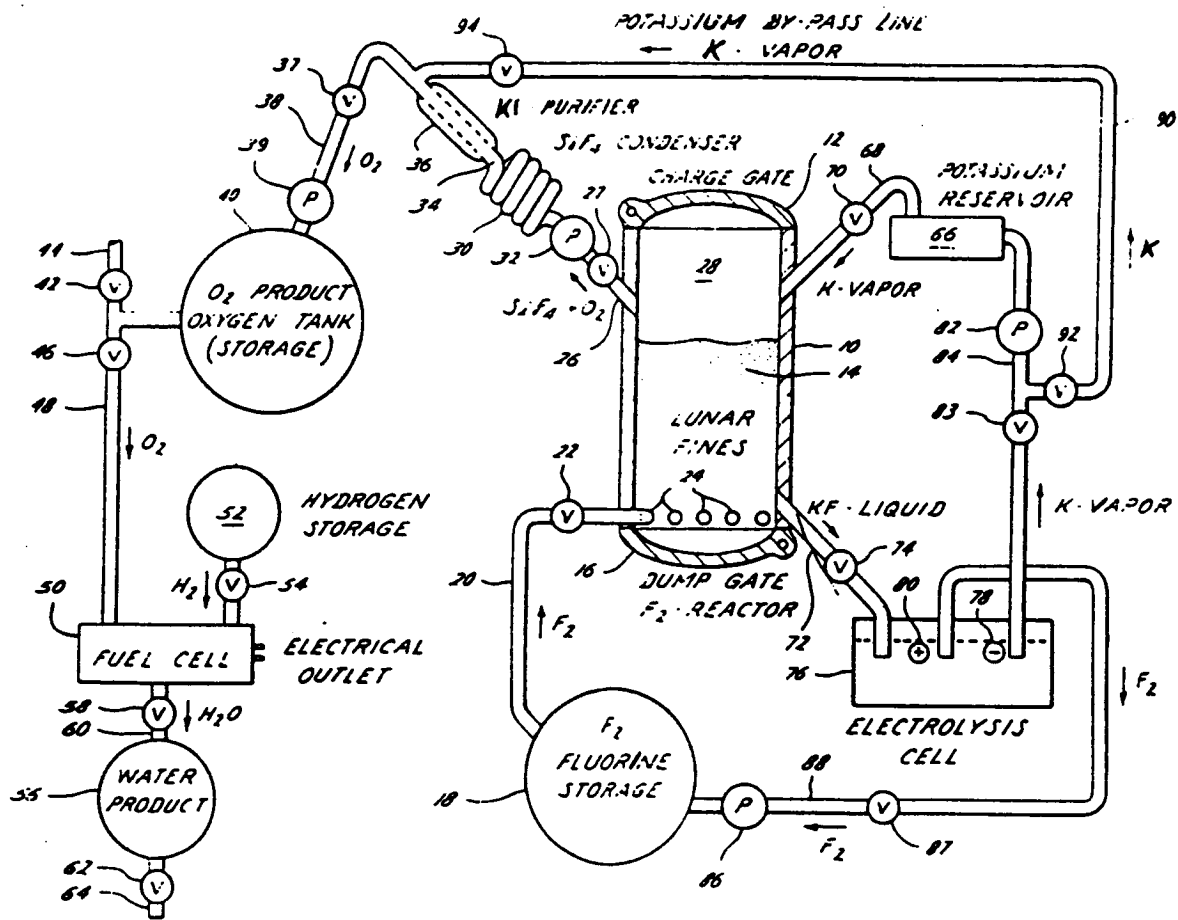


Figure 7.10.1 Outline of process scheme to obtain oxygen from lunar regolith using fluorine (After Downs, 1973).

ORIGINAL PAGE IS
OF POOR QUALITY

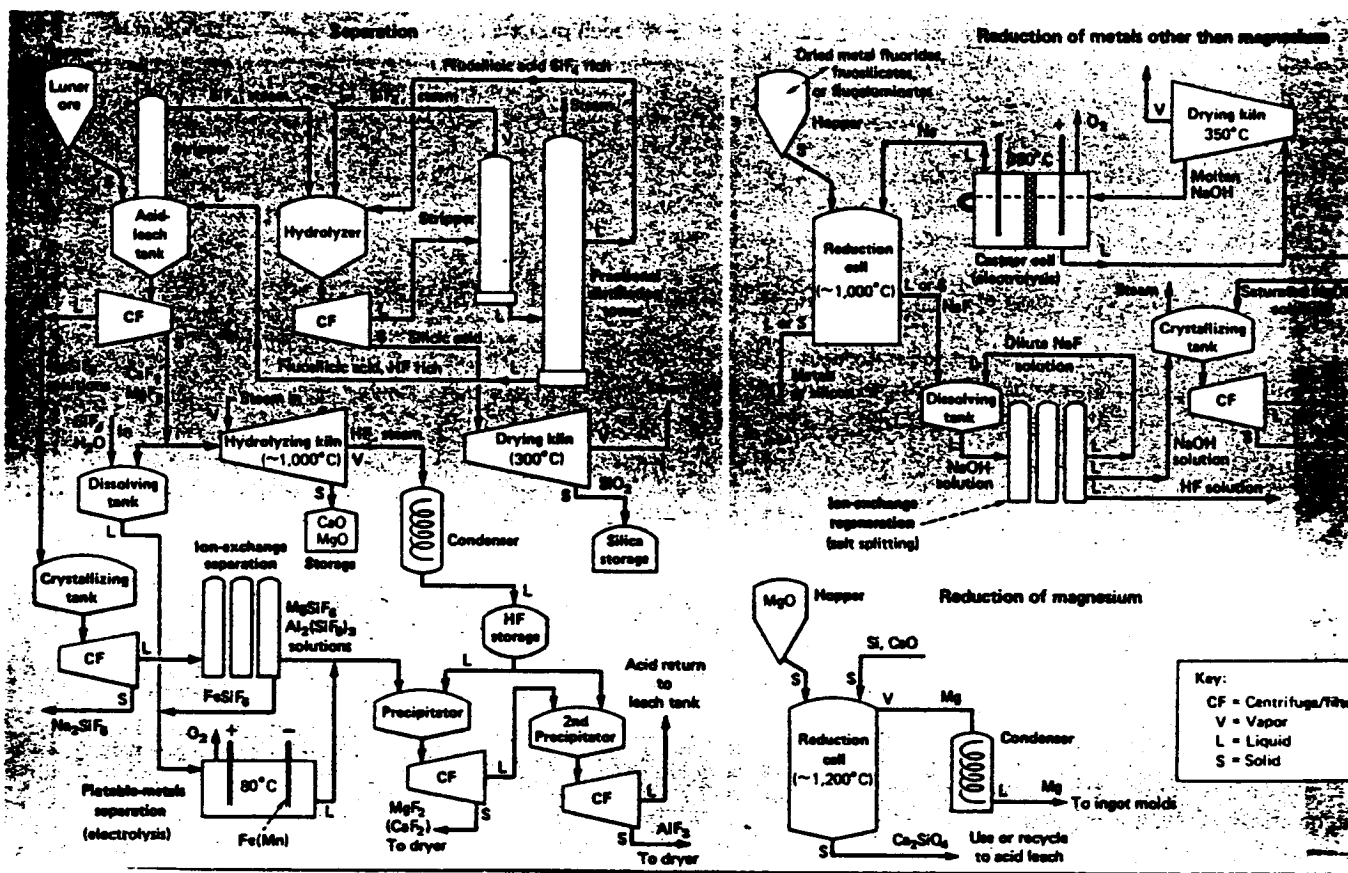


Figure 7.10.2 Flow chart outline of the HF acid leach process of oxygen production from lunar regolith (After Waldron, et al., 1980).

green glasses contain up to 600 ppm fluorine and associated basalts typically contain <100 ppm fluorine. Pyrolysis studies of volatile release patterns for lunar regolith do not typically reveal fluorine release at temperatures below 600° C (DesMarais, 1974a, 1974b, Criswell and Waldron, 1982; Gibson and Moore, 1976). Questions exist regarding the nature of chemical bonding of fluorine in the green and orange glasses studied by Goldberg, et al, (1976).

FEASIBILITY

Pro

- (1) Fluorine based chemical processes are attractive because bulk lunar regolith can be processed with high oxygen yields without modification or beneficiation.
- (2) Fluorine and HF acid reactions enable low temperature extraction of oxygen and of oxygen bearing H_2O . Relatively low direct energy inputs can derive substantial oxygen yields.

Con

- (1) Fluorine or hydrofluoric acid may need to be imported from earth initially, at a large cost. Low fluorine abundances characteristic of the lunar materials may prevent use of lunar fluorine as a potential resource.
- (2) Fluorine and hydrofluoric acid are very dangerous reagents in their terrestrial application; great care must be taken to insure against human exposure to these materials. In addition, container and handling problems inherent to these reagents must be considered.
- (3) The expected processing plant mass for any fluorine based oxygen extraction scheme will be large relative to that for other potential extraction methods (Cutler and Krag, 1985).

REFERENCES

- Criswell, D.R., Waldron, R.J., (1982) Materials processing in space. In: O'Leary (ed) Space Industrialization (Vol.2). CRC Press. Boca Raton, FL, pp 1-54
- Cutler, A.H. and Krag, P. (1985) A carbothermal scheme for lunar oxygen production. In: Mendell, W.W. (ed), Lunar bases and space activities of the 21st century. Lunar and Planetary Institute. Houston, TX pp 559-569.
- DesMarais, D.J., Hayes, J.M., Meinschein, W.G. (1974a) The distribution in lunar soil of hydrogen released by pyrolysis. Proc. Lunar Planet Sci Conf. 5: 1811-1822
- DesMarais, D.J., Hayes, J.M., Meinschein, W.G. (1974b) The distribution i lunar soil of carbon released by pyrolysis. Proc Lunar Sci Conf. 4: 1543-1558
- Downs, W.R. (1971) Oxygen and water from lunar surface material. NASA TM-X 58061. NASA JSC, Houston, TX, pp 21
- Downs, W.R. (1973) Method for obtaining oxygen from lunar of similar soil. U.S. patent no. 3,773,913. Nov. 20th, 1973
- Gibson, E.K., Moore, G.W. (1972) Inorganic gas release and thermal analysis study of Apollo 14 and 15 soils. Proc Lunar Planet Sci Conf 3: 2029-2040.
- Goldberg, R.H., Tombrello, T.A., Burnett, D.S. (1976) Fluorine as a constituent in lunar magmatic gases. Proc Lunar Planet Sci Conf. 7: 1597-1613.
- Waldron, R.D., Erstfield, T.E., Criswell, D.R. (1980) The role of chemical engineering in space manufacturing. Chemical Engineering. Feb. 12, 1980, 86: 80-94.
- Waldron, R.D. (1983) Laboratory investigation of HF acid leach process for refining of lunar materials: preliminary results (abs). In: O'Neil (ed) Space manufacturing 1983, Proc 6th Princeton/AIAA Space Manufacturing Conference, 53. Am Astronautical Soc., San Diego, CA pp 335.

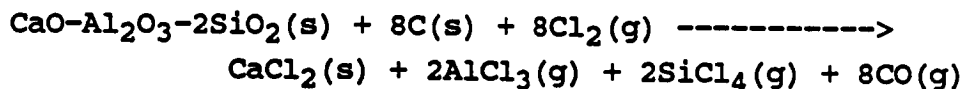
7.11 OTHER CHEMICAL METHODS

Carbochlorination

Rao et al., (1979), Waldron, et al., (1980), Erstfield and Williams (1979), and Steurer (1982) describe a carbochlorination method of producing aluminum from lunar anorthite. The pertinent reactions comprising this process are outlined below:



net reaction:



These reactions proceed optimally at 675-770 C. The product AlCl_3 can be recovered by condensing out other product species. CO is condensed after AlCl_3 (Fig. 7.11.1). This separation technique was developed as a precursor to dissociating AlCl_3 via an electrowinning process conceived by ALCOA.

CO can potentially be dissociated via a solid-state electrolysis cell such as are described above (see Ilmenite Reduction Solid-State Electrolysis, pp 25). Carbon produced by electrolysis can be recycled for use in the above reactions while oxygen can be condensed and stored. Should aluminum be extracted using the ALCOA process, product Cl from this process can also be effectively recycled. The overall carbochlorination scheme has received waning attention due to the potentially large plant mass and the probability of carbon and chlorine imports being necessary (Waldron, et al., 1980).

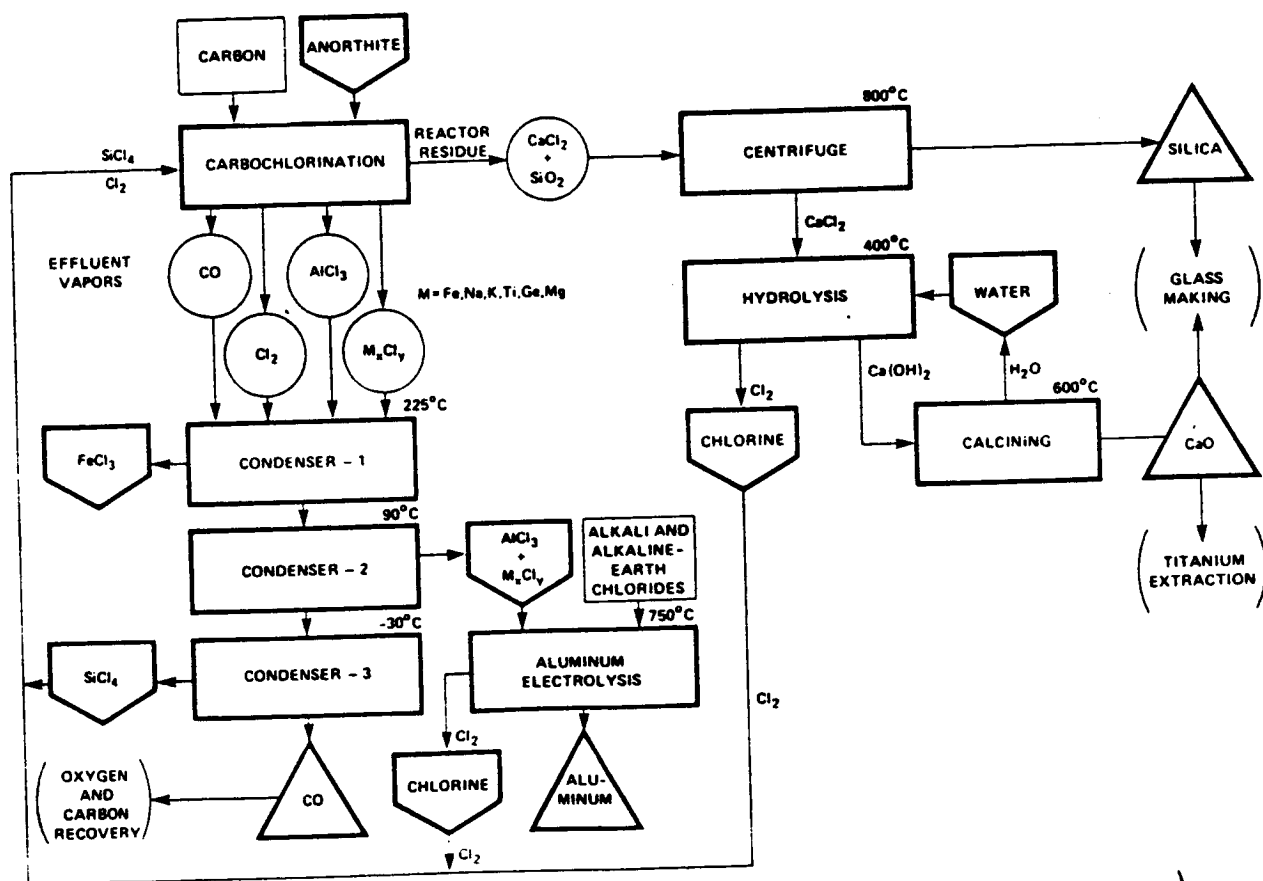


Figure 7.11.1 Flow chart of the carbochlorination method of aluminum and oxygen production (After Rao, et al., 1980).

REFERENCES

- Erstfield, T.E., Williams, R.J. (1979) High temperature electrolytic recovery of oxygen from gaseous effluents from carbochlorination of lunar anorthite and the hydrogenation of ilmenite: A theoretical study. NASA TM-58214. NASA Washington, DC, pp 51
- Rao, D.B., Choudary, U.V., Erstfield, T.E., Williams, R.J., Chang, Y.A. (1979) Extraction processes for the production of aluminum, titanium, iron, magnesium, and oxygen from non-terrestrial sources. In: O'Leary, B., Billingham, J., Gilbreath, W., Gosset, B., (eds) Space resources and space settlements. NASA SP-428. NASA Washington, DC. pp 257-274
- Steurer, W.H. (1982) Extraterrestrial materials processing. JPL pub. 82-41. Pasadena, CA
- Waldron, R.D., Erstfield, T.E., Criswell, D.R. (1980) The role of chemical engineering in space manufacturing. Chemical Engineering. Feb. 12, 1980, 86: 80-94.

Sodium Reduction

Waldron (1983) conceived a process by which Na is reacted with metal oxides derived from a separate process (such as HF acid leaching, above) to produce various sodium compounds (Na_2SiO_3 , Na_2TiO_3 , NaFeO_2) and sodium oxide (Na_2O). Sodium compounds can be directly dissociated by pyrolysis to yield sodium oxide. Sodium is then recovered by reaction with either pure nickel or copper or FeO:



Pyrolysis of the metal oxide products from these reactions at elevated temperatures of $1500^\circ - 2200^\circ \text{C}$ will yield oxygen vapor which can be recovered. The pure sodium vapor product from the above reactions can be recycled for further reduction of lunar-derived metal oxides. This process would most likely involve a large two-stage processing plant to produce metal oxides from regolith followed by sodium reduction and recovery. Additionally, handling of pure sodium vapor could present difficulties.

Waldron, R.D. (1983) Non-electrolytic route to oxygen and metallic elements from lunar soil. In: O'Neil (ed) Space Manufacturing 1983, Proc 6th Princeton Space Manufacturing Conf. Am Astronautical Soc., San Diego, CA 297-314.

7.12 COMPARISON OF METHODS/SUGGESTIONS FOR FUTURE RESEARCH

In contrasting feasibilities of the processes outlined above an important first order trade-off between costs of importing raw materials and the cost of energy production becomes apparent.

Vapor phase reduction, magma electrolysis, and possible fluorine leaching require no import of raw material; bulk lunar regolith can be processed directly. Vapor phase reduction techniques require substantially more energy than does magma electrolysis, however, oxygen yields by vapor phase reduction are much higher than for other processes. In addition, selective ionization yields an extremely pure oxygen product relative to other extraction techniques. On the other hand, chemical reduction processes operate at lower temperatures than either vapor phase techniques or magma electrolysis, which could mean substantial savings in energy consumption. The main drawback to any of the chemical processes proposed above is the likely need for import of necessary reagents such as H, C, F, or Na. Although liberation of oxygen by fluorine or HF is attractive because bulk regolith can be directly processed at low temperatures, complicated and dangerous chemistry and a potentially large and complex processing plant may not warrant implementation of this technique.

Magma electrolysis and electrowinning of lunar material for oxygen production are fraught with significant problems of anode and cathode wear and containment problems, in addition to large energy inputs necessary to sustain a molten electrolyte indicates that magma electrolysis can only be considered as a batch type process at present. Pending technological breakthroughs in solving these problems, magma electrolysis and electrowinning should not receive the attention which is deserved by other more tractable methods.

Hydrogen reduction of ilmenite involves relatively low temperature solid-state reaction chemistry and facilitates efficient recycling of both hydrogen and process heat in a continuous operating mode. In contrast, carbothermal reduction of lunar ilmenite requires melting, containing,

and handling batches of slag-metal mixtures and several chemical reaction consuming carbon (and hydrogen). These considerations favor implementing hydrogen reduction rather than carbothermal reduction. Carroll (1983) and many other workers (see Mendell, W.W., 1985) indicate that the discovery of water at the lunar poles would be the single greatest technological advance in terms of lowering the cost of a lunar base. Future remote sensing and/or unmanned efforts should be directed toward confirming or denying this possibility. Were such a hydrogen resource found, implementation of a hydrogen reduction plant would be straightforward. Research and development could then concentrate on reducing or preventing probable component deterioration by contaminants (such as H_2S , F, and Cl) and on enhancing reaction kinetics to increase the per-pass yield of water.

Solid-state electrolysis of $CO_2 - CO - H_2O$ products from chemical processes outlined above is a commonly recommended method of oxygen recovery. However, only one laboratory scale experimental study has been undertaken (Weissbart, et al., 1969). If processes which produce CO and H_2O gain favor as oxygen producing schemes, much research and development are desired toward producing efficient solid-state electrolytic cells capable of durable long-term operation.

Theoretical research into vapor phase reduction processes initiated at the Jet Propulsion Laboratory in 1981 has presently ceased. Since the above discussion favors either hydrogen reduction or vapor phase reduction, investigation into practical application of vapor phase processes should be revived. The effective use of solar energy is a key issue in lowering the costs of any lunar oxygen production scheme. Whether applied in direct solar furnace vaporization/dissociation, or in developing

necessary process heat to drive endothermic chemical reactions, use of solar energy where possible would greatly reduce electrical power consumption. Since electrical power plant mass is considered to be the largest and most costly entity in any lunar base (Simon, 1985), research into utilizing solar energy should remain a high priority. If, as suggested here, the choice boils down to either vapor phase reduction or hydrogen reduction processes, the ultimate decision will rest on an accurate assessment of overall energy and materials budgets of the two schemes. Namely, how does the cost (in energy consumption) of ilmenite beneficiation, hydrogen extraction or importation, and solid-state electrolysis compare to that necessary to vaporize and extract oxygen directly from bulk regolith.

7.13 SOLAR ENERGY AS A SOURCE OF PROCESS HEAT

Industrial process heat is the thermal energy used to prepare goods in manufacturing processes. These processes can range from the heat required to dry foods to the decomposition of compounds to their primary components.

Industrial process heat (IPH) can be characterized by three temperature ranges:

- a. Low temps. 100° C and below;
- b. Medium temps. 100 C to 350 C;
- c. High temps. +350° c

The types of IPH systems available are the following:

- a. Steam generated;
- b. Direct firing, as in a kiln;
- c. Hot air:
 - 1. Gas heating
 - 2. Steam flashing systems
 - 3. Solar boiler - auxiliary boiler system
- d. Hot water;
- e. Hot liquids.
- f. Solar

The solar systems comprise a collector field, a heat transport mechanism, a heat exchanger, and a controller.

The various types of collectors are:

- a. Solar ponds (up to 85° C);
- b. Flat plates (up to 100° C);
- c. Evacuated tubes (120° C to 300° C);
- d. Line focus (80° C to 320° C);
 - 1. Parabolic trough
 - 2. Hemispherical bowl
 - 3. Fresnel lens
 - 4. Multiple reflector (Fresnel mirrors)
- e. Point focus (300° C to 1500° C);
 - 1. Parabolic dish
 - 2. Fresnel lens
- f. Central receiver (300° C to 1200° C); -
- g. Distributed receiver (300° C to 1200° C)

Descriptions of the above types of IPH systems; collectors and their temperature ranges, along with the current status of IPH solar collector technologies are found in Appendix A ("Status Review and Prospects for Solar Industrial Process Heat"; F. Dreith, R. Davenport, and J. Feustel; J. Sol Energy Eng; 105: 385-400 Nov. 1983).

For high temperature processes (+350 C) Krieder, in Medium and High Temperature Solar Processes, 1979, state that to get a thermal performance of this magnitude one or two axes tracking solar concentrators must be used. Solar concentrators, devices which increase the flux at the absorber of a solar collector above ambient levels, and which have either reflecting or refracting elements that are located so that the solar flux is

focused or funneled onto a receiver component, can be broken down into the following types:

a. Compound curvature solar concentrators

1. Parabolic reflectors
2. Spherical reflectors
3. Fresnel lenses
4. Fresnel reflectors

b. Solar furnaces

1. Single heliostat
2. Multiple heliostat

On the paraboloidal concentrators, the focus occurs at a point instead of along a line. Thermal losses are small for these types of concentrators. The concentration ratio ranges from 500 to 3000. On the spherical reflector, the focus is along a line instead of at a point. These types of concentrators have lower concentration ratios (50 to 150), lower efficiencies, and the cost of solar heat is higher. In the use of the Fresnel lens (CR 100-1000), the lenses exhibit a prism effect called chromatic aberration. Sunlight is refracted differently for different wavelengths, thereby causing a beam spread. The concentration ratio for these devices are 100 to 1000. The Fresnel mirror concentrators (CR 1000-3000) consist of mirrors that track independently and which focus sunlight onto an absorber surface. The Fresnel mirrors are used in both solar furnace and central receiver solar thermal power plants.

Solar heliostat furnaces are large concentrators which achieve high temperatures. These devices do not require a working fluid absorber. Kreider (1979) defines a heliostat as a sun tracking planar reflector consisting of many small co-planar facets. The sun's rays are reflected from the heliostat onto a parabolic mirror which concentrates the solar flux.

Several examples of operating heliostats (see Kreider 1979, for specifications on physical properties and performance, pages 234-235) furnaces are:

a. Montlouis heliostat (Prof. Trombe of the Centre National de la Recherche Scientifique);

REFERENCES

- Carroll, W.F. (1983) Research on the use of space resources. JPL publication 83-36. Pasadena, CA 325 pp.
- Mendell, W.W. (ed) (1985) Lunar bases and space activities of the 21st century. Lunar Planet Sci Inst., Houston, TX 865 pp
- Simon, M.C. (1985) A parametric analysis of lunar oxygen production. In: Mendell, W.W. (ed) Lunar bases and space activities of the 21st century. Lunar Planet Sci Inst., Houston, TX pp 531-541